Bulletin of the Geological Society of Denmark

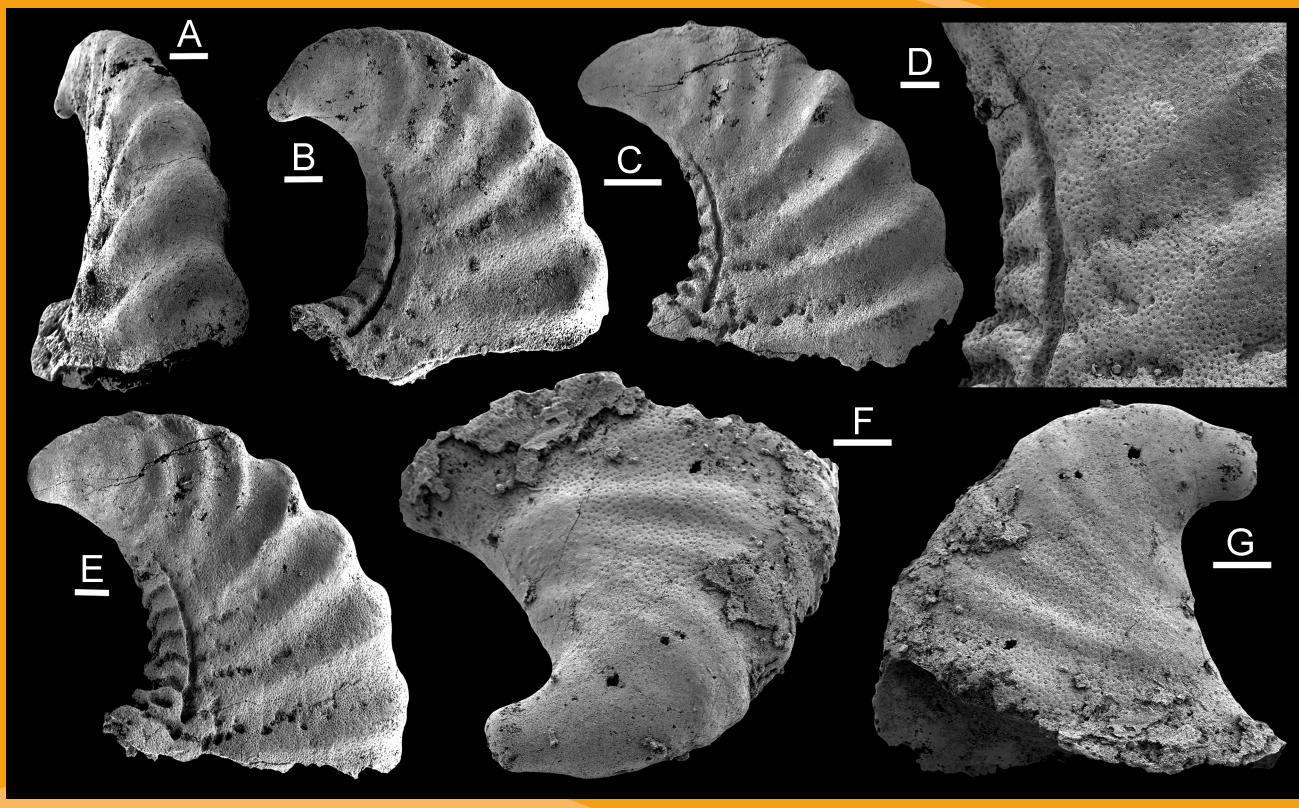

VOLUME 70 | 2022 | COPENHAGEN

DGF

Bulletin of the Geological Society of Denmark

is published by the Geological Society of Denmark (DGF, Dansk Geologisk Forening), founded in 1893

The *Bulletin* publishes contributions of international interest in all fields of geological sciences on results of new work on material from Denmark, the Faroes and Greenland. Contributions based on foreign material may also be submitted to the Bulletin if the subject is relevant for the geology of the area of primary interest. The rate of publishing is one volume per year. All articles are published as pdf-files immediately after acceptance and technical production.

Scientific editing and reviewing are done on an unpaid collegial basis; technical production expenses are covered by the membership fees.

The bulletin is freely accessible on the web page of the Geological Society of Denmark: www.2dgf.dk/publikationer/bulletin/index.html

---

Cover photo: Cambrian molluscs or mollusc-like fossils from the Henson Gletscher Formation, Peary Land, North Greenland. See this volume pp. 69–104: Peel, J.: Middle Cambrian (Miaolingian Series, Wuliuan Stage) molluscs and mollusc-like microfossils from North Greenland (Laurentia).

Vertebral size ratios and the ichthyosaurian vertebral column – a case study based on Late Jurassic fossils from North-East Greenland

THOMAS BANG HOLM, LENE LIEBE DELSETT & PETER ALSEN

Geological Society of Denmark
https://2dgf.dk

Received 15 December 2020
Accepted in revised form
31 January 2022
Published online
31 January 2022

Holm, T.B., Delsett, L.L. & Alsen, P. 2022. Vertebral size ratios and the ichthyosaurian vertebral column – a case study based on Late Jurassic fossils from North-East Greenland. Bulletin of the Geological Society of Denmark, Vol. 70, pp. 1–17. ISSN 2245-7070. https://doi.org/10.37570/bgsd-2022-70-01

Vertebral centra are some of the most common fossils from ichthyosaurs and thus valuable for understanding these marine reptiles. This study sets out to provide further information on the dimensional ratios of centra and how these might be used to obtain more information about an assemblage of Late Jurassic disarticulated centra found at Kingofjeldet on Kuhn Ø in North-East Greenland in 2017. The centra are used to test whether vertebral ratios (H:W and H:L) can be used to assign disarticulated and possibly weathered centra to a region in the vertebral column. In order to evaluate this, the ratios of the centra from Greenland were compared with those of five articulated and well-known ophthalmosaurid specimens, as well as classical traits based on morphology. Assigning the correct position in the vertebral column from ratios is, however, not straightforward. Firstly, comparing different ichthyosaur taxa gives different possible positions for the disarticulated centra. Secondly, centra from different vertebral regions commonly display similar ratios. Thirdly, ratios are sensitive to alteration by taphonomic processes. The ratios of the centra hints towards an ichthyosaur with a more regionalised vertebral column being present in the Late Jurassic sea of North-East Greenland. Further studies are needed to improve our understanding of the significance of the degree of regionalisation of the vertebral column among ichthyosaurs.

Keywords: Ichthyosaur, vertebrae, ratios, morphology, vertebral regionalisation, Ugpik Ravine Member, Kuhn Ø, Greenland.

Thomas Bang Holm [tholm@snm.ku.dk], Natural History Museum of Denmark, University of Copenhagen, Gothersgade 130, DK-1123 Copenhagen K, Denmark. Lene Liebe Delsett [DelsettL@si.edu], Department of Paleobiology, National Museum of Natural History, Smithsonian Institution, 1000 Madison Drive NW Washington, DC-20560, USA. Peter Alsen [pal@geus.dk], Geological Survey of Denmark and Greenland, Øster Voldgade 10, DK-1350 Copenhagen K, Denmark.

Ichthyosaurs first appeared during the Early Triassic (Olenekian) and existed until the early Late Cretaceous (Cenomanian), becoming one of the most successful groups of Mesozoic marine reptiles (Bardet 1992; Motani 2009; Motani *et al*. 2015; Jiang *et al*. 2016). Derived taxa were the first air-breathing vertebrates to adapt to a fully pelagic lifestyle, by developing fish-shaped bodies with a stiff trunk, a flexible tail with a vertical half-moon-shaped caudal fin and flipper-like front- and hind-limbs (Sander 2000; Buchholtz 2001; Motani 2005; Massare *et al*. 2006). Ichthyosaurs had a global distribution (Fernández & Maxwell 2012; Zammit 2012; Druckenmiller & Maxwell 2013; Delsett *et al*. 2017; Prasad *et al*. 2017). However, material from the world's largest island, Greenland, is scarce, hampering the understanding of palaeobiogeography and taxonomic relationships in northern latitudes (Marzola *et al*. 2018; Delsett & Alsen 2020). Newly described vertebrae from Late Jurassic ichthyosaurs from Kingofjeldet of North-East Greenland might answer these questions, but it has so far not been possible, as the assemblage only comprise vertebral centra (Delsett & Alsen 2020).

The robust vertebral centra are among the most

common fossil remains of ichthyosaurs, as they have a high preservation potential (McGowan & Motani 2003). Therefore, developing an understanding of vertebral centra and their usage in the studies of ichthyosaurs is of great interest and will allow more to be deduced about this group. Previous studies have used vertebral centra and the pattern of their changing dimensions along the vertebral column to describe ichthyosaurs and infer swimming style as well as possible taxonomic, intraspecific and/or ontogenetic variability (Buchholtz 2001; Massare *et al.* 2006; Fischer *et al.* 2012; Zammit *et al.* 2014; Delsett *et al.* 2017; Vakil *et al.* 2020). Many of the studies used relatively complete and articulated specimens, which are quite rare. It is far more common to find vertebrae isolated and/or disarticulated, such as the assemblage from Kingofjeldet, which is the focus in this study. Due to the high occurrence of isolated and/or disarticulated vertebrae, studies on these are also relevant and broadly applicable.

To effectively study the vertebral column of ichthyosaurs, the centra must be appropriately aligned along the vertebral column in their original positions. Normally, disarticulated vertebral centra from ichthyosaurs are assigned a position in the vertebral column (henceforth referred to as PVC) based on their morphology, which varies from region to region (McGowan & Motani 2003). Especially the position and appearance of the rib-facets on the lateral surfaces of the centra are used (Buchholtz 2001; McGowan & Motani 2003; Massare *et al.* 2006). Among many ichthyosaur taxa, the ratios of vertebral centra (dorsoventral height:mediolateral width and height:anteroposterior length) also vary considerably through the vertebral column (Buchholtz 2001). This provides the possibility of using the ratios of disarticulated centra to help assign them PVCs. A method based on vertebral ratios will provide a quantitative method for assigning PVCs and it will help narrowing down the possible PVCs of a disarticulated vertebra. This will especially be of great use when having to assign PVCs to weathered or broken centra, missing their rib facets and other morphological features, or to centra with anomalously positioned rib-facets (e.g., Vakil *et al.* 2020). Correct positioning of such centra will allow for a larger number of centra being used to reconstruct the ichthyosaurian vertebral column and provide further knowledge of anatomy, locomotion and possibly taxonomic, intraspecific and/or ontogenetic variability.

This study uses the disarticulated Kingofjeldet centra as a case study to test and discuss the efficiency of the method of using ratios of ichthyosaur centra to assign PVCs to isolated, disarticulated vertebrae. Furthermore, the ratio method will be compared with the classical method of using morphological features such as rib-facets. Therefore, this study serves to fill some of the gaps still present in our knowledge of how vertebrae can be used to study ichthyosaurs. The results will also be used to discuss vertebral anatomy and the possible taxonomy of the Kingofjeldet centra, thereby improving our poor understanding of ichthyosaurs from this region.

Geological setting and location

The assemblage of fossil vertebrae studied herein was collected from a stratigraphic level close to the base of the Ugpik Ravine Member (Bernbjerg Formation) on Kingofjeldet, Kuhn Ø, North-East Greenland (Figs 1–2). Kuhn Ø is situated in the northern part of the Wollaston Forland area and the associated Wollaston Forland Basin in North-East Greenland (Fig. 1a; Maync 1947; Surlyk 1977; Alsgaard *et al.* 2003). The Wollaston Forland Basin stretches from Hochstetter Forland in the north to Clavering Ø in the south.

The Wollaston Forland Basin is part of the late Palaeozoic to Mesozoic, East Greenlandic rift-basin complex, which was formed prior to and during the opening of the Atlantic, where Greenland and Norway ended up drifting apart (Surlyk 2003). During the Mesozoic, the area was situated at 45–50°N, at the western margin of a 500 km wide and 2000 km long epicontinental sea between Greenland and Norway (Surlyk 2003). The Wollaston Forland Basin was formed in the Middle Jurassic. Subsidence of the area resulted in marine transgression of the basement rocks (Surlyk 2003). Faulting during the Middle Jurassic to the earliest Cretaceous rifting resulted in the fragmentation of the Wollaston Forland – Kuhn Ø block that was divided into several smaller blocks (Surlyk 2003). Individual blocks rotated with a general dip in a W–SW-direction, forming several half grabens in the area (Alsgaard *et al.* 2003; Surlyk 2003). The whole Wollaston Forland area was covered by the sea from the Middle to Late Jurassic due to repeated transgressions (Surlyk 1977).

On Kuhn Ø, the Middle Jurassic Pelion Formation is resting directly on crystalline basement. The Pelion Formation is overlain by the Payerdal Formation, which is overlain by the Upper Jurassic Bernbjerg Formation. Only the lower sandy and grey mudstone-dominated Ugpik Ravine Member of the latter formation is preserved at the studied locality at Kingofjeldet, where the sedimentary succession is unconformably overlain by plateau basalts (Fig. 1b; Maync 1947). The Ugpik Ravine Member is sand-dominated at the base and becomes upwards progressively more fine-

grained and is dominated by laminated mudstones at the top (Maync 1947; Surlyk 1977). Therefore, the Ugpik Ravine Member represents a transition from the shoreface/shelf sandstone of the underlying Payer Dal Formation to the black, offshore mudstones of the Bernbjerg Formation. The Ugpik Ravine Member is approximately 43 m thick at Kingofjeldet (Maync 1947). At Kingofjeldet, the Ugpik Ravine Member consists of seven sandy, heterolithic coarsening-upward cycles, which are 5–14 m thick, each representing a shallowing upward cycle from an offshore environment to a shoreface environment (Fig. 2; Alsgaard *et al*. 2003). The cycles are separated from each other by transgressive erosion surfaces and sometimes layers of belemnite-breccia (Maync 1947; Alsgaard *et al*. 2003).

The ichthyosaur vertebrae are assumed to be

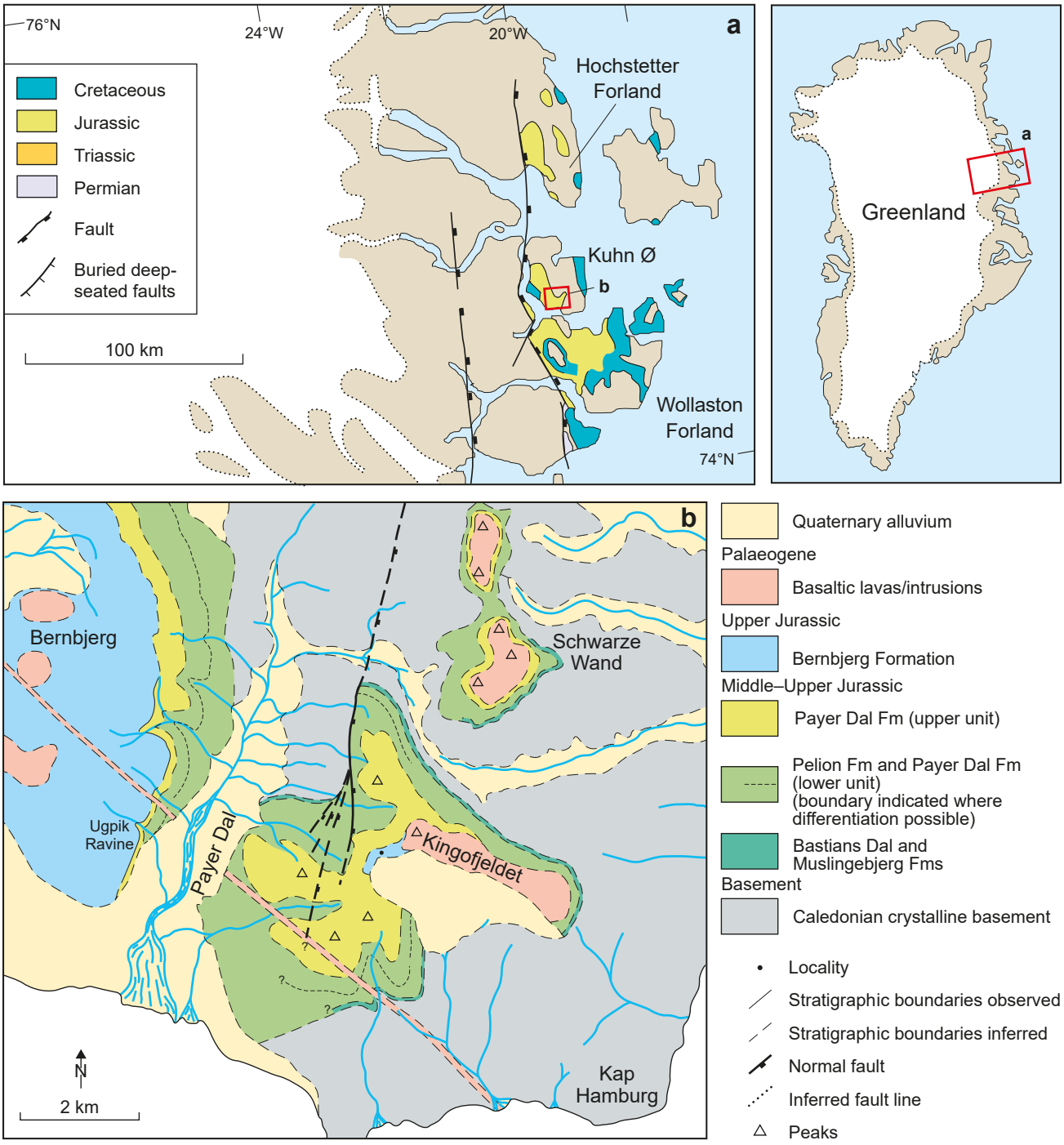

Fig. 1. a: Simplified geological map of the Kuhn Ø region in North-East Greenland. **b:** A more detailed geological map of the study area around Kingofjeldet. Modified from Alsgaard *et al*. (2003).

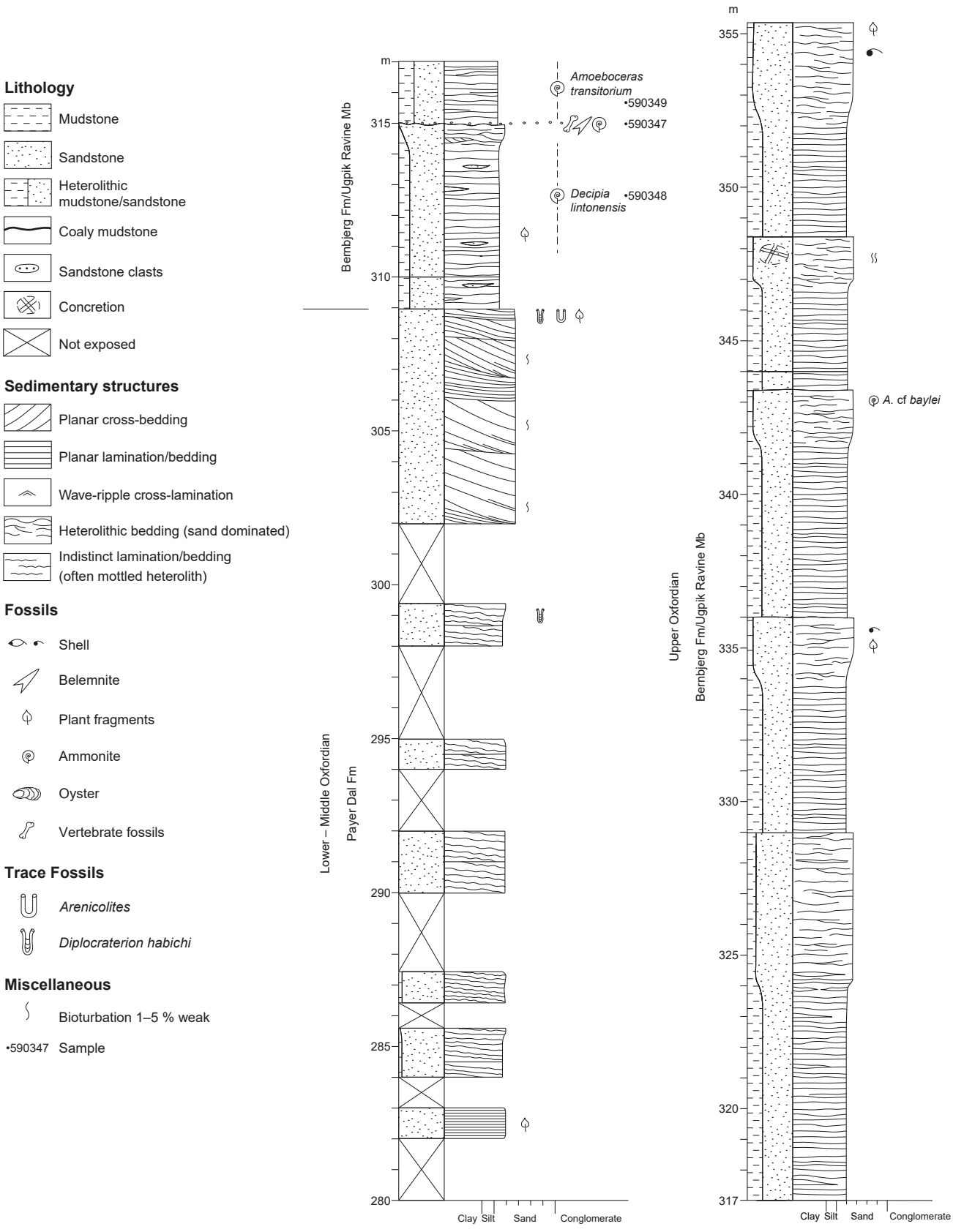

Fig. 2. Sedimentological log of the Payer Dal Formation and Bernbjerg Formation/Ugpik Ravine Member at Kingofjeldet on Kuhn Ø. The stratigraphic level yielding the fossil assemblage (GEUS 590347) is marked. The log was measured by Henrik Vosgerau in 1994.

from one of these shallow-marine, reworked layers (belemnite-breccia), as they were found together with an abundance of belemnites. The age of the fossil assemblage has been estimated to late Oxfordian based on the presence of the ammonites *Decipia lintonensis* (found as an imprint a few metres above the base of the unit) and *Amoeboceras transitorium* (found together with the fossil vertebrae; Delsett & Alsen 2020). These species are indicative of the Ilovaiskii subzone of the Glosense Zone (Callomon & Birkelund 1980).

Materials and methods

The vertebrae described by Delsett & Alsen (2020) were found on a weathered surface at Kingofjeldet on Kuhn Ø, North-East Greenland. They are all assumed to be from the same level in the succession and therefore of the same age (late Oxfordian; Delsett & Alsen 2020). A few of the centra were found embedded in the deposits, whereas most have been exposed to weathering. Several of the centra only consist of smaller fragments, in seven cases successfully pieced together to complete centra. The assemblage was given the sample number GEUS 590347 and the individual centra were given sub-numbers 1–72. However, illustrated fossils will have their repository at the type collections of the Natural History Museum of Denmark (NHMD) and are therefore assigned NHMD numbers as well (Table 1). The centra are referred to as the Kingofjeldet centra.

The aim of this study is to assign a PVC to each of the centra based on their ratios, in order to evaluate whether this is a reliable method. As the Kingofjeldet centra are all disarticulated, their ratios will be compared with those of centra belonging to articulated ichthyosaur specimens, whose ratios and PVCs are known from the literature. Each Kingofjeldet centrum will be tentatively assigned to a PVC, based on their similarity to ratios of the articulated ichthyosaurs. These PVCs will be compared with the PVCs indicated by the morphological features of the Kingofjeldet centra, based on criteria outlined below. Thus, PVCs obtained from morphology are used to evaluate the PVCs obtained from dimensional ratios. Based on previous studies (Buchholtz 2001; McGowan & Motani

Table 1. Measurements, ratios and positions of the Kingofjeldet centra

GEUS no	NHMD no	Height	Width	Dorsal length	Ventral length	Mean length	H:W	H:L	PVC morphology
590347-01	657919	58.45	65.23	29.02	28.56	28.79	0.90	2.03	Cervical
590347-02	608564	46.82	46.40	17.46	18.19	17.83	1.01	2.63	Cervical
590347-03		33.78	34.58	13.46	11.38	12.42	0.98	2.72	Cervical
590347-05		68.03	61.85	28.18	28.33	28.26	1.10	2.41	Cervical
590347-06	608565	46.39	48.28	22.40	19.02	20.71	0.96	2.24	Cervical
590347-07	657920	44.72	46.89	17.16	18.68	17.92	0.95	2.50	Posterior dorsal
590347-08		30.12	32.36	11.85	13.32	12.59	0.93	2.39	Cervical
590347-09		38.56	41.53	13.97	17.26	15.62	0.93	2.47	Cervical
590347-10	657921	50.59	52.00	11.68	13.42	12.55	0.97	4.03	Preflexural caudal
590347-11		46.11	43.20	18.05	17.99	18.02	1.07	2.56	Posterior dorsal/ prefexural caudal
590347-12	657922	44.54	47.04	14.55	15.11	14.83	0.95	3.00	Preflexural caudal
590347-13		29.19	32.98	11.50	12.02	11.76	0.89	2.48	Cervical
590347-14	657923	32.51	38.11	10.19	10.11	10.15	0.85	3.20	Preflexural caudal
590347-15		48.92	47.96	15.31	16.02	15.67	1.02	3.12	Preflexural caudal
590347-16	657924	23.10	35.66	13.92	12.96	13.44	0.65	1.72	Preflexural caudal
590347-17	608566	71.28	75.73	29.50	28.13	28.82	0.94	2.47	Preflexural caudal
590347-18		49.32	52.27	14.60	16.11	15.36	0.94	3.21	Preflexural caudal
590347-19		32.79	32.63	10.47	11.26	10.87	1,00	3.02	Preflexural caudal
590347-20		38.27	44.13	15.50	16.17	15.84	0.87	2.42	Preflexural caudal
590347-21	657925	46.66	52.14	16.73	17.72	17.23	0.89	2.71	Preflexural caudal
590347-22	657926	38.06	39.83	12.91	13.92	13.42	0.96	2.84	Posterior dorsal/ preflexural caudal
590347-23	608567	35.72	42.42	13.23	13.31	13.27	0.84	2.69	Preflexural caudal
590347-24	657927	20.71	18.31		11.72	11.72	1.13	1.77	Postflexural caudal
590347-25		23.63	22.01	12.62	12.25	12.44	1.07	1.90	Postflexural caudal

Measurements are in mm, and the positions in the vertebral column (PVC) are based on morphology.

2003), the morphology of the Kingofjeldet centra are assumed to give a good indication of where in the vertebral column the centra were actually placed, which is referred to as the correct PVC. If the two methods yield the same PVC, it could indicate that ratios are a good indicator of the PVCs of the centra.

Different terminologies have been used to subdivide the ichthyosaurian vertebral column into different regions (Fig. 3; Kirton 1983; Buchholtz 2001; McGowan & Motani 2003). In this study, the vertebral column of ichthyosaurs will be divided into five different regions: cervical, anterior dorsal, posterior dorsal, preflexural caudal (tail stock) and postflexural caudal (fluke; Fig. 3). The two latter regions are often combined into the caudal region. It is not possible to define sharp boundaries between the different regions, as the transition from one region to another and the change in centrum morphology happen gradually (McGowan & Motani 2003). A method of using the morphology of vertebral centra to assign disarticulated vertebrae to one of the vertebral regions have been well-known for a long time and thoroughly described by for example Buchholtz (2001) and McGowan & Motani (2003). The following criteria for morphology are commonly used:

- Cervical centra: two rib facets (diapophysis and parapophysis) sit dorsally high on each lateral surface with the diapophyses being confluent with the neural arch facets and the parapophyses positioned further ventrally. Some of these centra have a ventral keel, giving them a pentagonal/heart shape in ante-

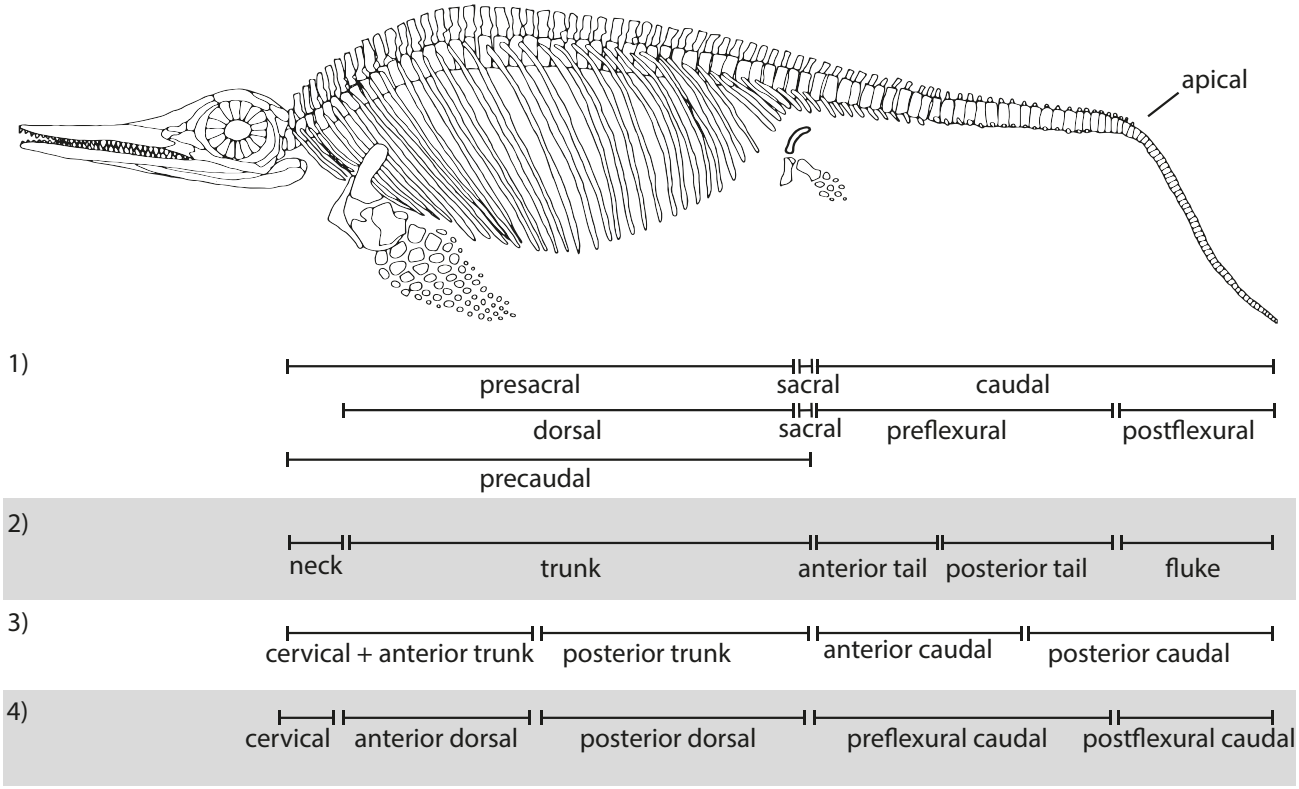

Fig. 3. Summary of the different terminologies used for subdivision of the ichthyosaurian vertebral column. Several of these definitions are sometimes used in other combinations. 1) McGowan & Motani 2003. Presacral vertebrae = from the atlas to the centrum at the distal end of the ilium. Dorsal = presacral vertebrae posterior to the level of the anterior margin of the pectoral girdle. Preflexural = caudal vertebrae anterior to apex of tailbend. Postflexural = posterior to apex of tailbend. Precaudal is used for the combination of presacral and sacral vertebrae. 2) Buchholtz 2001. Trunk = starts at the rapid increase in centrum width and height and includes the sacral vertebrae at the approximate location of the pelvis or where the ribs are rapidly decreasing in length. Anterior tail = the highest and widest centra, nearly round in cross section. Posterior tail = height decreases abruptly into dorsoventrally compressed centra with greater relative length. Fluke = starts at the change into laterally compressed centra. 3) Kirton 1983. No clear separation between cervical and anterior trunk vertebrae. Division between anterior and posterior trunk vertebrae is where the neural arch facet loses contact with the diapophysis. The anteriormost caudal vertebra is the one where the diapophysis and parapophysis merge to form a single rib facet and is associated with a sudden increase in centrum height. Posterior caudal vertebrae are small, slightly laterally compressed. 4) The subdivision of the ichthyosaurian vertebral column used in this study. See main text for explanations of the different regions.

rior and posterior view (Buchholtz 2001; McGowan & Motani 2003).

- Anterior dorsal centra: the rib facets are placed in an increasingly ventral position on the lateral surfaces in more posteriorly placed vertebrae, resulting in the diapophyses losing contact with the neural arch facets and the centra are generally round in anterior and posterior view (Buchholtz 2001; McGowan & Motani 2003).
- Posterior dorsal centra: the rib facets are positioned on the ventral half of the lateral surfaces and the centra are round in anterior and posterior view (Buchholtz 2001; McGowan & Motani 2003).
- Preflexural caudal centra: only one rib facet (apophysis) found on the ventral half of each lateral surface and the centra are very disc-shaped and increasingly dorsoventrally compressed in the posterior part of this region (Buchholtz 2001; McGowan & Motani 2003).
- Postflexural caudal centra: these are positioned posterior to the tail bend and are typically laterally compressed with no rib facets (Buchholtz 2001; McGowan & Motani 2003).

The dimensions of the Kingofjeldet centra were measured with a digital caliper. Width, height as well as dorsal and ventral length were measured for each centrum, if allowed by their preservational state. Centrum width (W) was measured as the maximum mediolateral width without rib facets. Centrum height (H) was measured as the maximum dorsoventral height without diapophyses and neural arch facets. The dorsal length (DL) was measured as the maximum dorsal anteroposterior length and always within the mediolateral extent of the pit of the neural canal. The ventral length (VL) was measured as the maximum ventral anteroposterior length. Mean lengths (L) of the centra were calculated from the dorsal length and ventral length measurements. From the measurements, H:W and H:L ratios were calculated.

In order to assign PVCs, the ratios of the Kingofjeldet centra were compared with the ratios of centra from five well-known Late Jurassic/Cretaceous ichthyosaur specimens, which have larger parts of their vertebral column preserved. As these specimens are more or less articulated, the correct PVCs of their centra are known. *Keilhauia nui* (PMO 222.655) consists of an articulated, partial skeleton with dorsal and preflexural caudal vertebrae preserved (Delsett *et al.* 2017). Zverkov & Prilepskaya (2019) considered *Keilhauia nui* a *nomen dubium*, referring it to *Arthropterygius* instead. The necessary H:W and H:L ratios were provided for five dorsal vertebrae and 20 preflexural caudal vertebrae (Delsett *et al.* 2017). H:W and H:L ratios were read from a plot (Delsett *et al.* 2017, fig. 6) with a margin of error of ±0.05. *Ophthalmosaurus icenicus* (PMAG R340) consists of a nearly complete skeleton with 101 vertebrae running continuously from the atlas to the mid of the postflexural caudal region (Buchholtz 2001). The necessary H:W and H:L ratios were provided for nine cervical, 27 dorsal, 36 preflexural caudal and 25 postflexural caudal vertebrae (Buchholtz 2001). H:W and H:L ratios were read from a plot (Buchholtz 2001, fig. 4A) with a margin of error of ±0.01. *Ophthalmosaurus natans* (UW 24205 and UW 34786) consists of a composite vertebral column going from the cervical region to the postflexural caudal region (Massare *et al.* 2006). The necessary H, W and L measurements needed for H:W and H:L ratios were provided for ≈ nine cervical, ≈ 25 dorsal and 34 preflexural caudal vertebrae (Massare *et al.* 2006). H, W and L measurements were read from a plot (Massare *et al.* 2006, fig. 3A) with a margin of error of ±1 mm. *Platypterygius americanus* (UW 5547) consists of a partially complete skeleton with 65 centra, the anterior dorsal region being partially disarticulated and with some of the mid-dorsal region missing (Maxwell & Kear 2010). The necessary H, W and L measurements needed for H:W and H:L ratios were provided for 16 cervical, 14 dorsal and 35 preflexural caudal vertebrae (Maxwell & Kear 2010). H, W and L measurements were read from a plot (Maxwell & Kear 2010, fig. 3A) with a margin of error of ±0.5 mm. *Sveltonectes insolitus* (IRSNB R269) consists of a nearly complete skeleton with a discontinuous series of 76 vertebrae (Fischer *et al.* 2011). The necessary H:W and H:L ratios were provided for 23 cervical, 16 dorsal, 22 preflexural caudal and 11 postflexural caudal vertebrae (Fischer *et al.* 2011). H:W and H:L ratios were read from a plot (Fischer *et al.* 2011, fig. 3A) with a margin of error of ±0.05. The measurements shown on plots were more precisely read with the described margins of errors by adding additional gridlines to the plots.

Comparisons of ratios with the Kingofjeldet centra were carried out by making bivariate plots of ratios in the statistical software PAST (version 4.03; Hammer *et al.* (2001)). The bivariate plots show the distribution of the centra from the different regions of the vertebral column of the known ichthyosaur specimens based on their ratios (H:W and H:L), together with the ratios of the Kingofjeldet material. Convex hulls in the bivariate plots each represent a vertebral region of the known ichthyosaur specimen and contains all H:W/H:L ratio pairs for the centra of that particular region. For each bivariate plot, a PVC for each Kingofjeldet centrum was assigned based on a qualitative assessment of which region-field its ratios most closely resembled. Close resemblance was considered to be the case if the ratios of a Kingofjeldet centrum were within the convex hull of a certain region. If the ratios of a

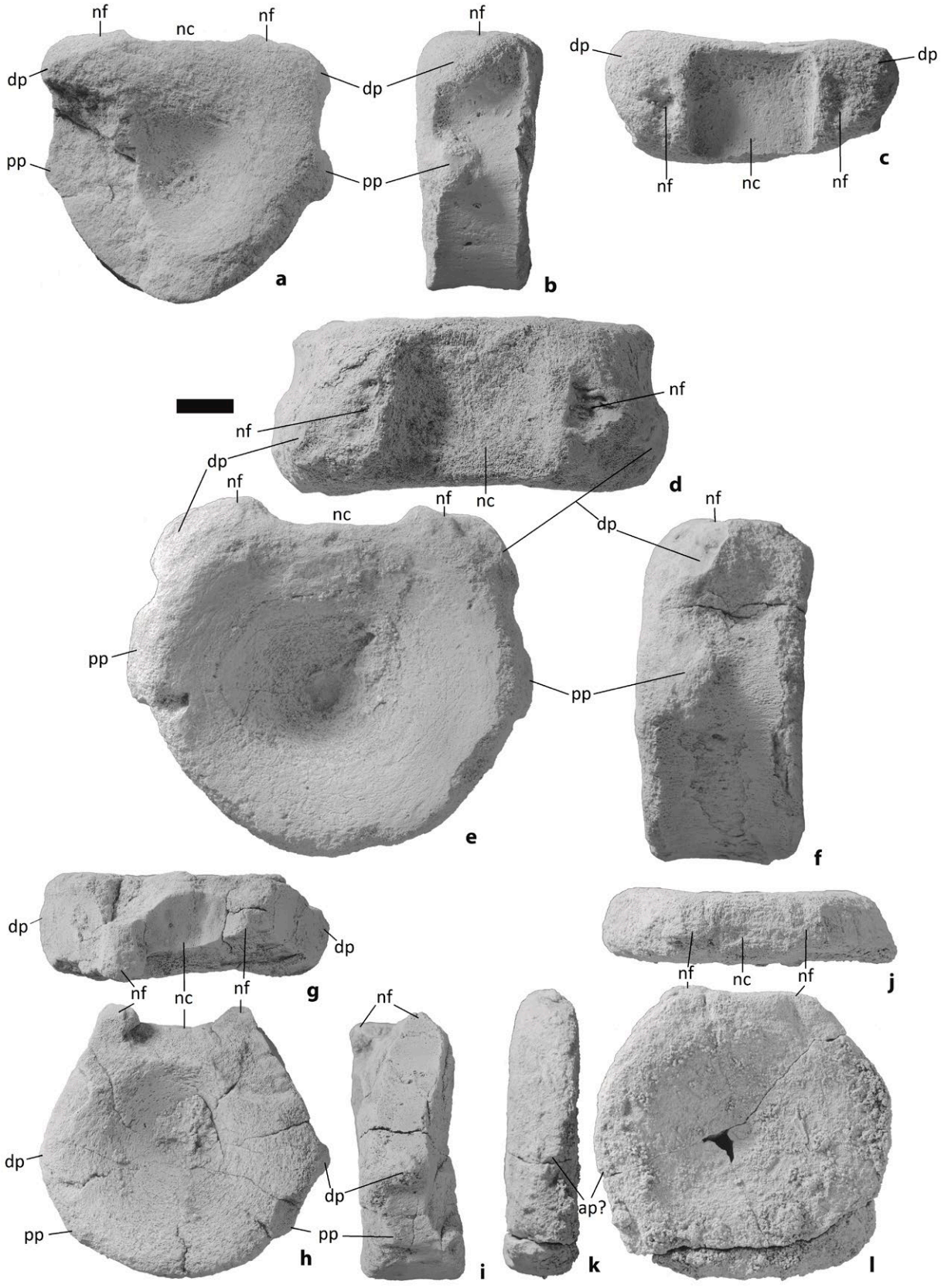

Fig. 4. Selected vertebral centra of GEUS 590347, coated with ammonium chloride. NHMD 608565 (cervical) in anterior **(a)**, left lateral **(b)** and dorsal **(c)** view. NHMD 657919 (cervical) in dorsal **(d)**, anterior **(e)** and left lateral **(f)** view. NHMD 657920 (posterior dorsal) in dorsal **(g)**, anterior/posterior? **(h)** and lateral **(i)** view. NHMD 657921 (preflexural caudal) in dorsal **(j)**, lateral **(k)** and anterior/posterior? **(l)** view. Scale bar is 1 cm. ap: apophysis, dp: diapophysis, nf: neural arch facet, nc: neural canal, pp: parapophysis.

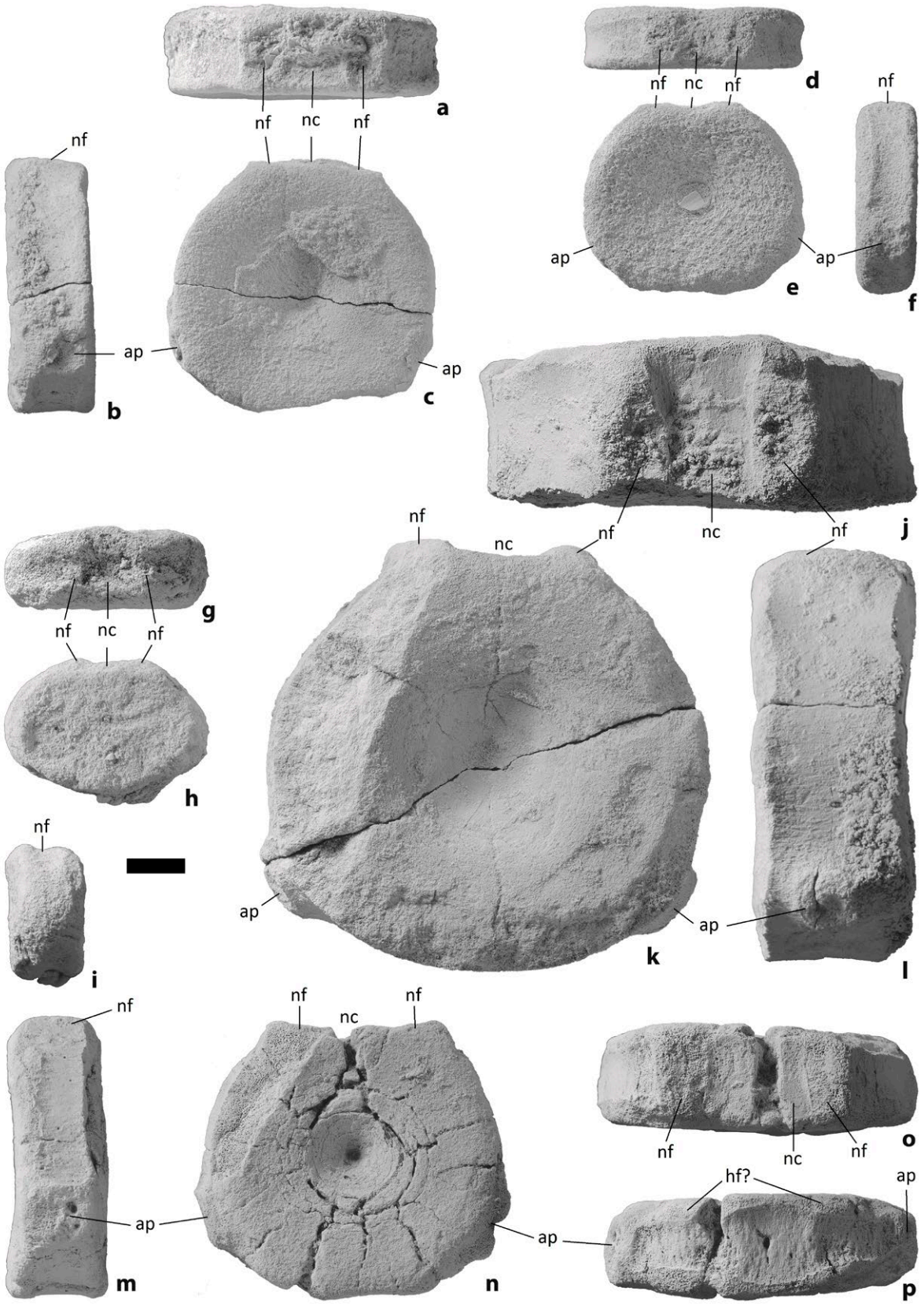

Fig. 5. Selected vertebral centra of GEUS 590347, coated with ammonium chloride. NHMD 657922 (preflexural caudal) in dorsal **(a)**, lateral **(b)** and anterior/posterior? **(c)** view. NHMD 657923 (preflexural caudal) in dorsal **(d)**, anterior/posterior? **(e)** and lateral **(f)** view. NHMD 657924 (preflexural caudal) in dorsal **(g)**, anterior/posterior? **(h)** and lateral **(i)** view. NHMD 608566 (preflexural caudal) in dorsal **(j)**, anterior/posterior? **(k)** and lateral **(l)** view. NHMD 657925 (preflexural caudal) in lateral **(m)**, anterior/posterior? **(n)**, dorsal **(o)** and ventral **(p)** view. Scale bar: 1 cm. ap: apophysis, hf: haemal arch facet, nf: neural arch facet, nc: neural canal.

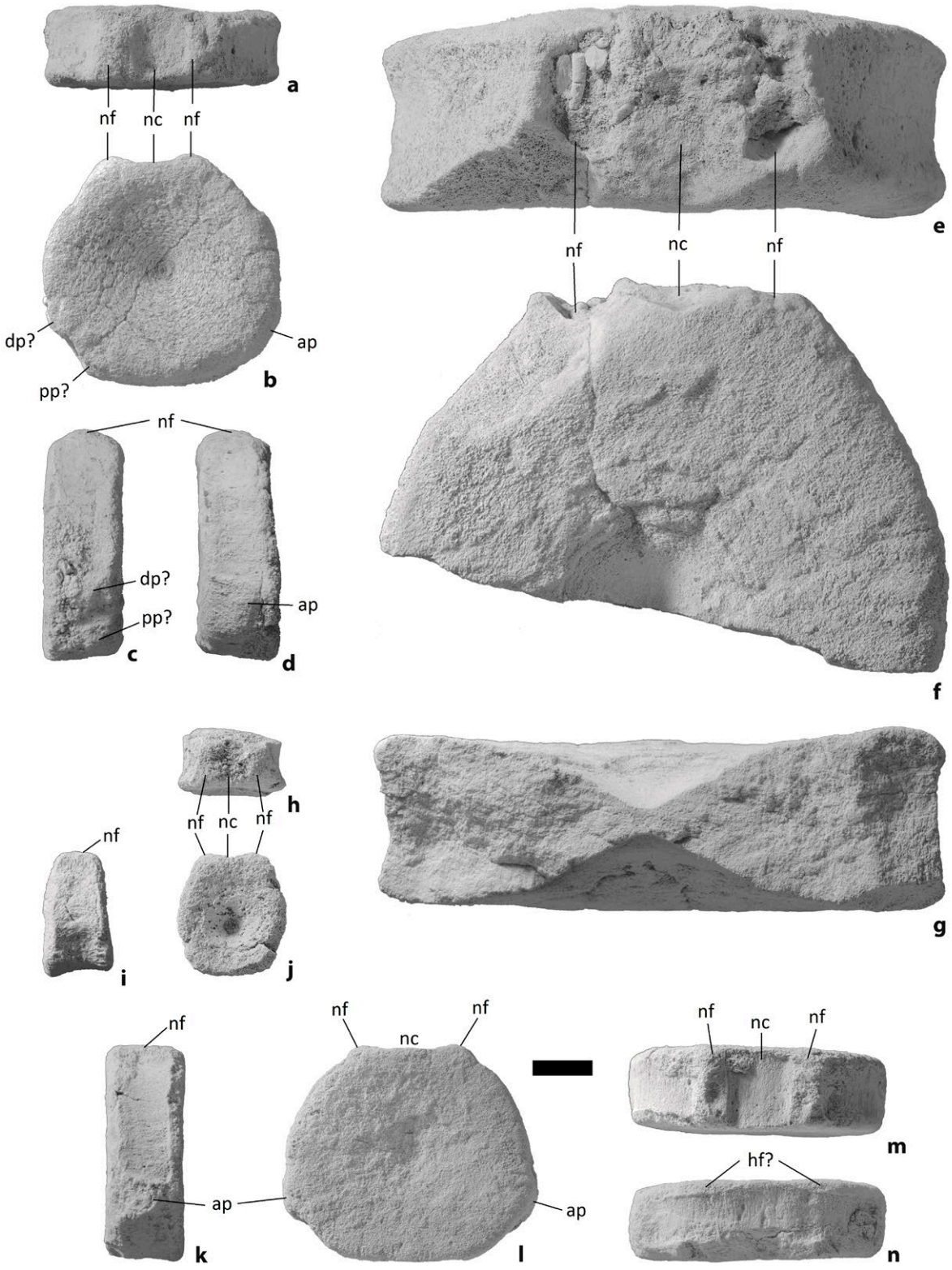

Fig. 6. Selected vertebral centra of GEUS 590347, coated with ammonium chloride. NHMD 657926 (posterior dorsal/preflexural caudal) in dorsal **(a)**, anterior/posterior? **(b)** and lateral **(c–d)** view. NHMD 657928 (preflexural caudal) in dorsal **(e)**, anterior/posterior? **(f)** and ventral **(g)** view. NHMD 657927 (postflexural caudal) in dorsal **(h)**, lateral **(i)** and anterior/posterior? **(j)** view. NHMD 608567 (preflexural caudal) in lateral **(k)**, anterior/posterior? **(l)**, dorsal **(m)** and ventral **(n)** view. Scale bar: 1 cm. ap: apophysis, dp: diapophysis, hf: haemal arch facet, nf: neural arch facet, nc: neural canal, pp: parapophysis.

Kingofjeldet centrum were outside the convex hulls of the different regions, comparison of ratios was not possible and no PVC was given based on ratios. When comparing PVCs based on ratios with the PVCs based on morphology, the two PVCs were considered to be in agreement, if they indicated the same vertebral region. The ratios of some of the Kingofjeldet centra were within the convex hull of multiple vertebral regions in the bivariate plots, indicating multiple possible PVCs for these centra. In these cases, the PVC based on ratios was considered inconclusive and could not be matched with the PVC based on morphology.

Results

Description of the fossils
Ichthyosauria *indet.* (Reptilia: Ichthyopterygia)

Referred specimens. Twenty-five complete and 44 incomplete vertebral centra (GEUS 590347-01–590347-25 and GEUS 590347-31–590347-72). Some of the better-preserved centra are illustrated in Figs 4–6. The referred specimens have previously been described by Delsett & Alsen (2020) who suggested that they represent several ichthyosaur specimens. The vertebrae likely belong to the family Ophthalmosauridae, although the material cannot be referred to this family with certainty because of the lack of skull, flipper and girdle material (Delsett & Alsen 2020). Based on this assumption the Kingofjeldet centra have been compared with centra from other ophthalmosaurids.

Taphonomy. The vertebral centra vary in preservation: some are well preserved, whereas others are weathered, broken into several pieces; and some are incomplete, missing half or more of the centrum. For some vertebrae, one or both neural arch facets have been heavily eroded. This is also the case for some rib facets on the lateral surfaces of some of the centra. Only the complete and nearly complete, three-dimensional centra (GEUS 590347-01 to 590347-25, except 590347-04) are used in the analysis and are in a suitable condition for having their height, width and length measured.

Vertebral region based on morphology. Based on the morphological features of the centra, it was possible with some certainty to assign the 24 most well-preserved specimens to regions of the vertebral column (Table 1; Buchholtz 2001; McGowan & Motani 2003). The vertebrae assigned to the cervical region possess a diapophysis positioned in the dorsal portion on the lateral surface, close to the dorsal surface of the centra. The parapophysis is situated below the diapophysis in the dorsal half (Buchholtz 2001; McGowan & Motani 2003). In some of the vertebrae, the diapophysis is clearly confluent with the neural arch facet (GEUS 590347-01, -02, -03 and -06, Fig. 4a–f), whereas this is less apparent on others due to weathering and erosion (GEUS 590347-05, -08, -09 and -13). The cervical vertebrae are approximately oval (GEUS 590347-01, -08 and -13, Fig. 4d–f) or almost heart-shaped (GEUS 590347-02, -03, -06 and -09, Fig. 4a–c) in anterior/posterior view, the heart-shape resulting from a ventral keel. The rib facets of these vertebrae tend to lie at/be confluent with the anterior margin of the lateral surface of the centrum. The posterior surface of GEUS 590347-09 is eroded to such a degree that it is no longer concave.

Only one vertebra (GEUS 590347-07, Fig. 4g-i) was confidently assigned to the posterior dorsal region based on the presence of a diapophysis in the middle of the lateral surface and the parapophysis positioned even further ventrally. It is approximately circular in anterior and posterior view (Buchholtz 2001; McGowan & Motani 2003). Due to its circular appearance in anterior and posterior view and the apparent lack of rib facets on the dorsal half of the lateral surfaces, GEUS 590347-11 might also be a posterior dorsal vertebra. Because it is heavily eroded and misses part of one lateral surface, a preflexural caudal position cannot be excluded.

The majority of the Kingofjeldet centra were assigned to the preflexural caudal region, based on the presence of only one apophysis on the ventral half of each lateral surface and the generally circular and disc-shaped appearance in anterior and posterior view, for example GEUS 590347-10, -12 and -17 (Figs 4j–l, 5a–c, 5j–l; Buchholtz 2001; McGowan & Motani 2003). Some of the centra are dorsoventrally compressed, which give them a characteristic ellipse-shaped appearance in anterior and posterior view, for example GEUS 590347-14, -16, -21 and -23 (Figs 5d–i, 5m–p, 6k–n). Some of the preflexural caudal centra (GEUS 590347-12, -16, -19, -21 and -23) have a thick anterior and posterior margin laterally on the ventral surface, which narrows anteroposteriorly in a medial direction, thereby outlining a spindle-shaped depression on the mid-ventral surface (Figs 5p, 6n). This might be haemal arch facets, as also proposed by Prasad *et al*. (2017). GEUS 590347-15 was assigned to the preflexural caudal region, in contrast to its dorsal position suggested by Delsett & Alsen (2020). In contrast to the other centra, GEUS 590347-16 is not biconcave and has a flat anterior and posterior surface, without preserved rib facets, which might be due to erosion (Fig. 5g–i). A larger, but broken preflexural caudal centrum (GEUS 590347-31, Fig. 6e–g), is also identified, without rib facets on the dorsal half. GEUS 590347-22 is identified as a preflexural caudal vertebra. However, it

might also belong to the posterior dorsal region, as one lateral surface seems to have two separate rib facets on the ventral half, whereas the other lateral surface has one elongate rib facet on the ventral half (Fig. 6a–d). The latter is possibly the result from the fusion of the diapophysis and parapophysis.

Two vertebrae (GEUS 590347-24 and -25) were assigned to the postflexural caudal region, based on their mediolaterally compressed shape in anterior and posterior view and lack of rib facets (Fig. 6h–j; Buchholtz 2001; McGowan & Motani 2003). GEUS 590347-24 is only concave on one side (Fig. 6j), the other is flattened.

Measurements, plots of ratios and positioning of centra

The height, width and length measurements of GEUS 590347-01–590347-25 are shown in Table 1 together

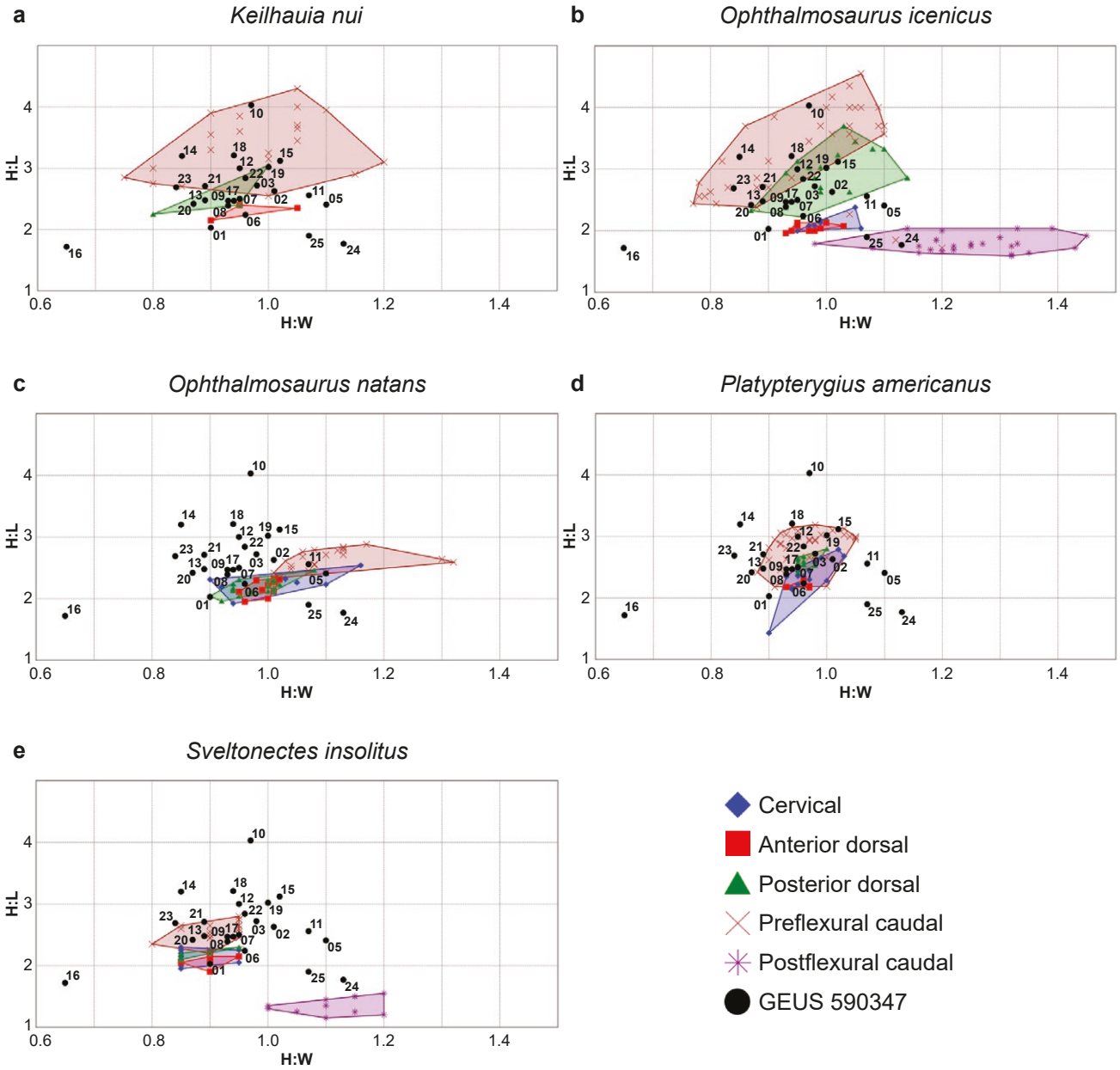

Fig. 7. Bivariate plots for comparison of ratios of vertebral centra from *Keilhauia nui* **(a)**, *Ophthalmosaurus icenicus* **(b)**, *Ophthalmosaurus natans* **(c)**, *Platypterygius americanus* **(d)** and *Sveltonectes insolitus* **(e)** with GEUS 590347. The bounded region-areas are based on ratios of vertebral centra from the known ophthalmosaurids. GEUS 590347-01–590347-25 are plotted according to their H:W and H:L ratios and have been assigned positions based on which region-field they lie within on the plots. The plots are based on data from Delsett *et al.* (2017; a), Buchholtz (2001; b), Massare *et al.* (2006; c), Maxwell & Kear (2010; d) and Fischer *et al.* (2011; e).

with the ratios (H:W and H:L). The ratios of the Kingofjeldet centra were compared with those of *K. nui*, *O. icenicus*, *O. natans*, *P. americanus* and *S. insolitus* (Fig. 7). For *O. icenicus*, a few centra plotted far away from the rest of the centra from the same region and were considered anomalous for the respective regions and therefore not included in the bounding of the different vertebral region-fields (Fig. 7b). This included a cervical vertebra, which plotted outside of the displayed ratio-intervals of Fig. 7 and three preflexural caudal vertebrae. For *O. natans*, cervical centra were included in the trunk region in Massare *et al.* (2006). It was therefore uncertain how many centra were in fact cervical centra. By comparison with the vertebral column of *O. icenicus*, which has approximately the same number of vertebrae, it was estimated that the first eight to ten centra in the vertebral column of *O. natans* are cervical centra (Fig. 7c).

The different ophthalmosaurid taxa show different ratios in the different vertebral regions, even though the ratios of the same vertebral regions in the different ophthalmosaurids to some extent overlap each other (Fig. 7). The five taxa show different degrees of overlap between the vertebral regions of its own vertebral column (Fig. 7). The vertebral regions of *O. natans*, *P. americanus* and *S. insolitus* exhibit considerable overlap, whereas the vertebral columns of *K. nui* and *O. icenicus* exhibit lesser overlap between regions. The H:L ratios of the vertebral centra of *K. nui* and *O. icenicus* become progressively higher and more extreme compared with the H:L ratios of *O. natans*, *P. americanus* and *S. insolitus* when moving posteriorly from the cervical to the preflexural caudal region (Fig. 7). The plotting of the Kingofjeldet centra show that these centra have dispersed ratios, with values and a distribution more similar to the ratios of *K. nui* and *O. icenicus* than to the ratios of *O. natans*, *P. americanus* and *S. insolitus* (Fig. 7).

The assigned PVC for each Kingofjeldet centrum based on ratios and how it compares to the PVC based on morphology can be seen in Table 2. Comparison of Kingofjeldet centrum ratios with those of *K. nui* and

Table 2. Assigned position in the vertebral column (PVC) for each vertebral centrum of GEUS 590347

GEUS no	NHMD no	*Keilhauia nui*	*Ophthalmosaurus icenicus*	*Ophthalmosaurus natans*	*Platypterygius americanus*	*Sveltonectes insolitus*	PVC (morphology)
590347-01	657919	NA	NA	PD	NA	C/AD	C
590347-02	608564	PrC	PD	NA	C/PrC	NA	C
590347-03		PrC	PD	NA	PD/PrC	NA	C
590347-05		NA	NA	C/PrC	NA	NA	C
590347-06	608565	AD	PD	C/PD	C/AD/PrC	NA	C
590347-07	657920	PD	PD	NA	C/PD/PrC	PrC	PD
590347-08		PD	PD	NA	PrC	PrC	C
590347-09		PD	PD	NA	PrC	PrC	C
590347-10	657921	PrC	PrC	NA	NA	NA	PrC
590347-11		NA	NA	PrC	NA	NA	PD/PrC
590347-12	657922	PrC	PD/PrC	NA	PrC	NA	PrC
590347-13		PD	PD/PrC	NA	PrC	PrC	C
590347-14	657923	PrC	PrC	NA	NA	NA	PrC
590347-15		PrC	PD	NA	PrC	NA	PrC
590347-16	657924	NA	NA	NA	NA	NA	PrC
590347-17	608566	PD	PD	NA	PrC	PrC	PrC
590347-18		PrC	PrC	NA	NA	NA	PrC
590347-19		PrC	PD	NA	PrC	NA	PrC
590347-20		PD	PrC	NA	NA	PrC	PrC
590347-21	657925	PrC	PrC	NA	NA	PrC	PrC
590347-22	657926	PD/PrC	PD/PrC	NA	PrC	NA	PD/PrC
590347-23	608567	NA	PrC	NA	NA	NA	PrC
590347-24	657927	NA	PoC	NA	NA	NA	PoC
590347-25		NA	PoC	NA	NA	NA	PoC

Column three to seven show the ratio-based PVCs of each centrum depending on which ophthalmosaurid they were compared with. NA marks cases where the ratios of the centrum in question did not plot within the ratios of the different vertebral regions of the ophthalmosaurid, which it was compared with. The last column shows the PVC of the centra based on their morphology.
Colours: green: PVC based on ratios matches with the PVC based on morphology, blue: PVC based on ratios does not match with the PVC based on morphology. AD: anterior dorsal, C: cervical, PD: posterior dorsal, PoC: postflexural caudal, PrC: preflexural caudal.

O. icenicus gave the highest number of PVCs agreeing with the PVCs based on morphology, which is nine and ten correctly positioned centra respectively. Some of the Kingofjeldet centra were assigned more than one possible PVC for each ophthalmosaurid they were compared with (Table 2). The analysis and bivariate plots show that when multiple PVCs are possible, it is not necessarily two adjacent regions within the vertebral column, but it might also be two non-adjacent regions (Fig. 7; Table 2). For example, four Kingofjeldet centra were assigned to a cervical position and a posterior dorsal or a preflexural caudal position when compared with either *O. natans* or *P. americanus* (Table 2). Cervical, posterior dorsal and preflexural caudal to some degree overlap with each other at lower H:L values (e.g., Fig. 7c–e). The ratio-based PVCs of each Kingofjeldet centrum also show that cervical centra (based on morphology) are often assigned a posterior dorsal or preflexural caudal position based on ratios (Table 2).

Discussion

Ratio-based positioning of the vertebral centra

Comparison with *O. icenicus* gave the highest amount of correctly positioned centra based on vertebral ratios (ten correct PVCs). That the highest amount of correctly positioned centra based on ratios represents just under half of the Kingofjeldet centra suggest that ratios cannot always be used on their own to assign centra to a vertebral region with certainty. Several factors seem to complicate the process of using vertebral centrum ratios to position disarticulated centra within the different regions of the vertebral column.

Firstly, the ratios for a certain vertebral region vary between the different ophthalmosaurid taxa to which the Kingofjeldet centra were compared. This will result in different possible PVCs for a disarticulated centrum, depending on which ophthalmosaurid it is compared with, which influences the analysis of the Kingofjeldet centra. This problem can be solved if comparisons of the ratios of disarticulated centra are restricted to centra from taxa known to have approximately the same degree of regionalisation of the vertebral column. Obviously, comparing with the same species is optimal, but when only looking at a few disarticulated centra, it is close to impossible to know the species and the degree of regionalisation. In addition, even among individuals of the same species, variation in ratios occurs within the same vertebral region, for example observed for *Acamptonectes densus* and *Platypterygius australis* (Fischer *et al*. 2012; Vakil *et al.* 2020). Such variation might represent ontogenetic stages, sexual dimorphism, intraspecific variation, or differential weathering and/or deformation of the centra.

Secondly, a gradual transition between the different vertebral regions and the lack of a unidirectional change in ratios along the vertebral column means that centra of adjacent and non-adjacent regions may have similar, overlapping ratios. This is clearly seen in Fig. 7 and is also apparent from previous studies of ichthyosaurian vertebral columns (e.g., Buchholtz 2001; McGowan & Motani 2003; Massare *et al*. 2006; Vakil *et al*. 2020). Therefore, a disarticulated centrum may be assigned to multiple regions based on its ratios, as was the case in this study. Some centra were here assigned both to the posterior dorsal and preflexural caudal regions or the cervical, posterior dorsal and/or preflexural caudal regions (Table 2). The postflexural caudal region seems to be the only clearly distinguishable region based on both ratios and morphology of the centra, for example in *O. icenicus* and *S. insolitus* (Fig. 7b, e). GEUS 590347-22 serves as an example on how difficult it can be to mark a sharp boundary between different regions based on ratios but also morphology. GEUS 590347-22 could be part of the transitional area from the posterior dorsal region to the preflexural caudal region, indicated by its ratios when compared with *K. nui* and *O. icenicus* and by its morphology. The distinction between the different regions of the vertebral column based on ratios becomes even less apparent in less regionalised ichthyosaurs. Thus, it may be even more difficult to assign a disarticulated centrum to one specific region based on its ratios when comparing it with less regionalised taxa.

Thirdly, several of the Kingofjeldet centra plotted outside of the defined regions based on the ratios of the five known ophthalmosaurids, which meant that assigning a PVC based on ratios was inconclusive (Fig. 7; Table 2). This might be a result of inadequate data for comparison caused by a relatively sparse set of measured centra from more or less articulated specimens. Inconclusive ratios can also be a result of weathering and/or deformation/compression. Such processes can alter the dimensions and ratios of the centra, causing them to plot differently than they would without being affected by these processes. The Kingofjeldet centra were found in the muddy sandstone deposits of the Ugpik Ravine Member, which might have been subject to some compression. It is common for disarticulated vertebrae to be compressed in an anteroposterior direction (e.g., Delsett *et al*. 2016), causing them to attain higher H:L ratios. Besides causing the centra to plot differently, this might also explain why so many cervical centra were identified as posterior dorsal and preflexural caudal vertebrae based on their ratios. The posterior dorsal region and

especially the preflexural caudal region tend to have higher H:L ratios than the cervical region (Fig. 7). Possible dorsoventral compression could also explain the very low H:W and H:L ratio of GEUS 590347-16, which plots far from all the other Kingofjeldet centra and the centra of the five known ophthalmosaurids.

Biological implications of the vertebral centra

Previous studies have used centrum ratios, their gradual change through the vertebral column and regionalisation as a way to distinguish between different ophthalmosaurid taxa (Massare *et al.* 2006; Maxwell & Kear 2010; Vakil *et al.* 2020). Based on the bivariate plots in this study, it is fairly easy to distinguish the more regionalised ophthalmosaurids from the less regionalised ophthalmosaurids (Fig. 7). *Keilhauia nui* and *O. icenicus* have more strongly regionalised vertebral columns (Buchholtz 2001, fig. 4A; Delsett *et al.* 2017, fig. 5) with more dispersed and less overlapping regions (Fig. 7a–b). A more complete vertebral column of *K. nui* is required to give a more precise estimate of the regionalisation of the vertebral column and the dispersal of regions within a bivariate plot. *Ophthalmosaurus natans*, *P. americanus* and *S. insolitus* show a weaker degree of regionalisation of the vertebral column (Massare *et al.* 2006, fig. 3A; Maxwell & Kear 2010, fig. 3; Fischer *et al.* 2011, fig. 3B) with less dispersed and more overlapping regions (Fig. 7c–e). Changes in H:L ratios and not H:W ratios, seem to cause the greatest variation between the different regions of the vertebral column and between the more regionalised and less regionalised ophthalmosaurids. Vakil *et al.* (2020) showed a similar importance of centrum length and used it to distinguish between different specimens of *P. australis*. H:W ratios only seem to be important in the postflexural region related to the extreme mediolateral compression of vertebrae in this region.

In this study, comparisons with less regionalised ophthalmosaurids (*O. natans*, *P. americanus* and *S. insolitus*) result in more inconclusive PVCs of the Kingofjeldet centra than comparison with the stronger regionalised ophthalmosaurids (*K. nui* and *O. icenicus*; Table 2). This is because the Kingofjeldet centra have ratios that are less similar to those of less regionalised ophthalmosaurids than to those of more regionalised ophthalmosaurids. The ratios of the Kingofjeldet centra show values and a distribution similar to the ratios of *K. nui* and *O. icenicus*. Comparison with these two taxa also resulted in the highest amounts of Kingofjeldet centra being assigned a PVC based on ratios that matched the PVC suggested by morphology (Fig. 7, Table 2). This could indicate that the Kingofjeldet centra are from an ophthalmosaurid with a more regionalised vertebral column, bearing in mind that the Kingofjeldet centra might have been subjected to taphonomic processes. As mentioned earlier, this could have slightly altered their ratios through weathering and deformation, causing some centra (e.g., GEUS 590347-10) to appear more like those from more regionalised ichthyosaurs than is the case.

Despite the clear difference between more regionalised and less regionalised ophthalmosaurids in the bivariate plots, regionalisation does not seem to bear any taxonomic signal, at least not above species level. This is indicated by the similarities between the plots of *K. nui* and *O. icenicus* (Fig. 7a–b) and the similarities between the plots of *O. natans*, *P. americanus* and *S. insolitus* (Fig. 7c–e), the only exception being the preflexural caudal region of *O. natans*. These similarities are probably a consequence of regionalisation being an adaptive trait associated with locomotion and preferred swimming style (Buchholtz 2001) and is therefore a character affected by homoplasy (Paparella *et al*. 2017).

Generally, the taxonomic value of isolated centra have been questioned (McGowan & Motani 2003; Zammit 2010). However, it is worth noting that the ratios of the Kingofjeldet centra resemble those of *O. icenicus*. Only four centra are outside the range of the ratios of *O. icenicus* (Fig. 7b) and ten out of 24 centra were correctly positioned when compared with *O. icenicus* (Table 2). The morphology of the Kingofjeldet centra also have a certain resemblance to the vertebral centra of *O. icenicus* (Moon & Kirton 2016). This is especially the case for GEUS 590347-02, -06, -12, -14, -17, -21 and -23.

Conclusion

The ratios of 24 disarticulated vertebral centra from Ugpik Ravine Member, Greenland, were compared with those of five different ophthalmosaurids and based on this the centra were assigned positions in the vertebral column (PVCs). Multiple factors complicated the assigning of the correct PVCs to the centra when only ratios were considered. Firstly, it is uncertain which ophthalmosaurid is most suitable for the comparison. Comparison with arbitrary ophthalmosaurids in this study often resulted in inconclusive PVCs. Secondly, it is possible to obtain multiple different PVCs for a centrum due to weak regionalisation of the vertebral column and/or due to gradual transitions and a lack of a unidirectional change in ratios from one vertebral region to another. Thirdly, the method is sensitive to taphonomic alterations of the ratios through weathering and/or compaction, potentially causing centra to attain anomalous ratios or ratios resembling that of centra from other vertebral regions. Postflexural caudal centra were the only centra with

ratios clearly separating them from the other regions. A prerequisite for assigning PVCs to disarticulated centra based on their ratios, is that they belong to an ichthyosaur with a relatively regionalised vertebral column, which seems to be the case for the Kingofjeldet centra, bearing in mind potential diagenetic alterations of ratios. If the vertebral column is only weakly regionalised, it becomes difficult to place the centra and it will be more precise to use morphology. In conclusion, effective positioning of centra based on their ratios requires strongly regionalised vertebral columns where the ratios of the different regions can be clearly distinguished from each other. However, the studied ophthalmosaurids show that this is rarely the case. Yet, the pattern and difference in overlap of vertebral regions in the bivariate plots for more regionalised columns and less regionalised columns is interesting to note. More studies into these differences might help to better distinguish between more regionalised ichthyosaurs and less regionalised ones and improve our understanding of their different adaptive traits and the related locomotory importance.

Acknowledgements

Arne Thorshøj Nielsen is warmly thanked for supervision and help with formalities regarding writing the bachelor thesis upon which this study is based. GEUS supplied the material and equipment for the study. In addition, we appreciate Bent Lindow at NHMD for collection assistance and the Lethaia Foundation for sponsoring an educational visit to the Natural History Museum of Oslo and their collection of ichthyosaur material. Jørn Hurum is also thanked for giving access to the vertebrate palaeontology collection of the Natural History Museum of Oslo as well as Øyvind Hammer for evaluating the bivariate plots, Jette Halskov for drafting Figure 1 and Henrik Vosgerau for the log of the strata at Kingofjeldet. The reviewers Judy A. Massare and Benjamin P. Kear are thanked for comments that helped improve the manuscript. Finally, special thanks go to Sophie Boe Booker for reviewing the grammar of this paper.

References

Alsgaard, P.C., Felt, V.L., Vosgerau, H. & Surlyk, F. 2003: The Jurassic of Kuhn Ø, North-East Greenland. In: Ineson, J.R. & Surlyk, F. (eds): The Jurassic of Denmark and Greenland. Geological Survey of Denmark and Greenland Bulletin 1, 865–892. https://doi.org/10.34194/geusb.v1.4691

Bardet, N. 1992: Stratigraphic evidence for the extinction of the ichthyosaurs. Terra Nova 4, 649–656. https://doi.org/10.1111/j.1365-3121.1992.tb00614.x

Buchholtz, E.A. 2001: Swimming Styles in Jurassic Ichthyosaurs. Journal of Vertebrate Paleontology 21, 61–73. https://doi.org/10.1671/0272-4634(2001)021[0061:SSIJI]2.0.CO;2

Callomon, J.H. & Birkelund, T. 1980: The Jurassic transgression and the mid-late Jurassic succession in East Greenland. Geological Magazine 117, 211–226. https://doi.org/10.1017/S0016756800030442

Delsett, L.L. & Alsen, P. 2020: New marine reptile fossils from the Oxfordian (Late Jurassic) of Greenland. Geological Magazine 157, 1612–1621. https://doi.org/10.1017/S0016756819000724

Delsett, L.L., Novis, L.K., Roberts, A.J., Koevoets, M.J., Hammer, Ø., Druckenmiller, P.S. & Hurum, J.H. 2016: The Slottsmøya marine reptile *Lagerstätte*: depositional environments, taphonomy and diagenesis. In: Kear, B.P. *et al*. (eds): Mesozoic Biotas of Scandinavia and its Arctic Territories. Geological Society, London, Special Publications 434, 165–188. https://doi.org/10.1144/SP434.2

Delsett, L.L., Roberts, A.J., Druckenmiller, P.S. & Hurum, J.H. 2017: A New Ophthalmosaurid (Ichthyosauria) from Svalbard, Norway, and Evolution of the Ichthyopterygian Pelvic Girdle. PLoS ONE 12, e0169971. https://doi.org/10.1371/journal.pone.0169971

Druckenmiller, P.S. & Maxwell, E.E. 2013: A Middle Jurassic (Bajocian) ophthalmosaurid (Reptilia, Ichthyosauria) from the Tuxedni Formation, Alaska and the early diversification of the clade. Geological Magazine 151, 41–48. https://doi.org/10.1017/S0016756813000125

Fernández, M.S. & Maxwell, E.E. 2012: The genus *Arthropterygius* Maxwell (Ichthyosauria: Ophthalmosauridae) in the Late Jurassic of the Neuquén Basin, Argentina. Geobios 45, 535–540. https://doi.org/10.1016/j.geobios.2012.02.001

Fischer, V., Masure, E., Arkhangelsky, M.S. & Godefroit, P. 2011: A new Barremian (Early Cretaceous) ichthyosaur from western Russia. Journal of Vertebrate Paleontology 31, 1010–1025. https://doi.org/10.1080/02724634.2011.595464

Fischer, V., Maisch, M.W., Naish, D., Kosma, R., Liston, J., Joger, U., Krüger, F.J., Pérez, J.P., Tainsh, J., Appleby, R.M. 2012: New Ophthalmosaurid Ichthyosaurs from the European Lower Cretaceous Demonstrate Extensive Ichthyosaur Survival across the Jurassic-Cretaceous Boundary. PLoS ONE 7, e29234. https://doi.org/10.1371/journal.pone.0029234

Hammer, Ø. & Harper D.A.T. 2001: PAST: Paleontological statistics software package for education and data analysis. Palaeontologia Electronica 4, 1–9.

Jiang, D.Y., Motani, R., Huang, J.D., Tintori, A., Hu, Y.C., Rieppel, O., Fraser, N.C., Ji, C., Kelley, N.P., Fu, W.L. & Zhang, R. 2016: A large aberrant stem ichthyosauriform indicating early rise and demise of ichthyosauromorphs in the wake of the end-Permian extinction. Scientific Reports 6, 26232. https://doi.org/10.1038/srep26232

Kirton, A. M. 1983: A review of British Upper Jurassic Ich-

thyosaurs, 366 pp. Unpublished PhD thesis, University of Newcastle upon Tyne.

Marzola, M., Mateus, O., Milán, J. & Clemmensen, L.B. 2018: A review of Palaeozoic and Mesozoic tetrapods from Greenland. Bulletin of the Geological Society of Denmark 66, 21–46. https://doi.org/10.37570/bgsd-2018-66-02

Massare, J.A., Buchholtz, E.A., Kenney, J.M. & Chomat A.M. 2006: Vertebral Morphology of *Ophthalmosaurus natans* (Reptilia: Ichthyosauria) from the Jurassic Sundance Formation of Wyoming. Paludicola 5, 242–254.

Maxwell, E.E. & Kear, B.P. 2010: Postcranial Anatomy of *Platypterygius Americanus* (Reptilia: Ichthyosauria) from the Cretaceous of Wyoming. Journal of Vertebrate Paleontology 30, 1059–1068. https://doi.org/10.1080/02724634.2010.483546

Maync, W. 1947: Stratigraphie der Jurabildungen Ostgrönlands zwischen Hochstetterbugten (75°N.) und dem Kejser Franz Joseph Fjord (73°N.). Meddelelser Om Grønland 132, 1–223.

McGowan, C. & Motani, R. 2003: Ichthyopterygia. In: Sues, H.D. (eds): Handbook of Paleoherpetology, Part 8, 175 pp. Munich: Verlag Dr. Friedrich Pfeil.

Moon, B.C. & Kirton, A.M. 2016: Ichthyosaurs of the British Middle and Upper Jurassic Part 1, *Ophthalmosaurus*. Monograph of the Palaeontographical Society 170, 84 pp. https://doi.org/10.1080/02693445.2016.11963958

Motani, R. 2005: Evolution of fish-shaped reptiles (Reptilia: Ichthyopterygia) in their physical environments and constraints. Annual Review of Earth and Planetary Sciences 33, 395–420. https://doi.org/10.1146/annurev.earth.33.092203.122707

Motani, R. 2009: The evolution of marine reptiles. Evolution: Education & Outreach 2, 224–235. https://doi.org/10.1007/s12052-009-0139-y

Motani, R., Jiang, D.Y., Chen, G.B., Tintori, A., Rieppel, O., Ji, C. & Huang, J.D. 2015: A basal ichthyosauriform with a short snout from the Lower Triassic of China. Nature 517, 485–488. https://doi.org/10.1038/nature13866

Paparella, I., Maxwell, E.E., Cipriani, A., Roncacé, S. & Caldwell, M.W. 2017: The first ophthalmosaurid ichthyosaur from the Upper Jurassic of the Umbrian–Marchean Apennines (Marche, Central Italy). Geological Magazine 154, 837–858. https://doi.org/10.1017/S0016756816000455

Prasad, G.V.R., Pandey, D.K., Alberti, M., Fürsich, F.T., Thakkar, M.G. & Chauhan, G.D. 2017: Discovery of the first ichthyosaur from the Jurassic of India: Implications for Gondwanan palaeobiogeography. PloS ONE 12, e0185851. https://doi.org/10.1371/journal.pone.0185851

Sander, P.M. 2000: Ichthyosauria: their diversity, distribution, and phylogeny. Paläontologische Zeitschrift 74, 1–35. https://doi.org/10.1007/BF02987949

Surlyk, F. 1977: Stratigraphy, tectonics and palaeogeography of the Jurassic sediments of the areas north of Kong Oscars Fjord, East Greenland. Geology of Greenland Survey Bulletin 123, 56 pp. https://doi.org/10.34194/bullggu.v123.6665

Surlyk, F. 2003: The Jurassic of East Greenland: a sedimentary record of thermal subsidence, onset and culmination of rifting. In: Ineson, J.R. & Surlyk, F. (eds): The Jurassic of Denmark and Greenland. Geological Survey of Denmark and Greenland Bulletin 1, 659–722. https://doi.org/10.34194/geusb.v1.4674

Vakil, V., Webb, G.E. & Cook, A.G. 2020: Can vertebral remains differentiate more than one species of Australian Cretaceous ichthyosaur? Alcheringa: An Australasian Journal of Palaeontology 44, 537–554. https://doi.org/10.1080/03115518.2020.1853809

Zammit, M. 2010: A review of Australasian ichthyosaurs. Alcheringa 34, 281–292. https://doi.org/10.1080/03115511003663939

Zammit, M. 2012: Cretaceous Ichthyosaurs: Dwindling Diversity, or the Empire Strikes Back. Geosciences 2, 11–24. https://doi.org/10.3390/geosciences2020011

Zammit, M., Kear, B.P. & Norris, R.M. 2014: Locomotory capabilities in the Early Cretaceous ichthyosaur *Platypterygius australis* based on osteological comparisons with extant marine mammals. Geological Magazine 151, 87–99. https://doi.org/10.1017/S0016756813000782

Zverkov, N.G. & Prilepskaya, N.E. 2019: A prevalence of *Arthropterygius* (Ichthyosauria: Ophthalmosauridae) in the Late Jurassic–earliest Cretaceous of the Boreal Realm. PeerJ 7, e6799. https://doi.org/10.7717/peerj.6799

New record of the genus *Ptychodus* Agassiz, 1834, (Chondrichthyes, Elasmobranchii) from the Upper Cretaceous of Bornholm (Denmark)

IBAN GOÑI & GILLES CUNY

Geological Society of Denmark
https://2dgf.dk

Received 12 July 2021
Accepted in revised form
25 January 2022
Published online
3 March 2022

Goñi, I & Cuny, G. 2022. New record of the genus *Ptychodus* Agassiz, 1834, (Chondrichthyes, Elasmobranchii) from the Upper Cretaceous of Bornholm (Denmark). Bulletin of the Geological Society of Denmark, Vol. 70, pp. 19–25. ISSN 2245-7070. https://doi.org/10.37570/bgsd-2022-70-02

Nine shark teeth were collected at Arnager in the south-western part of the island of Bornholm (Baltic Sea, Denmark). They all come from the basal conglomerate of the Coniacian (Upper Cretaceous) Arnager Limestone Formation and belong to the genus *Ptychodus* Agassiz, 1834. Three different species are identified: *P. altior*, *P. latissimus* and *P. mammillaris*, which were hitherto unknown in Denmark.

Keywords: *Ptychodus*, shark tooth, Late Cretaceous, Coniacian, Bornholm, Denmark.

Iban Goñi [iban.goni@etu.univ-lyon1.fr] and Gilles Cuny [gilles.cuny@univ-lyon1.fr], both Univ Lyon, Université Claude Bernard Lyon 1, CNRS, ENTPE, UMR 5023 LEHNA, F-69622 Villeurbanne, France.

Nine shark teeth belonging to the genus *Ptychodus* Agassiz, 1834 (see Giusberti *et al.* 2018; Brignon 2019) were collected by three amateur palaeontologists (Mette Hofstedt [7 teeth: DK 858 A-G], Marianne Nattestad [1 tooth: DK 858 I] and Niels Hemmer [1 tooth: DK 858 H]) in the south-western part of the island of Bornholm at Arnager (Denmark, 55°03'N, 14°46'E; Fig. 1). The whole set was declared 'Danekræ' in 2016 as the 'Danekræ' law that was enacted in 1989 stipulates that "Whoever in Denmark finds a botanical or zoological object of fossil or sub-fossil origin or a geological object of unique scientific or display value, shall offer the object to the State […]. If the State wishes to acquire the object, the finder or owner shall be paid a reward" (Christensen & Hald 1990). Until now, only the species *Ptychodus rugosus* Dixon, 1850 had been officially recorded from Denmark (Blume 1979; Radwanski & Marcinowski 1996), excluding Greenland from where a tooth of *Ptychodus decurrens* Agassiz, 1835 was described from the late Turonian–Early Coniacian by Hoch (1992). In addition, one tooth from the collection of the Natural History Museum of Denmark (NHMD) is attributed to *P. rugosus* (Fig. 2). It was deposited, and probably identified, on May 5th 1950 by A. Rosenkrantz under the number 1950.150, that was later registered as NHMD 167591. According to the original label, it also comes from Arnager.

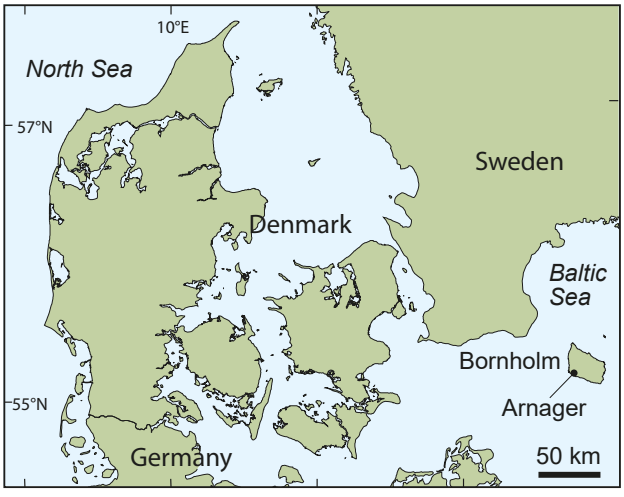

Fig. 1. Map showing the location of Arnager on Bornholm Island.

Teeth of *Ptychodus* are easily recognizable due to their peculiar morphology. The crown is divided into two parts: the marginal area and the cusp. In most species the cusp is ornamented with distinct transverse ridges, whereas the marginal area is variously ornamented, ranging from a granular texture to fine ridges. A few

species display radiating ridges instead of transverse ridges. The cusp is dome-shaped and elevated to varying degrees, dependent on the species and position of the teeth in the jaws. This general morphology suggests that this shark was durophagous. It was a large shark that could reach up to 10 m in length (Shimada *et al.* 2010; Hamm 2020). *Ptychodus* is a genus known from the Middle Cenomanian to the Early Campanian in North and South America, Europe, Africa, Asia and Australia (Hamm 2020). Its phylogenetic affinities among elasmobranchs have long been a point of contention (Cuny 2008), however a consensus that *Ptychodus* was a neoselachian shark seems to have emerged (Hoffman *et al.* 2016; Hamm 2020). Its precise relationships among neoselachians remain, however, enigmatic, although it has been suggested that it could be related to Lamniformes (Rozefelds 1993; Hamm 2010).

Fig. 2. Tooth of *Ptychodus latissimus* in apical view (NHMD 167591), originally ascribed to *P. rugosus*, with its original label. Scale bar = 10 mm.

Geological setting

All nine teeth were recovered from the basal phosphorite conglomerate of the Arnager Limestone Formation near Arnager Pynt in the south-western part of Bornholm. The formation is 12–20 m thick at this location, but can reach up to 40 m towards the north-west along Stampe Å. The basal conglomerate is, however, only visible near Arnager Pynt. The Arnager Limestone Formation has been dated as Early to Middle Coniacian and was deposited in a rather deep outer shelf environment, although not far from the coastline (Schiøler 1992; Hart *et al.* 2012; Svennevig & Surlyk 2019). Svennevig & Surlyk (2019) noted that the Arnager Limestone occupied a much more proximal position than most other Upper Cretaceous Chalk in North-West Europe. The presence of a conglomerate at the base of the Arnager Limestone, which is separated from the underlying Arnager Greensand by a hiatus (Svennevig & Surlyk 2019), suggests a high-energy environment indicative of a period of regression/lowered sea level. This certainly explains why some specimens are fragmentary.

Material and method

All nine teeth are housed in the Danekræ collection (DK) of the Natural History Museum of Denmark (NHMD) at the University of Copenhagen under the collection number DK 858 A-I. Because of the peculiar arrangement of the teeth in the oral cavity, where they form straight, parallel tooth files directed anteroposteriorly (cranio-caudally), the typical vocabulary to describe elasmobranch teeth is adapted. The usual mesial and distal sides are replaced by anterior (facing anteriorly) and posterior (facing caudally) sides, whereas the lingual side faces towards the inside of the mouth and the labial one towards the outside of the mouth (Hamm 2020). All the teeth were photographed at the NHMD by Sten Lennart Jakobsen. All measurements were made using a calliper with an accuracy of a tenth of a millimetre. Important characters in the description of a *Ptychodus* tooth are the elevation of the cusp, the shape and number of the transverse ridges and the ornamentation pattern of the marginal area. A transverse ridge is defined here as a continuous unit crossing the apex of the crown from the lingual to the labial side. Observation of the details of the ornamentation was made using a stereomicroscope Leica MZ7.5. Specimen DK 858 B was broken during manipulation after it was photographed. The cusp was separated from the marginal area and part of the basal part of the cusp was lost. The systematic scheme

adopted here follows Hoffman *et al.* (2016) and Hamm (2019) in attributing the genus *Ptychodus* to neoselachian sharks and Hamm (2019) in attributing it to the Order Ptychodontiformes.

Systematic palaeontology

Class Chondrichthyes Huxley, 1880

Subclass Elasmobranchii Bonaparte, 1838

Subcohort Neoselachii Compagno, 1977

Order Ptychodontiformes Hamm, 2019

Family Ptychodontidae Jaeckel, 1898

Genus *Ptychodus* Agassiz, 1834

General description. The teeth measure between 5 and 14.5 mm antero-posteriorly. A posterior sulcus, which allows the tooth to be oriented, is visible only when the tooth is complete and/or well preserved. However, for every specimen described below, either the tooth is broken, or part of the tooth is hidden in the matrix. No root is visible. We could therefore not differentiate the lingual side from the labial one. Thus, they are defined as lateral sides. The apical surface is flat or convex and represents the best-preserved region in each tooth. It bears three to eight transverse ridges. Three main morphologies of the crown can be defined:

Morphotype 1: The apical part of the cusp is ovoid, but it is less elongated antero-posteriorly than in morphotype 2 below. The antero-posterior length of the central elevation exceeds its height.

Morphotype 2: The apical part of the cusp is ovoid in outline, longer antero-posteriorly than labio-lingually. The antero-posterior length of the central elevation does not exceed its height.

Morphotype 3: The apical part of the cusp is square and the associated central elevation is low.

Ptychodus mammillaris Agassiz, 1835

Material. DK 858 D (Fig. 3B), DK 858 F (Fig. 3C), and DK 858 I (Fig. 3A).

Description. These three teeth belong to morphotype 1. Their apical surface is flat to slightly convex. Six to eight thick transverse ridges cross the whole of the cusp labio-lingually. Their extremities are discontinuous, forming an alignment of tubercles that merge with the ornamentation of the marginal area. The labial and lingual extremities of the posterior ridges curve anteriorly whereas those of the anterior ridges curve posteriorly. The transverse ridges of DK 858 F (Fig. 3C) appear distinctly thinner than those of DK 858 D (Fig. 3B) and DK 858 I (Fig. 3A). The ornamentation of the marginal area is composed of discontinuous tubercles that can be quite elongate, forming a concentric pattern around the cusp in apical view.

Comparison. The orientation of the extremities of the transverse ridges described above is reminiscent of that seen in NHMD 167591 (Fig. 2). Nevertheless, the cusp is not as high and NHMD 167591 belongs to morphotype 3 (see below). The presence of six to eight parallel, thick and clearly delineated transverse ridges in DK 858 I (Fig. 3A) and DK 858 D (Fig. 3B) is in agreement with *P. mammillaris,* the teeth of which usually show five to ten ridges in medial and lateral files (Hamm 2020). The wide marginal area of DK 858 I, the only tooth in our sample in which this area is preserved, displays a coarse and concentric ornamentation, also characteristic of *P. mammillaris* (Hamm 2020). Teeth of this species can reach up to 45 mm labio-lingually (Longbottom & Patterson 2002), whereas our largest and best-preserved tooth (DK 858 I) measures 14.5 mm labio-lingually. This suggests that these teeth belong to the 2nd-4th tooth file position in the jaw (S. Hamm, personal communication October 2021).

Ptychodus altior Agassiz, 1835

Material. DK 858 A (Fig. 3D), DK 858 B (Fig. 3E), and DK 858 E (Fig. 3F).

Description. These three teeth belong to morphotype 2. The crown is flared at the base and can be subdivided into three main units: the marginal area, the base and the apex of the cusp. The lateral and posterior sides of the base of the cusp are very abrupt, almost vertical, whereas the anterior side is less steep. There are three or four straight to wavy transverse ridges, roughly parallel to each other, that cross the convex apex of the cusp labio-lingually before fading away, leaving the lateral sides of the cusp devoid of ornamentation. On the other hand, the anterior and posterior sides may display faint, irregular ridges or tubercles in DK 858 A (Fig. 3D) and DK 858 E (Fig. 3F). The transition between the base of the cusp and the marginal area is sharp, the latter being ornamented by discontinuous ridges displaying a concentric pattern around the cusp.

Comparison. Four species of *Ptychodus* possess teeth belonging to morphotype 2: *Ptychodus altior, P. rugosus, P. anonymus* Williston, 1900 and *P. whipplei* Marcou,

1858. Teeth of *P. anonymus* display transverse ridges that are closely spaced and extend to the base of the cusp. Moreover, this species has so far only been reported from the Cenomanian (Hamm 2020). The apical cusp of *P. whipplei* teeth display a more circular outline compared to DK 858 A (Fig. 3D), DK 858 B (Fig. 3E) and DK 858 E (Fig. 3F), and the transverse ridges reach the marginal area (Hamm 2020). Teeth of *Ptychodus rugosus* differ from the Danish specimens by displaying more irregular transverse ridges that cross the apex of the cusp (Radwanski & Marcinowski 1996; Hamm 2020). DK 858 A (Fig. 3D), DK 858 B (Fig. 3E) and DK 858 E (Fig. 3F) are therefore attributed to *P. altior* based on their transverse ridges that are confined to the apex of the cusp and their smooth lateral sides (Amadori *et al.* 2019). *Ptychodus altior* has so far only been recovered from Europe and Angola (Amadori *et al.* 2019).

***Ptychodus latissimus* Agassiz, 1835**

Material. NHMD 167591 (Fig. 2), DK 858 C (Fig. 3G) and DK 858 H (Fig. 3H).

Description. These teeth belong to morphotype 3. A complete marginal area is not preserved in any of the three samples. In anterior or posterior view the cusp is slightly convex. Six thick transverse ridges, the extremities of which point posteriorly in DK 858 H (Fig. 3H), cross the whole of the cusp labio-lingually. In NHMD 167591 (Fig. 2) and DK 858 C (Fig. 3G) only the first three transverse ridges point posteriorly. The extremities of some of the transverse ridges are discontinuous, forming an alignment of tubercles that merge with the ornamentation of the marginal area. The tubercles are predominantly elongated

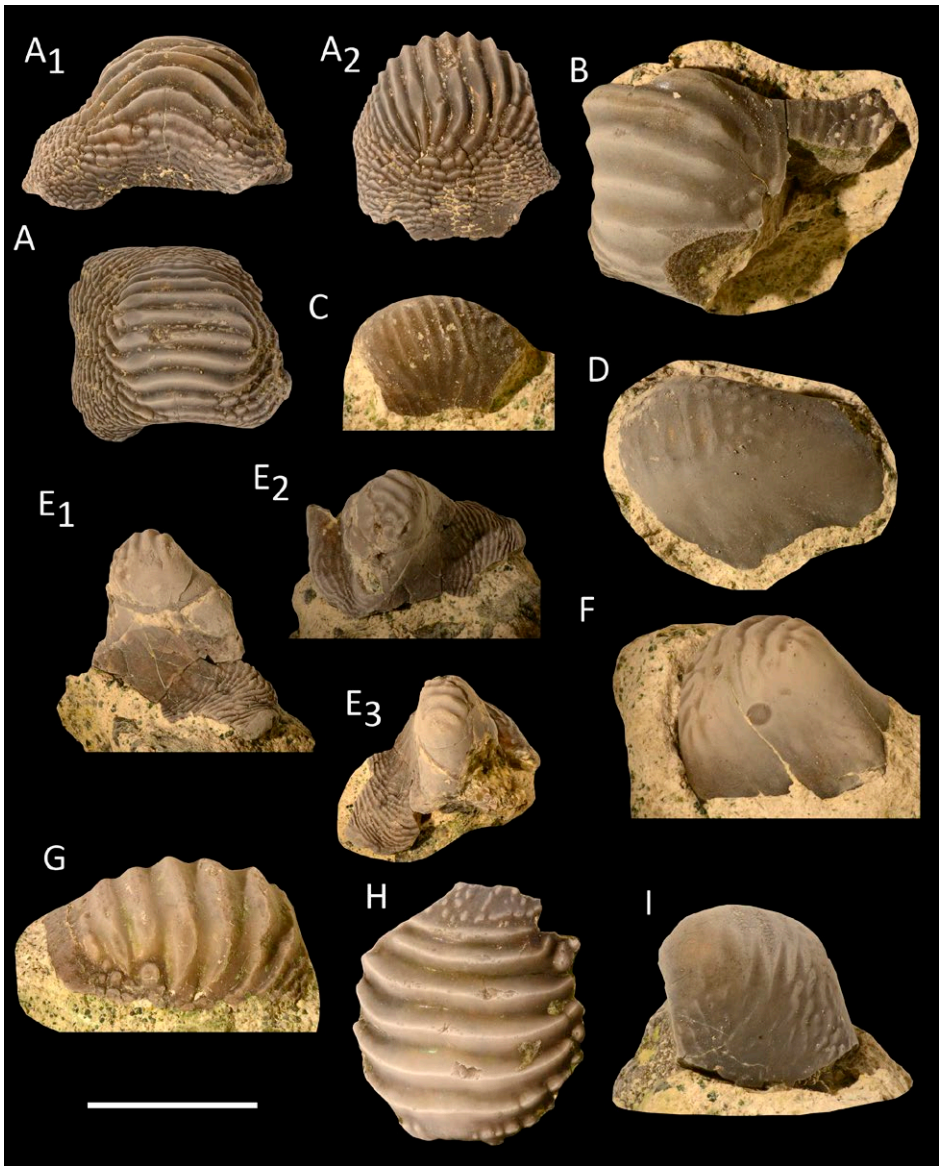

Fig. 3. *Ptychodus* teeth from Bornholm Island. **A-C:** *Ptychodus mammillaris*. **A**: DK 858 I; A_1, posterior view; A_2, lateral view; A_3, apical view. **B**: DK 858 D, latero-apical view. **C**: DK 858 F, latero-apical view. **D-F**: *Ptychodus altior.* **D**: DK 858 A, latero-apical view. **E**: DK 858 B; E_1, lateral view; E_2, postero-apical view; E_3, antero-apical view. **F**: DK 858 E, latero-apical view. **G-H**: *Ptychodus latissimus.* **G**: DK 858 C, latero-apical view. **H**: DK 858 H, apical view. **I:** *Ptychodus* sp. DK 858 G, lateral view. Scale bar for A, E, H, I = 10 mm. Scale bar for B, C, D, F, G = 5 mm.

and irregular, both in shape and orientation. There is a gradual transition between the cusp and the marginal area.

Comparison. NHMD 167591 (Fig. 2) was attributed to *P. rugosus*, probably by A. Rosenkrantz based on its original museum label; to the best of the authors' knowledge this specimen was never published. However, this tooth is not as high and its transverse ridges are better developed and more regular than typically seen in *P. rugosus* (Radwanski & Marcinowski 1996; Hamm 2020). This identification must therefore be rejected. The number and the morphology of the curved transverse ridges of NHMD 167591, as well as of DK 858 C (Fig. 3G) and DK 858 H (Fig. 3H), are more reminiscent of the species *P. latissimus*. The latter species possesses three to eight thick and widely spaced ridges across a low cusp (Hamm 2020). The ornamentation pattern of DK 858 D (Fig. 3B) is also reminiscent of that of *P. latissimus*, but the crown is too high for that tooth to be attributed to the latter species. Adult teeth of *P. latissimus* can reach 60 mm (Longbottom & Patterson 2002), whereas the largest tooth in our sample, NHMD 167591 (Fig. 2), is roughly 24 mm antero-posteriorly.

***Ptychodus* sp.**

Material. DK 858 G (Fig. 3I).

Description. This tooth belongs to morphotype 2. Only the cusp is preserved. The transverse ridges are almost completely worn away, but four straight ridges parallel to each other can be observed. They do not reach the base of the cusp (Fig. 3I). Anterior and posterior sides are ornamented with discontinuous and irregular ridges. Lateral sides are ornamented with thinner, sparse and irregular ridges.

Comparison. DK 858 G (Fig. 3I) displays four ridges on the apex that do not reach the base of the cusp. However, contrary to the teeth of *P. altior*, the lateral faces of the cusp are not completely smooth, even when their ornamentation is sparse. The tooth cannot be assigned to the species *P. mammillaris* because the transverse ridges do not reach the marginal area. In addition, teeth of *P. mammillaris* display at least five transverse ridges, and the crown of DK 858 G is too high to correspond to a posterior tooth with a reduced number of ridges (Hamm 2020). Morphologically, DK 858 G (Fig. 3I) appears to be an intermediate between *P. altior* and *P. mammillaris*, although admittedly closer to the former than to the latter. Because of the incomplete nature and worn appearance of the single specimen available, it is treated here in open nomenclature.

Discussion

Ptychodus latissimus and *P. mammillaris* have frequently been described from the same stratigraphic levels (Welton & Farish 1993; Trbušek 1999; Longbottom & Patterson 2002), so their association in the Bornholm specimens is not surprising. All teeth described above are small and certainly come from lateral tooth files. According to the geological setting (Svennevig & Surlyk 2019) the conglomerate's genesis was likely due to lowered sea level, hence higher energy, allowing disarticulation and winnowing of teeth of specimens into a lower energy environment. Efficient sorting has concentrated teeth of similar size, between 5 and 15 mm labio-lingually, in the conglomerate. This explains the absence of large lower symphysial and upper paramedial teeth from the collection.

Although NHMD 167591 (Fig. 2) cannot be attributed to *Ptychodus rugosus,* the tooth illustrated by Radwanski & Marcinowski (1996: pl. 2, fig. 6), which displays a high cusp crossed by irregular ridges, is indeed typical of *P. rugosus*. Unfortunately, the whereabouts of this tooth are unknown and no details were given by the authors. Blume (1979) figures a single tooth of *Ptychodus* that was not identified to species level. The cusp displays at least nine ridges and is not elevated, which excludes the possibility that it could belong to *P. rugosus,* as the elevated cusp of *P. rugosus* never displays more than six ridges (Hamm 2020). Although the tooth illustrated by Blume (1979) may superficially look similar to NHMD 167591 (Fig. 2), its transverse ridges are too numerous and closely spaced for this tooth to be attributed to *P. latissimus*. The same character indicates that this specimen can also not be assigned to either *P. altior* or *P. mammillaris*. It is therefore likely that there is at least one more species, and perhaps two if we take into account DK 858 G (Fig. 3I), present in the Upper Cretaceous of Bornholm, but a precise identification based on a single photograph is premature, and without access to the specimen further conclusions are unattainable.

Ptychodus altior is reported for the first time from Denmark. This species has predominantly been reported from Europe, with a single report from south-western Africa (Amadori *et al*. 2019). *Ptychodus latissimus* and *P. mammillaris* on the other hand have a more cosmopolitan distribution (Hamm 2020). The three species have been found together in Angola (Antunes & Cappetta 2002) and in the English Chalk (Dixon 1850).

The Arnager Limestone has been dated as Early to Middle Coniacian based on dinoflagellate cysts (Schiøler 1992). This date has been supported by ammonites and inoceramid bivalves (Kennedy & Christensen 1991). The three species of *Ptychodus*

described above have a stratigraphic range restricted to the Middle Turonian–Early Coniacian interval (Hamm 2020), which is in good agreement with the accepted age for the Arnager Limestone. Interestingly, *P. rugosus* first appeared in the Late Coniacian and has never been recovered in association with the three other species documented herein (Hamm 2020). This casts some doubt on the exact origin of the *P. rugosus* tooth that was initially reported from the Arnager Greensand (Radwanski & Marcinowski 1996), which is Cenomanian in age (Svennevig & Surlyk 2019). One possibility is that this tooth was instead retrieved from the Bavnodde Greensand on Bornholm, but without access to the specimen such a hypothesis is untestable.

Conclusion

Three species are described among the nine teeth declared 'Danekræ' from Bornholm: *Ptychodus altior, Ptychodus latissimus* and *Ptychodus mammillaris*. The identification of DK 858 G (Fig. 3I) is more difficult and is therefore left in open nomenclature. Even though *Ptychodus rugosus* has not been described here, this species is present on Bornholm (Radwanski & Marcinowski 1996) although, based on its known stratigraphic range, it is unlikely that it belongs to the same assemblage as the three species described here.

Acknowledgements

We would like to thank Sten Lennart Jakobsen who provided the photographs of the teeth in Fig. 2 and Fig. 3, as well as Bent Lindow (Natural History Museum of Denmark) for his help, and Mette Hofstedt and Marianne Nattestad for sharing information on their discovery. Comments provided during the review process by Shawn Hamm and Romain Vullo greatly improved the quality of this manuscript. We are also thankful to Timothy Topper for improving the language of this manuscript.

References

Agassiz, L. 1833-43: Recherches sur les poissons fossiles. Tome 3 contenant l'histoire de l'ordre des placoïdes, 390 pp. Neufchâtel: Imprimerie de Petitpierre. https://doi.org/10.5962/bhl.title.4275

Amadori, M., Amalfitano, J., Giusberti, L., Fornaciari, E., Luciani, V., Carnevale, G. & Kriwet, J. 2019: First associated tooth set of a high-cusped *Ptychodus* (Chondrichthyes, Elasmobranchii) from the Upper Cretaceous of northeastern Italy, and resurrection of *Ptychodus altior* Agassiz, 1835. Cretaceous Research 93, 330–345. https://doi.org/10.1016/j.cretres.2018.10.002

Antunes, M.T. & Cappetta, H. 2002: Sélaciens du Crétacé (Albien-Maastrichtien) d'Angola. Palaeontographica Abteilung A 264, 85–146.

Blume, T. 1979: Gamle hajer. Varv 3, 86–95.

Bonaparte, C. L. J. 1832–1841: Iconografia della Fauna Italica, per le quattro classi degli animali vertebrati, tomo 3. Pesci, 553 pp. Rome: Dalla Tipografia Salviucci. https://doi.org/10.5962/bhl.title.70395

Brignon, A. 2019: Le *Diodon* devenu requin : l'histoire des premières découvertes du genre *Ptychodus* (Chondrichthyes), 100 pp. Bourg-la-Reine: Arnaud Brignon.

Christensen, E.F. & Hald, N. 1990: Danekræ, et nyt begreb i dansk museumslovgivning. Arkæologiske udgravninger i Danmark 1990, 7–16. Translated into English by Joan Davidson.

Compagno, L.J.V. 1977: Phyletic relationships of living sharks and rays. American Zoologist 17, 303–322. https://doi.org/10.1093/icb/17.2.303

Cuny, G. 2008: Mesozoic hybodont sharks from Asia and their relationships to the genus *Ptychodus*. Acta Geologica Polonica 58(2), 211–216.

Dixon, F. 1850: The geology and fossils of the Tertiary and Cretaceous formations of Sussex, 422 pp. London: Longman, Brown, Green and Longmans. https://doi.org/10.5962/bhl.title.14790

Giusberti, L., Amadori, M., Amalfitano, J., Carnevale, G. & Kriwet, J. 2018: Remarks on the nomenclature of the genera *Ptychodus* Agassiz, 1834 and *Buffonites* Sternberg, 1829 (Ptychodontidae, Chondrichthyes). Bolletino della Società Paleontologica Italiana 57, 251–253. https://doi.org/10.4435/BSPI.2018.15

Hamm, S.A. 2010: The Late Cretaceous shark *Ptychodus marginalis* in the Western Union seaway, USA. Journal of Paleontology 84, 538–548. https://doi.org/10.1666/09-154.1

Hamm, S.A. 2019: First associated tooth set of *Ptychodus anonymus* (Elasmobranchii: Ptychodontidae) in North America from the Jetmore Chalk in Kansas. Transactions of the Kansas Academy of Science 122, 1–18. https://doi.org/10.1660/062.122.0101

Hamm, S.A. 2020: Stratigraphic, geographic and paleoecological distribution of the Late Cretaceous shark genus *Ptychodus* within the Western Interior Seaway, North America. New Mexico Museum of Natural History & Science Bulletin 81, 1–94.

Hart, M.B., Bromley, R.G. & Packer, S.R. 2012: Anatomy of the stratigraphical boundary between the Arnager Greensand and Arnager Limestone (Upper Cretaceous) on Bornholm, Denmark. Proceedings of the Geologists' Association 123(3), 471–478. https://doi.org/10.1016/j.pgeola.2011.11.006

Hoch, E. 1992: First Greenland record of the shark genus *Pty-*

chodus and the biogeographic significance of its fossil assemblage. Palaeogeography, Palaeoclimatology, Palaeoecology 92, 277–281. https://doi.org/10.1016/0031-0182(92)90087-L

Hoffman, B.L., Hageman, S.A. & Claycomb, G.D. 2016: Scanning electron microscope examination of the dental enameloid of the Cretaceous durophagous shark *Ptychodus* supports neoselachian classification. Journal of Paleontology 90, 741–762. https://doi.org/10.1017/jpa.2016.64

Huxley, T.H. 1880: On the application of the laws of evolution to the arrangement of the Vertebrata, and more particularly of the Mammalia. Proceedings of the Zoological Society of London 1880, 649–662.

Jaekel, O. 1898: Ueber *Hybodus* Agassiz. Sitzungsbericht der Geselltschaft Naturforschenden Freunde 89, 135–146.

Kennedy, W.J. & Christensen, W.K. 1991: Coniacian and Santonian ammonites from Bornholm, Denmark. Bulletin of the geological Society of Denmark 38, 203–226.

Longbottom, A.E. & Patterson, C. 2002: Fishes. In: Smith, A.B. & Batten, D.J. (eds): Fossils of the Chalk, second edition, pp. 296–324. London: The Paleontological Association.

Marcou, J. 1858: Geology of North America: With Two Reports on the Prairies of Arkansas and Texas, the Rocky Mountains of New Mexico, and the Sierra Nevada of California, Originally Made for the United States Government, 144 pp. Zurich: Zürcher and Furrer. https://doi.org/10.5962/bhl.title.129806

Radwanski, A. & Marcinowski, R. 1996: Elasmobranch teeth from the mid-Cretaceous sequence of the Mangyshlak Mountains, Western Kazakhstan. Acta Geologica Polonica 46, 165–169.

Rozefelds, A.C. 1993: Lower Cretaceous Anacoracidae? (Lamniformes: Neoselachii); vertebrae and associated dermal scales from Australia. Alcheringa 17, 199–210. https://doi.org/10.1080/03115519308619604

Schiøler, P. 1992: Dinoflagellate cysts from the Arnager limestone formation (coniacian, late cretaceous), Bornholm, Denmark. Review of Palaeobotany and Palynology *72*(1–2), 1–25. https://doi.org/10.1016/0034-6667(92)90171-C

Shimada, K., Everhart, M.J., Decker, R. & Decker, P.D. 2010: A new skeletal remain of the durophagous shark, *Ptychodus mortoni,* from the Upper Cretaceous of North America: an indication of gigantic body size. Cretaceous Research 31, 249–254. https://doi.org/10.1016/j.cretres.2009.11.005

Svennevig, K. & Surlyk, F. 2019: A high-stress shelly fauna associated with sponge mud-mounds in the Coniacian Arnager Limestone of Bornholm, Denmark. Lethaia 52(1), 57–76. https://doi.org/10.1111/let.12290

Trbušek, J. 1999: Upper Cretaceous sharks and rays from the Prokop opencast mine at Březina near Moravská Třebová. Acta Universitatis Palackianae Olomucensis Facultas Rerum Naturalium, Geologica 36, 51–61.

Welton, B.J. & Farish, R.F. 1993: The collector's guide to fossil sharks and rays from the Cretaceous of Texas, 204 pp. Lewisville: Before Time.

Williston, S. W. 1900: Some fish teeth from the Kansas Cretaceous. Kansas University Quarterly 91, 27–42.

U-Pb zircon and titanite age of the Christiansø granite, Ertholmene, Denmark, and correlation with other Bornholm granitoids

TOD WAIGHT, MIKAEL STOKHOLM, BENJAMIN HEREDIA & TONNY B. THOMSEN

Geological Society of Denmark
https://2dgf.dk

Received 15 June 2021
Accepted in revised form
3 March 2022
Published online
23 March 2022

Waight, T., Stokholm, M., Heredia, B. & Thomsen, T.B. 2022: U-Pb zircon and titanite age of the Christiansø granite, Ertholmene, Denmark, and correlation with other Bornholm granitoids. Bulletin of the Geological Society of Denmark, Vol. 70, pp. 27–38. ISSN 2245-7070. https://doi.org/10.37570/bgsd-2022-70-03

A granitic sample from the Danish island of Christiansø in the Ertholmene island group north of Bornholm is described petrographically and geochemically, and dated using U-Pb in zircon and titanite. Zircon systematics in the sample are complicated by abundant Pb loss and a large population of zircons interpreted as being inherited. Removal of highly disturbed zircons, imprecise analyses, and assumed inherited zircons yield an upper intercept date of 1500 ± 18 Ma (MSWD = 13, n = 58). Removal of zircons with high common Pb from this population yields an identical result of 1500 ± 22 Ma (MSWD = 8, n = 34). Zircons that are ≤3% discordant give a weighted average $^{206}Pb/^{238}U$ age of 1458 ± 12 Ma (MSWD = 3.0, n = 18), and a weighted average $^{207}Pb/^{206}Pb$ age of 1495 ± 14 Ma (MSWD = 4.7, n = 19). Titanites from the sample yield a lower intercept age of 1448 ± 15 Ma (MSWD = 6.8, n = 45). The sample contains a significant number of inherited grains indicative of ages around 1.7–1.8 Ga. The relatively large MSWDs for these age determinations indicate geological complexity, likely reflecting Pb loss, and the possible presence of inherited zircons which suffered major Pb loss during incorporation in the granitic magma. The zircon and titanite dates agree reasonably well with previous age determinations on felsic lithologies from the Bornholm mainland, as well as from the Blekinge Province of southern Sweden. Petrographically and geochemically, the Christiansø granite is indistinguishable from, and can be correlated with, the A-type granites and gneisses which occur on Bornholm. The high abundance of disturbed and inherited zircons (c. 1.7–1.8 Ga) may indicate that the granite was intruded into and assimilated a nearby region of unexposed Transscandinavian Igneous Belt rocks. The somewhat altered nature of the rock, and overall disturbance of U-Pb zircon systematics, suggest alteration associated with fluid-flow along nearby faults defining the northern margin of the Sorgenfrei–Tornquist Zone.

Keywords: Granite, Bornholm, Ertholmene, U-Pb zircon, titanite.

Tod Waight [todw@ign.ku.dk], Department of Geosciences and Natural Resource Management (Geology Section), University of Copenhagen, Øster Voldgade 10, 1350 Copenhagen K, Denmark. Mikael Stokholm [mikael.stokholm@snm.ku.dk], Department of Geosciences and Natural Resource Management (Geology Section), University of Copenhagen, Øster Voldgade 10, 1350 Copenhagen K, Denmark. Benjamin Heredia [behe@geus.dk] and Tonny B. Thomsen [tbt@geus.dk], Geological Survey of Denmark and Greenland, Øster Voldgade 10, 1350 Copenhagen K, Denmark.

Christiansø is a small island (*c.* 0.25 km^2) that is part of the island group Ertholmene, located *c.* 20 km northeast of Bornholm, in the southern Baltic Sea (Fig. 1A). The island group has a long and rich human history, and although it is generally acknowledged that the basement block making up Ertholmene is geologically related to Bornholm, to our knowledge no detailed geological investigations have been published on the rocks of the island group. The islands are the only emergent portion of a horst that forms part of the

Bornholm–Skåne segment of the Sorgenfrei–Tornquist Zone (Fig. 1A), a major intracontinental fault zone separating the East European Platform and the Baltic Shield in the north from the sedimentary rocks of the Danish–Polish Trough to the south (e.g. EUGENO-S Working Group 1987; Krzywieca *et al.* 2003; Graversen 2009). The islands of Christiansø and Frederiksø are dominated by a reddish granitic gneiss. Outcrops of dolerite dykes and green sandstone dikes, as also observed on Bornholm (e.g. Katzung 1996; Holm *et al.* 2010) have also been noted (Kofoed 1961). In this contribution, we present a petrographic description, geochemical analysis, and U-Pb zircon and titanite age for a representative granite sample collected from the southern end of Christiansø (Fig. 1B).

Methods

Whole rock geochemistry of the sample was determined at ACTLABs using the 4LithoRes protocol, a combination of lithium metaborate/tetraborate fusion ICP-OES and ICP-MS analysis for major and trace element analysis, respectively. U-Pb geochronology on titanite was carried out on a double-polished thin section by laser ablation inductively coupled plasma mass spectrometry (LA-ICPMS) at the Geological Survey of Denmark and Greenland (GEUS), using a NWR 213 frequency-quintupled solid state Nd:YAG laser system from Elemental Scientific Lasers (ESL) mounted with a standard TV2 ablation cell coupled to an ELEMENT 2 double-focusing single-collector magnetic sector-field

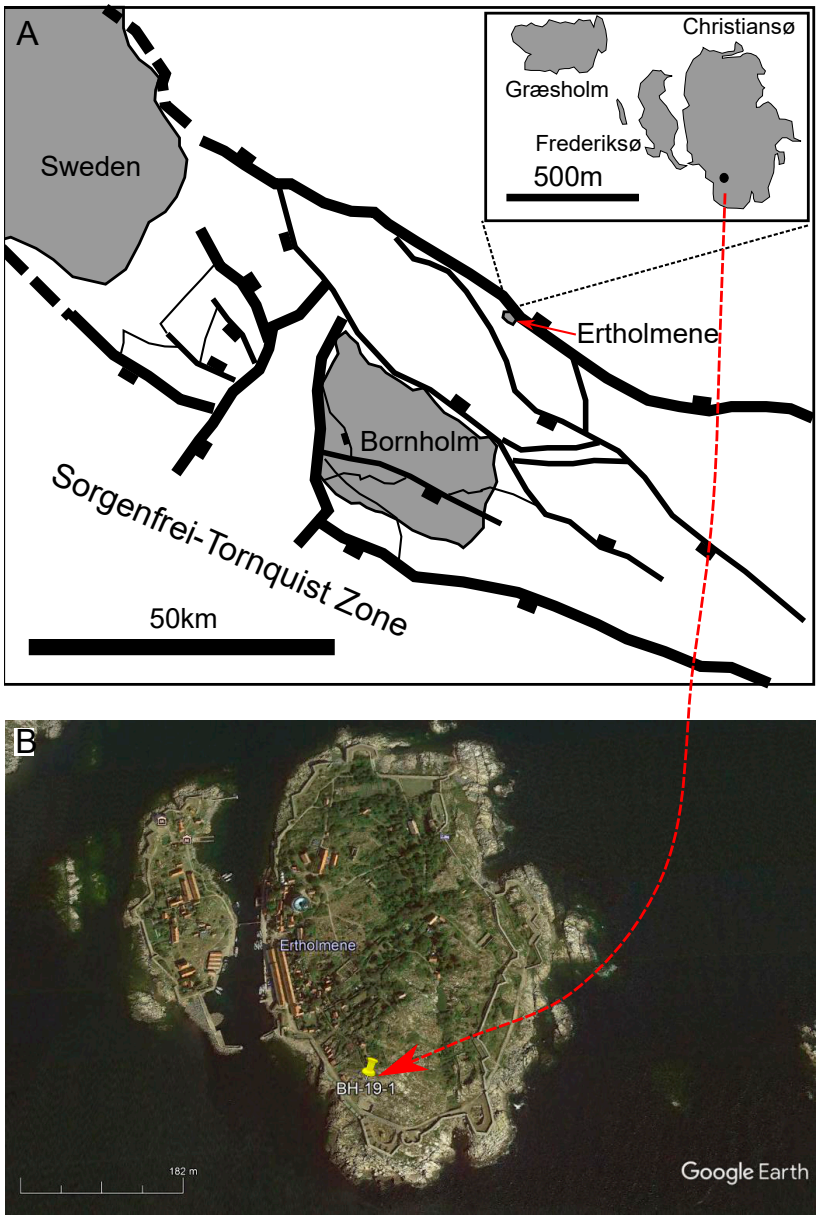

Fig. 1. A: Location map showing position of Bornholm and Ertholmene within the Sorgenfrei–Tornquist Zone (modified from Graversen 2009), tickmarks show downthrown side of fault blocks. **B:** Image of Christiansø and Frederiksø from Google Earth showing sample location.

ICPMS from Thermo-Fisher Scientific. The mass spectrometer is equipped with a new jet interface pump system and detector amplifier and employed Ni jet-type sampler and H-type skimmer cones. Operating conditions and data acquisition parameters are listed in the electronic appendix. Prior to loading, the thin section and standards were carefully cleaned with ethanol to remove surface contamination. To ensure stable laser output energy, the laser was heated prior to operation, providing a stable laser power and flat ablation craters by a 'resonator-flat' laser beam. The mass spectrometer was run for at least one hour before analysis to stabilise and minimise the background signal. The ablated material was swept by the helium carrier gas and mixed with argon gas *c.* 0.5 m before entering the mass spectrometer.

Before the start of analysis, the ICP-MS was optimised for dry plasma conditions through continuous linear ablation of the GJ-1 zircon standard. The signal-to-noise ratios for the heavy mass range of interest (i.e. ^{202}Hg to ^{238}U), emphasising on ^{238}U and ^{206}Pb, were maximised, while simultaneously opting for the lowest oxide production level by minimising the $^{254}UO_2/^{238}U$ ratio. To minimise instrumental drift, a standard-sample-standard analysis protocol was followed, bracketing 7–8 sample spots by 2–3 standard measurements. Standard analyses and results were validated by analyses of the natural titanite standards A1772 and A968 (provided by Y. Lahaye, GTK), the Seiland standard titanite (provided by Ø. Skår, NGU), and the Plešovice (Slama *et al.* 2008) and GJ-1 (Jackson *et al.* 2004) zircon standards, which all were analysed regularly throughout the analysis sequence. All standards demonstrated an averaged age accuracy within 3% deviation (2σ) from reference values, and internal uncertainties on individual spots of < 2–3% (2σ). Data processing was performed off-line using the software Iolite v. 2.5 (Hellstrom *et al.* 2008; Paton *et al.* 2010, 2011) with the VizualAge data reduction scheme (Petrus & Kamber 2012). Data were corrected for background, session drift and down-hole isotopic fractionation by using MKED1 as primary reference material (Spandler *et al.* 2016).

Data were acquired from single spot analyses using a laser spot size of 25 μm for the analyses and a pre-ablation spot size of 40 μm. A laser fluence of 3.5 to 4.4 J/cm^2 and a pulse rate of 5 Hz was applied. The acquisition sequence included 5 pre-ablation bursts followed by a 15 sec. background measurement, then laser ablation for 35 sec., and finally washout for 30 sec. Factory-supplied software was used for the acquisition of the transient data, obtained through an automated running mode of pre-set analytical locations. Analyses spots on the grains were placed at clear and inclusion-free locations free of cracks.

Titanites often contain a high proportion of common Pb, as shown by low $^{206}Pb/^{204}Pb$ and $^{207}Pb/^{204}Pb$ ratios and compositions that plot above the concordia in Tera-Wasserburg plots. An assumption that the common Pb ratio is invariant will mean that any error in the isotope ratios assigned to common Pb will result in a consistent bias, rather than a random variation, of the calculated $^{206}Pb/^{238}U$ and $^{207}Pb/^{206}Pb$ radiogenic ratios (Ludwig 1998). Thus, using a "SemiTotal–Pb/U isochron" approach (Tera & Wasserburg 1972), the background- and session-drift corrected ratios can be plotted on a Tera-Wasserburg concordia diagram without correction for common Pb. If (and only if) the true $^{206}Pb/^{238}U$ and $^{207}Pb/^{206}Pb$ radiogenic isotope ratios represent comparable dates, the non-common Pb corrected data will be dispersed along a line whose lower intercept with the concordia curve defines the age of their crystallisation or resetting (Ludwig 1998; see for example Spencer *et al.* 2013 and Chew *et al.* 2014). This is the case for the titanite grains in this study, and thus the lower intercept age reported here for the titanites is not corrected for common Pb, and assumed to represent the U/Pb isotopic age of the titanite resulting from a specific geological event.

U-Pb dating of zircon was performed at GEUS by LA-ICPMS (same instrumentation as above) using methods described in detail in Waight *et al.* (2017). Common Pb corrections were made using the method of Andersen (2002). For both titanites and zircons, diagrams and statistical information were produced using Isoplot 3.70 (Ludwig 2008). All age data are plotted and presented at 2 sigma level.

Results

The sample (BH19-1) was collected from blasted outcrops near Kongens Bastion at the southern end of Christiansø (Lat. 55°19'6.10"N, long. 15°11'17.64"E). In outcrop, the rock is a reddish, leucocratic, fine to medium-grained, equicrystalline granitic gneiss (*sensu lato*) with a foliation defined by a weak alignment of mafic phases (Fig. 2). No significant variations in the texture or mineralogy of the granite were noted in reconnaissance investigations of Christiansø and Frederiksø.

In thin section, the sample comprises abundant subhedral to anhedral quartz and anhedral microcline-twinned alkali feldspar up to 1 mm in diameter (Fig. 3). Some granophyric intergrowths are also observed. Plagioclase occurs as larger but subordinate subhedral crystals up to 3 mm in length, showing weak albite twinning and common alteration with many inclusions of fine-grained epidote. No primary biotite is

preserved in the rock, instead biotite has been altered to flakes of green chlorite up to 1 mm in length and showing anomalous purple interference colours. Rounded to square opaque phases (presumably magnetite) up to 0.5 mm in diameter are common, and often associated with anhedral titanite crystals of approximately the same size. Fine-grained hematite is evident along many grain boundaries and presumably contributes to the reddish colour of the rock.

A bulk geochemical analysis of the sample is presented in Table 1 and compared to analyses of granites and gneisses from Bornholm (Johansson *et*

Fig. 2. Close up of Christiansø granite from sampling location. Note the red colour which resembles leucocratic granite varieties on Bornholm (e.g. Hammer and Almindingen Granites).

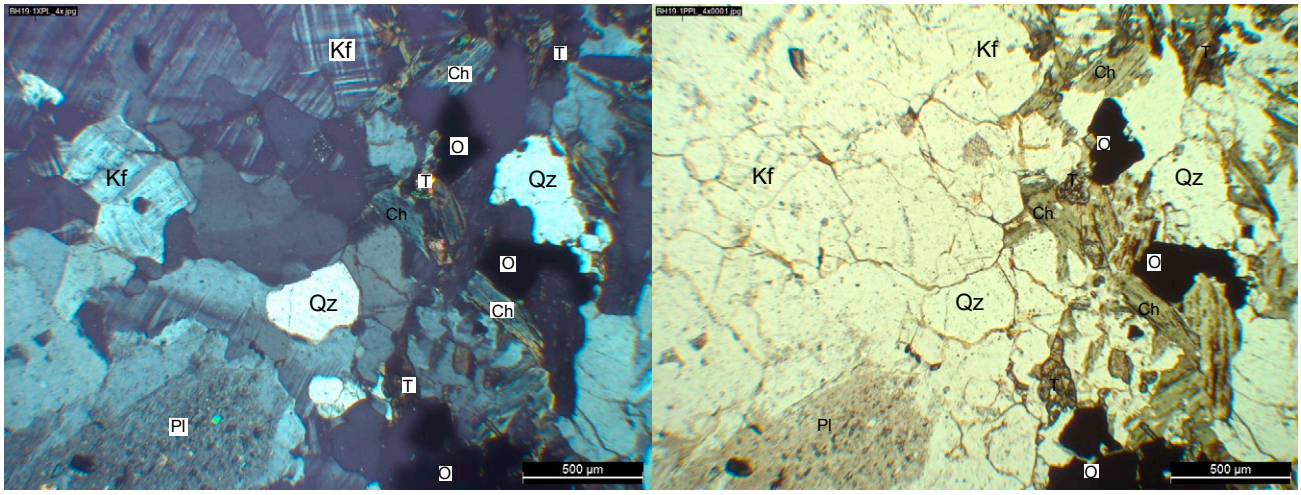

Fig. 3. Photomicrographs of sample BH19-1 (left = cross-polarised light, right =plain polarised light). Kf = alkali feldspar, Qz = quartz, Pl = plagioclase feldspar, T = titanite, Ch = chlorite, O = opaque.

Table 1. Geochemical analysis of sample BH19-1. Major elements are in weight percent, and trace elements in µg/g

SiO2	71.01	Sc	8	Sr	137	Ce	143	Lu	1.02
Al2O3	13.15	Be	4	Y	57.5	Pr	15.9	Hf	9.8
Fe2O3(T)	4.07	V	24	Zr	382	Nd	57.5	Ta	2.13
MnO	0.07	Cr	< 20	Nb	21	Sm	10.8	W	580
MgO	0.66	Co	75	Mo	< 2	Eu	1.94	Tl	0.6
CaO	1.67	Ni	< 20	Ag	0.9	Gd	9.2	Pb	25
Na2O	3.14	Cu	< 10	In	0.1	Tb	1.56	Bi	< 0.1
K2O	4.98	Zn	70	Sn	4	Dy	9.49	Th	21.4
TiO2	0.65	Ga	18	Sb	< 0.2	Ho	1.93	U	5.34
P2O5	0.16	Ge	1.5	Cs	1.2	Er	5.9		
LOI	0.78	As	< 5	Ba	1038	Tm	0.933		
Total	99.56	Rb	181	La	71.2	Yb	6.39		

al. 2016) in Fig. 4. The Christiansø granite has 71 wt.% SiO_2, plotting in the granite field in the total alkalies – silica diagram modified for plutonic rocks by Middlemost (1994; Fig. 4A). The rock is metaluminous (molar $Al_2O_3/(CaO+Na_2O+K_2O) = 0.97$), ferroan, and alkali-calcic (Figs 4B, C). The rock also shows similar trace element and rare earth element (REE) patterns as the granitoids and gneisses from Bornholm and is characterised by high field strength element (HFSE) enriched compositions such that it plots in the A-type / within-plate granite field in tectonic discrimination diagrams (Figs 4D, E, F).

A total of 137 zircons from the sample were analysed for U-Pb geochronology. The full data set is available as an electronic appendix to this article. Common Pb contents are variable, and a common Pb correction was applied when the estimated fraction of common Pb was over 0.05. Many of these analyses were subsequently discarded from age calculations on other grounds. The resultant data were highly scattered with many discordant analyses and evidence for open system behaviour and Pb loss. Consequently, filtering of the data was necessary. As the first part of this process, a purely mathematical approach was taken so as not to introduce any human-bias into the data sorting process. All analyses with negative correlation coefficients (n = 12) and/or internal errors on measured $^{207}Pb/^{235}U$ or $^{206}Pb/^{238}U$ greater than 10% (2 S.E.) (n = 47) were excluded from the data set. The data were separated visually into a group which we assume represent the original magmatic zircons (dark blue shaded and orange symbols in Fig. 5, n = 58), a second group we assume represents an inherited zircon population (green symbols in Fig. 5, n = 14), and a third group of highly discordant analyses likely also to represent older inherited zircons (possibly c. 2 Ga) that are excluded from further discussion (red symbols in Fig. 5, n=5). The first group yields a Model-2 upper intercept date of 1500 ± 18 Ma (MSWD = 13), with a lower intercept of *c.* 130 Ma (Fig. 5). These zircons have $^{207}Pb/^{206}Pb$ dates ranging from 1144 to 1596 Ma. Exclusion of zircons with a fraction of common Pb > 0.01 from this population (orange symbols in Fig. 5) yields an identical Model-2 upper intercept date of 1500 ± 22 Ma (MSWD = 8; n = 34 – blue shaded symbols in Fig. 5). The second presumed inherited population yields a Model 2 upper intercept date of 1727 ± 79 Ma (MSWD = 6.0), with a lower intercept also at *c.* 130 Ma (Fig. 5; green symbols) and is suggestive of an older population of zircons which have suffered partial lead loss. These zircons have $^{207}Pb/^{206}Pb$ dates ranging from 1672–1864 Ma. Those zircons within the first group that are within 3% of concordance yield a weighted average $^{207}Pb/^{206}Pb$ age of 1495 ± 14 Ma (MSWD = 4.7, n=19, Fig. 6A) and a weighted average $^{206}Pb/^{238}U$ date of 1458 ± 12 Ma (MSWD = 3.0, n = 18, Fig. 6B). The relatively high MSWDs for all these results clearly indicate a heterogeneous zircon population, which complicate determining a precise crystallisation age for this rock.

Fifty spot analyses were made in multiple grains of visually inclusion-free titanite in the polished section of BH19-1; the full data set is available as an electronic appendix to this article. These results define a line which plots above the concordia in a Tera-Wasserburg diagram, reflecting variable contents of common Pb. Following exclusion of six analyses (reflecting analytical challenges – i.e. have reverse slope of the semi-major axis on the ellipses and unusual eccentricity), and assuming an invariant initial Pb composition, the remaining analyses define a lower intercept date of 1448 ± 15 Ma (MSWD = 6.8, n = 44) (Fig. 7), which is in good agreement with the weighted average $^{206}Pb/^{238}U$ date for concordant, non-inherited zircons.

Discussion

U-Pb zircon analyses of granitoids and gneisses from Bornholm demonstrate that all felsic basement rocks were emplaced between 1470 and 1445 Ma (Zariņš &

Johansson 2009; Waight *et al.* 2012). No age distinction is possible between the largely undeformed granitoids and pervasively deformed gneisses within analytical uncertainty. However, ages for a gneiss sample of potentially supracrustal origin and a quartz-rich xenolith in the Svaneke Granite of *c.* 1480 Ma are slightly older and thus far the oldest ages determined for any rocks from Bornholm (Waight *et al.* 2017). The range of ages on Bornholm is in good agreement with age determinations of *c.* 1.45 Ga on granites in the Blekinge Province in southern Sweden and in the southern Baltic Sea (Åberg 1988; Kornfält 1993, 1996; Čečys *et al.* 2002; Čečys 2004; Obst *et al.* 2004; Krzeminska *et al.* 2021). Johansson *et al.* (2016) showed that the Bornholm granitoids and gneisses are ferroan, potassic rocks with features typical of A-type granitoids, and

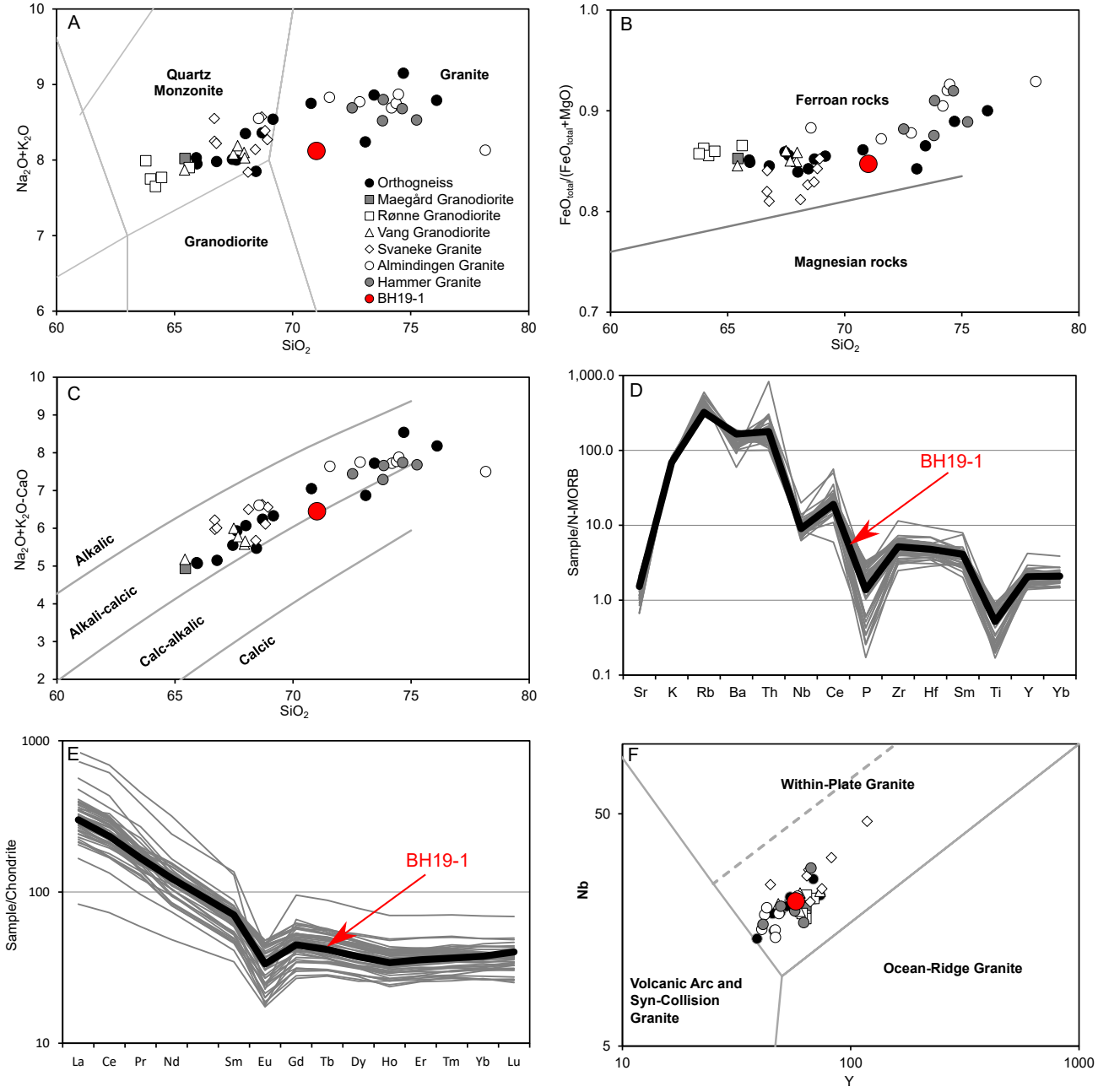

Fig. 4. Selected geochemical plots comparing Christiansø Granite (BH19-1) with granites and gneisses from Bornholm (data from Johansson *et al.* 2016). **A:** Total alkalies silica diagram from Middlemost (2003), **B:** FeO* vs SiO_2 classification plot of Frost & Frost (2008), **C:** Modified alkali-lime index classification plot of Frost *et al.* (2001), **D:** MORB-normalised multi-element diagram and **E:** Chondrite-normalised REE diagram (normalising values for MORB and Chondrite from Sun & McDonough (1989), various plutons are not distinguished for simplicity), **F:** Tectonic discrimination diagram of Pearce *et al.* (1984).

our new data indicate that the Christiansø granite has identical geochemical signatures. Combined, the geochronological and geochemical data indicate that the Bornholm and Blekinge Province rocks (including Christiansø) were generated in an intracontinental setting and are linked to the Danopolonian event in SE Sweden, Bornholm, Poland and Lithuania (e.g. Bogdanova *et al.* 2006). The relationship between this event and the penecontemporaneous tectonomagmatic Hallandian event in the Eastern Segment of the Sveconorwegian Orogen (e.g. Söderlund *et al.* 2002; Ulmius *et al.* 2015) remains unclear.

The complex nature of the U-Pb zircon data for the Christiansø granite complicate estimation of a precise crystallisation age. Both the weighted average zircon $^{206}Pb/^{238}U$ age of 1458 ± 12 Ma and the lower intercept titanite age of 1448 ± 17 Ma agree with the range of ages for granitoids and gneisses previously determined on Bornholm. However, we note that the weighted average $^{206}Pb/^{238}U$ date may have been moved to a somewhat younger date due to small amounts of Pb loss and discordance. The upper intercept zircon date of 1500 ± 18 Ma and the weighted average $^{207}Pb/^{206}Pb$ date of 1495 ± 14 Ma are significantly older than the ages obtained for other Bornholm granitoids and gneisses, although interestingly these dates are within error of the gneiss and xenolith ages presented in Waight *et al.* (2017). We note that we have made no attempt to remove potentially older zircons from the 'magmatic' population in sample BH19-1, and some of those zircons could represent potentially inherited zircon mineral grains (xenocrysts/restite) that lost large amounts of Pb during incorporation into the host magma. Incorporation of such zircons would shift results to slightly older ages. Because of the dominance of zircon analyses clustering towards the upper intercept, any geological significance of the lower intercept zircon ages for both the inherited and magmatic zircons is poorly constrained.

The Christiansø granite has a geochemical composition that is a perfect match for felsic basement rocks from Bornholm. The sample shows most petrographic and geochemical similarity to more silica-rich lithologies on Bornholm, specifically the Hammer and Almindingen granites and the more leucocratic red variants of orthogneisses present on Bornholm, to which the Christiansø granite also bears a strong physical resemblance. Therefore, we conclude that the basement rocks on Ertholmene can be confidently linked to basement rocks on Bornholm.

The relative abundance of potentially inherited zircons (19 out of 77 accepted analyses) in the Christiansø granite is unusual compared to most felsic basement rocks from Bornholm. In general, the abundance of inherited zircons on Bornholm is low (<5%). However, those that are found mostly have ages between 1.6 and

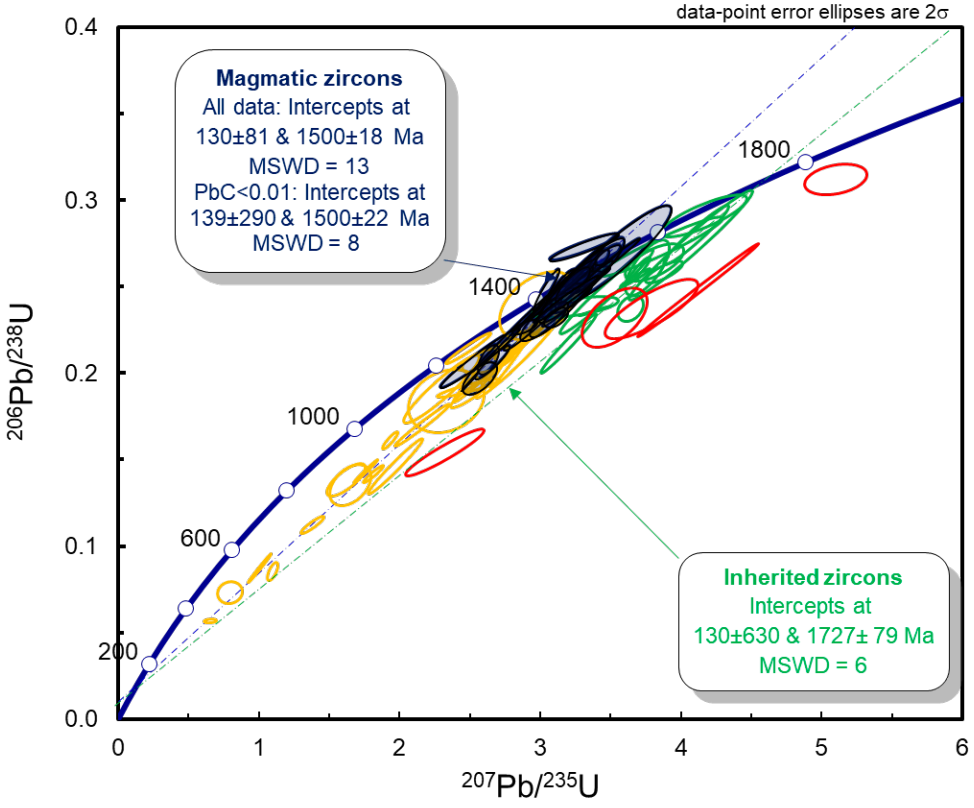

Fig. 5. Wetherill U-Pb Concordia diagram for zircons from sample BH19-1 (excessively discordant analyses, and all analyses with internal 2. S.E. errors > 10 % are excluded). Dark blue shaded ellipses (fraction of common Pb < 0.01) and orange ellipses (fraction of common Pb > 0.01) are interpreted as magmatic and are used to define the upper and lower intercept ages for the 'magmatic' zircons shown. Green ellipses are interpreted as inherited and are used to define the upper and lower intercept ages shown for inherited zircons. Red ellipses likely represent older (*c.* 2 Ga?) inherited zircons, but are not included in any age calculations. MSWD = the Mean Square of the Weighted Deviates (MSWD) for the isochron fit.

1.8 Ga (Waight *et al.* 2012), which is consistent with the involvement of Transscandinavian Igneous Belt rocks as an important source component (Johansson *et al.* 2016). We note that many zircons identified as potentially inherited in BH19-1 have U-Pb systematics consistent with dates of around 1.7–1.8 Ga, and subsequent relatively recent Pb loss (Fig. 5). No rocks of this timespan have been observed on Bornholm. However, they do occur to the north in the Blekinge Province (Johansson *et al.* 2006; Johansson 2016). The abundance of inherited zircons in the Christiansø sample suggests that this granite was emplaced into and contaminated by similar Blekinge or Transscandinavian Igneous Belt rocks.

The degree of disturbance of the zircon population in BH19-1 is also distinct from most felsic rocks from Bornholm where zircons are mostly relatively 'well-behaved', although zircons in a few samples show some evidence for Pb loss (Zariņš & Johansson 2009; Waight *et al.* 2012). We note that some zircons in the Almindingen sample (BH8) analysed by Waight *et al.* (2012) showed significant Pb loss. However, this Pb loss was relatively well-constrained to have occurred at around 400 Ma and likely reflected local disturbance related to intrusion of a nearby dike interpreted to be post-Silurian based on mineralogy and orientation (Jensen 1989). An additional sample from the same quarry dated by Zariņš & Johansson (2009) showed limited evidence for disturbance. Dated gneisses and granitoids from Bornholm are generally fresh and show only minor evidence for alteration (e.g. sericitisation of feldspars). We suggest that the more pronounced disturbance of the U-Pb isotopic system in the zircons from Christiansø, coupled with petrographic evidence for more extensive and higher temperature alteration (i.e. chloritised biotite and saussuritised plagioclase), is related to fluid flow along a nearby major fault, which defines the northern edge of the Christiansø Horst, and the northern margin of the Sorgenfrei–Tornquist Zone (Krzywieca *et al.* 2003; Graversen 2009). Although poorly constrained and of uncertain geological significance, lower intercept ages are consistent with this disturbance occurring during Mesozoic or younger movement on the Sorgenfrei–Tornquist Zone (e.g., Mogensen & Korstgård 2003).

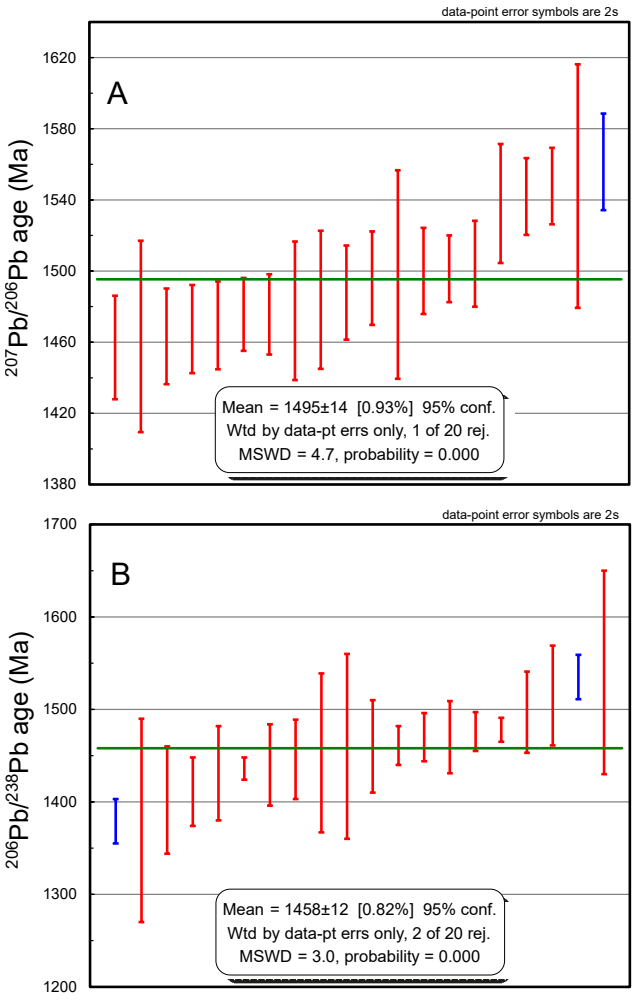

Fig. 6. Weighted mean of (**A**) ^{207}Pb/^{206}Pb and (**B**) ^{206}Pb/^{238}U dates for zircons that are within 3 % of concordance (Wetherill plot). Red bars are ages included in the mean, analyses in blue are excluded.

The general agreement in dates calculated for the near-concordant zircons and the titanites is evidence that both determinations are robust indicators of crystallisation age (albeit with relatively large uncertainties) and shows significant promise for expanded use of combining information from U-Pb in zircon and titanite as a geochronological tool. Titanite can provide important additional geological information due to its somewhat lower closure temperature (*c.* 500–650 °C; e.g. Cherniak 1993), a feature which has been used in for example cooling and metamorphic history studies (e.g. Willigers *et al.* 2001; Kirkland *et al.* 2017). We note, however, that several studies indicate that under some circumstances the closure temperature for Pb in titanite can be considerably higher (e.g. Kohn 2017; Hartnady *et al.* 2019) and thus it can also record crystallisation ages. Titanite can also form as a hydrothermal mineral, and can thus be used to constrain alteration and mineralisation events (e.g., Bell *et al.* 2017; Hart-Madigan *et al.* 2020). This is not the case on Bornholm and Christiansø where petrographic relationships indicate the titanite is a primary phase. U-Pb titanite dates from other felsic rocks from Bornholm are typically within error to 20 Ma younger than zircon dates from the same sample (Zariņš & Johansson 2009) and are consistent with initially rapid cooling, coupled with evidence from other geochronometers for subsequent relatively slow post-crystallisation cooling

on Bornholm (Waight *et al.* 2012). Given the relatively large errors on both the titanite and zircon dates for Christiansø, it is not possible to evaluate any discrepancies related to cooling history and differences in closure temperature between zircon and titanite, but the ages are consistent with crystallisation followed by initially rapid cooling.

The abundant evidence for Pb loss and disturbance in the zircons is interestingly not observed in the titanites, suggesting that the latter phase is more robust to Pb loss. It is beyond the scope of this contribution to discuss this in detail; however, it has been noted that diffusion rates for Pb in titanite are relatively slow and ineffective at temperatures below *c.* 800°C (Kohn 2017) and we speculate that the robust age obtained here may reflect the larger grain size of the titanite crystals compared to zircon, such that the larger crystal volumes of titanite mean that any effects of Pb loss are restricted to smaller grains or the rims of larger crystals (Kirkland *et al.* 2016). We also suggest that the apparent robustness of titanite U-Pb systematics may also reflect generally lower U contents in titanite than zircon and thus less radiation damage. Diffusion experiments in zircon suggest that it should be robust to Pb loss by diffusion alone even at high temperatures (Cherniak & Watson 2001). However, this is clearly not the case at lower temperatures, as U-Pb discordance in zircons is commonly attributed to Pb loss and can be related to degree of radiation damage, particularly if the zircons have been at relatively low temperatures (below natural annealing temperatures of *c.* 360° C) for long periods (e.g., Cherniak & Watson 2001). This is consistent with Rb-Sr ages for mica indicating the Bornholm granites have not been at temperatures over 300–350°C since *c.* 1.37 Ga (Waight *et al.* 2012). Finally, higher common Pb contents in titanite compared with zircon likely reflect the crystal lattice of titanite being more accommodating for incorporation of Pb. Therefore, the radiogenic Pb produced by U decay in titanite is more tightly bound to the crystal lattice than in zircon and less prone to Pb loss.

Conclusions

A sample of the granite making up the small islands of Christiansø and Frederiksø north of Bornholm was investigated petrographically and geochemically and dated isotopically using U-Pb in zircon and titanite. The sample is a reddish, equigranular, leucocratic biotite granite with evidence for alteration (epidote in plagioclase and biotite altered to chlorite). The granite is ferroan, metaluminous, alkali-calcic and has essentially identical major and trace element characteristics to other felsic basement rocks on Bornholm.

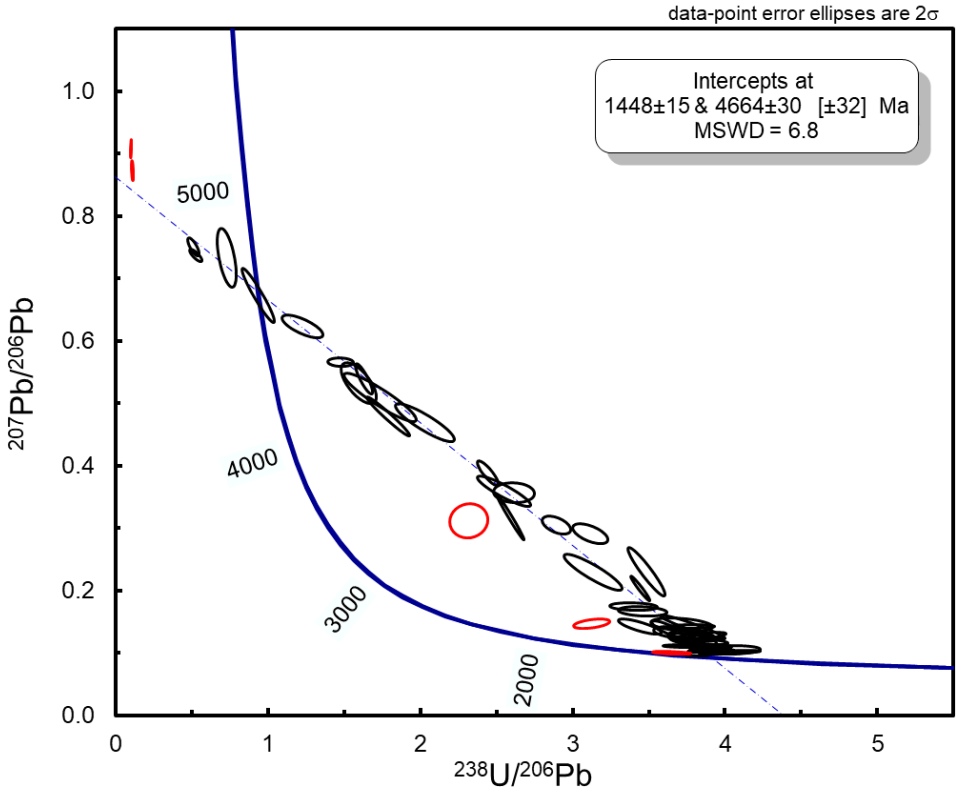

Fig. 7. Tera-Wasserburg plot for titanites from sample BH19-1. Black ellipses are used to define the lower intercept age shown, red ellipses are analyses excluded from the age calculation.

Zircon U-Pb systematics in the sample are complex, and include a significant number of zircon grains considered to be inherited. Many of the zircons have suffered relatively recent Pb loss. Removal of highly disturbed and imprecise analyses, and of inherited zircons, yields a poorly constrained upper intercept age of 1500 ± 18 Ma (MSWD = 13). Weighted average ages of 1495 ± 14 Ma (MSWD = 4.7) ($^{207}Pb/^{206}Pb$) and 1458 ± 12 Ma (MSWD = 3) ($^{206}Pb/^{238}U$) are obtained from those zircons that are within 3% of concordance. The discrepancy between these ages likely reflects inclusion of inherited zircons that suffered large degrees of Pb loss during incorporation in the host magma, and small amounts of Pb loss. U-Pb systematics in titanite yield an age of 1448 ± 15 Ma (MSWD = 6.8) that is within error of the weighted average $^{206}Pb/^{238}U$ zircon age. The disturbance of the zircons, and the alteration of the granite, are likely the result of the proximity to the major fault zone defining the northern edge of the Sorgenfrei–Tornquist Zone. Titanite does not show the same effects of Pb loss as zircon, suggesting that in this location it has been more robust during the Pb loss event. Most of the inherited zircons have suffered Pb loss, however they are mostly *c.* 1.7–1.8 Ga in age, consistent with inherited zircon ages observed on Bornholm. The greater abundance of inherited zircons compared to Bornholm may suggest intrusion into, and contamination by, nearby unexposed Transscandinavian Igneous Belt rocks.

Acknowledgements

Jens Peter Koefoed (Christiansø administration) and Jill Grønberg Nothlev (Naturstyrelsen, Bornholm, Miljø- og Fødevareministeriet) are thanked for permission to collect samples on Christiansø. Clara-Marie and Magnus Waight are thanked for being most excellent field assistants. Mojagan Alaei and other staff at GEUS are thanked for excellence in zircon separation and preparation. Åke Johansson and Paul Martin Holm are thanked for their insightful, thorough and helpful reviews, which helped sharpen the manuscript, and Richard Wilson is thanked for editorial handling and patience.

References

Åberg, G. 1988: Middle Proterozoic anorogenic magmatism in Sweden and worldwide. Lithos 21, 279–289. https://doi.org/10.1016/0024-4937(88)90033-3

Andersen, T. 2002: Correction of common lead in U–Pb analyses that do not report 204Pb. Chemical Geology 192, 59 – 79. https://doi.org/10.1016/S0009-2541(02)00195-X

Bell, R-M., Kolb, J., Waight, T.E., Bagas, L. & Thomsen, T. 2017: A Palaeoproterozoic multi-stage hydrothermal alteration system at Nalunaq gold deposit, South Greenland. Mineralium Deposita 52, 383–404. https://doi.org/10.1007/s00126-016-0667-7

Bogdanova, S., Gorbatschev, R., Grad, M., Guterch, A., Janik, T., Kozlovskaya, E., Motuza, G., Skridlaite, G., Starostenko, V. & Taran, L. 2006: EUROBRIDGE: new insight into the geodynamic evolution of the East European Craton. Geological Society, London, Memoirs 32, 599–625. https://doi.org/10.1144/gsl.mem.2006.032.01.36

Čečys, A. 2004: Tectonic implications of ca. 1.45 Ga granitoid magmatism at the southwestern margin of the East European Craton. LITHOLUND thesis 6, 29 pp.

Čečys, A., Bogdanova, S., Janson, C., Bibikova, E. & Kornfält, K.-A. 2002: The Stenshuvud and Tåghusa granitoids: new representatives of Mesoproterozoic magmatism in southern Sweden. GFF 124, 149–162. https://doi.org/10.1080/11035890201243149

Cherniak, D. 1993: Lead diffusion in titanite and preliminary results on the effects of radiation damage on Pb transport. Chemical Geology 110, 177–194. https ://doi.org/10.1016/0009-2541(93)90253-F

Cherniak, D.J. & Watson, E.B. 2001: Pb diffusion in zircon. Chemical Geology 172, 5–24. https://doi.org/10.1016/S0009-2541(00)00233-3

Chew, D.M., Petrus, J.A. & Kamber, B.S. 2014: U–Pb LA–ICPMS dating using accessory mineral standards with variable common Pb. Chemical Geology 363, 185–199. https://doi.org/10.1016/j.chemgeo.2013.11.006

EUGENO-S Working Group 1987: Crustal structure and tectonic evolution of the transition between the Baltic Shield and the North German Caledonides (the EUGENO-S Project). Tectonophysics 150, 253–348. https://doi.org/10.1016/0040-1951(88)90073-x

Frost, B. & Frost, C.D. 2008: A geochemical classification for feldspathic igneous rocks. Journal of Petrology 49, 1955–1969. https://doi.org/10.1093/petrology/egn054

Frost, B.R., Barnes, C.G., Collins, W.J., Arculus, R.J., Ellis, D.J. & Frost, C.D. 2001: A geochemical classification for granitic rocks. Journal of Petrology 42, 2033–2048. https://doi.org/10.1093/petrology/42.11.2033

Graversen, O. 2009: Structural analysis of superposed fault systems of the Bornholm horst block, Tornquist Zone, Denmark. Bulletin of the Geological Society of Denmark 57, 25–49. https://doi.org/10.37570/bgsd-2009-57-02

Hart-Madigan, L., Wilkinson, J.J., Lasalle, S. & Armstrong, R.N. 2020: U-Pb dating of hydrothermal titanite resolves multiple phases of propylitic alteration in the Oyu Tolgoi porphyry district, Mongolia. Economic Geology 115, 1605–1618. https://doi.org/10.5382/econgeo.4780

Hartnady, M.I.H., Kirkland, C.L., Clark, C., Spaggiari, C.V., Smithies, R.H., Evans, N.J. & McDonald, B.J. 2019: Titanite

dates crystallization: Slow Pb diffusion during supersolidus re-equilibration. Journal of Metamorphic Geology 37, 823–838. https://doi.org/10.1111/jmg.12489

Hellstrom, J., Paton, C., Woodhead, J. & Hergt, J. 2008: Iolite: software for spatially resolved LA-(quad and MC) ICPMS analysis. Mineralogical Association of Canada short course series 40, 343–348.

Holm, P.M., Pedersen, L.E. & Hojsteen, B. 2010: Geochemistry and petrology of mafic Proterozoic and Permian dykes on Bornholm, Denmark: Four episodes of magmatism on the margin of the Baltic Shield. Bulletin of the Geological Society of Denmark 58, 35–65. https://doi.org/10.37570/bgsd-2010-58-04

Jackson S.E., Pearson, N.J., Griffin, W.L. & Belousova, E.A. 2004: The application of laser ablation-inductively coupled plasma mass spectrometry to in situ U–Pb zircon geochronology. Chemical Geology 211, 47–69. https://doi.org/10.1016/j.chemgeo.2004.06.017

Jensen, Aa. 1989: The Bjergebakke dyke – a kullaite from Bornholm. Bulletin of the Geological Society of Denmark 37, 123–140.

Johansson, Å. 2016: U-Pb SIMS dating of some granitoids from eastern Blekinge, southern Sweden. GFF 138, 430–444. https://doi.org/10.1080/11035897.2016.1146328

Johansson, Å., Bogdanova, S. & Cecys, A. 2006: A revised geochronology for the Blekinge Province, southern Sweden. GFF 128, 287–302. https://doi.org/10.1080/11035890601284287

Johansson, Å., Waight, T.E., Andersen, T. & Simonsen, S.L. 2016: Geochemistry and petrogenesis of Mesoproterozoic A-type granitoids from the Danish island of Bornholm, southern Fennoscandia. Lithos 244, 94–108. https://doi.org/10.1016/j.lithos.2015.11.031

Katzung, G. 1996: Sandstone dykes in the Vang granite, northwestern Bornholm. Bulletin of the Geological Society of Denmark 43, 51–53. https://doi.org/10.37570/bgsd-1996-43-06

Kirkland, C.L., Hollis, J., Danišík, M., Petersen, J., Evans, N.J. & McDonald, B.J. 2017: Apatite and titanite from the Karrat Group, Greenland; implications for charting the thermal evolution of crust from the U-Pb geochronology of common Pb bearing phases. Precambrian Research 300, 107–120. https://doi.org/10.1016/j.precamres.2017.07.033

Kirkland, C.L., Spaggiari, C.V., Johnson, T.E., Smithies, R.H., Danišík, M. Evans, N., Wingate, W.W.D., Clark, C., Spenser, C., Mikucki, E. & McDonald, B.J. 2016: Grain size matters: Implications for element and isotopic mobility in titanite. Precambrian Research 278, 283–302. http://dx.doi.org/10.1016/j.precamres.2016.03.002

Kofoed, A.E. 1961: Christiansøs historie, 282 pp. Rønne: Bornholms Historiske Samfund.

Kohn, M. J. 2017: Titanite petrochronology. Reviews in Mineralogy and Geochemistry 83, 419–441. https://doi.org/10.2138/rmg.2017.83.13

Kornfält, K-A. 1993: U-Pb zircon ages of three granite samples from Blekinge County, south-eastern Sweden. Sveriges Geologiska Undersökning Serie C 823, 17–23.

Kornfält, K-A. 1996: U-Pb zircon ages of six granite samples from Blekinge County, southeastern Sweden. Sveriges Geologiska Undersökning Serie C 828, 15–31.

Krzeminska, E., Johansson, Å.E., Krzeminski, L., Wiszniewska, J., Williams, I.S., Zdzisław, P. & Sylwester, S. 2021: Basement correlation across the southernmost Baltic Sea: Geochemical and geochronological evidence from onshore and offshore deep drill cores, northern Poland. Precambrian Research 362, 106300. https://doi.org/10.1016/j.precamres.2021.106300

Krzywieca, P., Kramarskab, R. & Zientara, P. 2003: Strike-slip tectonics within the SW Baltic Sea and its relationship to the inversion of the Mid-Polish Trough – evidence from high-resolution seismic data. Tectonophysics 373, 93–105. https://doi.org/10.1016/s0040-1951(03)00286-5

Ludwig, K.R. 1998: On the treatment of concordant uranium-lead ages. Geochimica et Cosmochimica Acta 62, 665–676. https://doi.org/10.1016/S0016-7037(98)00059-3

Ludwig, K.R. 2008: User's Manual for Isoplot 3.70: A geochronological toolkit for Microsoft Excel. Berkeley Geochronology Center Special Publication 4, 76 pp.

Middlemost, E.A.K. 1994: Naming materials in the magma/igneous rock system. Earth-Science Reviews 37, 215–224. https://doi.org/10.1016/0012-8252(94)90029-9

Mogensen, T.E. & Korstgård, J.A. 2003: Triassic and Jurassic transtension along part of the Sorgenfrei–Tornquist Zone in the Danish Kattegat. Geological Survey of Denmark and Greenland Bulletin 1, 439–458.

Obst, K., Hammer, J., Katzung, J. & Korich, D. 2004: The Mesoproterozoic basement in the southern Baltic Sea: insights from the G 14-1 off-shore borehole. International Journal of Earth Sciences 93, 1–12. https://doi.org/10.1007/s00531-003-0371-6

Paton, C., Woodhead, J.D., Hellstrom, J.C., Hergt, J.M., Greig, A. & Maas, R. 2010: Improved laser ablation U-Pb zircon geochronology through robust downhole fractionation correction. Geochemistry, Geophysics, Geosystems 11, 1–36, Article number Q0AA06. https://doi.org/10.1029/2009GC002618

Paton, C., Hellstrom, J., Paul, B., Woodhead, J. & Hergt, J. 2011: Iolite: Freeware for the visualisation and processing of mass spectrometric data. Journal of Analytical Atomic Spectrometry 26, 2508–2518. https://doi.org/10.1039/C1JA10172B

Petrus, J.A. & Kamber, B.S. 2012: VizualAge: A novel approach to laser ablation ICP-MS U-Pb geochronology data reduction. Geostandards and Geoanalytical Research 36, 247–270. https://doi.org/10.1111/j.1751-908X.2012.00158.x

Pearce, J.A., Harris, N.B.W. & Tindle, A.G. 1984: Trace element discrimination diagrams for the tectonic interpretation of granitic rocks. Journal of Petrology 25, 956–983. https://doi.org/10.1093/petrology/25.4.956

Slama, J., Kosler, J., Condon, D.J., Crowley, J.L., Gerdes, A., Hanchar, J.M., Horstwood, M.S.A., Morris, G.A., Nasdala, L., Norberg, N., Schaltegger, U., Schoene, N., Tubrett, M.N. & Whitehouse, M.J. 2008: Plešovice zircon – a new natural reference material for U-Pb and Hf isotopic microanalysis. Chemical Geology 249, 1–35. https://doi.org/10.1016/j.chemgeo.2007.11.005

Söderlund, U., Möller, C., Andersson, J., Johansson, L. & Whitehouse, M. 2002: Zircon geochronology in polymetamorphic gneisses in the Sveconorwegian orogen, SW Sweden: ion microprobe evidence for 1.46–1.42 and 0.98–0.96 Ga reworking. Precambrian Research 113, 193–225. https://doi.org/10.1016/s0301-9268(01)00206-6

Spandler, C., Hammerli, J., Sha, P., Hilbert-Wolf, H., Hu; Y., Roberts, E. & Schmitz, M. 2016: MKED1: A new titanite standard for in situ analysis of Sm–Nd isotopes and U–Pb geochronology. Chemical Geology 425, 110–126. https://doi.org/10.1016/j.chemgeo.2016.01.002

Spencer, K.J., Hacker, B.R., Kylander-Clark, A.R.C., Andersen, T.B., Cottle, J.M., Stearns, M.A., Poletti, J.E. & Seward, G.G.E. 2013: Campaign-style titanite U–Pb dating by laser-ablation ICP: Implications for crustal flow, phase transformations and titanite closure. Chemical Geology 341, 84–101. http://dx.doi.org/10.1016/j.chemgeo.2012.11.012

Sun, S.S. & McDonough, W.F. 1989: Chemical and isotopic systematics of oceanic basalts. Implications for mantle composition and processes. In: Saunders, A.D. & Norry, M.J. (Eds.), Magmatism in Ocean Basins. Geological Society, London, Special Publication 42, 313–345. https://doi.org/10.1144/gsl.sp.1989.042.01.19

Tera, F. & Wasserburg, G. 1972: U-Th-Pb systematics in three Apollo 14 basalts and the problem of initial Pb in lunar rocks. Earth and Planetary Science Letters 14, 281–304. https://doi.org/10.1016/0012-821X(72)90128-8

Ulmius, J., Andersson, J. & Möller, C. 2015: Hallandian high temperature metamorphism at 1.45 Ga in continent Baltica: P-T evolution and SIMS U-Pb zircon ages of aluminous gneisses, SW Sweden. Precambrian Research 265, 10–39. https://doi.org/10.1016/j.precamres.2015.04.004

Waight, T.E., Frei, D. & Storey, M. 2012: Geochronological constraints on granitic magmatism, metamorphism, cooling and uplift on Bornholm, Denmark. Bulletin of the Geological Society of Denmark 60, 23–46. https://doi.org/10.37570/bgsd-2012-60-03

Waight, T.E., Serre, S.H., Næsby, S.H. & Thomsen, T.B. 2017: The ongoing search for Denmark's oldest rock: new U-Pb zircon ages for a quartz-rich xenolith and country rock from the Svaneke Granite, Bornholm. Bulletin of the Geological Society of Denmark 65, 75–86. https://doi.org/10.37570/bgsd-2017-65-06

Willigers, B.J.A., Krogstad, E.J. & Wijbrans, J.R. 2001: Comparison of thermochronometers in a slowly cooled granulite terrain: Nagssugtoqidian Orogeny, West Greenland. Journal of Petrology 42, 1729–1749. https://doi.org/10.1093/petrology/42.9.1729

Zariņš, K. & Johansson, Å. 2009: U–Pb geochronology of gneisses and granitoids from the Danish island of Bornholm: new evidence for 1.47–1.45 Ga magmatism at the southwestern margin of the East European Craton. International Journal of Earth Sciences (Geologische Rundschau) 98, 1561–1580. https://doi.org/10.1007/s00531-008-0333-0

Macrofossil studies of Lateglacial sediments from Regstrup, north-west Sjælland, Denmark

OLE BENNIKE, LONE CLAUDI-HANSEN, BETINA MAGNUSSEN & PETER WIBERG-LARSEN

Geological Society of Denmark
https://2dgf.dk

Received 1 December 2021
Accepted in revised form
20 February 2022
Published online
30 March 2022

Bennike, O., Claudi-Hansen, L., Magnussen, B. & Wiberg-Larsen, P. 2022: Macrofossil studies of Lateglacial sediments from Regstrup, north-west Sjælland, Denmark. Bulletin of the Geological Society of Denmark, Vol. 70, pp. 39–51. ISSN 2245-7070. https://doi.org/10.37570/bgsd-2022-70-04

Studies of macrofossils indicate that the vegetation near Regstrup in north-west Sjælland, Denmark, from *c.* 13 600 to 13 500 cal. years BP was dominated by dwarf-shrub heaths. *Betula pubescens* (downy birch) arrived at *c.* 13 500 cal. years BP and became common after *c.* 13 200 cal. years BP. Open forests with *B. pubescens* and *Populus tremula* (aspen) dominated until *c.* 12 500 cal. years BP, indicating that an Allerød-type environment persisted for *c.* 350 years after the cooling at the onset of the Younger Dryas, which is dated to *c.* 12 850 years BP in ice cores from Greenland. Betula nana was common after *c.* 12 500 cal. years BP, indicating a return to a tundra-like landscape with dwarf-shrub heaths. The fauna included *Rangifer tarandus* (reindeer), *Castor fiber* (Eurasian beaver) and possibly *Lemmus lemmus* (Norway lemming). The lake deposits contain remains of many species of aquatic plants and animals, including three species of fish. The flora and fauna indicate that the lake water was fairly nutrient-rich and alkaline.

Keywords: Lateglacial, Allerød, Younger Dryas, vegetation history, fauna history, Denmark.

Ole Bennike [obe@geus.dk], Geological Survey of Denmark and Greenland (GEUS), C.F. Møllers Allé 8, DK-8000 Aarhus C, Denmark. Lone Claudi-Hansen [lch@vestmuseum.dk], Museum Vestsjælland, Forten 10, DK-4300 Holbæk, Denmark. Betina Magnussen [betina.magnussen@sund.ku.dk], GLOBE Institute, SUND, University of Copenhagen, Øster Voldgade 5-7, DK-1350 København K. Peter Wiberg-Larsen [pwl@ecos.au.dk], Institute for Ecoscience, Aarhus University, Vejlsøvej 25, DK-8600 Silkeborg, Denmark.

Prior to the extension of the Holbæk highway towards the west, Museum Vestsjælland conducted archaeological investigations. South of the village Regstrup, two small basins with Lateglacial sediments were encountered (Fig. 1). During the excavations, a fragment of a small antler and a mandible of reindeer (*Rangifer tarandus*) were found, as well as jaws with teeth of pike (*Esox lucius*), bones and scales of perch (*Perca fluviatilis*) and a leaf of *Dryas octopetala*. The fauna and flora, thus, indicated a Lateglacial age and finds of a scraper of flint and some flint flakes show that hunters visited the area.

The basins probably formed after the last deglaciation by melting of bodies of buried stagnant ice. Plant and animal remains were well-preserved and it was decided to conduct macrofossil analyses of samples that had been collected during the archaeological field work. The samples were taken from open sections from trenches.

Studies of the vegetation history of Denmark go back almost 200 years, but many details of Lateglacial and Holocene vegetation and environmental changes are still poorly known (Bennike & Mortensen 2018). The aim of this paper is to describe and interpret the results of the macrofossil studies of the sediments from Regstrup, from small basins in north-west Sjælland, Denmark. The study is the first radiocarbon dated macrofossil study of Lateglacial deposits from this region (Mortensen *et al.* (2014a). We compare the results with other recent detailed palaeoecological studies of Lateglacial deposits in Denmark (Bennike *et al.* 2004; Mortensen *et al.* 2011, 2014a, b; Fischer *et al.* 2013; Bennike & Mortensen 2018; Wiberg-Larsen *et al.* 2019).

Study area

The studied basins are located in north-western Sjælland, *c.* 9 km south-west of Holbæk (Fig. 1). The basins are small and measure only some tens of metres across. Because of the small size of the basins, they are suitable for plant macrofossil analyses. The sites are located *c.* 32 m above sea level and the basins may have formed as bodies of stagnant ice melted – or perhaps simply as groundwater filled depressions in the glacial landscape. The geographical coordinates of the sites are 55.66°N, 11.61°E (site 1, all samples except JP335) and 55.66°N, 11.64°E (site 2, sample JP 335). The distance between the basins is 1400 m.

The region was glaciated during the last glacial maximum and was deglaciated about 17 000 years BP, according to cosmogenic surface exposure dating of large erratic boulders from the region (Houmark-Nielsen *et al.* 2012). However, bodies of stagnant ice characterised the region for a long time after active glacier ice disappeared. The pre-Quaternary strata of the region are dominated by Paleocene clay, but Danian limestone and Cretaceous chalk is found to the north and east (Håkansson & Pedersen 1992) and the tills in the region are rich in fragments of limestone and chalk. The Regstrup area is dominated by clayey till with small areas of glaciofluvial sand (Milthers 1943) and nowadays by farmland with villages and it has probably been deforested for several millennia. The natural vegetation would probably be *Fagus sylvestris* dominated forests on well-drained soils and *Alnus glutinosa* dominated forests on wet soils. The climate is temperate; the mean July temperature was 16.2°C and the mean annual precipitation was 584 mm during the period from 1961 to 1990 (DMI 2019).

Methods

Profiles through the Lateglacial lake sediments were exposed by excavating trenches through the basins and the sediments were mapped and described by archaeologists from Museum Vestsjælland. Samples were collected from open sections. The samples consisted of a 1 m long sediment monolith and several kg-large bulk sediment samples. The monolith was carefully cleaned, and 50 contiguous samples of 2 cm length were taken for macrofossil analysis. The samples were wet sieved on 0.4 and 0.2 mm sieves and sub-samples on a 0.1 mm sieve. The residues left on the sieves were transferred to petri dishes and analysed using a dissecting microscope. Plant and animal remains were identified using reference material as well as keys and illustrations in various books and scientific papers such as Kaiser (1977), Henderson (1990), Brooks *et al.* (2007) and Rinne & Wiberg-Larsen (2017).

Selected identified macrofossils of terrestrial plants from four levels from the monolith and from one of the bulk samples were dried and submitted for accelerator mass spectrometry (AMS) radiocarbon dating. Dating was carried out at the Ångström Laboratory, University of Uppsala and at Aarhus AMS Centre, Aarhus University. The samples were treated with HCl to remove carbonates and with NaOH to remove humic acids, which may represent contamination

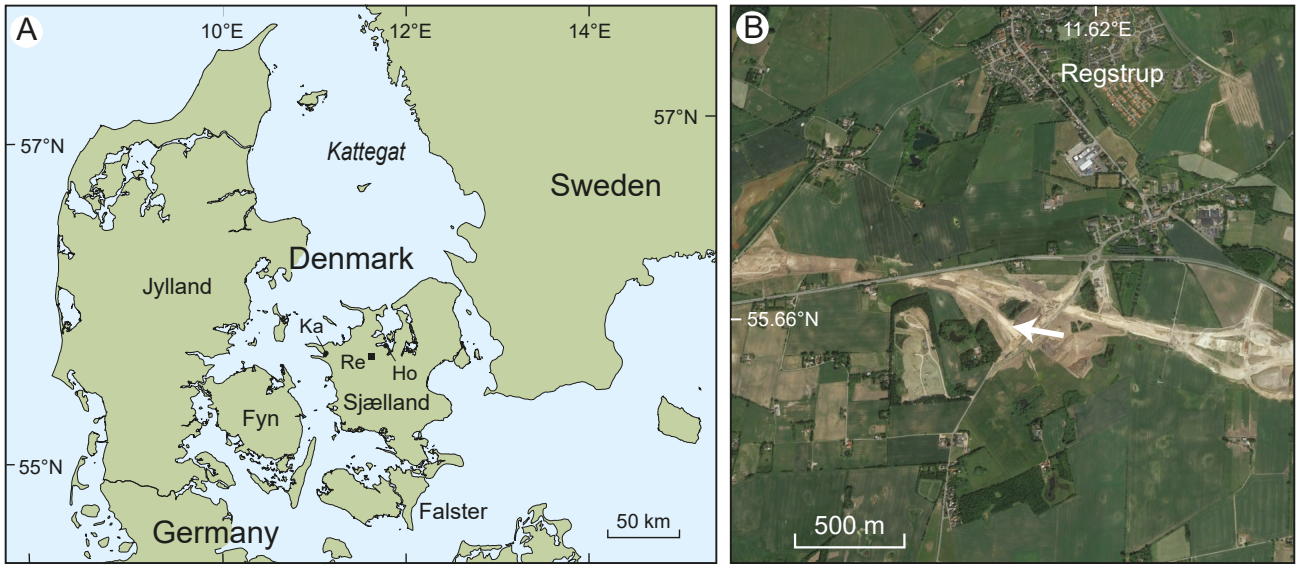

Fig. 1. A. Map of Denmark showing the location of the study sites. Re: Regstrup, Ho: Holbæk, Ka: Kalundborg. **B.** Google Earth satellite image of the study area.

Table 1. AMS radiocarbon age determinations from Regstrup, north-west Sjælland, Denmark
The samples are from site 1, except JP335 that is from site 2

Laboratory number	Depth cm/sample	Layer	Species	Age (^{14}C years BP)[1]	Calibrated age (years BP)[2]	Cal. age (yrs BP)[3]	Cal. age (years BC)[2]
Ua-58868	38–40	8	*Menyanthes trifoliata*	10514 ± 43	12206–12678	12550	10257–10729
Ua-58869	55–56	8	*Betula pubescens*	10663 ± 44	12514–12738	12691	10565–10789
Ua-58870	76–78	9	*Betula pubescens*	10838 ± 44	12728–12833	12766	10779–10884
Ua-58871	96–98	12	*Betula pubescens*	11726 ± 47	13482–13746	13568	11533–11797
Ua-58872	JP 314	10	*Arctostaphylos uva-ursi*	11367 ± 45	13164–13323	13244	11215–11374
AAR-29889	JP 335	6	*Menyanthes trifoliata*	10912 ± 48	12743–12918	12815	10794–10969
Ua-59941	1082x200		*Rangifer tarandus*	5853 ± 33	6560–6746	6674	4611–4797
Ua-59941	1082x200		*Rangifer tarandus*	5775 ± 99	6318–6791	6575	4369–4842

[1]Radiocarbon ages are reported in conventional radiocarbon years BP (before present = 1950; Stuiver & Polach (1977)).
The C ages have been corrected for isotopic fractionation by normalizing to a δ^{13}C value of –25 ‰.
[2]Calibration to calendar years BP/BC is according to the INTCAL20 data (Reimer et al. 2020). [3]Median probability ages.

from younger deposits. A reindeer antler was also dated, using the collogen fraction. The radiocarbon ages were calibrated to calendar years before present (BP) using the CALIB program (Stuiver *et al.* 2021), which calibrates to calendar years according to the INTCAL20 calibration curve (Reimer *et al.* 2020). The widespread occurrence of carbonate-rich glacial deposits in Denmark results in large hard-water effects, and thus it is important to use remains of terrestrial plants or animals for dating. Four samples from the monolith and one sample from the bulk sample were dated (Table 1).

Results and discussion

Sediments, dating and sedimentation rates

The Lateglacial sediments consisted of mineral-rich and organic-rich sediments. The organic-rich sediments were described as peat in the field, but the occurrence of numerous remains of fish and other aquatic animals and plants show that the sediments should be classified as coarse detritus gyttja. The succession at site 1 consisted of sand and gravel, clayey gyttja, calcareous gyttja, detritus gyttja, sandy clay, decomposed peat and clay. At site 2 the succession consisted of grey gyttja, coarse detritus gyttja and decomposed peat.

Four samples from the monolith from site 1 were dated, yielding median probability ages between 12 550 and 13 568 cal. years BP (Table 1). Calibrated ages for the monolith are plotted versus depth in Fig. 2. According to the age–depth curve the sedimentation rate was *c.* 0.25 mm/year in the lower part of the succession, and *c.* 1.52 mm/year in the middle and upper part. The chronology in the middle and upper part of the dated succession is well constrained, whereas the chronology of the lower part of the succession is more uncertain. An endocarp of *Arctostaphylos uva-ursi* from bulk sediment sample JP 314 gave a median probability age of 13 244 cal. years BP, corresponding to the Allerød period. Dating of seeds of *Menyanthes trifoliata* from bulk sample JP 335 from site 2 gave a median probability age of 12 815 cal. years BP, corresponding to an earliest Younger Dryas age (Table 1). Finally, a cast reindeer antler fragment gave a Mid-Holocene age (Bennike *et al.* 2021).

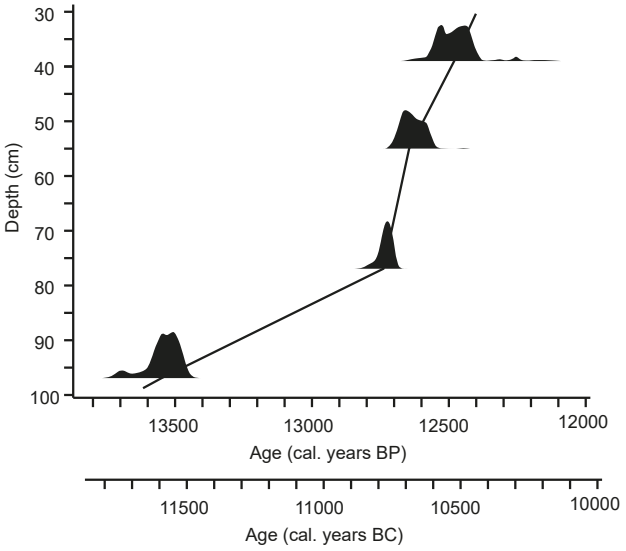

Fig. 2. Age–depth model for the succession from site 1 from Regstrup, north-west Sjælland.

Macrofossils

The results of the macrofossil analyses are presented in a macrofossil concentration diagram (Fig. 3) and in Table 2. The diagram is divided by visual inspection into four local macrofossil assemblage zones that are described and discussed in the following. The upper part of the succession did not contain any macrofossils, hence the diagram only covers *c.* 70 cm.

Zone 1 (13 500–13 600 cal. years BP)

Zone 1 is characterised by the woody plants *Dryas octopetala* and *Betula nana*. In addition, a few remains of *Salix* sp. were found. Herbaceous plants are represented by *Minuartia* sp. and bryophytes are represented by *Distichium* sp. and *Ditrichum* sp., which are often pioneer species on calcareous soils. The bryophyte *Tomentypnum nitens* and the rush *Juncus* sp. often grows in wet soil. Remains of macrolimnophytes are rare and represented by a few endocarps of *Potamogeton natans*, *P. perfoliatus* and *Stuckenia filiformis* (syn. *Potamogeton filiformis*). Aquatic invertebrates are represented by chironomids (head capsules), *Sialis* sp. (alder fly, mandibles) and the small bivalve *Pisidium* sp. Plants and invertebrates began to colonise the small lake and decreasing content of clay, silt and sand in the sediment shows that inwash of minerogenic sediment to the lake decreased. The vegetation around the lake was characterised by dwarf-shrub heaths with *D. octopetala*, *B. nana* and *Salix* sp., with some *B. pubescens*.

Zone 2 (12 650–13 500 cal. years BP)

Betula pubescens remains dominate this zone and in addition, rare remains of *Populus tremula* are found. Remains of *Dryas octopetala* were found in two samples; other woody plants are represented by *Salix* sp. and a single endocarp of *Rubus saxatilis*.

Herbaceous plants are represented by *Minuartia* sp., *Thalictrum alpinum* and *Taraxacum* sp. Plants characteristic of wet soils include *Selaginella selaginoides* that is represented by two megaspores and several species of bryophytes. Aquatic plants are dominated by *Carex rostrata*, in addition fruits of *Ranunculus* sect. *Batrachium* sp., *Hippuris vulgaris* and five species of *Potamogeton* were found. Remains of aquatic invertebrates include egg cocoons of the leaches *Erpobdella* sp. and *Piscicola geometra*, mandibles of the alder fly *Sialis* sp., shells of gastropods and numerous shells of *Pisidium* spp. and statoblasts of the bryozoan *Cristatella mucedo*. The common remains of macrolimnophytes and freshwater invertebrates clearly show that the deposit is of lacustrine origin. The lake housed a rich flora and fauna that indicate that the water was alkaline. Only little clay, silt and sand was washed out into the basin. The vegetation around the lake was dominated by open birch forests with scattered *Populus tremula*, *Dryas octopetala* and other woody plants, herbs and mosses.

Zone 3 (12 500–12 650 cal. years BP)

This zone is also dominated by *Betula pubescens;* in adition remains of *Betula nana* are found and *Populus*

Table 2. Macrofossils in bulk samples from Regstrup, Denmark. The samples are from site 1, except JP335 that is from site 2

	Terrestrial plants															Swamp plants				Aquatic plants																		Aquatic invertebrates								
	Betula nana	*Betula pubescens*	*Populus tremula*	*Salix* sp.	*Arctostaphylos uva-ursi*	*Potentilla* sp.	*Papaver* sect. *Scapiflora*	*Urtica dioeca*	*Selaginella selaginoides*	*Distichium* sp.	*Hylocomium splendens*	*Comarum palustre*	*Climacium dendroides*	*Tomenthyphum nitens*	*Chara* sp.	*Batrachium* sp.	*Menyanthes trifoliata*	*Carex rostrata*	*Alisma plantago-aquatica*	*Nuphar pumila*	*Myriophyllum* sp.	*Hippuris vulgaris*	*Sparganium erectum*	*Potamogeton natans*	*Potamogeton alpinus*	*Potamogeton perfoliatus*	*Potamogeton praelongus*	*Potamogeton obtusifolius*	*Potamogeton pusillus*	*Stuckenia filiformis*	*Erpobdella* sp.	*Piscicola geometra*	*Valvata cristata*	*Valvata piscinalis*	*Hippeutis complanatus*	*Stagnicola palustris*	*Armiger crista*	*Pisidium* sp.	*Cristatella mucedo*
JP 314	–	a	12	–	2	–	–	–	1	–	c	–	1	–	a	–	–	–	–	–	–	1	1	6	–	5	–	–	–	8	2	–	1	1	–	–	2	a	c
JP 320	2	a	–	1	–	–	–	–	–	1	–	–	–	–	r	–	–	a	–	–	1	1	–	–	–	–	–	–	–	1	–	c	c	–	–	–	a	–
JP 321	–	a	–	–	2	–	–	–	1	–	–	–	–	–	1	–	–	a	1	–	1	–	–	c	–	2	–	–	–	r	–	2	1	c	–	–	–	c	a
JP 322	a	a	c	r	–	5	–	–	–	–	r	1	–	–	a	1	a	a	–	–	–	1	2	c	5	–	1	–	–	1	1	–	–	r	2	–	–	r	a
JP 332	2	4	–	–	–	–	–	–	–	–	–	–	–	1	r	1	–	a	–	–	–	–	–	8	–	4	–	–	–	1	–	–	–	c	–	–	–	a	3
JP 334	–	c	1	–	–	–	–	–	–	–	–	–	–	–	r	1	6	c	–	–	1	–	–	3	5	–	–	–	–	–	1	–	–	–	–	–	–	–	r
JP 335	–	c	–	–	–	–	1	6	–	–	–	–	–	–	r	10	2	c	–	1	–	7	–	c	c	–	–	1	c	–	1	1	r	c	–	2	–	c	3

r: rare, c: common, a: abundant

tremula remains are surprisingly common. Herbaceous plants are only represented by two achenes of *Potentilla* sp. Remains of aquatic plants are also in this zone dominated by achenes of *Carex rostrata* and in addition, seeds of *Menyanthes trifoliata* are frequent, whereas *Myriophyllum* sp. remains are rare. *Potamogeton* spp. are represented by the same five species as in zone 2. Invertebrate remains are confined to an egg capsule of *Erpobdella* sp., a few mandibles of *Sialis* sp. and some statoblasts of *Cristatella mucedo*. The vegetation around the lake was still dominated by *Betula* forests, but *Populus tremula* played an important role. Dwarf shrubs and herbs were apparently rare and the forests around the lake may have been so dense that heliophytes became rare.

It should be noted that no remains of *Pinus sylvestris* were recorded. In Danish Lateglacial deposits pollen grains of *Pinus* are often abundant, and it has been proposed that pine had immigrated to Denmark during the Allerød period (Iversen 1947, 1954, 1973). However, so far no macrofossils of pine have been reported (Mortensen *et al.* 2014a) even though macrofossil studies have been conducted from a fairly large number of Lateglacial sites in Denmark. Thus it appears that pine did not grow in Denmark during the Lateglacial.

Zone 4 (12 400–12 500 cal. years BP)

In zone 4 only few remains of *Betula pubescens* were found. Instead, remains of *Betula nana* are common, and *Populus tremula* is missing. A few remains of *Potentilla* sp. and *Selaginella selaginoides* were found. Macrolimnophytes are represented by *Ranunculus* sect. *Batrachium* sp., *Menyanthes trifoliata* and *Carex rostrata* that are found in the lower part of the zone, where *Cristatella mucedo* also occurs. Apparently, macrolimnophyte vegetation disappeared from the lake during zone 4, and the sediment changes from gyttja to poorly sorted gravel that was probably deposited in the lake basin due to solifluction. The vegetation around the lake became more open and tree birch was replaced by dwarf birch; the warmth-demanding *P. tremula* disappeared. The area was, thus, characterised by an open tundra landscape with dwarf shrub heaths, presumably due to cooling during the Younger Dryas period.

The shift from *Betula pubescens* dominated forests with *Populus tremula* to *Betula nana* dominated tundra is dated to *c.* 12 500 cal. years BP. In the Greenland ice cores the shift from the relatively warm Greenland Interstadial 1 to the cold Greenland Stadial 1 is dated to *c.* 12 850 years BP. This raises the following questions: Are the dates from Regstrup too young or did the climate change occur at different times in Greenland and Denmark? Or did birch forests persist for some time into the Younger Dryas period?

There are only few well-dated Lateglacial sites from eastern Denmark. However, Mortensen *et al.* (2014b) studied Lateglacial sediments from Hasselø on Falster and dated the transition from an Allerød-type vegetation to a Younger Dryas-type vegetation to *c.* 12 575 cal. years BP, close to the result from Regstrup.

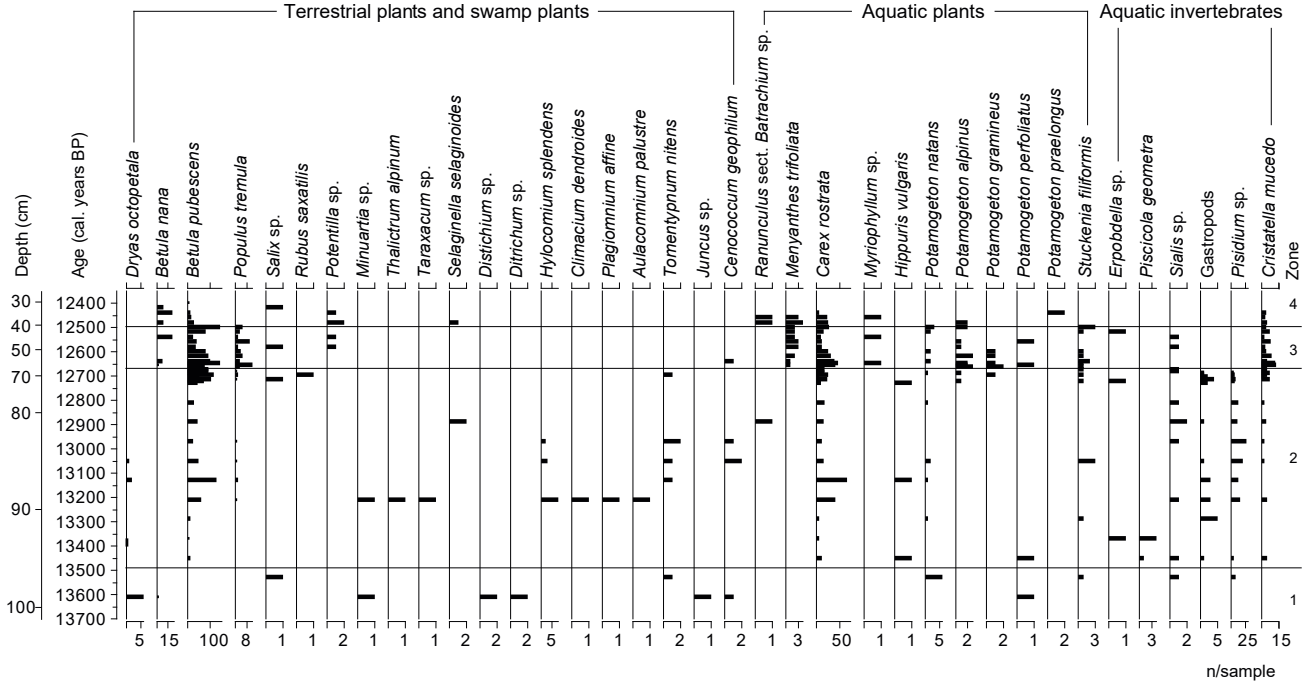

Fig. 3. Simplified macrofossil concentration diagram for site 1 from Regstrup.

Analyses of bulk samples

The results of analyses of large bulk samples appear from Table 2. The common occurrence of fresh water aquatic plants and animals show that the samples consist of detritus gyttja. Because of the large sample size, a number of species was found that did not appear in the monolith samples. Among the plants are *Arctostaphylos uva-ursi*. Endocarps of this dwarf-shrub are fairly frequent in Lateglacial deposits, in particular from the Allerød period. A radiocarbon age of 13 244 cal. years BP was obtained on *A. uva-ursi* endocarps from Regstrup (Table 1).

Achenes of the bog plant *Comarum palustre* are also fairly common in Lateglacial depsoits in Denmark. In contrast, fruits of *Sparganium erectum* have to our knowledge not previously been reported from Lateglacial deposits in Denmark. There is only a single previous record of *Alisma plantago-aquatica* from Lateglacial deposits; from Trollesgave near Holmegårds Mose in southern Sjælland (Fischer *et al.* 2013). The latter two species are relative warm demanding, but it is not surprising that they grew in Denmark because other species with similar temperature requirements have been reported (Johansen 1904; Iversen 1954). Based on beetle remains it is estimated that the mean summer temperature was 9 to 11°C during the Allerød period, and somewhat higher during the Bølling period (Coope *et al.* 1998).

Because remains of *Rangifer tarandus* (reindeer) and *Esox lucius* (pike) were found during the excavation we hoped that more vertebrate remains would turn up in the samples. However, in addition to *E. lucius* remains, we only found a pelvic spine of the small fish *Gasterosteus aculeatus* (stickleback).

The bulk sample JP 335 from site 2 that was dated to 12 770 cal. years BP (early Younger Dryas) was rich in remains of insect larvae (Table 3). The fauna was dominated by head capsules of larvae of chironomids (non-biting midges), but the sample also contained frequent remains of Trichoptera (caddisflies), *Sialis* (alderflies) and oribatid mites. The fauna resembled an invertebrate fauna recorded from submarine Lateglacial lake deposits from the Kattegat (Wiberg-Larsen *et al.* 2019). The lake deposit at site 2 near Regstrup was of limited extent, but the insect fauna indicates that the lake may have been fairly large. The record of *Simulium* cf. *equinum*, confined to running waters, indicates the presence of an inlet stream that might have been fairly large (as this species primarily inhabits larger streams). Several of the taxa such as *Sialis sordida*, *Micropsectra insignilobus*-type, *Micropsectra radialis*-type and *Zalutschia* type B can be classified as northern taxa that indicate lower temperatures than at present, pointing at cooling in the beginning of the Younger Dryas period. *Corynocera ambiqua*, which was the most common chironomid has also been considered an indicator of cold conditions, but the species is common in Denmark at the present (Brodersen & Lindegaard 1999).

Table 3. Arthropod remains from sample JP 335 from Regstrup, Denmark. The sample was dated to *c.* 12 800 cal. years BP

Group	Taxon	Remains	Notes
Oribatida	Oribatidae A, cf. *Hydrozetes*	4 exoskeletons	
	Oribatidae B	7 exoskeletons	Large, dark
Megaloptera	*Sialis sordida* *	4 frontoclypea	
	Sialis sp.	22 mandibles	
Trichoptera, Polycentropodidae	*Cyrnus flavidus*	1 frontoclypeus	
Trichoptera, Phryganeidae	*Agrypnia* cf. *varia*	3 frontoclypea	
Trichoptera, Limnephilidae	*Chaetopteryx sahlbergi/villosa*	1 frontoclypeus	
	Limnephilus A	15 pronotae	The frontal 1/3 part is darker than the rest
	Limnephilus B	5 frontoclypea	*Asynarchus* cf. *lapponicus* *
Simuliidae	*Simulium* cf. *equinum*	1 frontoclypeus	
Chironomidae[1]	*Chironomus anthracinus*-type	21 head capsules	
	Corynocera ambiqua (*)	65 head capsules	
	Micropsectra insignilobus-type *	18 head capsules	
	Micropsectra radialis-type *	3 head capsules	
	Chaetocladius type B	1 head capsule	
	Psectrocladius sordidellus-type	1 head capsule	
	Zalutschia type B *	1 head capsule	

[1] The nomenclature of Chironomidae follows Brooks *et al.* (2007). * Northern taxon.

Notes on selected species

Species living on land

Betula pubescens was represented by numerous nutlets and catkin scales. Hence, bulk samples JP 314 and JP 322 each contained at least 100 nutlets and 50 catkin scales. The rich occurrence of the species shows that the vegetation around the lake was characterised by birch forests during the time period from *c.* 13 200 to *c.* 12 500 cal. years BP. The lowest sample from the monolith contained a few remains of *B. pubescens*; this sample is dated to *c.* 13 600 cal. years BP. At Slotseng in southern Jylland the oldest macrofossils of *B. pubescens* were dated to *c.* 13 500 cal. years BP (Mortensen *et al.* 2011), at Hasselø on Falster to *c.* 13 600 cal. years BP (Mortensen *et al.* 2014b), at Staalsø near Kalundborg in north-west Sjælland to *c.* 13 700 cal. years BP (Mortsensen & Bennike, unpublished data), at Martin Holms Mose on the island of Samsø in central Denmark to *c.* 13 600 cal. years BP (Mortensen *et al.* 2014a), and at Søndre Kobberdam in north-east Sjælland to *c.* 13 330 cal. years BP (Bennike & Mortensen 2018). These ages imply that the species arrived in Denmark during the mid-Allerød. *Betula pubescens* was the first tree species that colonised Denmark after the last deglaciation, however, the species can occur as a fairly large tree, a small tree or a bush, depending on the local growth conditions. It is impossible to determine the growth form from fossil nutlets or catkin scales.

Danish lake deposits rich in remains of *Betula pubescens* are usually referred to the Allerød period. However, the radiocarbon ages from Regstrup show that *Betula pubescens* was also common in the early part of the Younger Dryas period at this site. Mortensen et al. (2014b) showed that the Allerød environment in Falster in south-eastern Denmark continued until *c.* 12 575 cal. years BP before the ecosystem collapsed and was replaced by a Younger Dryas type vegetation. The same appears to be the case in the Regstrup region in north-west Sjælland. It also appears that *Betula pubescens* survived into the Younger Dryas near Birkerød in north-east Sjælland (Mortensen et al. 2014a).

Betula nana was also represented by numerous nutlets and catkin scales. The species does not grow in Denmark anymore, but it occurs in bogs in southern Sweden and is common in heaths in northern Scandinavia and in low arctic regions. Remains of this shrub are common in Lateglacial deposits in Denmark and *Betula nana* was among the first woody plants to immigrate after the last deglaciation. There are also a few Early Holocene finds of this light-demanding species from Denmark (Jensen 1985; Bennike & Jensen 2011).

Populus tremula remains were surprisingly common in the samples from Regstrup. Until now only few fossils of this species were found in Lateglacial deposits in Denmark. A few pollen grains were reported from a clay pit near Ruds-Vedby in western Sjælland (Krog 1954) and a few scattered finds of macrofossils have been reported (e.g., Nielsen & Sørensen 1992; Bennike & Mortensen 2018). All securely dated finds from Denmark come from the Allerød period. However, at Regstrup the species continued to grow until 12 500 cal. years BP, i.e. in the early part of the Younger Dryas period. The beginning of cold conditions is dated to *c.* 12 850 years BP in ice cores from Greenland (Rasmussen *et al.* 2009) and the invertebrate fauna from sample JP 335 also indicate relatively cold conditions at *c.* 12 800 cal. years BP, as mentioned above.

Danish Lateglacial finds of *P. tremula* are confined to the southern and eastern part of Denmark, where summer temperatures are higher than in the north-western part of the country. The samples from Regstrup only contained bud scales – no catkin scales were found. This implies, together with the sparse occurrence of pollen grains reported in earlier studies of Lateglacial deposits that flowering and in particular fruiting were uncommon. Vegetative reproduction is currently common in *P. tremula* near the northern range limit of the species; it was probably also a common phenomenon in Lateglacial populations of the species in Denmark.

A single fruit stone of *Rubus saxatilis* was recorded. The species has previously been reported from Allerød-period layers from the classical Allerød site, from Frihedens Mose and from Hasselø on Falster in south-eastern Denmark (Hartz 1902; Jessen 1920; Mortensen et al. 2014b).

Arctostaphylos uva-ursi was represented by four endocarps. The species is rare in Denmark at present, but common in northern Scandinavia where it grows in dwarf-shrub heaths. Fruit stones of the species are fairly frequent in Allerød layers from Denmark, but it is also recorded from Younger Dryas layers (Bennike & Jensen 1995; Bennike *et al.* 2004a). Five finds from eastern Denmark have been dated to the mid-Allerød (Bennike *et al.* 2020; Bennike unpublished data).

A few leaf fragments of *Dryas octopetala* were found in the lower part of the monolith. *Dryas octopetala* is a common plant in Arctic regions, but the species may also grow in open non-shaded areas south of the Arctic. It prefers carbonate-rich soil and it can thrive in nutrient-poor conditions because it lives in symbiosis with nitrogen-fixating micro-organisms. The species was common in Denmark during the Lateglacial, but the forest in the southern and eastern parts of the country were so dense during the Allerød period that the species almost disappeared. In the north-western part of Denmark, the species was one of the dominating plants throughout the Allerød period (Bennike *et*

al. 2004b; Mortensen et al. 2014a). From north-western Sjælland the species has been reported from Vinde-Helsinge Mose near Gørlev, Ruds-Vedby (Krog 1954) and Raklev near Kalundborg (Bennike & Barry 2009).

Ten small achenes of *Potentilla* could not be identified to species. Most species of *Potentilla* are small herbs that grow in dry soils. The genus *Potentilla* includes many species in Arctic and northern boreal regions.

Papaver sect. *Scapiflora* sp. (arctic poppy) was represented by a single seed. To our knowledge it is the first record of this taxon from Lateglacial deposits in Denmark.

Six achenes of *Urtica dioeca* (common nettle) were found in sample JP 335. The species is rare in Lateglacial Danish deposits (Jensen 1985); it is nitrophilous and indicate nutrient-rich soils. Such soils may have formed locally due to the presence of reindeers or roosting birds.

A single achene belonged to *Comarum palustre* that grows in wet soil in bogs and along lake shores, in boreal or low-arctic climates. The species has been recorded from several Lateglacial sites in Denmark.

Thalictrum alpinum was also represented by a single achene. *Thalictrum alpinum* is a small heliophilous herb that today grows in heaths and copses in arctic and alpine regions (Fig. 4). Achenes of the species are rare in Lateglacial deposits, but they have been reported from Hasselø on the island of Falster in south-eastern Denmark, from sediments dated from 12 600 to 14 200 cal. years BP (Mortensen *et al.* 014b) and from sites in England and elsewhere in north-western Europe (Tralau 1963).

Taraxacum sp. was represented by a fragment of a nutlet. *Taraxacum* is a rare record for Lateglacial deposits in Denmark, but it has likewise been reported from Hasselø, in a sample dated to *c.* 13 700 cal. years BP. *Taraxacum* spp. are today fairly common in arctic regions, often growing in pioneer communities

A few megaspores of the small plant *Selaginella selaginoides* were found, the megaspores are fairly common in Danish Lateglacial deposits. The species grows in moist or wet sites, for example in calcareous mires.

The flora from Regstrup includes the bryophytes *Climacium dendroides*, *Hylocomium splendens*, *Aulacomnium palustre*, *Tomentypnum nitens*, *Calliergon* sp., *Ditrichum* sp., *Distichium* sp., *Plagiomnium affine*, *Bryum* sp. and *Sphagnum* sp. that have previously been recorded from a few Lateglacial sites in Denmark (Jessen 1924; Odgaard 1981). Most of the species grow in mires and several of them, especially *Distichium* sp., are calciphiles. Remains of *Sphagnum* are rare in Lateglacial deposits, presumably because most species of the genus grow in acid soils, which were rare during the Lateglacial.

Rangifer tarandus (reindeer). During the excavation two fragments of *R. tarandus* were found in layer 7. One is a fragment of a lower jaw of an animal that was 5½ to 6½ years old (Magnussen 2019). The other is a fragment of a small, slender cast antler probably from a female reindeer that was found in the uppermost part of layer 7. The antler was dated to *c.* 6600 cal. years

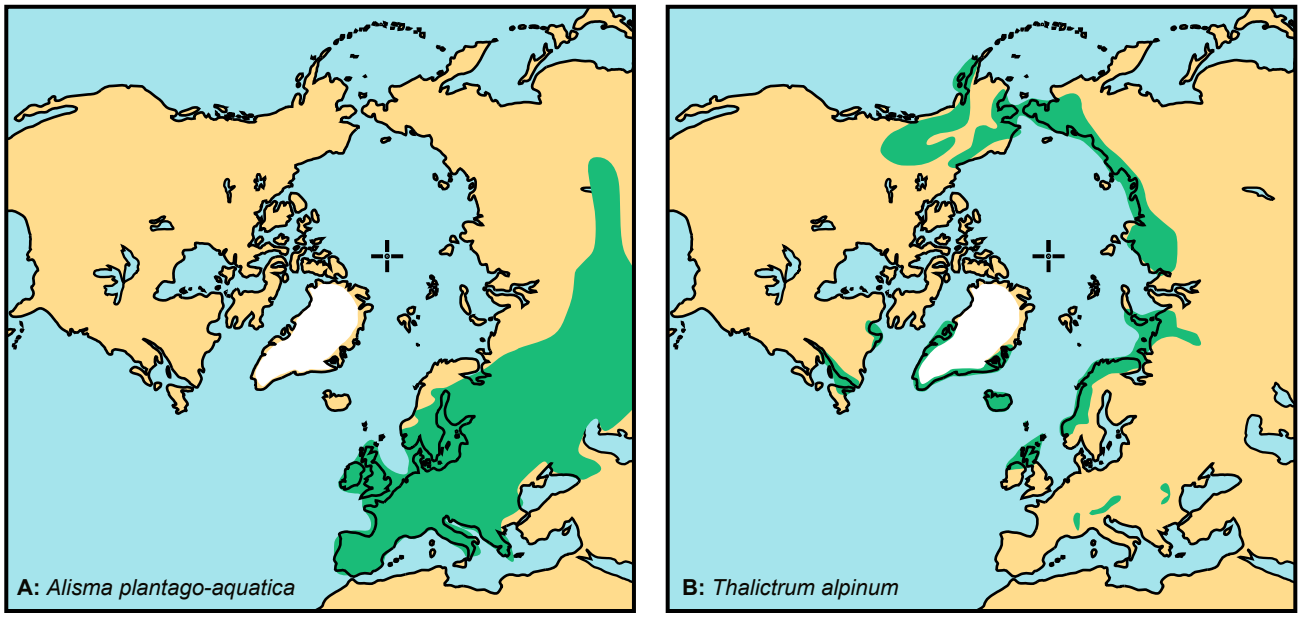

Fig. 4. Modern-day distribution of a warmth-demanding species (**A:** *Alisma plantago-aquatica*) and a cold-adapted species (**B:** *Thalictrum alpinum*), of which remains were found in the Lateglacial sediments from Regstrup. Modified from Hultén & Fries (1986).

BP (Table 1). This most surprising age for a Danish reindeer find was discussed by Bennike *et al.* (2021). The identification based on a visual inspection of the antler fragment was confirmed by protein sequencing by liquid chromatography tandem mass spectrometry (LC-MS/-MS). The reindeer antler may have come to Sjælland from Norway or Sweden as a result of trade.

Layer 7 with the jaw fragment is dated to the Younger Dryas. The former presence of reindeer in Denmark was discussed by Degerbøl & Krog (1959) and by Aaris-Sørensen *et al.* (2007). Radiocarbon dating of reindeer remains shows that the species lived in Denmark during the time period from *c.* 14 500 to 10 300 cal. years BP. This means that it persisted in Denmark into the early part of the Holocene. During this period temperatures were increasing but the increase was interrupted by the cold Preboreal oscillation centred at *c.* 11 400 cal. years BP (Björck *et al.* 1997). Several reindeer remains have previously been reported from north-west Sjælland, but only one find has been radiocarbon dated; it gave an age of *c.* 11 800 cal. years BP (Aaris-Sørensen *et al.* 2007).

Castor fiber (Eurasian beaver) was represented by a lumbar vertebra from layer 8. Two samples of plant macrofossils from this layer yielded ages of *c.* 12 550 and 12 690 cal. years BP (Table 1), corresponding to a mid-Younger Dryas age. Bones of beaver or beaver-gnawed branches have been reported from a few localities with Lateglacial sediments in Denmark. None of these finds are directly dated but they are referred to the Allerød period (Aaris-Sørensen 1995). Thus, the find from Regstrup may be the first record of bones of the species from Younger Dryas sediments. The beaver is primarily a boreal species that lives in rivers and streams, where it constructs dams.

?*Lemmus lemmus* (Norway lemming). A humerus fragment of a small rodent was with hesitation referred to *Lemmus lemmus*. Remains of the species have previously been recorded from Middle and Late Weichselian deposits in Denmark (Bennike *et al.* 1994; Heiberg 1995; Aaris-Sørensen 1995).

Aquatic plants

Three fruits of *Sparganium erectum* were found; the species appears to be new to the Lateglacial flora of Denmark. *Sparganium erectum* is a fairly warmth-demanding spccies but there are scattered finds of it from northern Sweden and northern Finland (Hultén & Fries 1986).

One fruit of *Alisma plantago-aquatica* was recorded, the species is another warmth-demanding plant, extending north almost to the arctic tree line (Fig. 4). It grows in shallow water along the shores of nutrient-rich lakes, in ponds and streams, and it is often one of the first water plants to colonise newly formed ponds (Moeslund *et al.* 1990). The species has been recorded from Lateglacial deposits from Holmegårds Mose in southern Sjælland (Fischer *et al.* 2013).

Three seeds of *Nuphar pumila* were found in JP 335. This species of water-lily is rare in Lateglacial deposits in Denmark (Jensen 1985). It is relatively warmth-demanding, but the geographical range extends to the arctic treeline.

Seven species of pondweeds (*Potamogeton* and *Stuckenia*) were found – all of them have been recorded from Lateglacial deposits in Denmark before (Jensen 1985).

Fruits of *Carex* were abundant in some of the samples. Some of the fruits had the perigynium preserved and could be identified to *Carex rostrata*, and most of the fruits without perigynium probably also belong to this species. The species grows in shallow water in lakes or in mires. Fruits of *C. rostrata* are common in Lateglacial deposits from Denmark.

Aquatic animals

Aquatic invertebrates included gemmules of Spongillidae indet., egg cocoons of leaches (*Erpobdella* sp. and *Piscicola geometra*). These taxa are common in Lateglacial deposits in Denmark.

Cladocerans were represented by ephippia of *Daphnia pulex*, *Simocephalus vetulus* and head shields and shells of *Chydorus sphaericus*. *Daphnia pulex* and *Chydorus sphaericus* remains are common in Lateglacial deposits, whereas *Simocephalus vetulus* remains are rare. Ephippia of *S. vetulus* have previously been reported from southern Sjælland (Poulsen 1944).

Ostracodes were represented by *Candona* sp., *Limnocythere* sp., *Cyclocypris laevis* and *Herpetocypris reptans*. The latter species appears to be new to the Lateglacial fauna of Denmark, but it has been reported from Lateglacial deposits in Germany (Absolon 1973). It is a warmth-demanding species that is found today to the north to Trondheim in Norway (Sars 1925). It mainly lives in nutrient-rich ponds and small lakes rich in macrophytes.

Freshwater molluscs were represented by several species of gastropods and bivalves such as *Valvata cristata*, *V. piscinalis*, *Ampullaceana balthica* (syn. *Radix balthica*, *Lymnaea peregra*), *Stagnicola palustris* (syn. *Lymnaea palustris*), *Gyraulus laevis*, *Hippeutis complanatus*, *Armiger crista*, *Pisidium* spp. and *Sphaerium* sp. All species have previously been recorded from Danish Lateglacial lake deposits (Johansen 1904), although *Stagnicola palustris* only rarely.

Statoblasts of three bryozoan taxa were found: *Cristatella mucedo*, *Plumatella* sp. and *Fredericella* sp. The latter is rarely recorded but the statoblasts are common in lake deposits. The taxa have wide geographical ranges but in the Arctic they are confined to the low arctic.

Finally, remains of three fish species were recorded:

Gasterosteus aculeatus, *Esox lucius* and *Perca fluviatilis*. *G. aculeatus* (three-spined stickleback) was represented by a pelvic spine in sample JP 320. Remains of the species have been reported from the classical Lateglacial Bølling site in Jylland (Rosenlund 1976) and from northern Sjælland (Bennike & Mortensen 2018; Bennike *et al*. 2020). *Gasterosteus aculeatus* can be found in large numbers in shallow, vegetation-rich water of lakes where it is an important prey for larger fish and birds. It is widely distributed in temperate and low-Arctic regions in the northern Hemisphere.

Esox Lucius (pike) was represented by 127 bones, which represent at least four individuals. The total length of the individuals was about 30 to 70 cm. *Perca fluviatilis* (perch) was represented by 454 fragments, of which 400 were scales. Remains of at least three individuals are present in the material – one of them was *c.* 32 cm long, the others somewhat smaller. Both pike and perch have been reported from fairly many sites with Lateglacial deposits in Denmark (Rosenlund 1976; Skousen 2008). Pike and perch may be found in a wide range of habitats, but they are most common in vegetation-rich lakes. They do not occur in the Arctic.

Further discussion

Lateglacial deposits with remains of arctic plants were first demonstrated in Denmark by the Swedish geologist Alfred Nathorst (Nathorst 1914). Later, in a clay pit south of Allerød in northern Sjælland, signs of a warm period during the Lateglacial were found (Hartz & Milthers 1901) and some decades later an older warm period was described from Bølling Sø in Jylland (Iversen 1942, 1954). These warm periods were partly recognised from sedimentological criteria. In the Allerød clay pit, the major part of the Lateglacial sediments consisted of clay, but during the Allerød period organic-rich gyttja was deposited. In Bølling Sø the Lateglacial deposits are dominated by sand and sandy clay and silt, but during the Allerød period gyttja rich in microalgae accumulated. In the Allerød pit the clay layers contained leaves of *Betula nana*, *Dryas octopetala* and other arctic plants, whereas leaves of *Betula pubescens* (downy birch) were found in the gyttja layer. In Bølling Sø the mineral-rich layers contained pollen of *B. nana*, whereas the gyttja layer contained pollen of tree birch, according to Iversen (1942).

The earliest analyses of plant remains from the Lateglacial were based on studies of macrofossils (Hartz 1902), but after the introduction of pollen analysis plant macrofossils have often been ignored. However, plant macrofossils have some advantages compared to pollen: macrofossils can often be identified to species. It is for example not possible to identify pollen grains of *Thalictrum* to species, whereas fruits can be identified. Hence, it is possible to decide if fruits belong to *T. alpinum* or the more warmth-demanding *T. flavum*, both of which occur in Lateglacial deposits in Denmark.

Another problem about pollen analysis is that some species produces vast quantities of pollen and some pollen types are being spread far by the wind. During the Lateglacial when the local pollen production was relatively small this means that a large part of the pollen rain may come from non-local trees. This problem is specially pronounced for *Pinus*, the pollen of which are abundant in Danish Lateglacial deposits, even though no macrofossils of this tree has so far been found.

Pollen grains can also be subject to reworking and redeposition, which may hamper interpretation of Lateglacial pollen diagrams. In Bølling Sø it was estimated that up to 80% of the pollen grains were reworked from older deposits (Iversen 1942). Some types of macrofossils, such as seeds and fruits with hard walls may also be reworked, but usually such fossils become worn. Fragile plant macrofossils such as leaves can hardly survive reworking.

Finally, pollen analysis only gives information about plants that produce pollen and spores. Macrofossil analysis also provides information about the animal life of the past. In the samples from Regstrup, we found remains of many animals, which bear witness about a rich life in and around the former lake basins.

Based on pollen analysis it was proposed that all of Denmark was dominated by birch forests during the Allerød period (Iversen 1973). However, analyses of macrofossils indicate that the northern and western parts of Denmark were dominated by dwarf-shrub heaths with *B. nana* (Mortensen et al. 2014a). Clearly, it is important to conduct analyses from different parts of the country if we want to achieve a better understanding of regional variations in vegetation and fauna that may be determined by differences in climate, soil and immigration history.

Conclusions

The analyses from the basins near Regstrup indicate that the area was covered by open forests during the younger part of the Allerød period and the older part of the Younger Dryas period. The forests were dominated by *B. pubescens*, but *Populus tremula* was also quite common, until it disappeared *c.* 200 years into the Younger Dryas period. The area also housed light-demanding species such as *Dryas octopetala*,

Rubus saxatilis, *Minuartia* sp., *Potentilla* sp., *Thalictrum alpinum* and *Taraxacum* sp. Plants growing on wet and moist ground included several species of bryophytes, *Carex* sp. and *Comarum palustre*. Shallow water near the margin of the basins housed a rich vegetation dominated by *Carex rostrata* and including *Ranunculus* sect. *Batrachium* sp., *Hippuris vulgaris*, *Myriophyllum* sp., *Menyanthes trifoliata*, *Alisma plantago-aquatica* and *Sparganium erectum*. The flora in deeper water included charophytes and several pondweed species. The vertebrate fauna included *Rangifer tarandus*, *Castor fiber* and a small rodent, probably *Lemmus lemmus*.

The basins housed a rich fauna of invertebrates, including two species/genera of leeches, water fleas, ostracodes, larvae of beetles, chironomids, alderflies, caddisflies, gastropods, bivalves and bryozoans. The invertebrates are well-know prey for fish and remains of perch, pike and three-spined stickleback were found.

The common presence of bud-scales of the fairly warmth-demanding plant *Populus tremula* and finds of fruits of *Alisma plantago-aquatica* and *Sparganium erectum*, as well as other finds of warmth-demanding plants in south-eastern Denmark indicates that summer temperatures during the Allerød and early Younger Dryas periods were higher in the southern and eastern parts of Denmark than in the the northern and western parts of the country. Before and after the forested period the area around the basins were characterised by dwarf-shrub heaths with *Dryas octopetala*, *Betula nana*, herbs and mosses.

Acknowledgements

We are grateful to Morten Fischer Mortesen who saw the potential for macrofossil analyses of the sediments from Regstrup. Radiocarbon dating was carried out under the supervision of Göran Possnert in Uppsala (samples marked Ua) and Jesper Olsen in Aarhus (sample marked AAR). Comments by journal referees Anthony Ruter, Copenhagen and Bent Odgaard helped to improve the paper.

References

Aaris-Sørensen, K. 1995: Palaeoecology of a LateWeichselian vertebrate fauna from Nørre Lyngby, Denmark. Boreas 24, 355–365. https://doi.org/10.1111/j.1502-3885.1995.tb00785.x

Aaris-Sørensen, K., Mühldorff, R. & Petersen, E.B. 2007: The Scandinavian reindeer (Rangifer tarandus L.) after the last glacial maximum: time, seasonality and human exploitation. Journal of Archaeological Science 34, 914–923. https://doi.org/10.1016/j.jas.2006.09.014

Absolon, A. 1973: Ostracoden aus einigen Profilen spat- und postglazialer Karbonatablagerungen in Mitteleuropa. Mitteilungen der Bayersichen Staatssamlung für Paläontologie und historische Geologie 13, 47–94.

Bennike, O. & Jensen, J.B. 1995: Near shore Baltic Ice Lake deposits in Fakse Bugt, southeast Denmark. Boreas 24, 185–195. https://doi.org/10.1111/j.1502-3885.1995.tb00772.x

Bennike, O. & Barry, D. 2009: Plante- og dyrelivet på Herredsåsen i jægerstenalderen – om landets ældste andemad og tidligste salamandre. I: Pedersen, L. (red.): Årets gang på Kalundborg Museum 2008, 80–85.

Bennike, O. & Jensen, J.B. 2011: Postglacial relative shore level changes in Lillebælt, Denmark. Geological Survey of Denmark and Greenland Bulletin 23, 37–40. https://doi.org/10.34194/geusb.v23.4834

Bennike, O. & Mortensen, M.F. 2018: A multi-disciplinary macrofossil study of late glacial to early Holocene sediments from Søndre Kobberdam, Hareskovene, Denmark. Bulletin of the Geological Society of Denmark 66, 113–122. https://doi.org/10.37570/bgsd-2018-66-05

Bennike, O., Houmark-Nielsen, M., Böcher, J. & Heiberg, E.O. 1994: A multi-disciplinary macrofossil study of Middle Weichselian sediments at Kobbelgård, Møn, Denmark. Palaeogeography, Palaeoclimatology, Palaeoecology 111, 1–15. https://doi.org/12.1016/0031-0182(94)90344-1

Bennike, O., Jensen, J.B., Lemke, W., Kuijpers, A. & Lomholt, S. 2004a: Late- and postglacial history of the Great Belt, Denmark. Boreas 33, 18–33. https://doi.org/10.1080/03009480310006952

Bennike, O., Sarmaja-Korjonen, K. & Seppänen, A. 2004b: Reinvestigation of the classic late-glacial Bølling Sø sequence, Denmark: chronology, macrofossils, Cladocera and chydorid ephippia. Journal of Quaternary Science 19, 465–478. https://doi.org/10.1002/jqs.852

Bennike, O., Pantmann, P. & Aarsleff, E. 2020: Lateglacial and Holocene floras and faunas from the Salpetermosen area, north-east Sjælland, Denmark. Bulletin of the Geological Society of Denmark 68, 231–244. https://doi.org/10.37570/bgsd-2020-68-10

Bennike, O., Jensen, T.Z.T., Taurozzi, A.J., Mackie, M., Claudi-Hansen, L. & Magnussen, B. 2021: A Mid-Holocene reindeer antler from Regstrup, Sjælland, Denmark. Danish Journal of Archaeology 10, 1–8.

Björck, S., Rundgren, M., Ingólfsson, Ó. & Funder, S. 1997: The Preboreal oscillation around the Nordic Seas: terrestrial and lacustrine responses. Journal of Quaternary Science 12, 455–465. https://doi.org/10.1002/(SICI)1099-1417(199711/12)12:6<455::AID-JQS316>3.0.CO;2-S

Brodersen, K.P. & Lindegaard, C. 1999: Mass occurrence and sporadic distribution of *Corynocera ambigua* Zetterstedt (Diptera, Chironomidae) in Danish lakes. Journal of Paleolimnology 22, 41–52. https://doi.org/10.1023/A:1008032619776

Brooks, S.J., Langdon, P.G. & Heiri, O. 2007: The identification and use of Palaearctic Chironomidae larvae in palaeoecol-

ogy. Quaternary Research Association Technical guide 10, 276 pp.

Coope, G.R., Lemdahl, G., Lowe, J.J. & Walking, A. 1998: Temperature gradients in northern Europe during the last glacial-Holocene transition (14–9 14C kyr BP) interpreted from coleopteran assemblages. Journal of Quaternary Science 13, 419–433. https://doi.org/10.1002/(SICI)1099-1417(1998090)13:5<419::AID-JQS410>3.0.CO;2-D

Degerbøl, M & Krog, H. 1959: The Reindeer (*Rangifer tarandus* L.) in Denmark. Det kongelige Danske Videnskabernes Selskab, Biologiske Skrifter 10, 4, 165 pp.

DMI 2019: https://www.dmi.dk/vejr/arkiver/normaler-og-ekstremer/klimanormaler-dk/.

Fischer, A., Mortensen, M.F., Henriksen, P.S., Mathiassen, D.R. & Olsen, J. 2013: Dating the Trollesgave site and the Bromme culture e chronological fix-points for the Lateglacial settlement of Southern Scandinavia. Journal of Archaeological Science 40, 4663–4674. https://doi.org/10.1016/j.jas.2013.06.026

Håhansson, E. & Pedersen, S.A.S. 1992: Geologisk kort over den danske undergrund. København: Varv. (Map sheet).

Hartz, N. 1902: Danmarks senglaciale Flora og Fauna. Danmarks Geologiske Undersøgelser II række, 11, 80 pp. https://doi.org/10.34194/raekke2.v11.6793

Hartz, N. & Milthers, V. 1901: Det senglaciale Ler i Allerød Teglværksgrav. Meddelelser fra Dansk Geologisk Forening 2, 31–60.

Heiberg, E.O. 1995: Sen- og Postglaciale mindre gnavere (Rodentia) og insektædere (Insectivora) fra Danmark, 274 pp. Unpublished cand. scient. Thesis, University of Copenhagen, Denmark.

Henderson, P.A. 1990: Freshwater ostracods. Synopses of the British Fauna (New series) 42, 228 pp.

Houmark-Nielsen, M., Linge, H., Fabel, D., Schnabel, C., Xue, S., Wilcken, K.M. & Binnie, S. 2012: Cosmogenic surface exposure dating the last deglaciation in Denmark: discrepancies with independent age constraints suggest delayed periglacial landform stabilisation. Quaternary Geochronology 13, 1–17. https://doi.org/10.1016/j.quageo.2012.08.006

Hultén, E. & Fries, M. 1986: Atlas of North European vascular plants I-III. Koeltz Scientific Books: Königstein.

Iversen J. 1942: En pollenanalytisk Tidsfæstelse af Ferskvandslagene ved Nørre Lyngby. Meddelerser fra Dansk Geologisk Forening 10, 130–151.

Iversen, J. 1947: Plantevækst, dyreliv og klima i det senglaciale Danmark. Geologiska Föreningens i Stockholm Förhandlingar 69, 67–78. https://doi.org/10.1080/11035894709454075

Iversen, J. 1954: The Late-Glacial flora of Denmark and its relation to climate and soil. Danmarks Geologiske Undersøgelse II række, 80, 87–119.

Iversen, J. 1973: The development of Denmark's nature since the Last Glacial. Danmarks Geologiske Undersøgelse V. række, 7-C, 120 pp. https://doi.org/10.34194/raekke5.v7.7020

Jensen, H.A. 1985: Catalogue of late- and post-glacial macrofossils of Spermatophyta from Denmark, Schleswig, Scania, Halland and Blekinge dated 13,000 B.P. to 1536 A.D. Danmarks Geologiske Undersøgelse, Serie A, 6, 95 pp. https://doi.org/10.34194/seriea.v6.7025

Jessen, K. 1920: Moseundersøgelser i det nordøstlige Sjælland. Med bemærkninger om træers og buskes indvandring og vegetationens historie. Danmarks Geologiske Undersøgelse II. Række, Vol. 34, 268 pp. https://doi.org/10.34194/raekke2.v34.6820

Jessen, K 1924: Et bjørnefund i Allerødytje. Meddelelser fra Dansk Geologisk Forening 6, 24, 11 pp.

Johansen, A.C. 1904: Om den fossile kvartære Molluskfauna i Danmark og dens relationer til forandringer i klimaet, 137 pp. Copenhagen: Gyldendalske Boghandel.

Kaiser, E.W. 1977: Æg og larver af 6 Sialis-arter fra Skandinavien og Finland (Megaloptera, Sialidae). Flora og Fauna 83, 65–79.

Krog, H. 1954: Pollen analytical investigations of a C-14-dated Alleröd-section from Ruds-Vedby. Danmarks Geologiske Undersøgelse, II. Række 80, 120–139.

Magnussen, B. 2019: Rute 23, MHO1082-8. Et knoglemateriale fra Rute 23, hvor de ældste lag dateres til Hamburg-Bromme kultur og de yngste lag dateres til Neolitikum-jernalder. ArchaeoScience 14, 8 pp. Unpublished report in the archives of the Zological Museum, Copenhagen.

Milthers, V. 1943: Nordvestsjællands geologi. Danmarks Geologiske Undersøgelse V række, 6, 185 pp. https://doi.org/10.34194/raekke5.v6.7019

Moeslund, B., Løjtnant, B., Mathiesen, H., Mathiesen, L., Pedersen, A., Thyssen, N. & Schou, J.C. 1990: Danske vandplanter, 187 pp. Copenhagen: Miljøstyrelsen.

Mortensen, M.F., Birks, H.H., Christensen, C., Holm, J., Noe-Nygaard, N., Odgaard, B.V., Olsen, J. & Rasmussen, K.L. 2011: Late-glacial vegetation development in Denmark – new evidence based on macrofossils and pollen from Slotseng, a small-scale site in southern Jutland. Quaternary Science Reviews 30, 2534–2550. https://doi.org/10.1016/j.quascirev.2011.04.018

Mortensen, M.F., Henriksen, P.S & Bennike, O. 2014a: Living on the good soil: relationships between soils, vegetation and human settlement during the late Allerød time period in Denmark. Vegetation History and Archaeobotany 23, 195–205. https://doi.org/10.1007/s00334-014-0433-7

Mortensen, M.F., Henriksen, P.S., Christensen, C., Petersen, P.V. & Olsen, J. 2014b: Vegetation development in south-east Denmark during the Weichselian Late Glacial: palaeoenvironmental studies close to the Palaeolithic site of Hasselø. Danish Journal of Archaeology 3, 33–51. https://doi.org/10.1080/21662282.2014.994281

Nathorst, A.G. 1914: Minnen från Samarbete med Japetus Steenstrup 1871 och från en därpå följande tjugofemårig Korrespondens. In: Jungersen, H.F.E. & Warming, E. (eds), Mindeskrift i anledning af hundredaaret for Japetus Steenstrups fødsel, no. 5, 22 pp. Copenhagen: Bianco Lunos Bogtrykkeri.

Nielsen, H. & Sørensen, I. 1992: Taxonomy and stratigraphy of lateglacial *Pediastrum*-taxa from Lysmosen, Denmark – a preliminary study. Review of Palaeobotany and Palynology 74, 55–75. https://doi.org/10.1016/0034-6667(92)90138-7

Odgaard, B.V. 1981: The Quaternary bryoflora of Denmark. I. Species list. Danmarks Geologiske Undersøgelse, Årbog 1980, 45–74.

Poulsen, E.M. 1944: Entomostraceans from a late-glacial lacustrine deposit at Næstved, Denmark. Meddelelser fra dansk Geologisk Forening 10, 405–416.

Rasmussen, S.O. *et al*. 2014: A stratigraphic framework for abrupt climatic changes during the Last Glacial period based on three synchronized Greenland ice-core records: refining and extending the INTIMATE event stratigraphy. Quaternary Science Reviews 106, 14–28. https://doi.org/10.1016/j.quascirev.2014.09.007

Reimer, P. *et al*. 2020: The IntCal20 Northern Hemisphere radiocarbon age calibration curve (0-55 cal kB). Radiocarbon 62, 725–757. https://doi.org/10.1017/rdc.2020.41

Rinne, A. & Wiberg-Larsen, P. 2017: Trichoptera larvae of Finland. Identification key to the caddis larvae of Finland and nearby countries, 152 pp. Helsinki: Trificon Books.

Rosenlund, K. 1976: Catalogue of subfossil Danish Vertebrates, fishes, 108 pp. Copenhagen: Zoologisk Museum.

Sars, G.O. 1925: An account of the Crustacea of Norway with short descriptions and figures of all the species. Vol. 9. Ostracoda, 73–208. Bergen: Bergen Museum.

Skousen, H. 2008: Arkæologi i lange bander. Undersøgelser forud for anlæggelsen af motorvejen nord om Århus 1998-2007, 348 pp. Aarhus: Forlaget Moesgaard.

Stuiver, M. & Polach, H.A. 1977: Discussion of reporting ^{14}C data. Radiocarbon 19, 355–363. https://doi.org/10.1017/s0033822200003672

Stuiver, M., Reimer, P.J. & Reimer, R.W. 2021: CALIB 8.2 [WWW program] at http://calib.org, accessed 2021-11-14

Tralau, H. 1963: The recent and fossil distribution of some boreal and arctic-montane plants in Europe. Arkiv för Botanik ser. 2, vol. 5, 533–581.

Wiberg-Larsen, P., Bennike, O. & Jensen, J.B. 2019: Submarine Lateglacial lake deposits from the Kattegat, southern Scandinavia. Journal of Quaternary Science 34, 165–171. https://doi.org/10.1002/jqs.3089

An Eocene conger eel (Teleostei, Anguilliformes) from the Lillebælt Clay Formation, Denmark

GIORGIO CARNEVALE, WERNER SCHWARZHANS, ANE ELISE SCHRØDER & BENT ERIK KRAMER LINDOW

Geological Society of Denmark
https://2dgf.dk

Received 2 February 2022
Accepted in revised form
2 April 2022
Published online
08 April 2022

Carnevale, G., Schwarzhans, W., Schrøder, A.E. & Lindow, B.E.K. 2022: An Eocene conger eel (Teleostei, Anguilliformes) from the Lillebælt Clay Formation, Denmark. Bulletin of the Geological Society of Denmark, Vol. 70, pp. 53–67. ISSN 2245-7070. https://doi.org/10.37570/bgsd-2022-70-05-rev

A conger eel (Anguilliformes, Congridae) is described from the lower Lutetian concretionary nodules of the Lillebælt Clay Formation exposed at Trelde Næs, eastern Jutland, based on two partially complete articulated cranial skeletons. One of the cranial specimens exhibits an otolith void from which a cast was taken, used by Schwarzhans (2007) to describe the extinct *Pseudoxenomystax treldeensis*, which is placed herein within the new genus *Smithconger* gen. nov. *Smithconger treldeensis* (Schwarzhans, 2007) is characterized by well-developed lateral processes on the frontals, supraoccipital crest absent, sphenotic spine rather large, anteriorly pointed and exposed on the flattened surface of the skull roof, otic bullae considerably reduced, maxilla almost straight and distally pointed, maxillary and dentary teeth numerous and arranged in multiple rows, dentary with slightly convex ventral profile, opercle with smooth posterior margin and subopercle short. The otoliths of *Smithconger treldeensis* show high dorsal rim, broad and deep dorsal depression, no ventral furrow, sulcus straight, shallow, centrally positioned with anteriorly reduced colliculum, and ostial channel at anterior tip of colliculum short, not reaching the predorsal rim. The otolith-based species *Bathycongrus waihaoensis* Schwarzhans, 2019 from the Kaiatan (Bartonian/Priabonian) of New Zealand is also assigned to the genus *Smithconger*. *Smithconger* is tentatively referred to the congrid subfamily Congrinae due to the lack of hypohyals in the hyoid bar. This new Eocene genus of conger eel shows a certain degree of similarity with the extant *Bassanago*. The diversity and relationships of other Eocene congrids is also briefly discussed.

Keywords: Anguilliformes, Congridae, *Smithconger* gen. nov., Eocene, Lutetian, Lillebælt Clay Formation, eastern Jutland.

Giorgio Carnevale [giorgio.carnevale@unito.it], Dipartimento di Scienze della Terra, Università degli Studi di Torino, Via Valperga Caluso 35, I-10125 Torino, Italy. http://orcid.org/0000-0002-3433-4127. Werner Schwarzhans [wwschwarz@aol.com], Ahrensburger Weg 103, D-22359 Hamburg, Germany; also Natural History Museum of Denmark, Universitetsparken 15, DK-2100 Copenhagen Ø, Denmark. http://orcid.org/0000-0003-4842-7989. Ane Elise Schrøder [aneelises@snm.ku.dk], Natural History Museum of Denmark, Universitetsparken 15, DK-2100 Copenhagen Ø, Denmark; also Fossil and Moclay Museum, Museum Mors, Skarrehagevej 8, DK-7900 Nykøbing Mors, Denmark. https://orcid.org/0000-0001-9371-400X. Bent Erik Kramer Lindow [lindow@snm.ku.dk], Natural History Museum of Denmark, Universitetsparken 15, DK-2100 Copenhagen Ø, Denmark. https://orcid.org/0000-0002-1864-4221.

Eel-like fishes of the order Anguilliformes constitute a distinctive lineage of elopomorph teleosts that comprises more than 900 extant species arranged in 19 families (Anguillidae, Chlopsidae, Congridae, Cyematidae, Derichthyidae, Eurypharyngidae, Heterenchelyidae, Monognatidae, Moringuidae, Muraenesocidae, Muraenidae, Myrocongridae, Nemichthyidae, Nettastomatidae, Ophichthidae, Protanguillidae, Saccopharyngidae, Serrivomeridae, Synaphobranchidae), which occupy a variety of environments from freshwaters to shallow marine biotopes, to abyssal depths (Nelson *et al*. 2016). The extremely elongate anguilliform body

plan is unique within the Teleostei, being characterized, among the other features, by dorsal and anal fins confluent with caudal fin, ethmoid fused with the vomer, palatine absent, gill arches free from the neurocranium and displaced posteriorly, uppermost branchiostegal rays curving dorsally behind the opercle, and a ribbon-like 'leptocephalus' larva (e.g., Regan 1912; Trewavas 1932; Robins 1989; Johnson *et al*. 2012). The appearance of anguilliforms in the fossil record dates back to the late Cenomanian (about 94 Ma; Marramà *et al*. 2016), with several taxa collected from the Sannine Limestone in Lebanon (Hay 1903; Belouze 2002; Belouze et al. 2003a, b; Forey *et al*. 2003). However, the origin of the extant lineages took place primarily at the end of the Cretaceous and during the Palaeogene (e.g., Santini *et al*. 2013), being well documented by the diverse anguilliform assemblage of Monte Bolca (Blot 1978, 1984; Pfaff *et al*. 2016), but also by the fossils from other localities (e.g., Bonde 1966; Casier 1967; Taverne & Nolf 1978; Young 1993; Bannikov & Parin 1997; Belouze 2002). The otolith record of anguilliforms is relatively rich and diverse, especially that of the Congridae (Schwarzhans 2019b), whose members appear to be present since the Campanian (Nolf & Dockery 1990) and are well documented since the Maastrichtian (Schwarzhans 2010). Conversely, the skeletal record of congrids is rather poor and the earliest skeletal remains of conger eels are represented by four species (*Bolcyrus bajai*, *Bolcyrus formosissimus*, *Paracongroides heckeli*, *Voltaconger latispinus*) from the late Ypresian of Monte Bolca (Blot 1978), plus some isolated bones referred to *Paraconger sauvagei* from the Lutetian Sables de Lede (Taverne & Nolf 1978), where otoliths assigned to the same species were reported by Stinton & Nolf (1970). In addition, partially complete articulated skeletons of conger eels are also known from Oligocene of Northern Caucasus, Russia, with the species *Pavelichthys daniltshenkoi*, and from the Oligocene of Apsheron Peninsula, Azerbaijan, with the species *P. perekischylika* (Prokofiev 2007). The goal of this paper is to describe the skeletal remains pertaining to the family Congridae discovered in the concretionary nodules of the Eocene Lillebælt Clay Formation, Denmark. One of these specimens, a partially complete neurocranium, exhibits an otolith void *in situ*, thereby providing a unique opportunity to link the skeletal and otolith records of an Eocene conger eel and to define in much detail its distribution in space and time (Schwarzhans & Carnevale 2017).

Geological setting

The specimens documented herein primarily consist of incomplete and partially articulated skeletal remains embedded into concretions collected along the south-eastern coast of Trelde Næs, a small peninsula in the eastern Jutland, close to the town of Fredericia (Fig. 1). The fossils were collected from the Lillebælt Clay Formation, an Eocene fossiliferous grey-green, non-calcareous clay that commonly includes mixed carbonate and phosphatic concretions (Heilmann-Clausen *et al*. 1985), which is well-exposed along the coastal cliffs at Trelde Næs. Heilmann-Clausen *et al*. (1985) subdivided the Lillebælt Clay Formation into six lithological units, of which the first two are considered of late Ypresian age. According to Schnetler & Heilmann-Clausen (2011), the transition between the second and third lithological units seems to define the boundary between Ypresian and Lutetian. Concretions occur in the third, fourth, fifth and (possibly) sixth lithological cycles (Heilmann-Clausen *et al*. 1985). There is no information about the lithological cycle from which the concretionary nodules containing the fossils described herein were collected (see also Collins & Jakobsen 2003), but it is reasonable to conclude that they date back to the early Lutetian. The fine-grained sediments of the Lillebælt Clay Formation accumulated in the North Sea Basin, about 300 km from the Swedish coasts (Thomsen *et al*. 2012) at depths between 100 and 350 meters (Schnetler & Heilmann-Clausen 2011; Carlsen & Cuny 2014).

The fossiliferous content of the Lillebælt Clay Formation is quite abundant. Bonde (1968) reported the occurrence of brachiopods, echinoderms, annelids, molluscs (e.g., Schnetler & Heilmann-Clausen 2011) and crustaceans (e.g., Collins & Jakobsen 2003) at Trelde Næs. Vertebrates are represented by cartilaginous and bony fishes. Hansen *et al*. (2013) described associated skeletal and dental remains of an odontaspidid shark, while Carlsen & Cuny (2014) provided a detailed analysis of a diverse elasmobranch assemblage, comprising more than 30 taxa. Bony fishes are represented by isolated teeth (Carlsen & Cuny 2014) and bones (Heilmann-Clausen *et al*. 1985), as well as by otolith voids from which casts were taken (Schwarzhans 2007) and rare partially complete articulated skeletal remains (Bonde *et al*. 2008) preserved in the concretionary nodules, including those described in this study.

Material and methods

The present study is based on four specimens, a single partially complete neurocranium (Fig. 2) (which includes the impression of an otolith; Fig. 3A), an incomplete articulated skeleton represented by the head and the anterior portion of the abdominal region (Fig. 4), plus two otolith casts housed in the collections of

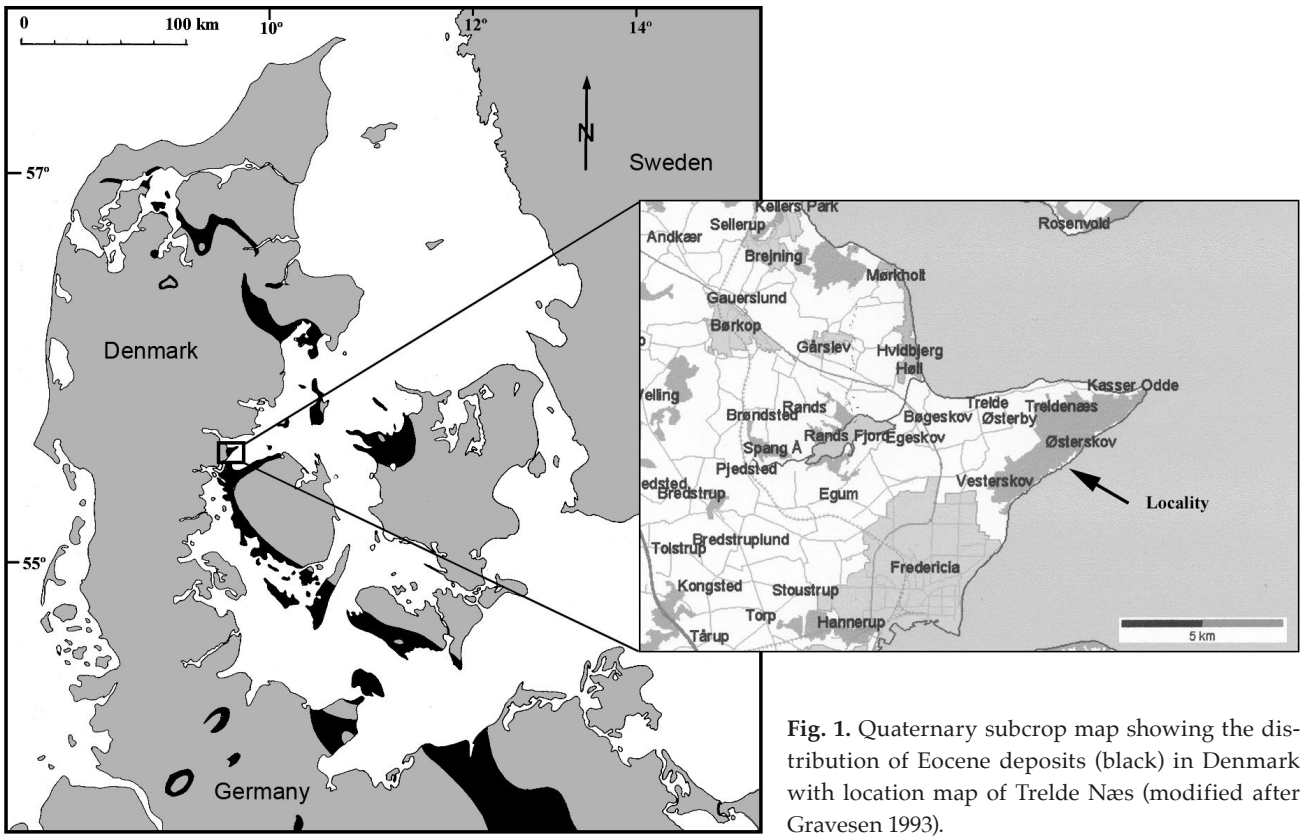

Fig. 1. Quaternary subcrop map showing the distribution of Eocene deposits (black) in Denmark with location map of Trelde Næs (modified after Gravesen 1993).

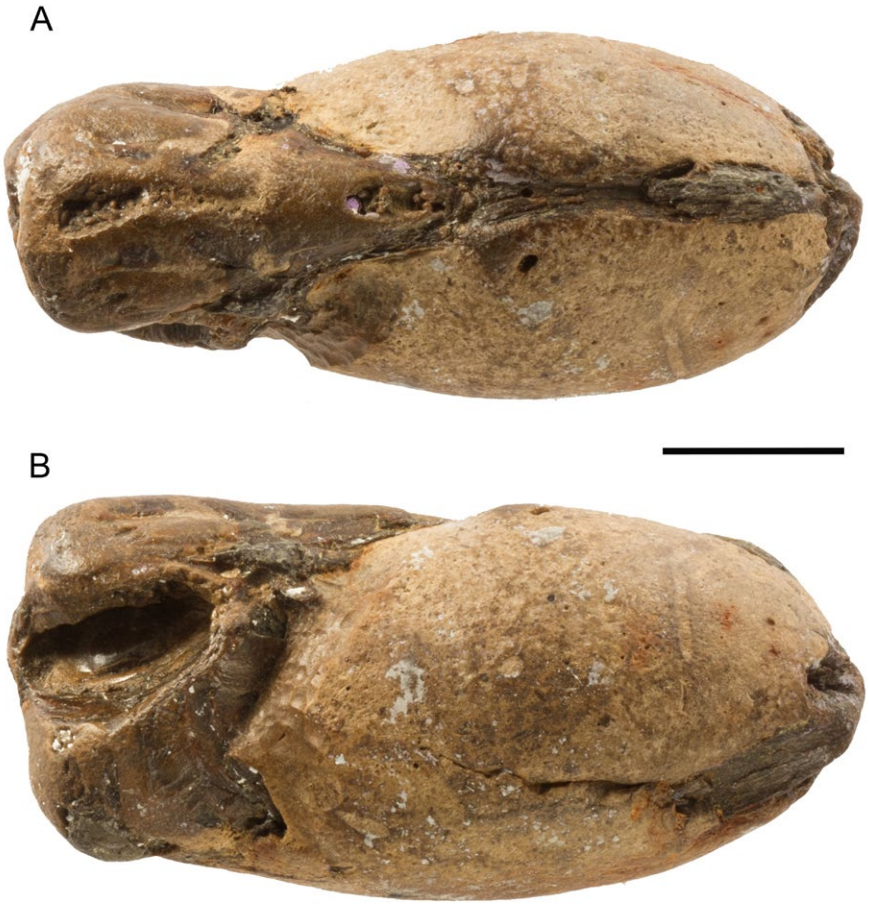

Fig. 2. *Smithconger treldeensis* (Schwarzhans 2007) from the Eocene of Trelde Næs, eastern Jutland, Denmark. Holotype, NHMD-625030. **A**: Neurocranium in dorsal view. **B**: Neurocranium in right lateral view, with a large hollow cavity originally occupied by the saccular otolith. Scale bar 10 mm.

the Natural History Museum of Denmark, Copenhagen. The skeletal material was studied using a WILD Heerbrugg stereomicroscope equipped with a camera lucida drawing arm. The incomplete articulated skeleton required matrix removal before examination to allow investigations of its structure in as much detail as possible; this was achieved using thin entomological needles. During examination, the skeletal remains were moistened with alcohol to enhance some details of their anatomy. Measurements were taken with a dial caliper to the nearest 0.1 mm. Comparative morphological and osteological data were derived mainly from the literature.

Anatomical abbreviations: aa, anguloarticular; ach, anterior ceratohyal; bo, basioccipital; br, branchiostegal rays; bsp, basisphenoid; cl, cleithrum; ctb, ceratobranchial; d, dentary; ect, ectopterygoid; epb, epibranchial; epi, epioccipital; etv, ethmovomerine complex; exo, exoccipital; f, frontal; h, hyomandibula; iop, interopercle; lep, lateral ethmoid process; lfp, lateral frontal process; lvp, lateral vomerine process; mx, maxilla; op, opercle; pa, parietal; pas, parasphenoid; pch, posterior ceratohyal; pop, preopercle; pro, prootic; pte, pterosphenoid; pto, pterotic; q, quadrate; soc, supraoccipital; sop, subopercle; sph, sphenotic; uh, urohyal; v, vertebra.

Institutional abbreviations: MCSNV, Museo Civico di Storia Naturale, Verona; MGUH, Museum Geologica Universitas Hafniensis, Copenhagen; MNHN, Museum National d'Histoire Naturelle, Paris; NHMD,

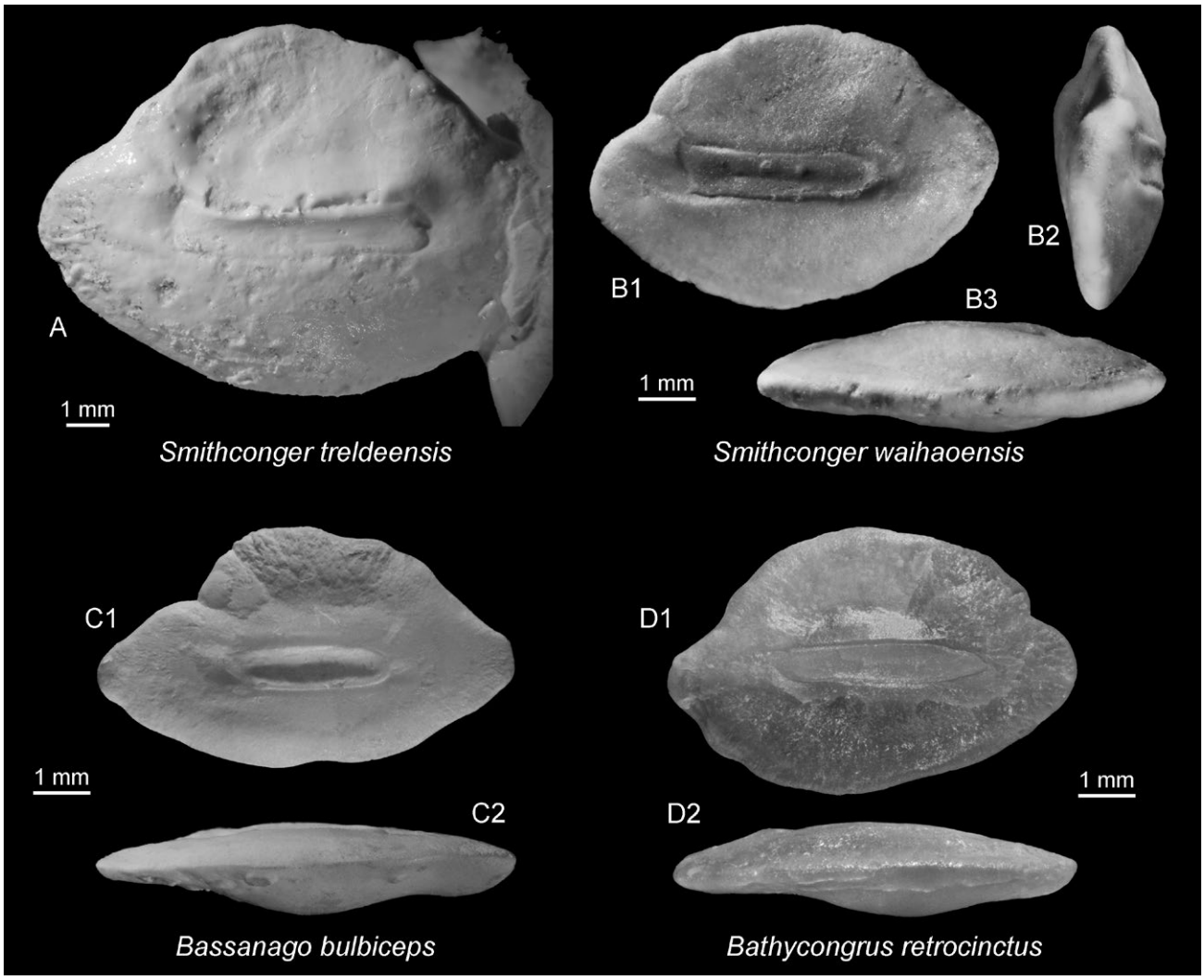

Fig. 3. Otoliths. **A**: *Smithconger treldeensis* (Schwarzhans 2007) from the Eocene of Trelde Næs, eastern Jutland, Denmark, holotype, MGUH 28368. **B**: *Smithconger waihaoensis* (Schwarzhans 2019) from the Kaiatan (Bartonian/Priabonian) of the Waihao River banks, New Zealand South Island, holotype, NMNZ S.46736; B1 inner face, B2 anterior view, B3 ventral view. **C**: *Bassanago bulbiceps* Whitley 1948, Recent, off Wellington, New Zealand, coll. Schwarzhans; C1 inner face, C2 ventral view. **D**: *Bathycongrus retrotinctus* (Jordan & Snyder 1901), Recent, off Dong-gang, Taiwan, ZMUC P2396514, leg. Ho; D1 inner face, D2 ventral view.

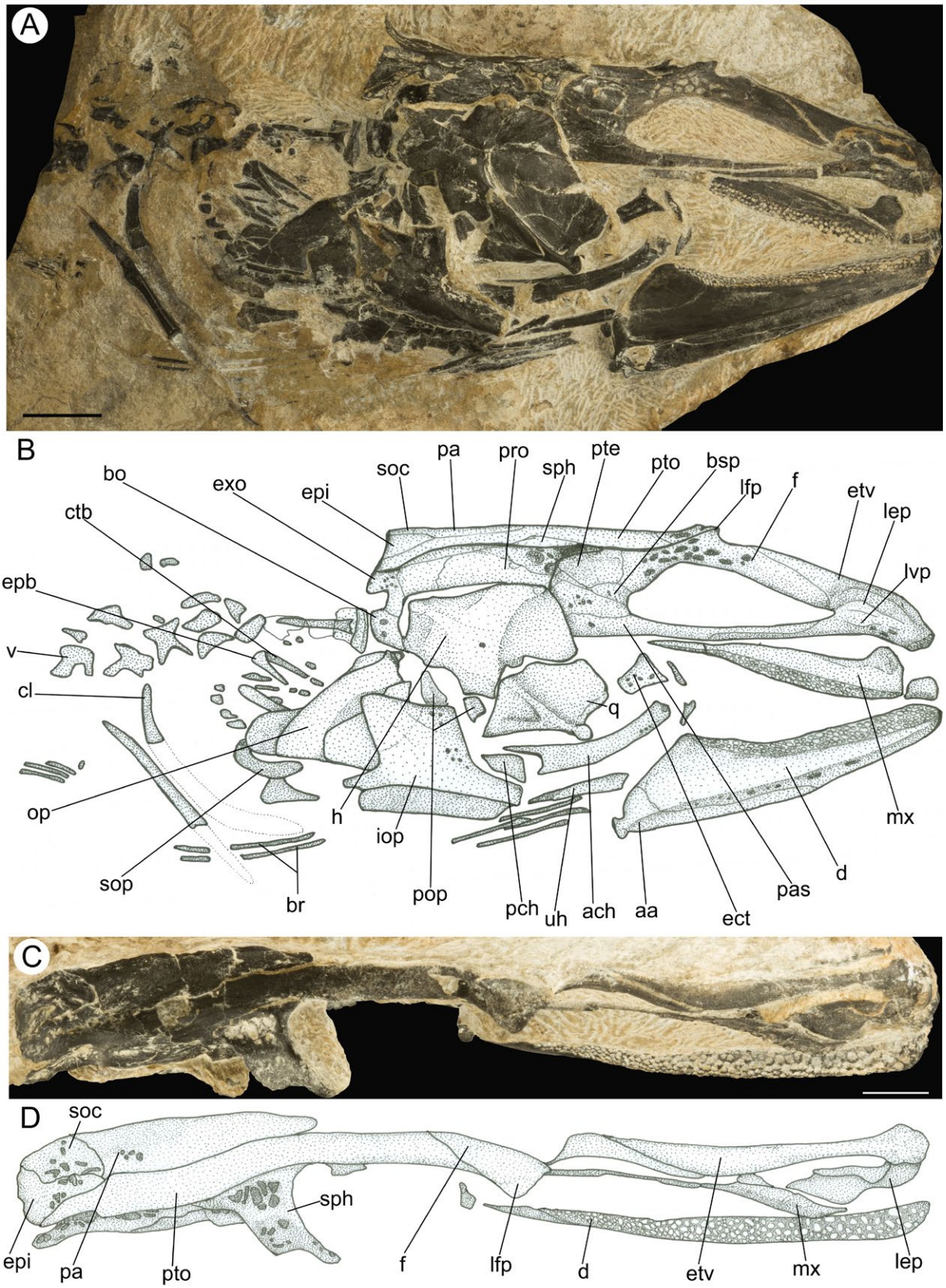

Fig 4. *Smithconger treldeensis* (Schwarzhans 2007) from the Eocene of Trelde Næs, eastern Jutland, Denmark. Paratype, NHMD-625415. **A**: Head and anterior portion of the axial skeleton, right lateral view. **B**: interpretative reconstruction. **C**: Neurocranium in dorsal view. **D**: interpretative reconstruction. Scale bars 10 mm.

Natural History Museum of Denmark, Copenhagen; NHMUK, Natural History Museum, London; NHMW, Naturhistorisches Museum, Vienna; NMNZ, Museum of New Zealand Te Papa Tongarewa, Wellington; ZMUC, Zoological Museum of the University of Copenhagen.

Systematic palaeontology

Order Anguilliformes Regan, 1909
Family Congridae Kaup, 1856

Genus *Smithconger* gen. nov.

Type species. *Smithconger treldeensis* (Schwarzhans 2007), syn. *Pseudoxenomystax treldeensis* Schwarzhans 2007.

Etymology. Named in honour of the American ichthyologist David G. Smith (plus the generic name *Conger*), in recognition of his outstanding contribution to the study of anguilliform fishes.

Diagnosis. A genus of Congridae unique in having the following combination of characters: frontals with well-developed lateral processes; supraoccipital crest absent; sphenotic large and anteriorly pointed, exposed on the flattened surface of skull roof; otic bullae considerably reduced; maxilla elongate, nearly straight, distally pointed, bearing a large paddle-like dorsal process on its anterodorsal extremity; oral jaw teeth numerous, arranged in multiple rows; ventral profile of the dentary convex; mandible not projecting anteriorly beyond the upper jaw; opercle with smooth posterior margin; subopercle short; otoliths oval with high dorsal rim, broad and deep dorsal depression, no ventral furrow; sulcus straight, narrow, shallow, centrally positioned with anteriorly reduced colliculum; ostial channel at anterior tip of colliculum short, not reaching the predorsal rim.

Discussion. Schwarzhans (2007) described the species *Pseudoxenomystax treldeensis* from the Lillebælt Clay based on three otolith casts. One of these otoliths, selected as the holotype (Fig. 3A), was found as a void *in situ* from a partially preserved neurocranium, which was not described nor figured by Schwarzhans (2007). Despite the inadequate preservation of the holotypic neurocranium (Fig. 2), a suite of morphological features reveals a substantial similarity in the overall proportions and general configuration with that of the paratype NHMD-625415. Due to the distinctiveness of these features, especially the relative size and orientation of the sphenotic spine and of the robust laterally-directed frontal process, these specimens are regarded herein as conspecific.

The extant genus *Pseudoxenomystax* was originally created by Breder (1927) and subsequently discussed by Castle (1960) and is currently not considered as valid with its formerly referred species assigned to the genera *Bassanago* and *Bathycongrus* (e.g., Smith 1989; Castle 1995). The neurocranial morphology of both these genera differs from that of the Eocene fossil from the Lillebælt Clay Formation described herein, thereby supporting its attribution to a new separate genus within the family Congridae.

Composition. Two fossil species are referred to the genus *Smithconger*; the type-species *Smithconger treldeensis* (Schwarzhans, 2007) from the early Lutetian of the Lillebælt Clay Formation of Denmark and *Smithconger waihaoensis* (Schwarzhans 2019), an otolith-based species (Fig. 3B) described by Schwarzhans (2019a) as *Bathycongrus waihaoensis* from the Kaiatan (Bartonian/Priabonian) of the Waihao River, South Island of New Zealand.

Smithconger treldeensis (Schwarzhans, 2007)
(Figs 2–3A, 4–5).

Holotype. NHMD-625030, a partially complete neurocranium exhibiting a large hollow cavity originally occupied by the saccular otolith (Fig. 2), measuring about 44.9 mm in length. The otolith (Fig. 3A) is registered with the number MGUH 28347.

Paratypes. NHMD-625415, a partially complete articulated skeleton represented by the head and a poorly preserved anterior portion of the abdominal region of the body (Fig. 4). Paratypic otoliths are registered with the numbers MGUH 28346 and 28357.

Type locality and horizon. Trelde Næs near Fredericia, eastern Jutland, Denmark, Lillebælt Clay Formation, Middle Eocene, early Lutetian.

Measurements (of the paratype NHMD-625415). Neurocranial length: 76.2 mm; neurocranial depth (measured at midlength of the orbit): 14.8 mm (19.4 % of neurocranial length); preorbital length: 13.6 mm (17.8 % of neurocranial length); orbital length: 28.7 mm (37.6 % of neurocranial length); postorbital length: 34.0 mm (44.6 % of neurocranial length); maxillary length: 33.9 mm (44.4 % of neurocranial length); mandible length: 44.8 mm (58.7 % of neurocranial length); lateral extension of the sphenotic spine: 7.5 mm (9.8% of neurocranial length).

Description. The holotypic neurocranium is inade-

quately preserved to allow an appropriate description of its structure (Fig. 2). Therefore, the descriptive osteology is mostly based on the paratype NHMD-625415 (Fig. 4). Overall, the paratypic specimen NHMD-625415 is largely incomplete, lacking most of the axial skeleton. The head skeleton is partially complete and most of the bones are in some ways displaced from their original position (Figs 4A–B). The axial skeleton is solely represented by at least five incomplete and poorly preserved (abdominal) vertebrae, a partially complete crescent-shaped cleithrum and some fragments of the pectoral-fin rays.

The neurocranium is elongate, slender and somewhat dorsally flattened (Figs 4A–B, 5); its depth measured at the midlength of the orbit reaches about one fifth of the neurocranial length. It is robust anteriorly and projects beyond the lower jaw. The orbit is elongated and occupies more than one third of the entire neurocranial length. Overall, the neurocranium is solidly ossified and some of the bones are ornamented by irregular and deep pits, which are quite abundant on the ventral surface of the frontal in the central and posterior sector of the orbit, but also on the prootic and the ventral surface of the sphenotic; due to the extensive ornamentation of certain neurocranial bones, it is very difficult to recognize the foramina for nerves. The original sutures between the bones are difficult to recognize due to considerable overlapping, as well as of inadequate preservation of the surface of certain bones.

The ethmovomerine complex is thick and bears a broad lateral ethmoid process with almost linear lateral margins emerging just in front of the orbit. The anteroventral portion of the ethmovomerine complex, which apparently comprises the entire dentigerous area, is slightly curved downwards (Figs 4A–B, 5). A small lateral vomerine process can be observed just below the lateral ethmoid process. The frontals are only partially exposed and form most of the dorsal border of the orbit (Figs 4–5). The two frontals are fused to each other into a single bone, which can be easily recognized in the holotype (Fig. 2). A prominent and thick triangular process projects laterally from the dorsal surface of the frontals (Figs 4C–D, 5). As reported above, the ventral surface of the frontals just above the origin of the prominent lateral process is extensively pitted. The parietals are rather large and articulate anteriorly with the fused frontals, laterally with the pterotic and posteriorly with the epioccipital and the small supraoccipital. There is no

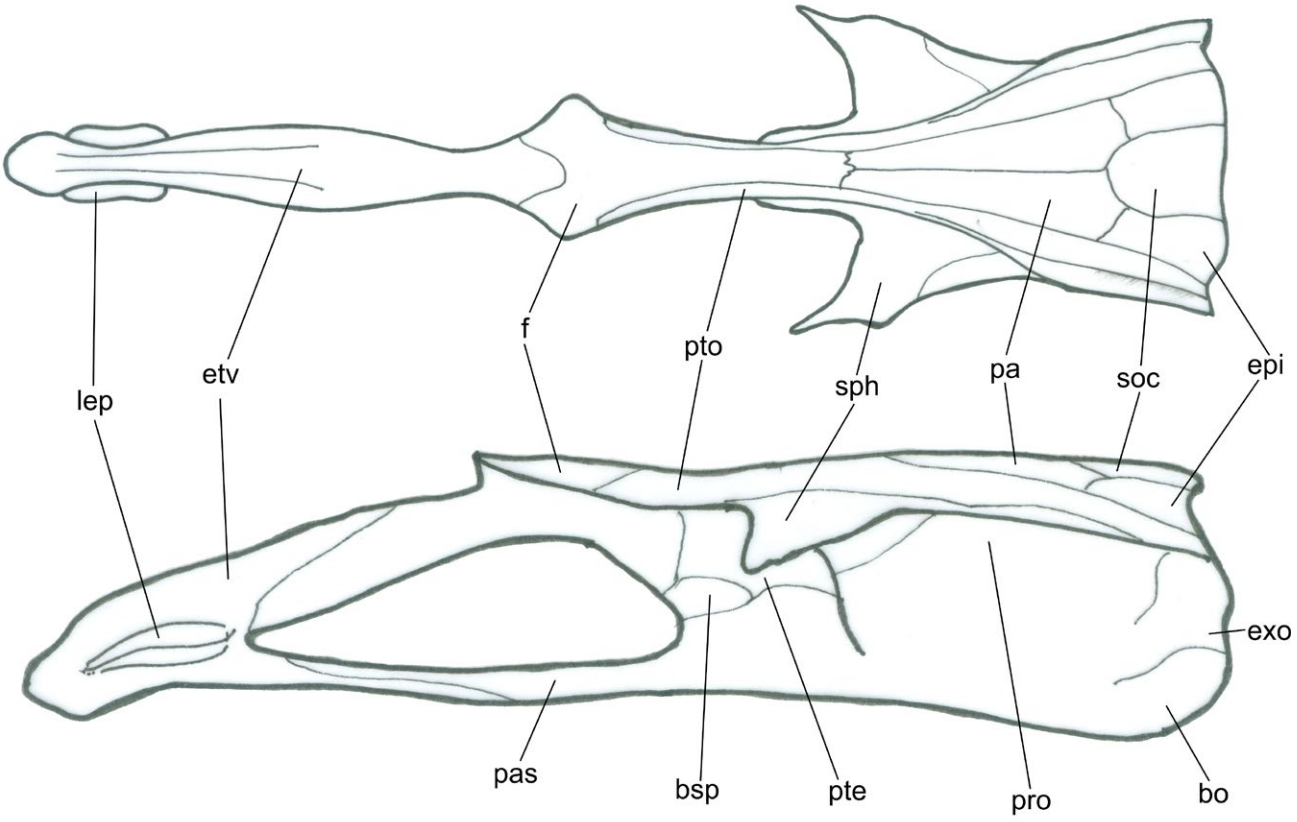

Fig. 5. *Smithconger treldeensis* (Schwarzhans 2007) from the Eocene of Trelde Næs, eastern Jutland, Denmark. Reconstruction of the neurocranium in dorsal (above) and lateral (below) view.

supraoccipital crest. The epioccipital occupies a small triangular surface in the posteriormost portion of the skull roof where it articulates with the parietal and supraoccipital medially and with the pterotic laterally. As in other anguilliform fishes, the pterotic is the major lateral longitudinal bone of the neurocranium; based on its overall morphology, with a smooth and solid outer surface, it is reasonable to hypothesize that the temporal sensory canal was enclosed within this bone. Due to the flattened dorsal aspect of the neurocranium, the sphenotic is clearly exposed on the skull roof (Fig. 5), showing a very high position on the neurocranium compared to most congrid taxa (Fig. 6), in which it contributes to form the lateral wall of the neurocranium (e.g., Smith 1989). The sphenotic is almost triangular in dorsal outline and projects antero-laterally as a pointed blade-like process; it articulates medially and posteriorly with the pterotic and ventrally with the pterosphenoid and prootic. The articular facet for the anterior articular head of the hyomandibula is clearly recognizable in NHMD-625415. The pterosphenoid forms part of the lateral wall of the neurocranium; it articulates with the frontal anteriorly, with the basisphenoid anteroventrally, with the sphenotic and pterotic dorsally, with the prootic posteroventrally, and with the parasphenoid ventrally. The basisphenoid is small and can be easily recognized along the posterior border of the orbit. The parasphenoid is greatly elongate, extending from the basioccipital almost to the anterior tip of the orbit. The prootic is mostly not exposed, covered by the hyomandibula in the paratype NHMD-625415. Although the prootics are only partially exposed in the holotype (Fig. 2), it seems that the otic bullae were consistently reduced in size in origin, resembling the condition observed in *Conger* (e.g., Takai 1959; Asano 1962; Smith 1989). The stout basioccipital forms the posteroventral corner of the neurocranium. The basioccipital articulates dorsally with the large exoccipital.

While the otolith is not preserved in the holotype, its outline is impressed in the cavity allowing the production of a cast (Fig. 3A) that was described by Schwarzhans (2007) as follows: "Large oval otoliths up to about 14 mm length. Ventral rim gently curving, smooth, deepest at its middle; dorsal rim more strongly curving, highest, most expanded just anterior of the middle, this portion sometimes slightly undulated. Anterior tip moderately pointed at its middle; posterior tip symmetrical, not completely preserved. Inner face markedly convex. Sulcus medial, narrow, straight, with well-marked, anteriorly reduced colliculum. Anterior part of ostium indistinctly outlined, without colliculum and thus colliculum centrally positioned on inner face. Ostial canal short, indistinct, beginning near anterior tip of colliculum, not reaching dorsal rim. Dorsal depression wide, deep; no ventral furrow. Outer face nearly flat to slightly convex, smooth".

Based on the relative size of the jaw bones and the limited forward inclination of the suspensorium, it is reasonable to conclude that the mouth gape was moderately large (Figs 4A–B). The upper border of the mouth gape is formed by the thick and robust maxilla. The maxilla is elongate, nearly straight, distally pointed and bears a large paddle-like dorsal process on its anterodorsal extremity that comprises the maxilla-ethmovomeral facet on its medial surface. The alveolar surface of the maxilla is fully covered by relatively small circular tooth sockets arranged in multiple rows. The mandible is solid, almost linear and nearly triangular in outline, and does not project anteriorly beyond the upper jaw. It is constituted by the dentary and the anguloarticular. The dentary is very large and bears a well-developed coronoid process posterodorsally. The alveolar surface of the dentary is completely covered by tooth sockets arranged in multiple rows identical to those of the maxilla (Fig. 4).

Although only partially complete, the suspensorium appears to be wider than deep, inclined forward and characterized by a very large hyomandibula (Figs 4A–B). The hyomandibula has an irregular trapezoid outline and possesses two prominent condyles for the cranial articulation. What appears to be a foramen can be observed on the main vertical shaft of the hyomandibula. The opercular process of the hyomandibula is extremely short and thick. The quadrate is large, fan-shaped, with an irregular dorsal margin. The dorsal margin of the quadrate fits well with the ventral margin of the hyomandibula, suggesting that these bones were remarkably consolidated into a strong functional complex. Only a fragment of the ectopterygoid, probably representing a disarticulated posterior extremity can be observed in the fossil.

The bones of the opercular apparatus are displaced from their original position and overlapped to each other (Figs 4A–B). Of the preopercle only some fragments can be recognized. The interopercle is plate-like, roughly trapezoid in outline. The opercle is only partially exposed; it appears to be fan-shaped, with a gently convex dorsal margin and a rounded and continuous posterior margin. The subopercle is sickle-shaped.

Of the hyoid arch (Figs 4A–B), a partially preserved hyoid bar with anterior and posterior ceratohyals, a largely incomplete urohyal and at least six incomplete branchiostegal rays can be recognized. There are no hypohyals.

Gill arches are represented by fragments of the ventral and dorsal portions, including what appear to be incomplete epibranchials and ceratobranchials (Figs 4A–B).

The affinities of Smithconger treldeensis (Schwarzhans, 2007)

In his fundamental study on the classification of eel-like fishes, Regan (1912) emphasized the diagnostic role of separated vs fused frontals in the subdivision of modern anguilliforms into well-defined groups. The shared possession of fused frontals allowed the recognition of a speciose and morphologically diverse lineage traditionally referred to as the Congroidei (Robins 1989), which includes, among the others, the families Congridae, Derichthyidae, Muraenesocidae, Nettastomatidae and Ophichthidae (Nelson *et al*. 2016). Within this group, the family Congridae is one of the largest and most diverse, currently comprising 194 species arranged in 30 extant genera (Fig. 6). A definition of the Congridae is problematic to provide because of the generalized morphology and substantial uniformity of the overall appearance of most of its members (Smith 1989). Although this family has been considered as non-monophyletic by molecular studies (e.g., Inoue *et al*. 2010; Johnson *et al*. 2012; Santini *et al*. 2013), the co-occurrence of certain morphological traits is almost exclusive of these fishes, making it possible to refer fossil taxa to this family. Therefore, despite the incompleteness of the available material, both the skeletal structure and otolith morphology concur to support the attribution to the anguilliform family Congridae. In particular, the combination of laterally compressed and massive ethmovomer, fused frontals, large sphenotics, otoliths with shallow sulcus, anteriorly reduced colliculum and broad dorsal depression, and forward inclined suspensorium substantially support the placement of the fossils described herein within the family Congridae (e.g., Asano 1962; Smith 1989; Ramon-Castro *et al*. 2021). Primarily based on the criteria proposed by Asano (1962), Smith (1989) subdivided the Congridae into three subfamilies, the Bathymyrinae, Congrinae and Heterocongrinae (the latter recognized as a subfamily by Böhlke 1957). The subfamily Bathymyrinae consists of seven genera (*Ariosoma*, *Bathymyrus*, *Chiloconger*, *Kenyaconger*, *Parabathymyrus*, *Paraconger*, *Rostroconger*; Smith & Karmovskaya 2003; Smith 2018), the subfamily Heterocongrinae contains two genera (*Gorgasia*, *Heteroconger*; Böhlke 1957), while at least 21 genera (*Acromycter*, *Bassanago*, *Bathycongrus*, *Bathyuroconger*, *Castleichthys*, *Conger*, *Congrhynchus*, *Congriscus*, *Congrosoma*, *Diploconger*, *Gnathophis*, *Japonoconger*, *Lumiconger*, *Macrocephenchelys*, *Poeciloconger*, *Promyllantor*, *Pseudophichthys*, *Rhynchoconger*, *Scalanago*, *Uroconger*, *Xenomystax*; Table 1) are implicitly referred to the subfamily Congrinae, considering that Karrer & Smith (1980) suggested that the genus *Blachea* might deserve a separate subfamilial status. According to Smith (1989), the Bathymyrinae and Heterocongrinae form a sister pair, supported by at least two synapomorphies, possession of a strut-like lateral ethmoid process (lost in *Heteroconger*; Fig. 6L) and unsegmented fin rays. This sister-group relationship has also been confirmed by a comparative study of their otoliths (Schwarzhans, 2019b).

As discussed above, there is no evidence of a strut-like lateral ethmoid process in *Smithconger* (Fig. 5), thereby excluding it from any possible attribution to the Bathymyrinae and Heterocongrinae. Moreover, *Smithconger* differs from the members of the Bathymyrinae by having a supraoccipital, which is reduced but present in the bathymyrine genera *Chiloconger* and *Paraconger* (Fig. 6Q; Table 1). The heterocongrines, commonly known as garden eels, are a specialized clade with a slender and greatly elongate body, a shortened head and a caudal fin stiffened for burrowing on sandy bottoms. These fishes are characterized by unique suite of features that clearly separate them from the other congrids, including a short and oblique mouth and lower jaw projecting beyond the upper one (Böhlke 1957; Rosenblatt 1967; Smith 1989); all of these features have not been observed in *Smithconger*. The Congrinae is the largest of the currently recognized subfamilies. Smith (1989) suggested the loss of hypohyals as a possible synapomorphy for the congrines. As described above, there is no evidence of hypohyals in *Smithconger,* thereby supporting its attribution to this subfamily, which can be also justified by the possession of a moderately large mouth gape and absence of a strut-like lateral ethmoid process. Within the congrines, *Smithconger* resembles in many ways *Bassanago* (see Fig. 6C, Table 1), especially in the well-developed laterally directed frontal processes, absence of a supraoccipital crest, convex ventral profile of the dentary, smooth posterior margin of the opercle, short subopercle and, more generally, in the overall proportions of the neurocranium (e.g., Smith *et al*. 2020). The otoliths of *Smithconger* resemble those of *Bassanago* (Fig. 3C) and, to a lesser extent, those of *Bathycongrus* (Fig. 3D) in having a horizontally positioned and anteriorly reduced sulcus with a single, centrally positioned colliculum, as well as for the presence of a distinctive and wide dorsal depression. However, *Smithconger* clearly differs from *Bassanago* in having considerably reduced (vs large) otic bullae, nearly straight and distally pointed (vs slightly curved and distally expanded) maxilla, basisphenoid with anterior smooth margin (vs with a distinct process) (see Smith *et al*. 2020). The otoliths of *Smithconger* show an indistinct and short ostial channel that is interpreted as plesiomorphic compared to the otoliths of the extant *Bassanago* (and *Bathycongrus*) in which the ostial channel is completely atrophied.

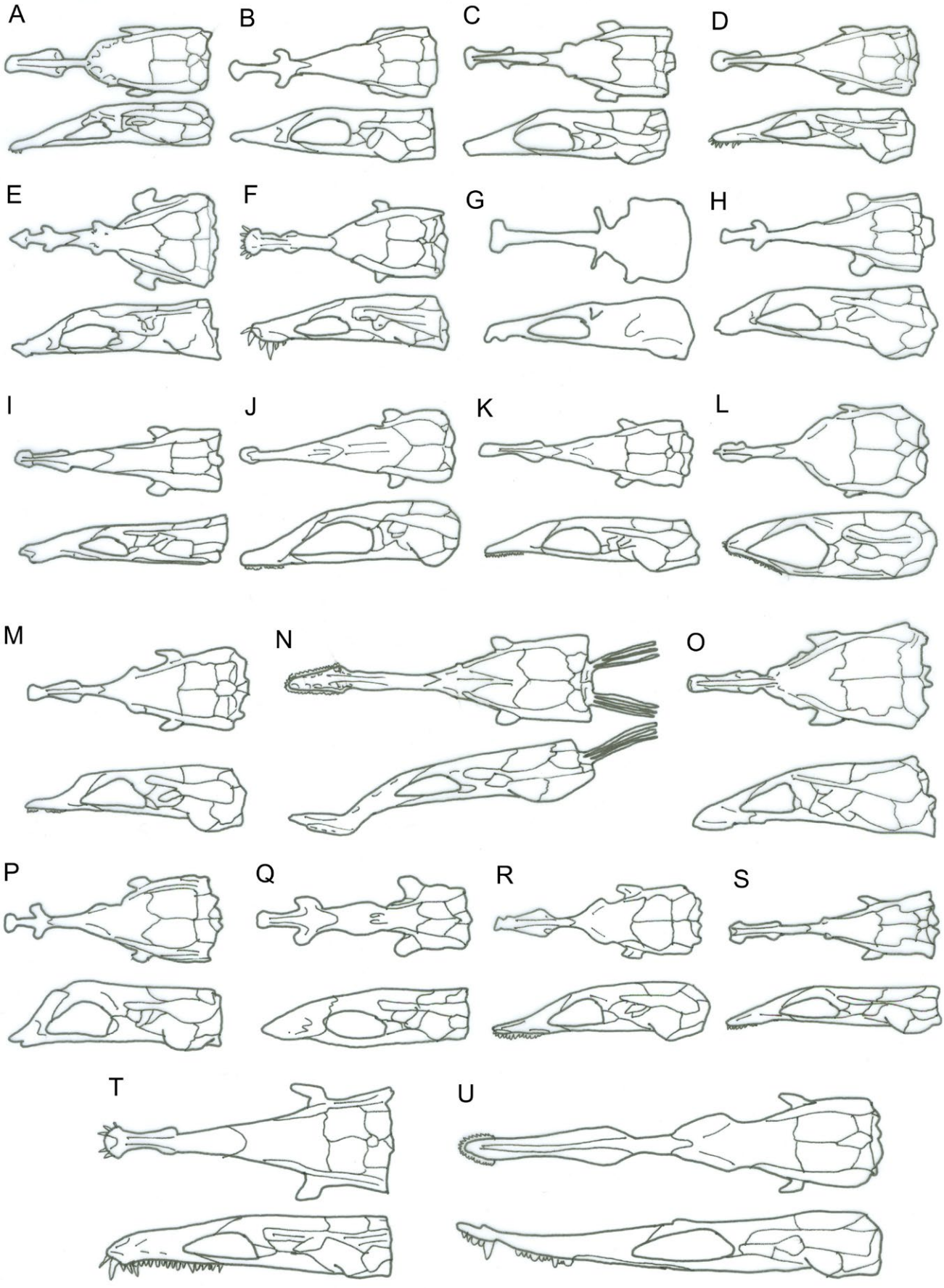
A
B
C
D
E
F
G
H
I
J
K
L
M
N
O
P
Q
R
S
T
U

Table 1. Synopsis of selected morphological characters for fossil and extant genera of the family Congridae

	supraoccipital	strut-like lateral ethmoid process	lateral process of the frontal	teeth in jaws	lower jaw projecting beyond upper	posterior opercular margin
Acromycter	present	absent	present or absent	multiple rows	no	lobate/fimbriated
Ariosoma	absent	present	present or absent	multiple rows	no	smooth
Bathymyrus	absent	present	present	single row	no	smooth
Bassanago	present	absent	present	multiple rows	no	smooth
Bathycongrus	present	absent	absent	multiple rows	no	serrated
Bathyuroconger	present	absent	absent	two or three rows	no	with strong spines
Blachea	present	absent	present	single row	no	smooth
Bolcyrus	present	absent	absent	multiple rows	yes	smooth
Castleichthys	?	?	?	single row	no	?
Chiloconger	present	present	absent	two or three rows	no	smooth
Conger	present	absent	present or absent	one or two rows	no	smooth
Congrhynchus	?	?	?	multiple rows	no	?
Congriscus	absent	absent	absent	one or two rows	no	smooth
Congrosoma	?	?	?	?	no	?
Diploconger	?	?	?	one to three rows	no	?
Gnathophis	present	absent	absent	multiple rows	no	smooth
Gorgasia	present	present	absent	multiple rows	yes	smooth
Heteroconger	present	absent	absent	multiple rows	yes	smooth
Japonoconger	present	absent	present, very short	multiple rows	no	weakly serrated
Kenyaconger	?	?	?	one or two rows	yes	?
Lumiconger	present	absent	present, very short	multiple rows	no	smooth
Macrocephenchelys	absent	absent	absent	multiple rows	no	with strong spines
Parabathymyrus	absent	present	present	one or two rows	no	smooth
Paraconger	present	present	present	one or two rows	no	smooth
Paracongroides	?	?	?	?single row	no	smooth
Pavelichthys	present	present	absent	multiple rows	yes	?smooth
Poeciloconger	?	?	?	multiple rows	no	?
Promyllantor	?	?	?	multiple rows	no	?
Pseudophichthys	absent	absent	present	multiple rows	no	with strong spines
Rhynchoconger	present	absent	present	multiple rows	no	serrated
Rostroconger	?	?	?	one or tow rows	no	?smooth
Scalanago	?	?	?	?	no	?smooth
Smithconger	present	absent	present	multiple rows	no	smooth
Uroconger	present	absent	absent	two rows	no	smooth
Voltaconger	present	absent	absent	single row	yes	smooth
Xenomystax	present	absent	present	three rows	no	smooth

Includes new data and data from Asano (1962), Blot (1978), Böhlke (1957), Castle (1960, 1963, 1968, 1988, 1995), Castle & Paxton (1984), Eagderi & Adriaens (2014), Ho et al. (2018), Kanazawa (1958, 1961), Karmovskaya (2006, 2011), Karmovskaya & Smith (2008), Karrer & Smith (1980), Prokofiev (2007), Ramos-Castro et al. (2021), Robins & Robins (1971), Rosenblatt (1967), Smith (1989, 2004, 2018), Smith & Kanazawa (1977), Smith et al. (2018, 2020), Smith & Karmovskaya (2003), Takai (1959).

◀ **Fig. 6.** Neurocranium of selected conger eel species in dorsal (above) and left lateral (below) view. **A**: *Acromycter perturbator* (Parr, 1932), redrawn from Smith (1989); **B**: *Ariosoma balearicum* (Delaroche, 1809), redrawn from Smith (1989); **C**: *Bassanago albescens* (Barnard, 1923), redrawn from Smith *et al*. (2020); **D**: *Bathycongrus thysanochilus* (Reid, 1934), redrawn from Smith (1989); **E**: *Bathymyrus smithi* Castle, 1968, redrawn from Castle (1968); **F**: *Bathyuroconger vicinus* (Vaillant, 1888), redrawn from Smith (1989); **G**: *Blachea xenobranchialis* Karrer & Smith, 1980, redrawn from Karrer & Smith (1980); **H**: *Chiloconger dentatus* (Garman, 1899), redrawn from Smith & Karmovskaya (2003); **I**: *Conger oceanicus* (Mitchill, 1818), redrawn from Smith (1989); **J**: *Congriscus megastoma* (Günther, 1877), redrawn from Asano (1962); *K*: *Gnathophis bathytopos* Smith & Kanazawa, 1977, redrawn from Smith (1989); **L**: *Heteroconger halis* (Böhlke, 1957), redrawn from Smith (1989); **M**: *Japonoconger carribeus* Smith & Kanazawa, 1977, redrawn from Smith (1989); **N**: *Lumiconger arafura* Castle & Paxton, 1984, redrawn from Castle & Paxton (1984); **O**: *Macrocephenchelys branchialis* Fowler, 1934, redrawn from Smith (1989); **Q**: *Paraconger caudilimbatus* (Poey, 1867), redrawn from Smith (1989); **R**: *Pseudophichthys splendens* (Lea, 1913), redrawn from Smith (1989); **S**: *Rhynchoconger gracilior* (Ginsburg, 1951(, redrawn from Smith (1989); **T**: *Uroconger syringinus* Ginsburg, 1954, redrawn from Smith (1989); **U**: *Xenomystax bidentatus* (Reid, 1940), redrawn from Smith (1989).

Compared to the Eocene congrid genera from Monte Bolca *Bolcyrus*, *Paracongroides* and *Voltaconger* and to the Oligocene *Pavelichthys*, *Smithconger* exhibits a substantially different neurocranial morphology (Fig. 7; Table 1), mandible not projecting beyond the upper jaw (Table 1), and different oral jaw teeth arrangement (Table 1). In particular, the neurocranium of *Smithconger* clearly differs from that of *Bolcyrus* (Figs 7A–B) by having a different outline and general proportions, well-developed (vs absent) laterally-directed frontal process, skull roof flattened (vs not flattened) bearing a large and acute sphenotic spine, and supraoccipital crest absent (vs present). In addition, *Bolcyrus* is characterized by mandible projecting anteriorly beyond the upper jaw (Fig. 7C; Table 1) and by a single hypohyal in the hyoid bar (Blot 1978). As far as *Paracongroides* is concerned (Fig. 7F), it clearly differs from *Smithconger* by having jaw teeth arranged in a single row (Table 1; see also Blot 1978). *Pavelichthys* differs from *Smithconger* in having a strut-like lateral ethmoid process and mandible projecting beyond the upper jaw and by lacking laterally-directed frontal processes (Table 1; see also Prokofiev 2007). Finally, *Voltaconger* is characterized by a different neurocranial morphology,

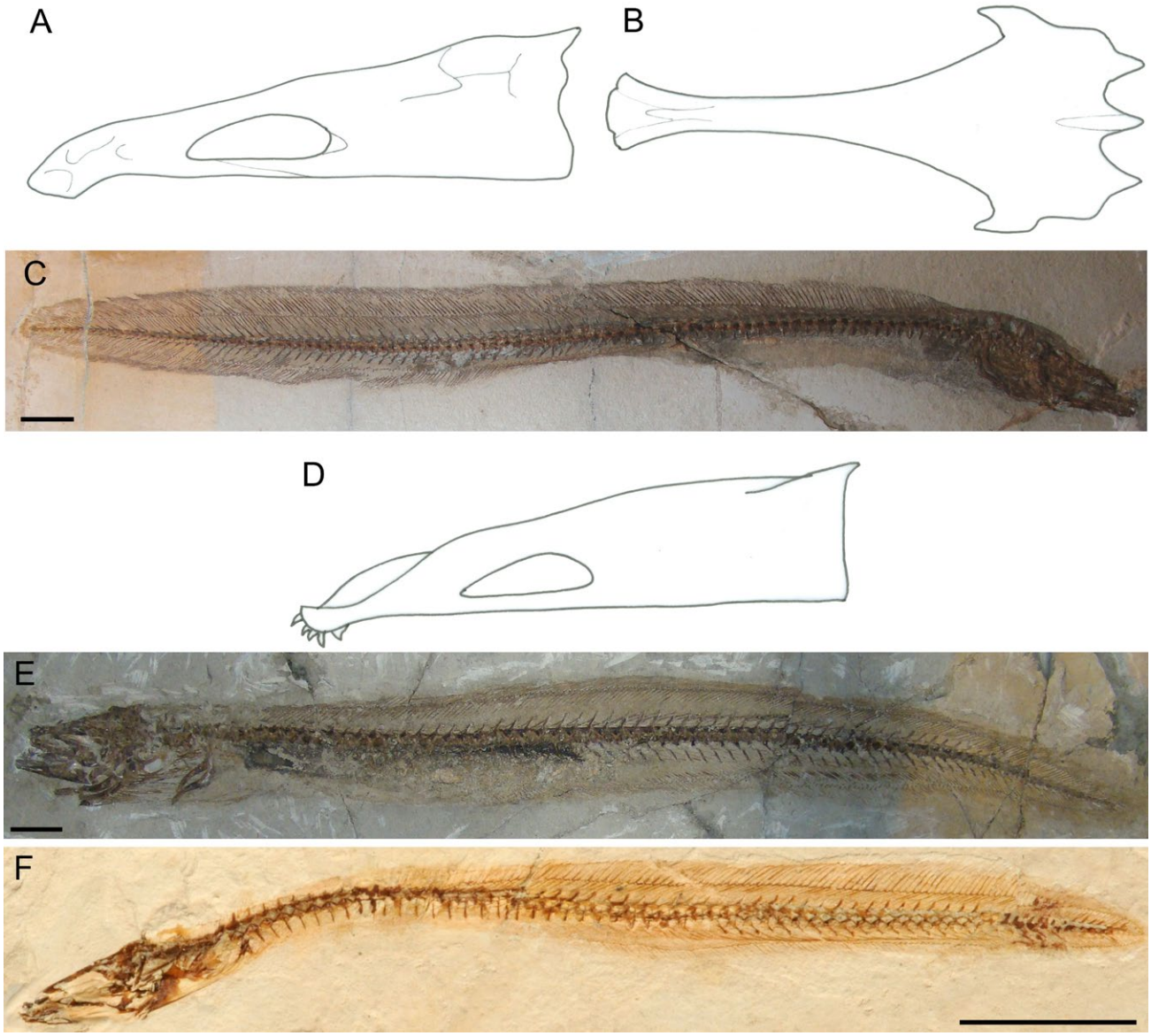

Fig 7. Eocene conger eels from Monte Bolca, Italy. **A–C**: *Bolcyrus formosissimus* (Eastman, 1905), reconstruction of the neurocranium in left lateral (A, based on MNHN 109609) and dorsal view (B, based on MCSNV IG24496); C: MCSNV T.442, right lateral view. **D–E**, *Voltaconger latispinus* (Agassiz, 1839); **D**: reconstruction of the neurocranium in left lateral view; **E**: NHMUK P17024, left lateral view. **F**: *Paracongroides heckeli* Blot, 1978, NHMW 1855/VI/70 – A3382, left lateral view. Scale bars 20 mm

which includes the lack of laterally-directed frontal processes and the presence of a supraoccipital crest (Fig. 7D), and by lower jaw projecting anteriorly beyond the upper one (Fig. 7E; Table 1).

The possible subfamilial attribution of these Palaeogene congrid genera was cursorily discussed by Prokofiev (2007), who concluded that *Bolcyrus* and *Voltaconger* may pertain to the Congrinae, whereas *Paracongroides* and *Pavelichthys* belong to the Bathymyrinae. However, while the attribution of *Paracongroides* and *Pavelichthys* to the Bathymyrinae seems to be reasonably supported by morphological evidence (preanal length of the body exceeding 40% of TL, fin rays not segmented, caudal fin reduced and apparently stiffened, and strut-like lateral ethmoid process in *Pavelichthys*; Blot 1978, Prokofiev 2007), the attribution of *Bolcyrus* and *Voltaconger* to the Congrinae appears to be much elusive. Both these genera are characterized by mandible projecting anteriorly beyond the upper jaw, plus a suite of generalized features commonly considered as diagnostic of the Congrinae (Smith 1989), including ectopterygoid stout, abdominal vertebrae representing less than 40% of the entire vertebral column, myorhabdoi absent, dorsal- and anal-fin rays segmented, caudal fin not reduced, and pectoral fin well-developed (Blot 1978). Moreover, *Voltaconger* lacks hypohyals in the hyoid bar, while *Bolcyrus* has a single hypohyal (Blot 1978). As discussed above, Smith (1989) considered the loss of hypohyals as a synapomorphic feature of the congrines, thereby suggesting that *Bolcyrus* cannot be confidently placed within the Congrinae; according to Johnson *et al*. (2012), however, hypohyals can probably be present in certain congrids. In summary, based on the available data, the subfamilial placement of *Bolcyrus* and *Voltaconger* appears to be not fully resolved. In this context, it is interesting to note that these two genera were placed outside the Congridae, associated with the genera of the extinct family Anguilloididae (*Anguilloides*, *Veronanguilla*), in the phylogenetic analysis published by Belouze (2002).

Acknowledgements

We would like to cordially thank Mogens Madsen (Fredericia) for collecting the holotype specimen and detecting the otolith impressions in the concretions of the Lillebælt Clay Formation and for preparing the formidable casts. We are particularly obliged to Emma Bernard (NHMUK), Gäel Clement (MNHN), Mathias Harzhauser (NHMW), Cathrin Pfaff and Jurgen Kriwet (University of Vienna), and Roberto Zorzin (MCSNV) for access to material in their care and for providing the photos of Eocene conger eels from Monte Bolca, including those used in this paper. We also thank H.-C. Ho (Pingtung, Taiwan) for his support with extant congrid otoliths. For reviewing the manuscript and providing constructive suggestions for its improvement we are particularly obliged to David G. Smith (National Museum of Natural History, Smithsonian Institution, Washington) and Tomáš Přikryl (Institute of Geology of the Czech Academy of Sciences, Prague). The research of GC was supported by a SYNTHESYS grant (DK-TAF-4928) and by grants (ex-60% 2021) from the Università degli Studi di Torino.

References

Asano, H. 1962: Studies on the congrid eels of Japan. Bulletin of the Misaki Marine Biological Institute, Kyoto University 1, 1–143.

Bannikov, A.F. & Parin, N.V. 1997: The list of marine fishes from Cenozoic (Upper Paleocene-Middle Miocene) localities in southern European Russia and adjacent countries. Journal of Ichthyology 37, 133–146.

Belouze, A. 2002: Compréhension morphologique et phylogénétique des taxons actuels et fossils rapportés aux anguilliformes («poissons», téléostéens). Travaux et Documents des Laboratoires de Géologie de Lyon 158, 1–401.

Belouze, A., Gayet, M. & Atallah, C. 2003a: Les premiers Anguilliformes : I. Révision des genres cénomaniens *Anguillavus* Hay, 1903 et *Luenchelys* nov. gen. Geobios 36, 241–273. 3. https://doi.org/10.1016/s0016-6995(03)00029-9

Belouze, A., Gayet, M. & Atallah, C. 2003b: Les premiers Anguilliformes : II. Paraphylie du genre *Urenchelys* Woodward, 1900 et relations phylogénétiques. Geobios 36, 351–378. https://doi.org/10.1016/s0016-6995(03)00036-6

Blot, J. 1978: Les apodes fossiles du Monte Bolca. Studi e Ricerche sui Giacimenti Terziari di Bolca 3, 1–260.

Blot, J. 1984: Les apodes fossiles du Monte Bolca II. Studi e Ricerche sui Giacimenti Terziari di Bolca 4, 61–238.

Böhlke, J. 1957: On the occurrence of garden eels in the western Atlantic, with a synopsis of the Heterocongrinae. Proceedings of the Academy of Natural Sciences of Philadelphia 109, 59–79.

Bonde, N. 1966: The fishes of the Mo-clay Formation (Lower Eocene): a short review. Meddelelser fra Dansk Geologisk Forening 16, 199–202.

Bonde, N. 1968: Nyligt fundne fossiler fra det 'plastiske ler'. Meddelelser fra Dansk Geologisk Forening 18, 148–151. https://doi.org/10.1016/0012-8252(68)90138-4

Bonde, N., Andersen, S., Hald, N. & Jakobsen S.L. 2008: Danekræ – Danmarks bedste fossiler, 225 pp. Copenhagen: Gyldendals forlag. https://doi.org/10.7146/gn.v0i3.3458

Breder, C.M. 1927: Scientific results of the first oceanographic expedition of the "Pawnee" 1925. Fishes. Bulletin of the Bingham Oceanographic Collection Yale University 1, 1–90.

Carlsen, A.W. & Cuny, G. 2014: A study of the shark and rays

from the Lillebælt Clay (Early-Middle Eocene) of Denmark, and their palaeoecology. Bulletin of the Geological Society of Denmark 62, 39–88. https://doi.org/10.37570/bgsd-2014-62-04

Casier, E. 1967: Poissons del'Eocene inferieur de Katharinenhof-Fehmarn (Schleswig-Holstein). Bulletin de l'Institut Royal des Sciences Naturelles de Belgique 43, 1–23.

Castle, P.H.J. 1960: Two eels of the genus *Pseudoxenomystax* from New Zealand waters. Transactions of the Royal Society of New Zealand 88, 463–472.

Castle, P.H.J. 1963: The systematics, development and distribution of two eels of the genus *Gnathophis* (Congridae) in Australasia waters. Zoological Publications from Victoria University of Wellington 34, 15–47. https://doi.org/10.1016/0011-7471(65)91373-2

Castle, P.H.J. 1968: Description and osteology of a new eel of the genus *Bathymyrus* from off Mozambique. Department of Ichthyology Rhodes University, Grahamstown, Special Publication 4, 1–12.

Castle, P.H.J. 1988: Two new species of the previously monotypic congrid eel genera *Poeciloconger* and *Macrocephenchelys* from Eastern Australia. Records of the Australian Museum 42, 119–126. https://doi.org/10.3853/j.0067-1975.42.1990.109

Castle, P.H.J. 1995: Alcock's congrid eels from the "Investigator" collections in Indian Seas 1888–1894. Copeia 1995, 706–718. https://doi.org/10.2307/1446768

Castle, P.H.J. & Paxton, J.R. 1984: A new genus and species of luminescent eel (Pisces: Congridae) from the Arafura Sea, Northern Australia. Copeia 1984, 72–81. https://doi.org/10.2307/1445036

Collins, J.S.H. & Jakobsen, S.L. 2003: New crabs (Crustacea, Decapoda) from the Eocene (Ypresian/Lutetian) Lillebælt Clay Formation of Jutland, Denmark. Bulletin of the Mizunami Fossil Museum 30, 63–96.

Eagderi, S. & Adriaens, D. 2014: Cephalic morphology of *Ariosoma gilberti* (Bathymyrinae: Congridae). Iranian Journal of Ichthyology 1, 39–50.

Forey, P.L., Yi, L., Patterson, C. & Davies, C.E. 2003: Fossil fishes from the Cenomanian (Upper Cretaceous) of Namoura, Lebanon. Journal of Systematic Paleontology 1, 227–330. https://doi.org/10.1017/s147720190300107x

Gravesen, P. 1993: Fossiliensammeln in Südskandinavien, 248 pp. Korb (Goldschneck).

Hansen, B.B., Cuny, G., Rasmussen, B.W., Shimada, K., Jacobs, P. & Heilmann-Clausen, C. 2013: Associated skeletal and dental remains of a fossil odontaspidid shark (Elasmobranchii: Lamniformes) from the Middle Eocene Lillebælt Clay Formation in Denmark. Bulletin of the Geological Society of Denmark 61, 37–46. https://doi.org/10.37570/bgsd-2013-61-03

Hay, O.P. 1903: On a collection of Upper Cretaceous fishes from Mount Lebanon, Syria, with descriptions of four new genera and nineteen new species. Bulletin of the American Museum of Natural History 19, 395–452.

Heilmann-Clausen, C., Nielsen, O.B. & Gersner, F. 1985: Lithostratigraphy and depositional environments in the Upper Paleocene and Eocene of Denmark. Bulletin of the Geological Society of Denmark 33, 287–323. https://doi.org/10.37570/bgsd-1984-33-26

Ho, H.-C., Smith, D.G. & Huang, J.-F. 2018: Notes on the two rare conger eel species (Anguilliformes: Congridae) found in Taiwanese waters. Zootaxa 4454, 233–237. https://doi.org/10.11646/zootaxa.4454.1.19

Inoue, J.G., Miya, M., Miller, M.J., Sado, T., Hanel, R., Hatooka, K., Aoyama, J., Minegishi, Y., Nishida, M. & Tsukamoto, K. 2010: Deep-ocean origin of the freshwater eels. Biology Letters 6, 363–366. https://doi.org/10.1098/rsbl.2009.0989

Johnson, G.D., Ida, H., Sakaue, J., Sado, T., Asahida, T. & Miya, M. 2012: A 'living fossil' eel (Anguilliformes: Protanguillidae, fam. nov.) from an undersea cave in Palau. Proceedings of the Royal Society B 279, 934–943. https://doi.org/10.1098/rspb.2011.1289

Kanazawa, R.H. 1958: A revision of the eels of the genus *Conger* with descriptions of four new species. Proceedings of the United States National Museum 108, 219–267. https://doi.org/10.5479/si.00963801.108-3400.219

Kanazawa, R.H. 1961: *Paraconger*, a new genus with three new species of eels (family Congridae). Proceedings of the United States National Museum 113, 1–14. https://doi.org/10.5479/si.00963801.113-3450.1

Karmovskaya, E.S. 2006: *Promyllantor atlanticus* (Anguilliformes, Congridae), a new species from the Continental Slope of Southwestern Africa. Journal of Ichthyology 46, 594–597. https://doi.org/10.1134/s0032945206080030

Karmovskaya, E.S. 2011: New species of the genus *Bathycongrus – B. parviporus* (Congridae, Anguilliformes) – from waters of Central Vietnam (Nha Trang and Van Phong Bays). Journal of Ichthyology 51, 417–425. https://doi.org/10.1134/s0032945211040060

Karmovskaya, E.S. & Smith, D.G. 2008: *Bathycongrus trimaculatus*, a new congrid eel (Teleostei: Anguilliformes) from the southwestern Pacific, with a redescription of *Bathycongrus bleekeri* Fowler. Zootaxa 1943, 26–36. https://doi.org/10.11646/zootaxa.4454.1.12

Karrer, C. & Smith, D.G. 1980: A new genus and species of congrid eel from the Indo-West Pacific. Copeia 1980, 642–648. https://doi.org/10.2307/1444440

Marramà, G., Villier, B., Dalla Vecchia, F.M. & Carnevale, G. 2016: A new species of *Gladiopycnodus* (Coccodontoidea, Pycnodontomorpha) from the Cretaceous of Lebanon provides new insights about the morphological diversification of pycnodont fishes through time. Cretaceous Research 61, 34–43. https://doi.org/10.1016/j.cretres.2015.12.022

Nelson, J.S., Grande, T.C. & Wilson, M.V.H. 2016: Fishes of the World. Fifth Edition, 707 pp. Hoboken: John Wiley & Sons.

Nolf, D. & Dockery, D.T. 1990: Fish otoliths from the Coffee Sand (Campanian of northeastern Mississippi). Mississippi Geology 10, 1–14.

Pfaff, C., Zorzin, R. & Kriwet, J. 2016: Evolution of the locomotory system in eels (Teleostei: Elopomorpha). BMC Evolutionary Biology 16, 159. https://doi.org/10.1186/s12862-016-0728-7

Prokofiev, A.M. 2007: A redescription and relationships of the

congrid eel *Pavelichthys danilshenkoi* (Anguilliformes: Congridae) from the Lower Oligocene of Northern Caucasus. Journal of Ichthyology 47, 335–340. https://doi.org/10.1134/s0032945207050013

Ramos-Castro, M., Loh, K.-H. & Chen, H.-M. 2021: A descriptive and comparative neurocranium morphology of Anguilliformes fishes in Taiwan waters. Zootaxa 5023, 509–536. https://doi.org/10.11646/zootaxa.5023.4.3

Regan, C.T. 1912: The osteology and classification of the teleostean fishes of the order Apodes. Annals and Magazine of Natural History 8, 377–387. https://doi.org/10.1080/00222931208693250

Robins, C.R. 1989: The phylogenetic relationships of the anguilliform fishes. In Böhlke, E.B. (ed.), Fishes of the western North Atlantic. Memoirs of the Sears Foundation for Marine Research 1(9), 9–21.

Robins, C.H. & Robins, C.R. 1971: Osteology and relationships of the eel family Macrocephenchelyidae. Proceedings of the Academy of Natural Sciences of Philadelphia 123, 127–150.

Rosenblatt, R.H. 1967: The osteology of the congrid eel *Gorgasia punctata* and the relationships of the Heterocongrinae. Pacific Science 21, 91–97.

Santini, F., Kong, X., Sorenson, L., Carnevale, G., Mehta, R.S. & Alfaro, M.E. 2013: A multi-locus molecular timescale for the origin and diversification of eels (Order: Anguilliformes). Molecular Phylogenetics and Evolution 69, 884–894. https://doi.org/10.1016/j.ympev.2013.06.016

Schnetler, K.I. & Heilmann-Clausen, C. 2011: The molluscan fauna of the Eocene Lillebælt Clay, Denmark. Cainozoic Research 8, 41–99.

Schwarzhans, W. 2007: Otoliths from casts from the Eocene Lillebælt Clay Formation of Trelde Næs near Fredericia (Denmark), with remarks on the diet of stomatopods. Neues Jahrbuch für Geologie und Paläontologie, Abhandlungen 246, 69–81. https://doi.org/10.1127/0077-7749/2007/0246-0069

Schwarzhans, W. 2010: Otolithen aus den Gerhartsreiter Schichten (Oberkreide: Maastricht) des Gerhartreiter Grabens (Oberbayern). Palaeo Ichthyologica 4, 1–100.

Schwarzhans, W. 2019a: Reconstruction of the fossil marine bony fish fauna (Teleostei) from the Eocene to Pleistocene of New Zealand by means of otoliths. Memorie della Società Italiana di Scienze Naturali e del Museo di Storia Naturale di Milano 46, 3–326. https://doi.org/10.5962/bhl.part.9960

Schwarzhans, W. 2019b: A comparative morphological study of recent otoliths of the Congridae, Muraenesocidae, Nattastomatidae and Colocongridae (Anguilliformes). Memorie della Società Italiana di Scienze Naturali e del Museo di Storia Naturale di Milano 46, 327–345. https://doi.org/10.5962/bhl.part.9960

Schwarzhans, W. & Carnevale, G. 2017: Otoliths in situ from Sarmatian (Middle Miocene) fishes of the Paratethys. Preface: a first attempt to fill the gap between the otolith and skeletal record of teleost fishes. Swiss Journal of Palaeontology 136, 1–6. https://doi.org/10.1007/s13358-017-0126-9

Smith, D.G. 1989: Family Congridae. In Böhlke, E.B. (ed.), Fishes of the western North Atlantic. Memoirs of the Sears Foundation for Marine Research 1(9), 460–567.

Smith, D.G. 2004: A new genus and species of congrid eel (Teleostei: Anguilliformes: Congridae) from Western Australia. Records of the Australian Museum 56, 143–146. https://doi.org/10.3853/j.0067-1975.56.2004.1416

Smith, D.G. 2018: A new genus and species of congrid eel from the Philippines (Anguilliformes: Congridae: Bathymyrinae). Zootaxa 4454, 78–83. https://doi.org/10.11646/zootaxa.4454.1.9

Smith, D.G. & Kanazawa, R.H. 1977: Eight new species and a new genus of congrid eels from the western North Atlantic with redescriptions of *Ariosoma analis*, *Hildebrandia guppyi*, and *Rechias vicinalis*. Bulletin of Marine Science 27, 530–543.

Smith, D.G. & Karmovskaya, E.S. 2003: A new genus and two new species of congrid eels (Teleostei: Anguilliformes: Congridae) from the Indo-West Pacific, with a redescription and osteology of *Chiloconger dentatus*. Zootaxa 343, 1–19. https://doi.org/10.11646/zootaxa.343.1.1

Smith, D.G., Ho, H.-C. & Sumod, K.S. 2018: Redescription of *Congrhynchus talabonoides* Fowler, 1934 (Anguilliformes: Congridae) based on specimens collected from the Philippines, Taiwan and India. Zootaxa 4454, 228–232. https://doi.org/10.11646/zootaxa.4454.1.18

Smith, D.G., Karmovskaya, E.S. & da Silva, J.P.C.B. 2020: A new congrid eel (Teleostei: Anguilliformes: Congridae) from the Western Pacific, with an analysis of its relationships. Zootaxa 4845, 191–210. https://doi.org/10.11646/zootaxa.4845.2.2

Stinton, F.C. & Nolf, D. 1970: A teleost otolith fauna from the Sands of Lede, Belgium. Bulletin de la Société Belge de Géologie, Paléontologie et Hydrologie 78, 219–234.

Takai, T. 1959: Studies on the morphology, ecology and culture of the important apodal fishes, *Muraenesox cinereus* (Forskål) and *Conger myriaster* (Brevoort). Journal of the Shimonoseki College of Fisheries 8, 209–555.

Taverne, L. & Nolf, D. 1978: Troisieme note sur les poissons des Sables de Lede (Eocene Belge): Les fossiles autres que les otolithes. Bulletin de la Société Belge de Géologie 87, 125–152. https://doi.org/10.1016/s0016-6995(78)80083-7

Thomsen, E., Abrahamsen, N., Heilmann-Clausen, C., King, C. & Nielsen, O.B. 2012: Middle Eocene to earliest Oligocene development in the eastern North Sea Basin: Biostratigraphy, magnetostratigraphy and paleoenvironment of the Kysing-4 borehole, Denmark. Palaeogeography, Palaeoclimatology, Palaeoecology 350–352, 212–235. https://doi.org/10.1016/j.palaeo.2012.06.034

Trewavas, E. 1932: A contribution to the classification of the fishes of the order Apodes, based on the osteology of some rare eels. Proceedings of the Zoological Society of London 1932, 639–659. https://doi.org/10.1111/j.1096-3642.1932.tb01089.x

Young, S.V.T. 1993: A neurocranium of the eel genus *Echelus* Rafinesque (Ophichthidae, Anguilliformes) from the Eocene of Hampshire and London Basins, and a review of the genera *Echelus* Rafinesque, *Rhynchorhinus* Woodward, *Eomyrus* Storms and *Goslinophis* Blot. Kaupia 2, 163–194. https://doi.org/10.1144/sp295.15

Middle Cambrian (Miaolingian Series, Wuliuan Stage) molluscs and mollusc-like microfossils from North Greenland (Laurentia)

JOHN S. PEEL & ARTEM KOUCHINSKY

Geological Society of Denmark
https://2dgf.dk

Received 14 December 2021
Accepted in revised form
4 April 2022
Published online
22 April 2022

Peel, J.S. & Kouchinsky, A. 2022. Middle Cambrian (Miaolingian Series, Wuliuan Stage) molluscs and mollusc-like microfossils from North Greenland (Laurentia). Bulletin of the Geological Society of Denmark, Vol. 70, pp. 69–104. ISSN 2245-7070. https://doi.org/10.37570/bgsd-2022-70-06

Diverse assemblages of helcionelloid molluscs and mollusc-like microfossils are described from the upper Henson Gletscher Formation (Cambrian, Miaolingian Series, Wuliuan Stage) of Lauge Koch Land and western Peary Land, North Greenland (Laurentia). The fauna compares closely to an assemblage of similar age from the Coonigan Formation of Australia, although the latter is preserved as silica replicas while the North Greenland fossils are dominantly preserved as phosphatized internal moulds. These internal moulds often retain a detailed impression of the inner surface of the shell, with a fine pitted texture typically present. Prominent deep grooves on the sub-apical surface in the erect helcionellids *Dorispira* and *Erugoconus*, corresponding to ridges on the shell interior, seem to be associated with control of water flow through the mantle cavity. Well-developed shell pores, preserved as tubercles on the internal mould, are common in species of the laterally compressed *Mellopegma*. New taxa: *Dorispira avannga* sp. nov., *Dorispira septentrionalis* sp. nov., *Dorispira tavsenensis* sp. nov., *Dorispira tippik* sp. nov., *Erugoconus acuminatus* gen. et sp. nov., *Scenella*? *siku* sp. nov., *Sermeqiconus* gen. nov., *Tavseniconus erectus* gen. et sp. nov., *Vendrascospira troelseni* gen. et sp. nov., *Vendrascospira frykmani* gen. et sp. nov.

Keywords: Molluscs, Henson Gletscher Formation, Miaolingian Series (Wuliuan Stage), North Greenland, Laurentia.

John S. Peel [john.peel@pal.uu.se], Department of Earth Sciences (Palaeobiology), Uppsala University, Villavägen 16, SE-752 36 Uppsala, Sweden. Artem Kouchinsky [artem.kouchinsky@gmail.com], Department of Palaeobiology, Swedish Museum of Natural History, Box 50007, SE-104 05 Stockholm, Sweden.

It was a surprise when the middle Cambrian microfossil *Protowenella* was reported from Denmark (Berg-Madsen & Peel 1978) and northernmost Greenland (Peel 1979) shortly after its original description by Runnegar & Jell (1976) from the Coonigan Formation and Currant Bush Limestone (Gowers Formation) in Australia, half a world away. However, since that time, *Protowenella* and various mollusc-like fossils from the Queensland and New South Wales assemblages described by Runnegar & Jell (1976, 1980) have been widely reported (MacKinnon 1985; Peel 1986, 2021a, b; Brock 1998; Gubanov *et al*. 2004; Vendrasco 2010, 2011; Kouchinsky *et al*. 2011). Their distribution demonstrates that the diversity of molluscs in assemblages of small shelly fossils described from the early Cambrian, originally mainly by Russian and Chinese workers (summaries of extensive literature by Geyer 1986; Bengtson *et al*. 1990; Skovsted 2004; Parkhaev & Demidenko 2010; Parkhaev 2019; Li *et al*. 2021), was maintained into the middle Cambrian (Miaolingian Series).

The present paper describes molluscs and mollusc-like fossils (Miaolingian Series, Wuliuan Stage; *Ptychagnostus gibbus* Zone) from the Henson Gletscher Formation of Lauge Koch Land and western Peary Land, North Greenland (Figs 1, 2). The diverse assemblages (Figs 3–16) are compared with the fauna of the Coonigan Formation of similar age. The Greenland fossils are mainly preserved as phosphatized internal moulds in contrast to the silica replicas of the Coonigan Formation, although phosphatized material has been described from the slightly younger Gowers

Formation (Drumian Stage; Runnegar & Jell 1976; Vendrasco *et al.* 2010, 2011). Numerous macromolluscs ('knock-out' specimens) have been described from the Miaolingian in North America (Geyer 1994 for references), but the present material represents the first substantial small shelly molluscan fauna of this age described from Laurentia.

The affinities of two conspicuous members of the Henson Gletscher Formation assemblage were reinterpreted recently and they are no longer considered to be molluscs, although their morphologies are mollusc-like (Fig. 3). Ironically, the isostrophically coiled *Protowenella* was transferred to Hyolitha by Peel (2021a) following the description of an inplace operculum of orthothecid type. The bivalved stenothecoids, which Yochelson (1968, 1969) established as a new class of molluscs, are now accepted as being more closely related to brachiopods on account of their inferred pedicle attachment (Rozov 1984; Johnston 2019; Peel 2021c; Johnston & Streng 2021a).

Anisostrophically coiled shells of pelagiellids are also prominent in the Henson Gletscher Formation assemblage. Pelagiellids are perhaps the most commonly reported and widely distributed mollusc-like small shelly fossils from the Cambrian, with Parkhaev (2001a) noting 30 named species. They have been assigned to various non-molluscan and torted or untorted molluscan groups, as summarized by Thomas *et al.* (2020) and Landing *et al.* (2021), although most modern workers have favoured placement within the molluscs (Kouchinsky *et al.* 2011; Li *et al.* 2017, 2021; Parkhaev 2019).

The remarkable description of bristles (setae) protruding from the aperture in specimens of *Pelagiella exigua* Resser & Howell, 1938 from the Kinzers Formation (Cambrian Series 2, Stage 4) of Pennsylvania prompted Thomas *et al.* (2020) to interpret *Pelagiella* as a mollusc and a member of Total group Gastropoda Cuvier, 1797. However, Landing *et al.* (2021) restricted *Pelagiella* Matthew, 1893 to the type species, *Pelagiella atlantoides* Matthew, 1893 from the Hanford Brook Formation (Cambrian Series 2, Stage 4) of New Brunswick, which they considered to be a mollusc. In a controversial action, Landing *et al.* (2021) interpreted other members of the *Pelagiella* morphological group as annelids. This opinion is not followed here, largely

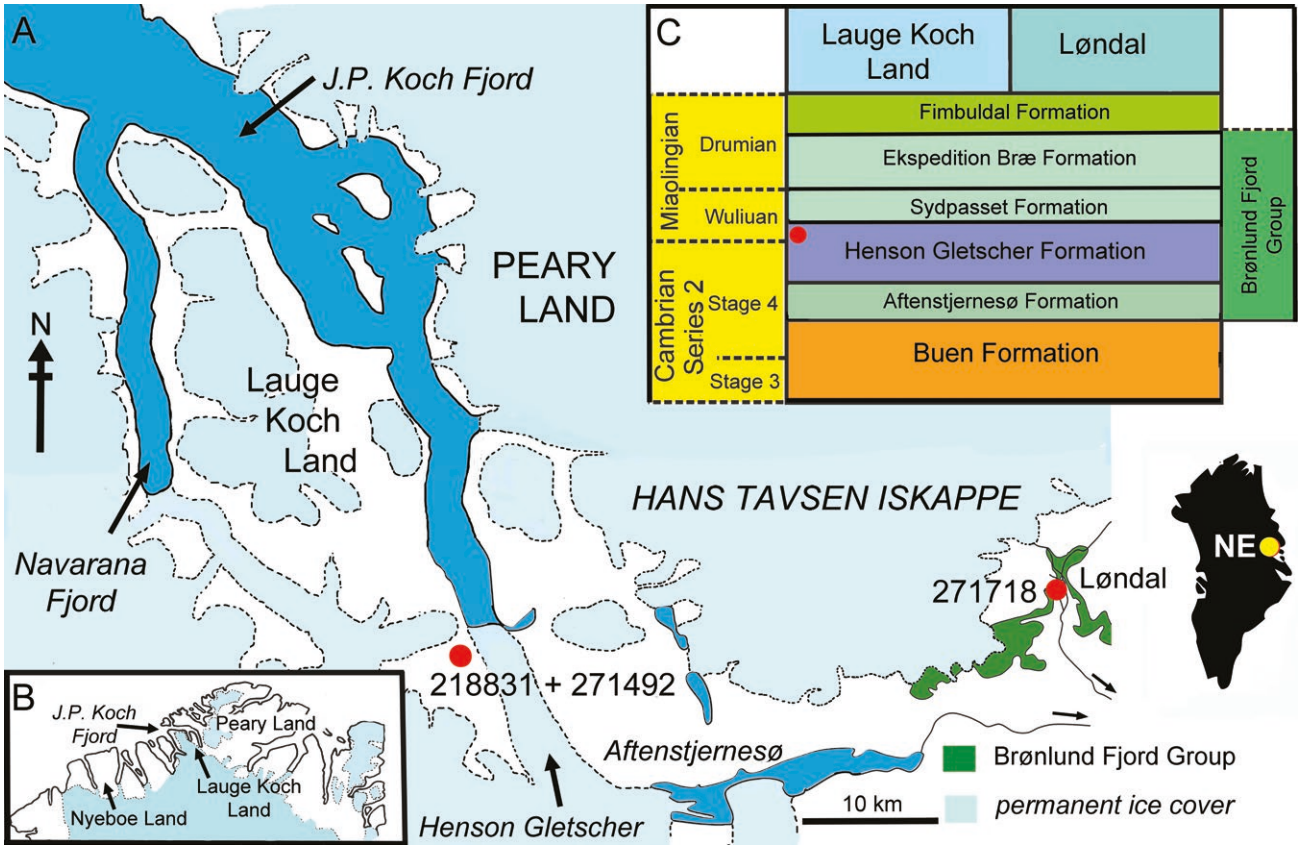

Fig. 1. Locality maps for GGU samples. **A**, southern Lauge Koch Land and Løndal region of southern Peary Land showing sample localities (filled circles), with inset of Greenland indicating North-East Greenland. **B,** overview of northern Greenland. **C,** Cambrian stratigraphy in Lauge Koch Land and Løndal, indicating derivation of GGU samples from the Henson Gletscher Formation (filled circle).

on account of descriptions of shell structure in pelagiellids by Kouchinsky (2000a), Vendrasco *et al*. (2010) and Li *et al*. (2017, 2021).

Geological background

The Henson Gletscher Formation in the Peary Land–Lauge Koch Land region of North Greenland (Fig. 1) is a highly fossiliferous unit within a prograding complex of shelf carbonates and siliciclastic sediments, referred to the Brønlund Fjord Group (Higgins *et al*. 1991; Ineson & Peel 1997; Geyer & Peel 2011; Peel *et al*. 2016). The formation is composed mainly of dark, recessive, bituminous and cherty limestones, dolostones and mudstones, with a middle member of pale fine-grained sandstones (Fig. 2). Thin carbonate debris flows occur sporadically. At its type locality in southern Lauge Koch Land, from which GGU samples 218831 and 271492 were collected, the Henson Gletscher Formation is 62 m thick (Figs 1A, 2A), but it

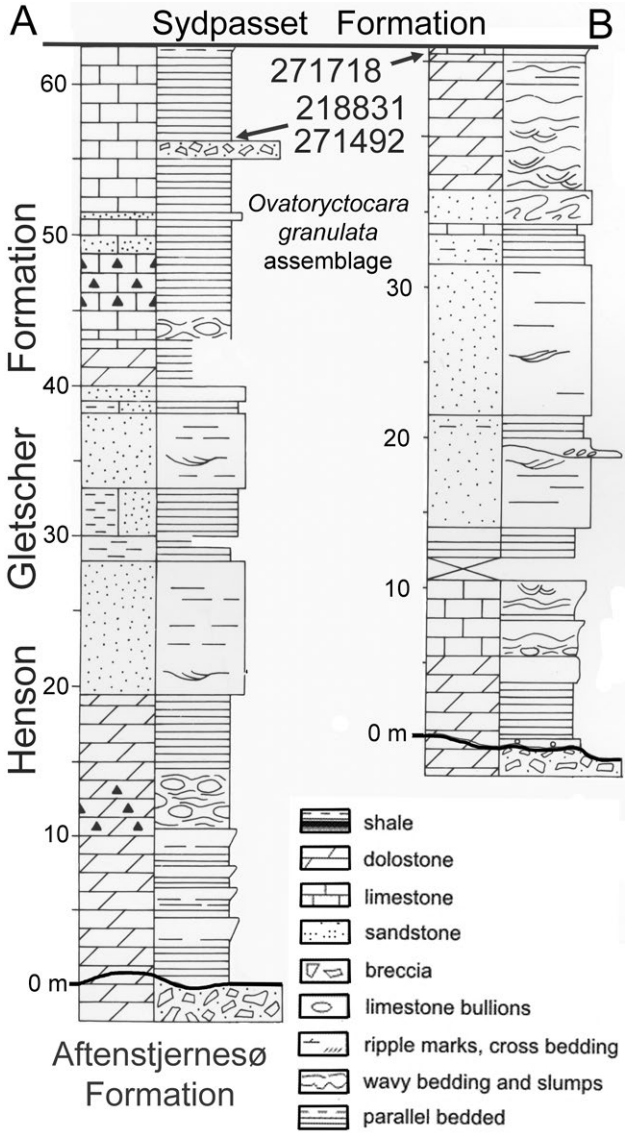

Fig. 2. Stratigraphic sections through the Henson Gletscher Formation at its type section in southern Lauge Koch Land (A) and in Løndal (B) showing derivation of GGU samples (after Jon R. Ineson).

GGU samples	218831	271492	271718
Phylum uncertain			
Class Hyolitha			
Order Orthothecida			
Protowenella flemingi	●	●	●
Phylum uncertain			
Class Stenothecoida			
Stenothecoides cf. *elongata*		●	
Stenothecoides terraglaciei		●	●
Stenothecella cf. *sibirica*		●	●
Phylum Mollusca			
Class uncertain			
Order Pelagiellida			
Costipelagiella cf. *nevadense*		●	●
Class Helcionelloida			
Dorispira accordionata		●	●
Dorispira cf. *arguta*			●
Dorispira avannga			●
Dorispira septentrionalis			●
Dorispira tavsenensis			●
Dorispira tippik		?	●
Dorispira? cf. *penecyrano*			●
Erugoconus acuminatus			●
Helcionella? sp.	●		
Helcionellid spp. indet.		●	●
Mellopegma chelata			●
Mellopegma cf. *georginense*			●
Mellopegma schizocheras		●	
Mellopegma sp.		●	
'*Obtusoconus*' sp.			●
Parailsanella sp.		●	
Scenella? *siku*			●
Sermeqiconus polaris	●		
Tavseniconus erectus			●
Vendrascospira troelseni		●	
Vendrascospira frykmani		●	

Fig. 3. Faunal list of molluscs and mollusc-like species from the Henson Gletscher Formation, North Greenland, Cambrian, Miaolingian Series, Wuliuan Stage.

thins to 47 m in Løndal in south-western Peary Land, to the east (Figs 1A, 2B).

Fossil assemblages from the Henson Gletscher Formation in southern Lauge Koch Land and Løndal range in age from Cambrian Series 2 (Stage 4) to the Miaolingian Series (Wuliuan Stage; *Ptychagnostus gibbus* Biozone), but Drumian Stage strata occur in Nyeboe Land along the northern coast of North Greenland (Higgins *et al.* 1991; Robison 1994; Blaker & Peel 1997; Ineson & Peel 1997; Geyer & Peel 2011; Fig. 1B). Trilobite faunas from the Henson Gletscher Formation have a dominantly Laurentian character but the assemblages include agnostoids and taxa that are important for international correlation with Siberia, the Altai Sayan foldbelt and South China (Blaker & Peel 1997; Geyer & Peel 2011). Elements of the diverse associated fauna were described by Clausen & Peel (2012), Peel *et* al. (2016) and Peel (2017, 2019, 2021c).

Derivation of samples. GGU samples 218831 and 271492 were collected at 56.5 m above the base of the Henson Gletscher Formation (thickness 62 m) at its type locality in Lauge Koch Land, in scours on the top of a 1 m thick mass flow deposit (82°10′N, 40°24′W; Ineson & Peel 1997, fig. 31; Geyer & Peel 2011, fig. 3; Figs 1A, 2A). GGU sample 218831 was collected by Peter Frykman on 24th June 1979; processed weight about 200 g. GGU sample 271492 was collected by J.S. Peel on 25th June 1978; processed weight about 2 kg.

GGU sample 271718 was collected by J.S. Peel on 15th July 1978 from a thin-bedded, phosphatized, dark dolomitic limestone occurring about 1 m below the top of the formation on the west side of Løndal (82°18′N, 37°03′W; Clausen & Peel 2012, fig. 1; Figs 1C, 2B), where the formation has thinned to 47 m. About 5 kg of limestone were processed.

Material. Specimens were hand-picked from wet sieved residues of limestone dissolved in 10% acetic acid prior to examination and imaging of selected specimens by scanning electron microscopy. The initial images were assembled in Adobe Photoshop CS4.

Preservation. Almost all examined specimens recovered from the acid residues are phosphatic internal moulds that display details of the inner surface of the original shell with great fidelity (Fig. 4A–C,E,G). The apertural margin is rarely preserved, indicating that phosphatization was usually confined to the earlier growth stages of the shell. The moulds have thin walls, with a granular or spherulitic inner surface, and the inner cavity is generally filled with phosphatized sediment (Fig. 4A). Exceptionally, encrustation on the shell exterior, in conjunction with the internal mould, provides an indication of the thickness of the dissolved calcareous shell (Figs 4H, 5D). However, the shell itself is not preserved and phosphatized details of its internal structure, as described by Kouchinsky (2000a, b) and Vendrasco *et al*. (2010, 2011), generally are not known. Rare specimens retain patches of phosphatized shell attached to the internal mould that show details of the ornamentation of the shell exterior such as fine spiral ribs and comarginal growth lines not usually visible on the internal moulds (Figs 4F,H,I, 5G). Transverse rugae are more acutely presented on the shell exterior than in corresponding internal moulds (Fig. 4F,H,I). As noted by Runnegar (1985, fig. 1) and Skovsted (2004, figs 3M,N,5R), rugae on internal moulds are not always expressed on the shell exterior in helcionelloids, as is also the case with the circumbilical channels on internal moulds of *Protowenella* (Fig. 5A–D).

Internal structures

Features of the surface of internal moulds include muscle scars (Fig. 6A,B,E,F) and a complex of spiral grooves and associated transverse segments deeply impressed into the subapical surface of several helcionelloids (Fig. 4A–C,E–H). Tubercles representing pores in the shell are characteristic of *Mellopegma* Runnegar & Jell, 1976 (Fig. 14), while development of a finely pitted surface is widespread (Figs 10L, 16D).

Spiral ridge and groove complex

Grooves on the sub-apical surface of internal moulds, corresponding to ridges on the internal surface of the helcionelloid shell, were described by Runnegar & Jell (1976) and Peel (1991a, fig. 23) in silicified specimens of *Dorispira merino* (Runnegar & Jell, 1976) from the Coonigan Formation of New South Wales. Similar structures were reported in Miaolingian material from Utah by Robison (1964) and by Hu *et al.* (2021) from China. Two deep grooves on the internal mould are usually present, but some specimens show four grooves that may even be flanked by a third, discontinuous pair (Fig. 4A,C). Peel (1991a) noted that the grooves appear suddenly on the sub-apical surface of the internal mould (Fig. 4A), were often L- or T-shaped in cross-section (Fig. 4E) and terminated just within the apertural margin (Fig. 4I). Runnegar & Jell (1976) and Peel (1991a) concluded that the ridges reflected folding in the mantle that probably helped control water currents to the mantle cavity. This function may parallel, or be partially equivalent to, the development of a snorkel on the subapical surface in yochelcionellid helcionelloids (Peel 1991a, 2006). However, the surface of the internal mould in the area between the

innermost pair of grooves often carries numerous transverse grooves representing ridges on the shell interior that intuitively are difficult to reconcile with the notion of control of longitudinal folding attributed to the larger spiral ridges (Fig. 4A,C, 9C–E). Large pits set into the finely pitted texture of the internal mould of some specimens, on the lateral surfaces of the shell adjacent to the ridges, appear to represent diagenetic crystal growth on the shell interior (Figs 4F,G).

Parkhaev (2000) rejected the mantle control function and suggested that the ridges and separating channels served to steer and support muscle threads that were attached to the shell in the sub-apical region, drawing comparison with the columellar folds of many gastropods. Such a function implies substantial extension of the soft parts beyond the shell margin in the subapical region since there would be little need for extensive muscle control if soft parts were restricted to the inner part of the shell without extension and withdrawal. Extension and withdrawal of the head-foot complex into the shell is a general adaptation against predation in heliciform gastropods but in cap-shaped forms, such as patelliform gastropods, tryblidiids and probably most helcionelloids, the soft parts do not extend substantially beyond the apertural margin and defence is achieved by clamping the shell down against the substrate. Restriction of the supposed muscle channels to the sub-apical surface does not suggest effective clamping at the supra-apical margin, but this would not be required in a model where soft parts were withdrawn into the shell. However, withdrawal would require that the principal muscle scars were attached deep within the shell, as in most heliciform gastropods and the morphologically similar isostrophic bellerophontoids (Peel 1976, 1982, 1991a, 1993, 2004), whereas the ridges on the shell interior in the present material terminate almost at the apertural margin (Figs 4H, 9E).

Circumbilical channels on the internal mould are a diagnostic character of *Protowenella* (Berg-Madsen & Peel 1978). The broad, rounded thickenings of the internal shell wall are distinct from the acute ridges

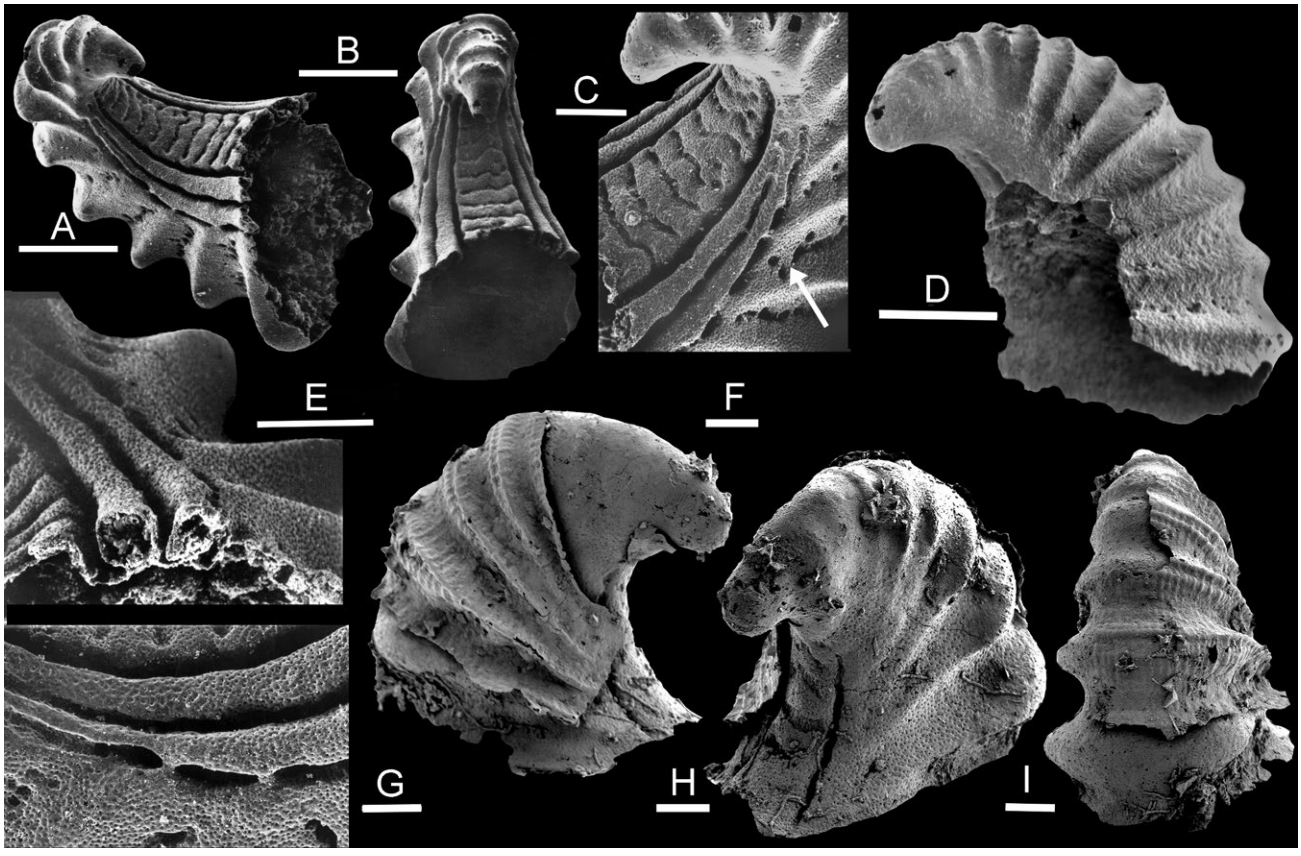

Fig. 4. Preservation of helcionelloids from the upper Henson Gletscher Formation, Miaolingian Series, Wuliuan Stage. **A–E, G:** *Dorispira tippik* sp. nov., MGUH 19561 from GGU sample 271718, Løndal, internal mould with details of groove complex on subapical surface. Arrow (C) indicates diagenetic crystal growth on shell interior. **D:** *Dorispira accordionata* (Runnegar & Jell, 1976), PMU 39172 from GGU sample 271492, Lauge Koch Land, phosphatic composite replica with trace of apical termination of spiral groove. **F, H, I:** PMU 39173 from GGU sample 271718, Løndal, internal mould with patches of thin phosphate encrustation formed on the outer surface preserving ornamentation. Scale bars: 500 μm (A, B), 400 μm (D), 200 μm (C, E), 100 μm (F–I).

seen in *Dorispira*. The channels in *Protowenella* were interpreted as possible sinuses in the apertural margin that might be related to inhalant currents entering the mantle cavity (Berg-Madsen & Peel 1978). Peel (2021a) noted that the channels did not result in sinuses on the outer shell surface and discounted a relationship to mantle currents. He suggested that the broad circumbilical thickenings may have acted as a support for the internal margin of the operculum, which also may have hinged against the termination of the ridges on opening. Peel (2021a) compared the channels on the internal mould of *Protowenella* to longitudinal furrows developed on the dorsal surface of some hyoliths (Malinky 2002; Marek et al. 1997).

There are only few published descriptions of muscle scars in helcionelloids. Parkhaev (2002) described muscle attachment scars on the supra-apical surface of *Bemella* Missarzhevsky *in* Rozanov & Missarzhevsky, 1966 and on the sub-apical surface of *Anhuiconus microtuberus* Zhou & Xiao, 1984, but these are low shells that expand rapidly in the direction of growth without sub-apical ridges. Li *et al.* (2021) described well preserved muscle scars in *Figurina figurina* Parkhaev, 2001a, which also has a low shell. Vendrasco *et al.* (2010) described a pair of muscle scars near the apex on the supra-apical surface of *Yochelcionella snorkorum* Vendrasco, Porter, Kouchinsky, Li & Fernandez, 2010 from the Miaolingian Gowers Formation of Australia, which is a tall shell but also lacks the ridges on the sub-apical surface.

Columellar folds in marine gastropods are often associated with burrowing high-spired forms at the present day (Signor & Kat 1984), but not exclusively so (Vermeij 2017). While some helcionelloids develop strong lateral compression that suggests a semi-infaunal mode of life (Gubanov *et al.* 1999; Peel 1991a), the wider aperture in most forms, including the present material, and often slightly flared margins are inconsistent with burrowing. A study of columellar muscle attachment in neogastropods by Price (2004) suggested that columellar folds did not guide the muscles as the snail extended or withdrew its soft parts.

Terrestrial snails often develop apertural barriers of teeth to resist predation and desiccation (Gittenberger 1994; Sulikowska-Drozd *et al.* 2014). The restriction of the ridges in the present marine material just to a small segment of the sub-apical apertural margin clearly refutes an effective defensive function in terms of the apertrure as a whole. Predation on helcionelloids was present in Cambrian seas, as documented by injuries described by Skovsted (2004) and Vendrasco *et al.* (2011), and illustrated here (Figs 7D,G, 14F).

The presence of the sub-apical ridges in such morphologically diverse taxa as the various species of the strongly rugose *Dorispira* (Figs 4, 7–9) and the smooth *Erugoconus* gen. nov. (Fig. 16F–K) may suggest that these forms comprise a distinct phylogenetic group of Miaolingian helcionelloids. However, it is considered premature to formalize such a step, with reference to the conclusions of Price (2004) that columellar folds in neogastropods evolved convergently on several occasions and that their function is not understood. The nature of the adaptation in helcionelloids remains problematic.

Pits, pores and polygons

A large proportion of the examined internal moulds displays a surface pattern of closely spaced fine pits with a diameter of 2–3 μm (Figs 4G, 9D, 10L). Occasionally, the pits are seen to be oriented in rows separated by low ridges (Fig. 14L) or lie centrally within a network of low ridges (Fig. 10D). Often, the apical area of specimens is smooth while the pitted texture is developed on the flanks (Fig. 10E). Bengtson *et al.* (1990) suggested that similar pits may reflect boring by endoliths, and traces of such activity may be widespread in Cambrian fossils (Runnegar 1985; Stockfors & Peel 2005), but not with the density, fineness and wide distribution seen here.

Vendrasco *et al.* (2010) described a similar pitted structure on internal moulds of molluscs and mollusc-like fossils from the Gowers Formation (Drumian) of Australia, which they considered to result from replacement of organic matrix associated with the prismatic microstructure of the shell, or as moulds of the crystal prisms after degradation of the organic meshwork. Li *et al.* (2021) illustrated similar pitting on internal moulds from the Xinji Formation (Cambrian Series 2) of North China. However, the pitting in some of the illustrated Australian specimens does not appear to show a high degree of correlation with prism boundaries and passes through several foliations (Vendrasco *et al.* 2010, pl. 4, figs 6–8, pl. 5, fig. 8). Furthermore, the pits are usually circular in cross-section in contrast to the polygonal form of the prisms. Peel (2021c) interpreted somewhat coarser pits in the apical area of juvenile stenothecoids to be the attachment sites of pedicle fibres, but such an interpretation is clearly not applicable to the widely distributed pits of the present context.

Internal moulds of *Tavseniconus erectus* gen. et sp. nov. (Fig. 16A–D) preserve a zone of larger pits (transverse diameter 5 μm) near the apertural margin that is set against a background of the fine pits on the flanks of the shell; the apical area is smooth (Fig. 16D). These larger pits slope down and inwards towards the apertural plane, giving them an elliptical shape on the mould surface, whereas the finer background pits penetrate perpendicular to the surface (Fig. 16D).

Internal moulds of *Mellopegma* show conical to sub-

cylindrical tubercles 5–8 μm in diameter, often with a blunt termination, that represent pores in the shell surface (Fig. 14D,E,I,K). The structures were described in detail by Vendrasco *et al.* (2011). They may be distributed randomly or follow a comarginal pattern associated with rugae (Fig. 14H). Vendrasco *et al.* (2011) considered that the pores extended through much or all of the shell wall and noted that similar structures had been described by Kouchinsky (2000a), Parkhaev (2006) and Feng & Sun (2006) in a variety of Cambrian helcionelloids. While some pores opened to the shell exterior, others appear to have been connected with the organic components of the shell structure and periostracum. Vendrasco *et al.* (2011) noted that the pores in *Mellopegma* were most similar to those developed in bivalves (Taylor *et al.* 1969) and suggested that shell pores might be a primitive character of the Phylum Mollusca.

Polygonal structures are widespread on phosphatized internal moulds of Cambrian helcionelloids (Parkhaev 2001; Skovsted 2004) and some may result from diagenesis. Ushatinskaya & Parkhaev (2005) suggested that they may represent imprints of the outer ephithelium of the mantle, and described similar structures in brachiopods, but a detailed review by Vendrasco *et al.* (2010, p. 125) concluded that the polygonal pattern of raised ridges or shallow grooves in Cambrian molluscs was a reflection of the organic framework of prismatic shell structure. Polygonal structures associated with muscle attachment areas in helcionelloids have been described by Parkhaev (2002), Vendrasco *et al.* (2010), Vendrasco *et al.* (2010) and Li *et al.* (2021).

Polygonal structures are not widely represented in the material from the Henson Gletscher Formation, but a weak pattern of polygonal grooves surrounding convex surfaces 8–10 μm in diameter is visible in some specimens of *Dorispira* and *Vendrascospira* gen. nov. (Figs 8E, H, 12D), comparable to that illustrated by Ushatinskaya & Parkhaev (2005, fig. 3) in *Oelandiella korobkovi* Vostokova, 1962 from the Tommotian of the Siberian Platform.

Age and faunal comparisons

Robison (1984) determined agnostoids from GGU sample 271492, including *Onymagnostus seminula* (Whitehouse, 1939), *Ptychagnostus gibbus* (Linnarsson, 1869) and specimens of *Ptychagnostus intermedius* (Tullberg, 1880) transitional to *P. atavus* (Tullberg, 1880), which were considered to be indicative of the *Ptychagnostus gibbus* Biozone (Wuliuan Stage). Subsequently, the last-named species was re-identified as *Ptychagnostus sinicus* Lu, 1957 (Ahlberg *et al.* 2007, p. 713). Poorly preserved agnostoids are present in GGU sample 271718 but this sample is considered to be a correlative of GGU sample 271492 on the basis of its lithostratigraphic position.

Strata of the upper Henson Gletscher Formation deposited during the Wuliuan Stage in Løndal and southern Lauge Koch Land yield diverse assemblages of molluscs and mollusc-like fossils (Figs 3–16). The main difference between the two areas concerns the abundance and diversity of *Dorispira* Parkhaev *in* Parkhaev & Demidenko, 2010 in GGU sample 271718 from Løndal relative to the samples from southern Lauge Koch Land. The mollusc faunas from the two areas are not closely similar, but this may result from the rarity of many individual taxa. Mollusc-like taxa such as *Protowenella* and stenothecoids occur in both areas.

Molluscs are less conspicuous in a fauna from the *Ovatoryctocara granulata* assemblage (Cambrian Series 2, uppermost Stage 4) of the Henson Gletscher Formation in Løndal that was described by Geyer & Peel (2011) and Peel *et al.* (2016) from about 13 m below GGU sample 271718 (Fig. 2B). The assemblage lacks the abundant specimens of *Dorispira* that characterize GGU sample 271718. Helical shells of pelagiellids are conspicuous in both faunas. *Yochelcionella* Runnegar & Pojeta, 1974 is well represented in the lower assemblage, where it occurs together with *Capitoconus* Skovsted, 2004 and *Mellopegma simesi* (MacKinnon, 1985), but all three are absent from the Wuliuan assemblage. Rare specimens of *Mellopegma* sp. (Peel *et al.* 2016, fig. 13N) may be referred tentatively to *Mellopegma georginense* Runnegar & Jell, 1976, which is also present in GGU sample 271718. *Coreospira* sp. of Peel *et al.* (2016, fig. 14N, O), a rare constituent of the *Ovatoryctocara granulata* assemblage, was considered to more closely resemble *Igorella* Missarzhevsky *in* Rozanov *et al.*, 1969 by Oh *et al.* (2021).

As in GGU sample 271718, an abundance of *Dorispira* is characteristic of the silicified fauna of the First Discovery Limestone (Coonigan Formation) of New South Wales (Runnegar & Jell 1976) of probable Ordian age, considered to be earliest middle Cambrian by Runnegar & Jell (1976), but late Cambrian Stage 4 by Geyer (2019). Percival *et al.* (2011) suggested that the formation was of slightly younger age (Templetonian Stage) but the age was regarded as uncertain, possibly Cambrian Series 2, Stage 4, by Smith *et al.* (2015, p. 44). The Coonigan Formation has also yielded three species of *Yochelcionella* but this genus is not known from the current Greenland material. However, *Yochelcionella gracilis* Atkins & Peel, 2004 occurs in Løndal within the *Ovatoryctocara granulata* assemblage (Cambrian Series 2, uppermost Stage 4) of the Henson Gletscher Forma-

tion and may be compared closely with *Yochelcionella ostentata* Runnegar & Jell, 1976 from the Coonigan Formation. The orthothecid hyolith *Protowenella* occurs in the Coonigan Formation and the current material from the Henson Gletscher Formation (Peel 2021a).

Mellopegma georginense Runnegar & Jell, 1976, from the Currant Bush Limestone (Gowers Formation) of the Georgina Basin, Australia (Runnegar & Jell 1976; Vendrasco *et al*. 2010) is tentatively identified from GGU sample 271718. In both areas, it occurs together with *Mellopegma schizocheras* Vendrasco, Kouchinsky, Porter & Fernandez, 2010, although the Australian occurrences are of Drumian age, compared to the Wuliuan material from the Henson Gletscher Formation in North Greenland. *Protowenella flemingi* Runnegar & Jell, 1976 and *Pseudomyona queenslandica* (Runnegar & Jell, 1976) also occur in the Currant Bush Limestone (Runnegar & Jell 1976). The former is present in the Wuliuan part of the Henson Gletscher Formation in North Greenland (Figs 3, 5A–D; Peel 2021b), whereas *Pseudomyona* Runnegar, 1983 occurs in the Ekspedition Bræ and Fimbuldal formations (Drumian) of North Greenland (Peel 2021b; Fig. 1C). *Yochelcionella* and *Eotebenna* Runnegar & Jell, 1976 occur in the Coonigan and Gowers formations (Runnegar & Jell 1976; Vendrasaco *et al*. 2010). While both genera occur in Cambrian Stage 4 strata of the Henson Gletscher Formation (Atkins & Peel 2004, 2008; Peel 1989; Peel *et al*. 2016), they are not recorded from the Wuliuan part of the Henson Gletscher Formation.

Brock (1998) described *Dorispira accordionata* (Runnegar & Jell, 1976) from Miaolingian limestone blocks within the Murrawong Creek Formation of New South Wales, associated with *Protowenella* and pelagiellids. A species assigned to *Mellopegma* is similar to *Mellopegma chelata* (Skovsted, 2006b) from GGU sample 271718. *Yochelcionella* described by Brock (1998) is not recorded from the present material but occurs in older and younger strata in North Greenland (Peel *et al*. 2016).

A diverse fauna of helcionelloids from Morocco and Spain was described by Geyer (1986). Moroccan material derived from the *Morocconus notabilis* and *Ornamentaspis frequens* biozones, corresponding to Cambrian Series 2, latest Stage 4 and the earliest Wuliuan Stage, respectively, contains *Marocella* Geyer, 1986, *Eotebenna* Runnegar & Jell, 1976 and *Yochelcionella* that are not represented in the current material from Greenland. *Protowenella*, pelagiellids and *Tavsenicoconus erectus* gen. et sp. nov. are present in both faunas. Strongly rugose helcionellids are common in both, although lower-shelled forms are more conspicuous in Morocco.

A silicified fauna derived from the Kuonamka Formation (upper Cambrian Stage 4–lower Drumian Stage) of northern Siberia shares *Costipelagiella* Horný, 1964 and *Protowenella* with the Henson Gletscher Formation (Gubanov *et al*. 2004; Kouchinsky *et al*. 2011), as well as *Pseudomyona queenslandica* (Runnegar & Jell, 1976) that occurs in Greenland in the Ekspedition Bræ Formation of Drumian age (Peel 2021b; Fig. 1C).

Systematic palaeontology

Institutional abbreviations and repositories. GGU prefix indicates a sample collected by Grønlands Geologiske Undersøgelse (Geological Survey of Greenland), now part of the Geological Survey of Denmark and Greenland (GEUS), Copenhagen, Denmark. Specimen repositories: Natural History Museum of Denmark, Copenhagen (MGUH prefix); Museum of Evolution, Uppsala University, Sweden (PMU prefix).

Unless otherwise stated, all figured specimens are derived from the upper Henson Gletscher, Cambrian, Miaolingian Series, Wuliuan Stage, *Ptychagnostus gibbus* Biozone in Lauge Koch Land (GGU samples 218831 and 271492) or Løndal (GGU sample 271718) and located in Figs 1–3.

This published work and the nomenclatural acts it contains have been registered in ZooBank: http://zoobank.org:pub:98433F3C-09EC-455C-A976-019CDAE6FBD8

Phylum uncertain

Class Hyolitha Marek, 1963

Order Orthothecida Marek, 1966

Family Protowenellidae Peel, 2021a

Genus *Protowenella* Runnegar & Jell, 1976

Type species. *Protowenella flemingi* Runnegar & Jell, 1976, Currant Bush Limestone (Gowers Formation), Queensland, Australia, Miaolingian Series, Drumian Stage.

Protowenella flemingi Runnegar & Jell, 1976

Fig. 5A–D

1976 *Protowenella flemingi* Runnegar & Jell, p. 133, fig. 6B–K.
1978 *Protowenella flemingi*; Berg-Madsen & Peel, p. 119, figs 4C–E, 6.
2021 *Protowenella flemingi*; Li *et al*., p. 556, fig. 25a–j.
2021a *Protowenella flemingi*; Peel, figs 3, 4 (includes additional citations).

Figured material. PMU 39329 from GGU sample 218831 and PMU 39333 from GGU sample 271492, southern Lauge Koch Land; PMU 38330, PMU 38331 from GGU sample 271718, Løndal.

Other material. More than 100 additional specimens from GGU samples 271492 and 271718.

Discussion. Following its original description from Drumian strata in Queensland by Runnegar & Jell (1976), *Protowenella* was redefined by Berg-Madsen & Peel (1978) on the basis of a specimen from Bornholm

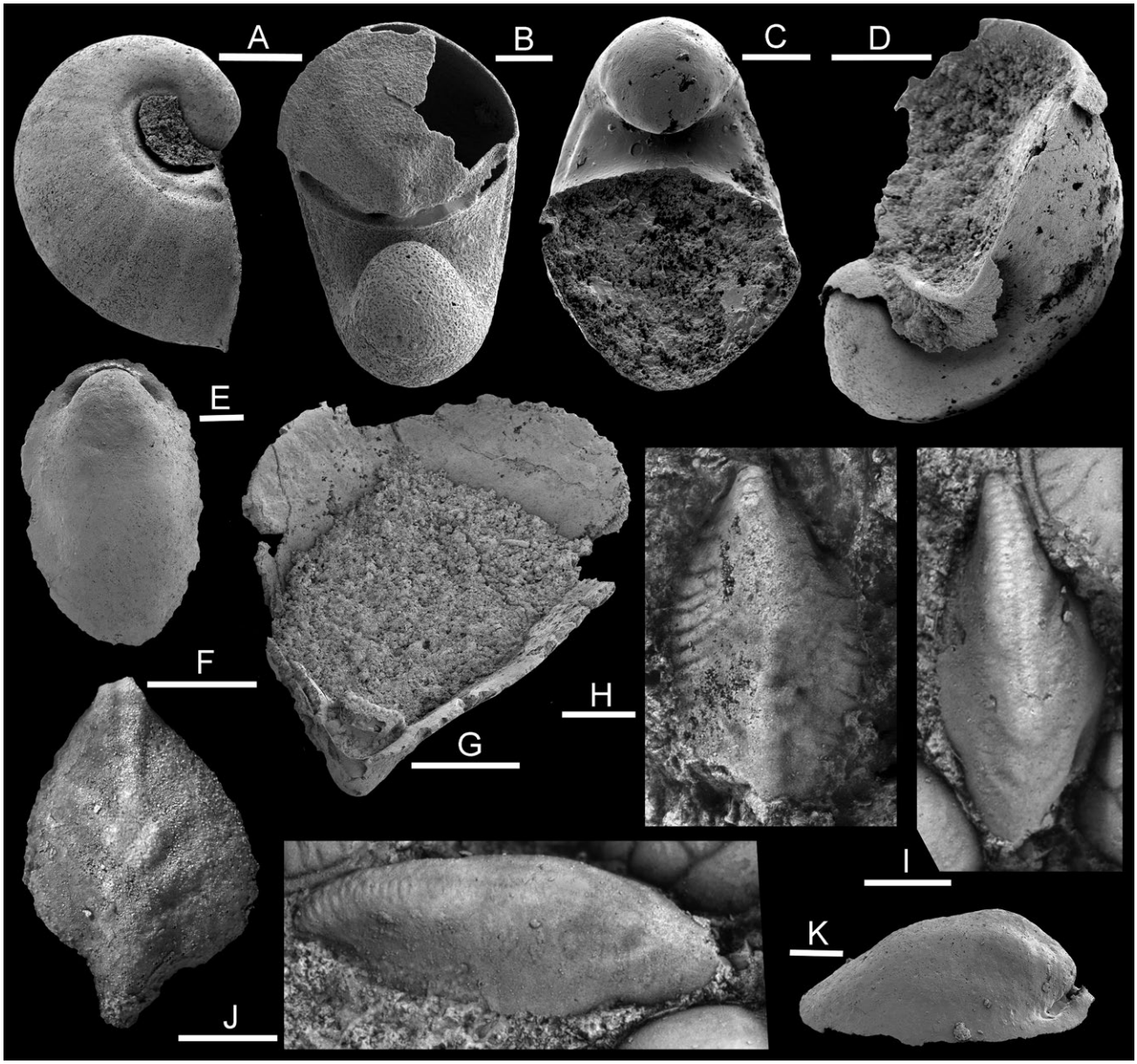

Fig. 5. Mollusc-like fossils, Henson Gletscher Formation, Cambrian, Miaolingian Series, Wuliuan Stage; internal moulds from GGU sample 271718 unless stated. **A–D:** *Protowenella flemingi* Runnegar & Jell, 1976. **A:** PMU 38330, lateral view. **B:** PMU 39329, apertural view with operculum in place from GGU sample 218331. **C:** PMU 38331 , apertural view. **D:** PMU 38333 from GGU sample 271492, oblique view of internal mould with phosphatization of external surface at apertural margin. **E–G, K:** *Stenothecoides terraglaciei* Peel, 2021b. **E:** PMU 38317 from GGU sample 271492, juvenile in plan view showing transverse sub-apical groove. **F:** PMU 38310. **G:** PMU 38322, holotype, internal view of ventral valve. **K:** PMU 38320 from GGU sample 271492, juvenile in lateral view showing sub-apical groove. **H:** *Stenothecoides* cf. *elongata* (Walcott, 1884), MGUH 33948 from GGU sample 271492 with lateral grooves on surface of internal mould. **I, J:** *Stenothecella* cf. *sibirica* Aksarina in Aksarina & Pelman, 1978, MGUH 33949 from GGU sample 271492, in plan (I) and oblique lateral (J) views. Scale bars: 1 mm (G), 100 μm (A, C–E, K), 50 μm (B).

to include the diagnostic circumbilical channels on the internal mould (Fig. 5A–C). It was reported from the Henson Gletscher Formation (GGU sample 271718) by Peel (1979). The history of research and phylogenetic placement of the genus were reviewed by Peel (2021a) who transferred *Protowenella* to Class Hyolitha on account of the presence of an in-place operculum of orthothecid type. *Protowenella* is widely distributed in Cambrian Series 2 and the Miaolingian Series (Wuliuan and Drumian stages).

Phylum uncertain

Class Stenothecoida Yochelson, 1968

Discussion. The bivalved stenothecoids were established as a new class of molluscs by Yochelson (1968, 1969) but their inferred pedicle attachment to the substrate promotes a closer relationship to brachiopods (Rozov 1984; Johnston 2019; Peel 2021c; Johnston & Streng 2021a). Rozov (1984) proposed a Phylum Stenothecata.

Genus *Stenothecoides* Resser, 1938

Type species. *Stenotheca elongata* Walcott, 1884, Eureka District, Nevada, Miaolingian Series, late Wuliuan Stage.

***Stenothecoides* cf. elongata (Walcott, 1884)**
Fig. 5H

1954 *Stenothecoides* cf. *S. elongata*; Rasetti, p. 63, pl. 11, figs 6–10, pl. 12 figs 1–4.
1957 *Stenothecoides* cf. *S. elongata*; Rasetti, p. 972, pl. 12, figs 1, 2.
1969 *Stenothecoides* cf. *elongata*; Yochelson, p. 55, fig. 4A–C.
2021c *Stenothecoides* cf. *elongata*; Peel, p. 390, fig. 7.

Figured material. MGUH 33948 from GGU sample 271492, internal mould, Lauge Koch Land.

Discussion. *Stenothecoides* cf. *S. elongata* is rare in GGU sample 271492, but the distinctive grooves on the internal mould, corresponding to ridges on the interior surface of the shell, perpendicular to the margin (Fig. 5H) compare well with material from the Mount Whyte Formation of British Columbia (Rasetti 1954; Yochelson 1969; Peel 2021c).

***Stenothecoides terraglaciei* Peel, 2021c**
Fig. 5E–G, K

2021c *Stenothecoides terraglaciei* Peel, p. 388, figs 4–6.

Figured material. PMU 38317 and PMU 38320 from GGU sample 271492, Lauge Koch Land; PMU 38310 and PMU 38322 (holotype) from GGU sample 271718, Løndal.

Discussion. *Stenothecoides terraglaciei* is common in GGU sample 271718. Internal moulds of numerous juveniles in GGU sample 271492, associated with rare specimens of *Stenothecoides* cf. *S. elongata*, cannot be distinguished from similarly preserved specimens in GGU sample 271718 and are therefore referred collectively to *Stenothecoides terraglaciei* (Peel 2021c).

Genus *Stenothecella* Aksarina in Aksarina & Pelman, 1978

Type species. *Stenothecella sibirica* Aksarina in Aksarina & Pelman, 1978, Kuznetsk Alatau, Altai–Sayan foldbelt, Siberia; Cambrian Series 2, Stage 4.

***Stenothecella* cf. *sibirica* Aksarina in Aksarina & Pelman, 1978**
Fig. 5I, J

2021c *Stenothecella* cf. *sibirica*; Peel, p. 391, fig. 8.

Figured material. MGUH 33949 from GGU sample 271492, Lauge Koch Land.

Discussion. The series of small muscle scars along the supra-apical surface of a well-preserved internal mould from GGU sample 271492 (Fig. 5I,J) compares well with the species described by Aksarina & Pelman (1978) from Cambrian Series 2, Stage 4, in Siberia (Peel 2021c). Several incomplete phosphatized internal moulds are also known from GGU sample 271718.

Phylum Mollusca Cuvier, 1797

Class uncertain

Order Pelagiellida MacKinnon, 1985

Genus *Costipelagiella* Horný, 1964

Type species. *Costipelagiella zazvorkai* Horný, 1964, Skryje Formation, Czech Republic; Cambrian, Miaolingian Series.

***Costipelagiella* cf. *nevadense* Skovsted, 2006b**
Fig. 6

Figured material. PMU 39174 – PMU 39178, PMU 39180

from GGU sample 271718, Løndal. PMU 39179 from GGU sample 271492, Lauge Koch Land.

Discussion. *Costipelagiella* cf. *nevadense* is common in GGU sample 271718, but rare in GGU sample 271492. The material from the Henson Gletscher Formation resembles material from the upper Emigrant Formation (Cambrian Series 2, Stage 4) of Nevada described by Skovsted (2006b) in the presence of well-developed comarginal ribs on the upper whorl surface (Fig. 6C,D,I), whereas such ribs are limited to the whorl periphery and base in the type species illustrated by Horný (1964, pl. 2, figs 1–3). Specimens assigned to *Costipelagiella* by MacKinnon (1985) from the Tasman Formation of New Zealand are lower spired and have more numerous comarginal ribs.

Internal moulds of pelagiellids are widespread in samples from Cambrian Series 2 and the Miaolingian Series in North Greenland but only rarely preserve traces of external ornamentation. *Costipelagiella kochi* Peel, 1988 from the Holm Dal Formation (Cambrian, Miaolingian Series, Guzhangian Stage) of western Peary Land, North Greenland, has a shell with a less inflated base and a more rounded whorl periphery (Peel 1988, fig. 20). In contrast, most specimens of *Costipelagiella* from the Henson Gletscher Formation have a flattened upper whorl surface and more angular periphery, although both features are variable. Peel *et al*. (2016) reported pelagiellids with a fine reticulate ornamentation from the Henson Gletscher Formation in Løndal (Cambrian Series 2, Stage 4) about 12 m below GGU sample 271718. Skovsted (2004) described well preserved specimens from Cambrian Series 2, Stage 4, in North-East Greenland with sub-spiral ribs forming a deep V-shaped pattern at the whorl periphery, unlike the simple comarginal ribs of *Costipelagiella* (Fig. 6C,D).

A pelagiellid from the Kuonamka Formation of Siberia, which Kouchinsky *et al*. (2011) compared to *Costipelagiella zazvorkai* Horný, 1964, shows comarginal corrugation seen in the illustrated Henson Gletscher Formation specimens (Fig. 6) but it differs in the greater height of the aperture.

Internal moulds from GGU sample 271718 often preserve a muscle scar at the suture with the previous whorl (Fig. 6A(arrow),B(arrow),E,J). Traces of euendolithic borings within the original calcareous shell are often visible as cord-like ridges on the internal mould (Fig. 6J, arrows).

Class Helcionelloida Peel, 1991b

Diagnosis. Emended by Geyer *et al*. (2019, p. 212): 'Generally bilaterally symmetrical univalves in which the calcareous shell is usually coiled through up to several whorls; the whorls may be in contact or open coiled and are often laterally compressed. The aperture is

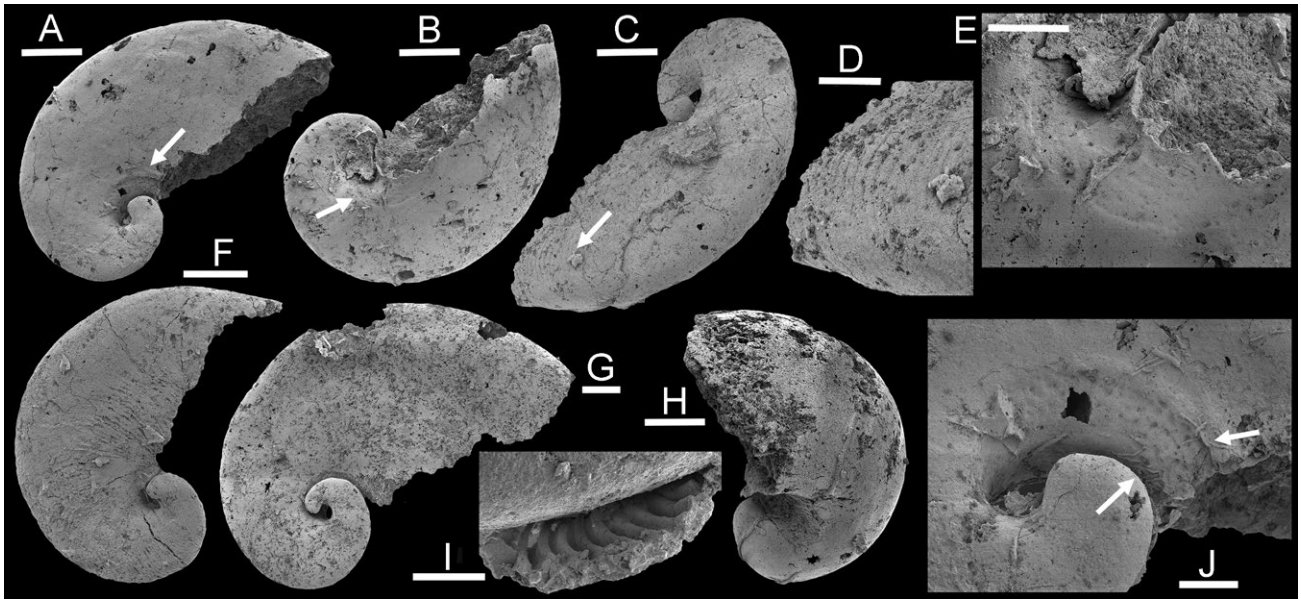

Fig. 6. *Costipelagiella* cf. *nevadense* Skovsted, 2006b, Henson Gletscher Formation, Cambrian, Miaolingian Series, Wuliuan Stage; internal moulds from GGU sample 271718 in Løndal unless stated. **A, J:** PMU 39174, apical view with arrow in A showing location of muscle scar (J); arrows in J show infilling of euendolithic borings. **B, E:** PMU 39175, umbilical surface showing detail of muscle scar (E). **C, D:** PMU 39176, oblique apical view with arrow in C locating detail of comarginal ribs (D). **F:** PMU 39177, apical view with traces of transverse ornamentation. **G:** PMU 39178, apical view. **H:** PMU 39179 from GGU sample 271492 from Lauge Koch Land, umbilical view. **I:** PMU 39180, showing impression of comarginal ribs from external surface. Scale bars: 200 μm (A–C, F, G), 100 μm (D, E, H), 50 μm (I, J).

oval, without re-entrant, but the sub-apical surface may develop a median sinus which in some taxa is deep and slit-like or trematose, with a single perforation at the end of an elongate tube termed the snorkel. In some forms, the lateral areas of the aperture may become prosocyrt, extended into weak lateral fields and producing broad emarginations in both the supra-apical and sub-apical surfaces astride the plane of symmetry. Ornamentation may include both comarginal and spiral elements; prominent comarginal rugae are common (modified from Peel 1991)'.

Discussion. There is no general agreement concerning the placement of helcionelloids in molluscan systematics. A series of papers by Parkhaev (2001a, b, 2002, 2017, 2019), Parkhaev & Demidenko 2010 and Parkhaev *in* Bouchet *et al.* (2017) has proposed that they should be placed as a separate Order Helcionelliformes Golikov & Starobogatov, 1989 (= Order Helcionelloida *sensu* Golikov & Starobogatov 1975) within the gastropod Subclass Archaeobranchia Parkhaev, 2001a, despite their interpreted untorted anatomy. Bellerophonts, a group of isostrophically coiled molluscs (Peel 1991a, b; Frýda 1999; Harper & Rollins 2000; Frýda *et al*. 2008; Ponder *et al*. 2020) often considered to be gastropods or untorted relatives of helcionelloids (or a polyphyletic grouping of both) were placed in a separate gastropod subclass by Parkhaev in Bouchet *et al.* (2017). Geyer *et al.* (2019) did not accept Parkhaev's archaeobranchian thesis and instead supported an opposing view that helcionelloids formed a Class Helcionelloida Peel, 1991b of untorted molluscs (Peel 1991a, 1991b; Jacquet & Brock 2016; Li *et al.* 2021), which is followed here. Discussion of other proposals and a historical review were given by Peel (1991a) and Ponder *et al.* (2020).

Missarzhevsky (1989, p. 171) proposed a new Order Eomonoplacophora for exogastric monoplacophorans without the muscle scars characteristic of *Tryblidium* Lindström, 1880, *Pilina* Koken & Perner, 1925 and their relatives. However, muscle scars are now known in several helcionelloid or helcionelloid-like genera (Rasetti 1954; Geyer 1994; Parkhaev 2002; Vendrasco *et al.* 2011; Li *et al.* 2021). Peel (1991a) generally accepted the content of Eomonoplacophora as helcionelloids but rejected the interpretation as exogastric and maintained the concept of Class Helcionelloida Peel, 1991b as endogastric molluscs. Eomonoplacophora has not gained widespread acceptance. However, Parkhaev in Bouchet *et al.* (2017) elevated Eomonoplacophora to a subclass of Class Monoplacophora Knight, 1952 but retained within it only one family (Maikhanellidae Missarzhevsky, 1989) of the eight families originally placed there by Missarzhevsky (1989, table 2). Most of the other seven families were considered to be gastropods of Subclass Archaeobranchia Parkhaev, 2001a (Parkhaev 2001a, 2002; Bouchet *et al*. 2017, p. 368, footnote 6) and placed within Order Helcionelliformes.

Parkhaev (2002) gave a detailed and valuable overview of the families and their included genera that he placed within Order Helcionelliformes (gastropod Class Archaeobranchia). Later versions were given by Bouchet *et al.* (2017) and Parkhaev (2019). Despite differences in the naming, content and placement of constituent families, most core genera are common to Eomonoplacophora *sensu* Missarzhevsky (1989), Helcionelloida (Peel, 1991a, b) and Helcionelliformes *sensu* Parkhaev (2001a, 2002).

Note on terminology. At numerous places in their text, Parkhaev & Demidenko (2010, pp. 1051, 1053, 1054) referred to the described helcionelloid genera as not having a 'planospiral' shell. The term is used also by Parkhaev (2017). Their meaning of planospiral is indicated by Parkhaev & Demidenko (2010, p. 1029) as "… shell does not form a complete whorl, so that the shell is not planospiral", which appears to indicate that planospiral reflects the degree of coiling (through at least one complete whorl) of a shell coiled in a single plane. 'Planospiral' is thus not synonymous in the usage of Parkhaev & Demidenko (2010) with the widely used 'planispiral' that means a shell coiled within a single plane, irrespective of the number of whorls (Knight *et al.* 1960, p. *I*132, see also Parkhaev 2000, 2001a). Such planispiral shells are not necessarily bilaterally symmetrical about that plane, but if so, they are described as isostrophic. Neither planospiral nor planispiral were used in Parkhaev (2019). Planospiral is sometimes used mainly in older literature as a synonym of planispiral in molluscs and foraminiferans, e.g. Cushman (1910). Planospiral is not used herein, where the degree of coiling is given as fractions of a shell whorl. This is less than a full revolution in most helcionelloids, but in a few forms such as *Coreospira* Saito, 1936 more than a full whorl may be present (Oh *et al.* 2021).

Family Helcionellidae Wenz, 1938

Genus *Dorispira* Parkhaev *in* Parkhaev & Demidenko, 2010

Type species. *Helcionella terraustralis* Runnegar & Jell, 1976 from the Coonigan Formation of New South Wales, Australia; Cambrian, Miaolingian Series, Wuliuan Stage.

Dorispira accordionata (Runnegar & Jell, 1976)

Figs 4D, 7A, E, F, J, N

1976 *Latouchella accordionata* Runnegar & Jell, p. 126, fig. 10C.1–C.18.

1998 *Latouchella accordionata*; Brock, p. 576, fig. 3.4–3.6.
2010 *Dorispira accordionata*; Parkhaev *in* Parkhaev & Demidenko, 2010, p. 1060.

Figured material. PMU 39172 from GGU sample 271492, Lauge Koch Land. PMU 339181 – PMU 39184 from GGU sample 271718, Løndal.

Description. Tall, laterally compressed, isostrophic shell coiled through half to two thirds of a whorl with a rectangular aperture, numerous prominent angular comarginal rugae and fine spiral threads. The shell exterior is preserved in a single specimen from GGU sample 271492 (Fig. 4D) but all other specimens are internal moulds in which the comarginal rugae are more rounded in crosssection (Fig. 7A,E,F,J,N). Specimens vary in curvature from tightly coiled, in which the apex substantially overhangs the sub-apical margin, as preserved (Fig. 7F), to tall, relatively slender forms (Fig. 7J). In the internal mould, the rounded apex is delimited by a shallow constriction from later growth stages (Fig. 7J). Two deep spiral grooves representing sharp ridges on the shell interior are present on the sub-apical surface in the latest half whorl, as preserved (Fig. 7A,F).

Discussion. *Dorispira accordionata* is abundant in GGU sample 271718. Specimens similar in shape to the slender form (Fig. 7J) were described by Brock (1998) from the Murrawong Creek Formation (Drumian Stage) of New South Wales. The sub-apical margin is extended in the larger silicified specimens illustrated by Runnegar & Jell (1976, fig. 10C) from the Coonigan Formation such that the apex does not extend beyond it. *Dorispira pearylandica* (Peel, 1988) from the Holm Dal Formation (Guzhangian Stage) of western Peary Land has a lower rate of whorl expansion.

Specimens from the Top Springs Limestone and Gum River Formation (Ordian Stage; Cambrian Stage 4–Wuliuan Stage) of Northern Territory, Australia, illustrated by Kruse (1991, 1998) often show a greater degree of coiling and more widely spaced comarginal rugae than material from North Greenland here referred to *Dorispira accordionata* (Fig. 7E,F,J,N). In this respect they more closely resemble *Dorispira tippik* sp. nov. (Fig. 7M,O,R). Kruse (1998) noted that the comarginal rugae often did not cross over the mid-dorsum in specimens from the Gum River Formation, a feature he attributed to erosion or exfoliation. Gubanov & Peel (1998) noted that restriction of prominent rugae to the lateral areas was the diagnostic feature of *Latouchella* Cobbold, 1921 from the Comley Limestone (Cambrian Stage 2) of Shropshire, England, although the name has been extensively applied to rugose Cambrian helcionelloids.

Tall specimens identified as *Oelandiella* cf. *accordionata* were described from the Tsinghsutung Formation (Cambrian Stage 4) of Guizhou, South China by Yang *et al.* (2012) and from the Miaolingian of Henan Province, North China by Hu *et al.* (2021) without reference to the establishment of *Dorispira* by Parkhaev & Demidenko (2010). The coarse rugae and the form of the aperture suggest placement in *Dorispira tippik* sp. nov., described below.

***Dorispira* cf. *arguta* (Resser, 1939)**
Fig. 8A–H

Figured material. PMU 39192 – PMU 39194 from GGU sample 271718, Løndal.

Description. Slowly expanding isostrophic cone coiled through half to two thirds of a whorl, with the uniformly curved supra-apical surface traversed by two broad, shallow constrictions (in available material) on the internal mould prior to the latest growth stage. Aperture subcircular, shell length about twice shell width, with shallow sub-apical fold along the median line. A pair of prominent spiral grooves extends from the first constriction to the aperture on the sub-apical surface of the internal mould, equivalent to sharp ridges on the shell interior. The apex of the internal mould is blunt, rounded, with slightly swollen apex. External ornamentation is not known, but the surface of the internal mould may show a pattern of low, meandering ridges (Fig. 8G,H).

Discussion. The few internal moulds placed here show the same pattern of broad comarginal rugae separated by narrow channels that is characteristic of *Dorispira arguta* (Resser, 1939) from the Miaolingian of Idaho (Geyer 1994, fig. 4). Type material of *Dorispira arguta* displays a fine reticulation of growth lines and spiral ridges on the shell exterior, whereas external ornamentation is not known in the Greenland specimens. In contrast, the spiral grooves on the sub-apical surface of the Greenland internal moulds have not been observed in material from Idaho.

The specimens from the Henson Gletscher Formation can be compared to the early growth stages of some specimens of *Dorispira merino* (Runnegar & Jell, 1976) from the Coonigan Formation of New South Wales (Runnegar & Jell 1976). Most illustrated specimens from the Coonigan Formation are silicified specimens that attain a length of about 6 mm, with the shell coiled through a full whorl. The dorsal and lateral areas of the shell surface are ornamented by prominent, pouch-like, transverse rugae, separated by deep channels. However, in the earliest half whorl of a partly exfoliated specimen illustrated by Runnegar

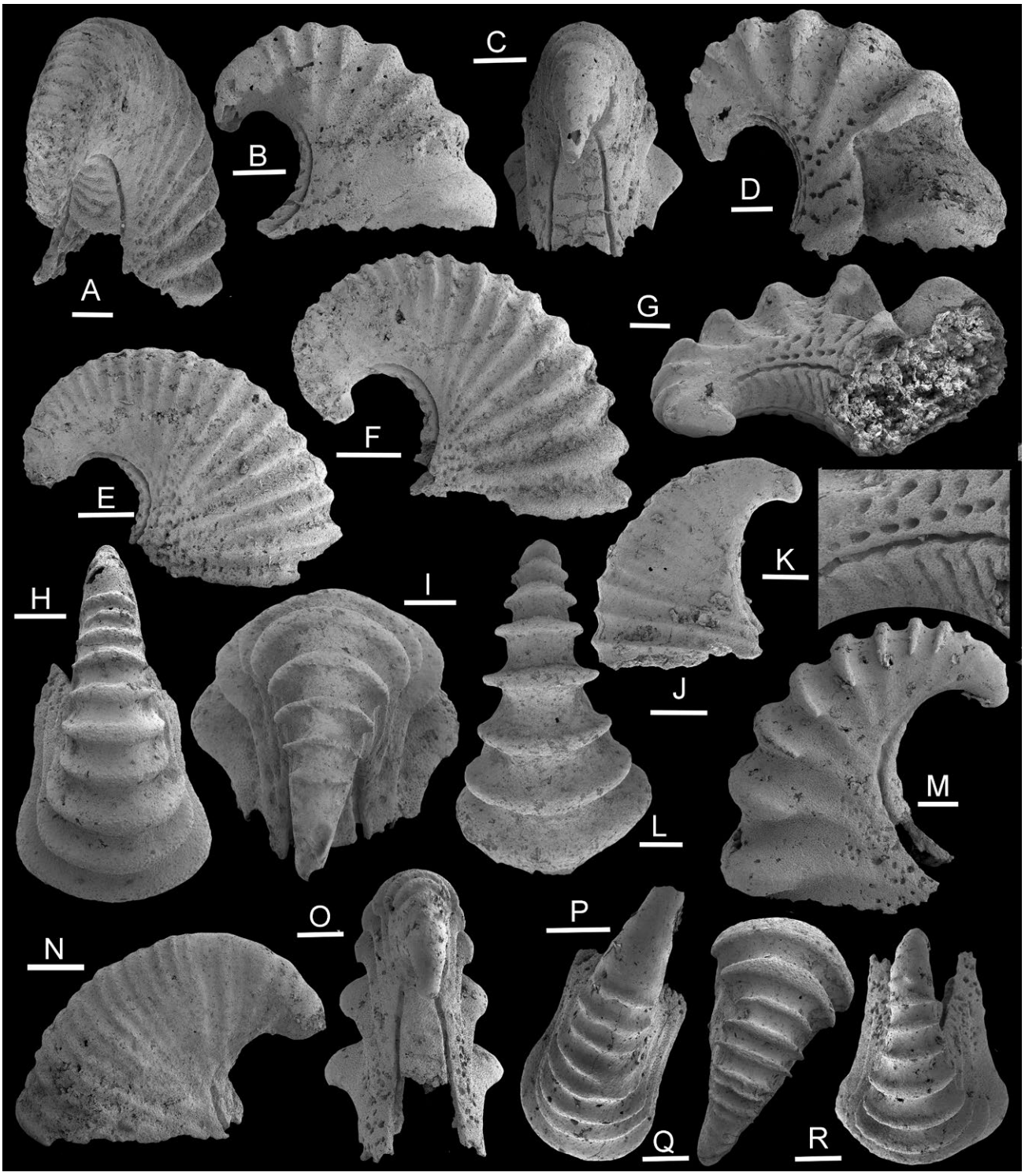

Fig. 7. *Dorispira*, upper Henson Gletscher Formation, Løndal, Peary Land, Miaolingian Series, Wuliuan Stage; internal moulds from GGU sample 271718. **A, E, F, J, N:** *Dorispira accordionata* (Runnegar & Jell, 1976). **A, F:** PMU 39181, oblique view of sub-apical surface. **E:** PMU 39182, lateral view. **J:** PMU 39183, lateral view. **N:** PMU 39184, lateral view. **B, C, D, G–I, K, L, M, O–R:** *Dorispira tippik* sp. nov. **B, C;** PMU 39185, lateral view (B) and sub-apical view with spiral grooves (C). **D, G, K:** PMU 39186, lateral view with repaired injury (D), oblique sub-apical view (G) with enlarged detail (K). **H:** PMU 39187, dorsal view. **I, L:** PMU 39188, dorsal (I) and supra-apical (L) views. **M, O, R:** PMU 39189, holotype in lateral (M), sub-apical (O) and dorsal (R) views. **P:** PMU 39190, dorsal view with concave lateral apertural margins. **Q:** PMU 39191, dorsal view. Scale bars: 400 μm (E, F, L), 200 μm (A–D, G–J, M–R), 100 μm (K).

& Jell (1976, fig. 9D.3), deep transverse channels on the internal mould are separated by broad transverse lobes that are lower in relief than the prominent lobes of the shell exterior at later growth stages This early stage closely resembles the small specimens (length about 1.3 mm) from the Henson Gletscher Formation (Fig. 8A–G).

***Dorispira avannga* sp. nov.**
Fig. 8K–N

Holotype. PMU 39197 from GGU sample 271718, Henson Gletscher Formation, Løndal, western Peary Land, North Greenland. Cambrian, Miaolingian Series, Wuliuan Stage.

Figured material. PMU 39196 from GGU sample 271718.

Diagnosis. Species of *Dorispira* with a circular aperture and numerous, closely spaced, angular comarginal rugae.

Derivation of name. From the Greenlandic 'avannga' meaning from the north.

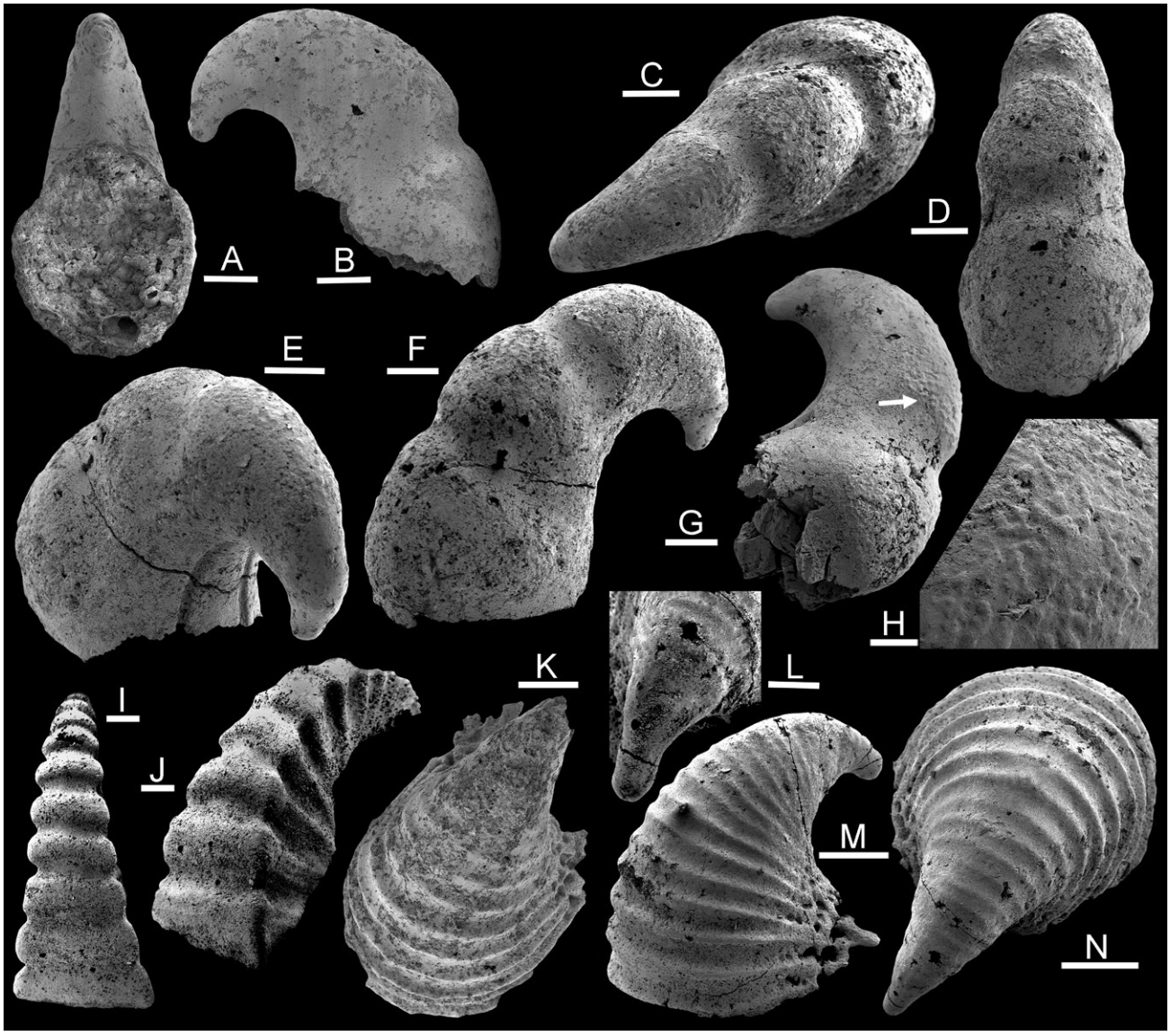

Fig. 8. *Dorispira*, upper Henson Gletscher Formation, Løndal, Peary Land, Miaolingian Series, Wuliuan Stage; internal moulds from GGU sample 271718. **A–H:** *Dorispira* cf. *arguta* (Resser, 1939). **A, B:** PMU 39192, apertural and lateral views. **C–F:** PMU 39193, dorsal (C, D) and oblique lateral (E, F) views. **G, H:** PMU 39194, lateral view, with detail of surface of internal mould (H, located by arrow in G). **I, J:** *Dorispira tavsenensis* sp. nov., PMU 39195, holotype, in dorsal (I) and dorso-lateral (J) views. **K–N:** *Dorispira avannga* sp. nov. **K:** PMU 39196. **L–N:** PMU 39197, holotype in oblique lateral (M) and dorsal (N) views with detail of early growth stage (L). Scale bars: 200 μm (A–G, I–K, M, N), 100 μm (L), 30 μm (H).

Description. Tall, isostrophic shell, coiled through half to two thirds of a whorl, in which the inflated shell has a circular apertural periphery (Fig. 8N). Supra-apical and lateral areas of the internal mould with numerous closely spaced, uniform, comarginal rugae, which become obscure on the subapical surface; traces of fine spiral ribs in the intervening concave channels. Apex strongly overhanging the sub-apical margin, with earliest growth stage smooth in the internal mould, subcylindrical and slightly constricted prior to transition to the rugose later growth stages (Fig. 8L). Two deep spiral grooves representing sharp ridges on the shell interior are present on the sub-apical surface of the internal mould in the latest half whorl, as preserved.

Discussion. *Dorispira avannga* sp. nov. is a rare species known only from internal moulds in GGU sample 271718. In terms of the shape and abundance of its comarginal rugae, *Dorispira avannga* closely resembles *Dorispira accordionata*. It is distinguished by the more inflated shell, with a circular aperture in plan view (Fig. 8N), when compared to the rectangular aperture of *Dorispira accordionata*. *Dorispira pearylandica* from the Holm Dal Formation (Guzhangian) of western Peary Land is more laterally compressed, with a lower rate of whorl expansion (Peel 1988).

***Dorispira septentrionalis* sp. nov.**
Figs 4F, H, I, 9A–E

Holotype. PMU 39173 from GGU sample 271718, Henson Gletscher Formation, Løndal, western Peary Land, North Greenland. Cambrian, Miaolingian Series, Wuliuan Stage.

Other figured material. PMU 39198 and PMU 39199 from GGU sample 271718.

Derivation of name. From the Latin 'septentrionalis' meaning northern.

Diagnosis. Tall, laterally compressed species of *Dorispira* in which the aperture narrows towards the sub-apical margin. Ornamentation of coarser comarginal rugae, cords and ribs crossed by spiral ridges.

Description. The aperture in the tall, laterally compressed, isostrophic shell narrows towards the sub-apical margin. The earliest growth stage is smooth with a round termination, and may be delimited from the later shell by a shallow constriction on the internal mould (Fig. 9B). Comarginal rugae are prominent on the supra-apical and lateral areas of the internal mould but much reduced or absent immediately below the apex. Ornamentation of comarginal cords and ribs crossed by spiral ridges to form a reticulate pattern. Internal mould with two deep spiral grooves on the sub-apical surface, its surface covered with fine pits (Fig. 9D).

Discussion. *Dorispira septentrionalis* sp. nov. differs from co-occurring species of *Dorispira* in terms of its greater lateral compression, with the aperture narrowing towards its sub-apical margin. *Dorispira accordionata* is distinguished by its more numerous, evenly developed and acute comarginal rugae (Fig. 4D). In silicified specimens of *Dorispira merino* illustrated from the Coonigan Formation by Runnegar & Jell (1976, fig. 9D), the shell is coiled through a full whorl and the comarginal rugae are more strongly developed, often pouch-like, with shallow emarginations on the lateral areas.

***Dorispira tavsenensis* sp. nov.**
Fig. 8I, J

Holotype. PMU 39195, partial internal mould from GGU sample 271718, Henson Gletscher Formation, Løndal, western Peary Land, North Greenland. Cambrian, Miaolingian Series, Wuliuan Stage.

Derivation of name. From Hans Tavsen (Tausen) Iskappe, western Peary Land (Fig. 1A).

Diagnosis. Species of *Dorispira* in which the flattened dorsal surface is perpendicular to the flat or shallowly concave lateral areas. Ornamentation of prominent transverse channels and rugae of similar width, the latter slightly nodose as they cross from the lateral areas to the dorsum.

Description. Isostrophic, laterally compressed, with the flattened dorsal (supra-apical) surface perpendicular to the flat to shallowly concave lateral areas (Fig. 8J). Surface with prominent comarginal rugae separated by deep U-shaped channels, with greatest width at nodes at the junction between the dorsal and lateral surfaces. The nodes create the impression of a spiral ridge on each whorl shoulder emphasised by the intervening channels being deepest close to the transition from the dorsum to the lateral areas. Rugae with fine comarginal cords and obscure spiral lines.

Discussion. *Dorispira tavsenensis* sp. nov. is known only from rare internal moulds in GGU sample 271718, amongst which the holotype, although broken, most clearly displays the quadratic transverse whorl profile (Fig. 8I, J). *Wakayella kandiingi* Kruse, 1998 from the Ranken Limestone (Ordian Stage; Cambrian Stage 4–Wuliuan Stage) of Northern Territory, Australia, dis-

plays a similar quadratic dorsal profile, with nodes at the transition from the dorsum to the lateral areas, but differs in its cap-shaped, rapidly expanding, strongly laterally compressed shell (Kruse 1998, fig. 40B).

Coreospira Saito, 1936, originally described from the middle Cambrian of Korea, has a similar quadratic whorl profile but the angulation between the dorsum and lateral areas is marked by a continuous prominent spiral cord (Oh *et al*. 2021).

***Dorispira tippik* sp. nov.**
Figs 4A–C, E, G, 7B, C, D, G–I, K, L. M, O–R

Holotype. PMU 39189 from GGU sample 271718, Henson Gletscher Formation, Løndal, western Peary Land, North Greenland. Cambrian, Miaolingian Series, Wuliuan Stage.

Other figured material. MGUH 19561 and PMU 39185 – PMU 39188, PMU 39190 and PMU 39191 from GGU sample 271718, Løndal.

Diagnosis. Species of *Dorispira* with the tall, laterally compressed shell coiled through about half a whorl and strongly defined comarginal rugae that are raised into turbercles at the transition from the supra-apical surface to the lateral areas.

Derivation of name. From the Greenlandic 'tippik' meaning the transverse supporting ribs of a boat, alluding to the prominent comarginal rugae.

Description. Tall, isostrophic, lateral compressed shell in which the aperture in later growth stages is key-shaped in plan view (Fig. 7H,P,R), with concave lateral areas. Apex of internal mould smooth, sometimes delimited from the later growth stages by a shallow constriction (Fig. 7O). Prominent, but narrow comarginal rugae originate at the junction between the sub-apical and lateral surfaces and increase in relief and become tuberculate as they cross the supra-apical (dorsal) surface (Fig. 7M). Sub-apical surface with one to three pairs of deep, continuous or slightly interrupted grooves (Fig. 4A) formed by ridges on the shell interior that may be L- or T-shaped in cross-section (Fig. 4E). Median area between the innermost pair of spiral grooves with comarginal grooves on the internal mould (Figs 4B, 7G). Surface of internal mould often covered with fine pits (Fig. 4G).

Discussion. Specimens of *Dorispira tippik* sp. nov. are abundant as internal moulds in GGU sample 271718 and rare specimens are identified tentatively on limestone surfaces from GGU sample 271492. Many specimens (Fig. 7L,M) have a similar erect shell with prominent comarginal rugae to *Dorispira iacobinica* (Geyer, 1986) from the *Morocconus notabilis* zone (Cambrian Series 2, upper Stage 4; Agzdian regional stage) of Morocco (Geyer 1986, pl. 3, figs 29, 30), while other Greenland specimens show a greater rate of whorl expansion in lateral perspective (Fig. 7B,D). *Dorispira iacobinica* differs in that the comarginal rugae are uniformly developed all around the shell whereas the rugae are much more prominent across the supra-apical surface of *Dorispira tippik* than on the sub-apical surface. However, the Moroccan holotype illustrated by Geyer (1986, pl. 3, fig. 29) preserves the shell exterior, with fine details of spiral ornamentation and transverse growth lines, in contrast to the internal moulds from Greenland.

Yang *et al*. (2012) described *Oelandiella* cf. *accordionata* from the Tsinghsutung Formation (Cambrian Stage 4) of Guizhou, South China, without reference to *Dorispira*. The erect shell and protruding sub-apical surface clearly distinguish the illustrated specimens from *Oelandiella* from the early Cambrian of the Siberian Platform (Vostokova 1962; Rozanov *et al*. 2010), as discussed by Parkhaev & Demidenko (2010). The coarse rugae suggest placement in *Dorispira tippik* sp. nov. An accompanying specimen in the Chinese fauna (Yang *et al*. 2012, pl. 2, figs 7, 8) is only slightly coiled and resembles the species described as *Helcionella callahani* Resser, 1938 from Cambrian Series 2, Stage 4 in the southern Appalachians, USA (Resser 1938), a shell form not known from the present North Greenland collections.

Hu *et al*. (2021) assigned Miaolingian (Drumian–Guzhangian) fossils from Henan Province, North China, to *Oelandiella accordionata* also without reference to *Dorispira*. The erect shell clearly distinguishes the illustrated specimens from *Oelandiella*, as discussed by Parkhaev & Demidenko (2010), and illustrated by Rozanov *et al*. (2010) and the coarse rugae and form of the aperture suggest placement in *Dorispira tippik* sp. nov.

***Dorispira*? cf. *penecyrano* (Runnegar & Jell, 1976)**
Fig. 9F, G

Figured material. PMU 39200 from GGU sample 271718.

Discussion. This rare member of the assemblage from GGU sample 271718 is known from laterally compressed internal moulds that display subdued comarginal transverse corrugation and an overhanging apex. The arched sinus in the apertural margin on the sub-apical surface characteristic of the silicified material from the Coonigan Formation is not seen, but its absence may reflect the much greater size (length up to 3 mm) of the Australian specimens. The

external ornamentation of fine spiral lirae illustrated by Runnegar & Jell (1976, fig. 10A) is not preserved on the internal moulds, which display the fine pits seen in many other specimens from the Henson Gletscher Formation material. The initial growth stage in the latter is blunt and delimited from the later parts of the internal mould by a shallow constriction (Fig. 9G).

Runnegar & Jell (1976) considered that the arched sinus in the apertural margin beneath the apex indicated a relationship to *Yochelcionella* Runnegar & Jell, 1974; it is not typically well developed in *Dorispira*. For this reason, and on account of the lack of spiral grooves on the sub-apical surface of the internal mould (Fig. 9F), the species is only tentatively assigned to *Dorispira*, where it was placed by Parkhaev (2019). Specimens from the Holm Dal Formation (Guzhangian Stage) of Peary Land described by Peel (1988) as *Latouchella holmdalense* Peel, 1988 are morphologically close to the Australian material described by Runnegar & Jell (1976). They differ from the specimens in GGU sample 271718 in having a prominent sub-apical arched sinus, coarser comarginal corrugation and a more overhanging apex, although these features may be in part be due to their greater size and preservation with retained shell. Robison (1964, pl. 92, fig. 14) illustrated a similar silicified specimen with a proportionately longer shell from the Drumian Stage of Utah.

Genus *Scenella* Billings, 1872

Type species. *Scenella reticulata* Billings, 1872, Cambrian Series 2, Conception Bay, Avalonian southeastern Newfoundland, Canada.

***Scenella? siku* sp. nov.**
Fig. 10G, K, M–O

Holotype. PMU 39207, internal mould from GGU sample 271718, Henson Gletscher Formation, Løndal, western Peary Land, North Greenland, Cambrian, Miaolingian Series, Wuliuan Stage.

Other figured material. PMU 39205 and PMU 39206, internal moulds from GGU sample 271718.

Derivation of name. From 'siku', one of many Greenlandic words for ice.

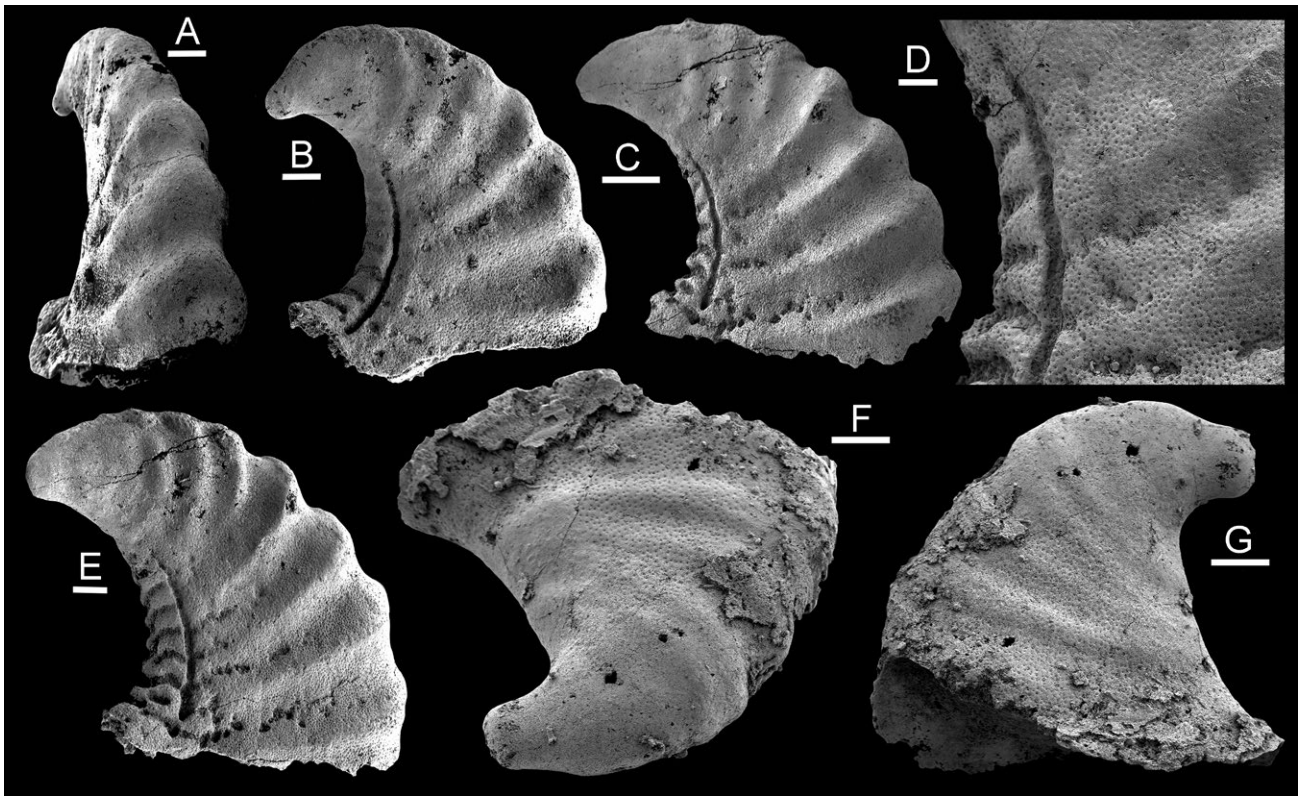

Fig. 9. *Dorispira*, upper Henson Gletscher Formation, Løndal, Peary Land, Miaolingian Series, Wuliuan Stage; internal moulds from GGU sample 271718. **A–E:** *Dorispira septentrionalis* sp. nov. **A, B:** PMU 39198, oblique lateral views. **C–E:** PMU 39199, oblique lateral (E) and lateral (C) views, with detail of pitted surface (D). **F, G:** *Dorispira*? *penecyrano* (Runnegar & Jell, 1976). PMU 39200, in lateral (G) and dorso-lateral (F) views. Scale bars: 200 μm (C), 100 μm (A, B, E–G), 50 μm (D).

Diagnosis. Tentatively a species of *Scenella* with an elongate form and the slightly overhanging apex lying close to the sub-apical margin.

Description. Isostrophic, low, limpet-like, in which the width of the elongate shell is about two thirds of its length. Apex lying close to the sub-apical margin, slightly overhanging the sub-apical wall. Supra-apical surface shallowly convex in lateral profile (Fig. 10G) with the point of greatest height above the apertural plane lying at about one fifth of the distance from the sub-apical margin to the supra-apical margin. Surface of internal mould may retain low, widely spaced rugae (Fig. 10K). External ornamentation not known.

Discussion. The question of the relationship between *Scenella* and *Protoconchioides* Shaw, 1962 has been discussed in detail by Geyer (1994). In *Protoconchioides douli* Geyer, 1994, from the Miaolingian of Idaho, the apex of the oval shell is located almost centrally, in

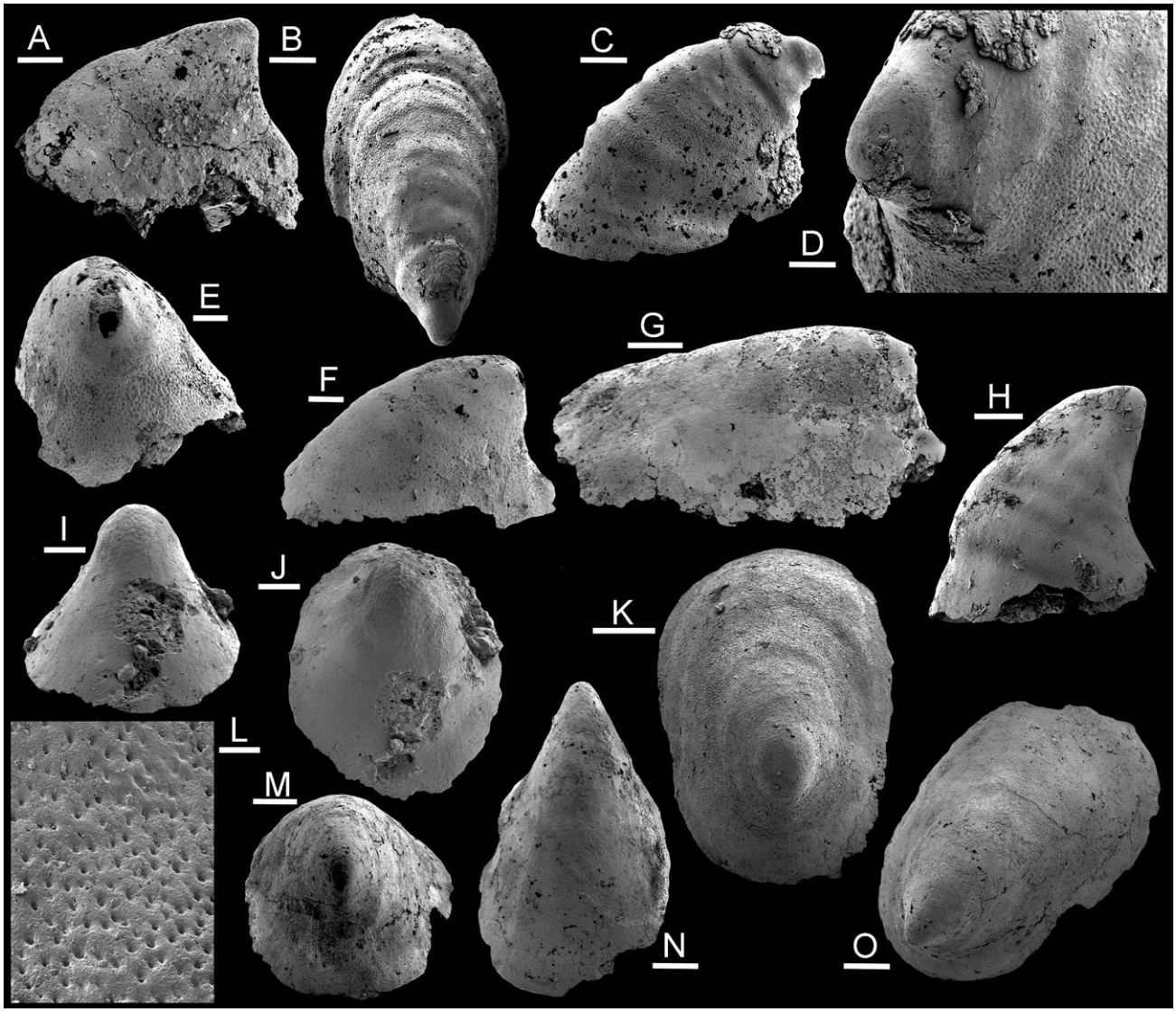

Fig. 10. Helcionellids, internal moulds from the Henson Gletscher Formation, Miaolingian Series, Wuliuan Stage, of Lauge Koch Land (GGU sample 271492) and Løndal (GGU sample 271718). **A, E, F, H,** Helcionellids spp. indet. **A:** PMU 39201 from GGU sample 271718, lateral view. **E, F,** PMU 39202 from GGU sample 271492, lateral view (F) and oblique view of sub-apical surface showing smooth surface around apex and pitted flanks (E). **H:** PMU 39203 from GGU sample 271718, lateral view. **B–D:** *Parailsanella* sp., PMU 39204 from GGU sample 271492, dorsal (B) and lateral (C) views with detail of early growth stage (D). **G, K, M–O:** *Scenella*? *siku* sp. nov. from GGU sample 271718. **G:** PMU 39205, lateral view. **K:** PMU 39206, apico-dorsal view. **M–O:** PMU 39207, holotype, in oblique apical (M), oblique dorsal (N) and oblique dorso-lateral (O) views. **I, J, L:** *Vendrascospira frykmani* gen. et sp. nov., PMU 39208 from GGU sample 271492, holotype, profile from supra-apical margin (I), dorsal view (J), detail of pitted surface (L). Scale bars: 200 μm (A–C, G, H, M–O), 100 μm (D–F, I–K), 20 μm (L).

contrast to its marginal position in *Scenella*? *siku*. This is also the case in *Protoconchioides*? *rasettii* Geyer, 1994, from the Mount Whyte Formation of British Columbia, originally described as *Scenella* sp. by Rasetti (1954). Described specimens of *Scenella*, including the type species (Knight 1941, pl. 2, fig. 5), also differ from *Scenella*? *siku* in having the apex placed more centrally and an oval to sub-circular dorsal plan. Comarginal rugae are only weakly developed, if present, and the shell exterior is ornamented with a fine reticulation of growth lines and radial ribs not known from *Scenella*? *siku*. *Scenella amii* (Matthew, 1902), abundant in the Burgess Shale of British Columbia, differs from *Scenella*? *siku* in the sub-circular dorsal plan and central location of the apex on the cap-shaped shell (Conway Morris & Peel 2013, fig. 1.6).

Genus *Parailsanella* Zhegallo in Voronova *et al.*, 1987

Type species. *Parailsanella acris* Zhegallo in Voronova *et al*., 1987 from Cambrian Series 2, Stage 3 (Montezuman Regional Stage) of Northwest Territories, Canada.

Discussion. *Helcionella* Grabau & Shimer, 1909 and *Bemella* Missarzhevsky *in* Rozanov & Missarzhevsky, 1966 are frequently cited helcionelloids with low cap-shaped shells and prominent comarginal rugae. Their relationship was recently discussed by Geyer *et al*. (2019) who discounted the significance of the globose apex overhanging the sub-apical margin that Missarzhevsky (in Rozanov *et al*. 1969) and Parkhaev (2001a, b) considered a diagnostic feature of *Bemella*. Instead, Geyer *et al*. (2019) placed emphasis on the differentiation of the early part of the shell from the later more strongly rugose teleoconch in *Bemella jacutica* Missarzhevsky in Rozanov & Missarzhevsky, 1966, as illustrated by Rozanov *et al*. (1969, pl. 4, fig. 3). The laterally compressed, early Cambrian genus *Parailsanella* Zhegallo in Voronova *et al*., 1987 also has a rugose shell but differs in that the apex is elevated above the plane of the aperture, such that a shallowly concave subapical wall is well developed (Kouchinsky *et al*. 2015, fig. 5). It is morphologically close to *Capitoconus* Skovsted, 2004, originally described from the Bastion Formation (Cambrian Series 2, Stage 4) of North-East Greenland, but the latter differs in terms of its strongly inflated protoconch (Skovsted 2004).

***Parailsanella* sp.**
Fig. 10B–D

Figured material. PMU 39204 from GGU sample 271492, Lauge Koch Land.

Discussion. This single internal mould lacks the apertural margin. It is laterally compressed (Fig. 10B) and coiled through about one quarter of a whorl, with the apex overhanging the sub-apical surface (Fig. 10C). Irregular comarginal rugae are most strongly developed on the supra-apical and lateral areas. The early growth stage preserves two prominent comarginal channels on the internal mould that seem to delimit the early growth stage which Geyer *et al*. (2019) considered to be diagnostic of *Bemella*. This interpretation is supported by the surface pattern developed on the internal mould in ontogenetic stages approximately adapertural of the second comarginal constriction, but absent from the apical area (Fig. 10C,D), although this is also a feature of the internal moulds of other North Greenland species (Figs 10E,13B). Initially this pattern is a fine reticulation of ridges, but it gradually transforms to a structure of fine pits as the aperture is approached. However, the sub-apical wall is well developed, such that the apex in lateral perspective is raised high above the plane of the aperture, motivating assignment to *Parailsanella*. The lateral profile is thus closely similar to internal moulds illustrated by Kouchinsky *et al*. (2015, fig. 15) from the Emyaksin Formation (Atdabanian Stage) of northern Siberia, although these have broader, more regular comarginal rugae than the North Greenland specimen.

Capitoconus borealis Peel, Streng, Geyer, Kouchinsky & Skovsted, 2016, from the the lower beds of the Henson Gletscher Formation in Løndal (Cambrian Series 2, Stage 4, *Ovatoryctocara granulata* beds), has a similar shell form to *Parailsanella* sp. from GGU sample 271492, but its protoconch is more prominent and comarginal rugae are lacking. Growth lines are crossed by fine spiral threads that have not been observed in *Parailsanella* sp.

A specimen from the Coonigan Formation described by Runnegar & Jell (1976, fig. 8A, 1-2) as *Anabarella* sp. was transferred to *Bemella* by Parkhaev (2019). The specimen is more than five times larger than *Parailsanella* sp. from North Greenland, more laterally compressed, with a well-developed sub-apical surface and flanks with coarser and more widely spaced rugae. Runnegar & Jell (1976, fig. 9A.1–9A.5) described as *Vallotheca* [sic] sp. a silicified, strongly rugose specimen from the Coonigan Formation that exhibits a similar lateral profile and elongate form to *Parailsanella* sp. from the Henson Gletscher Formation. The latter specimen lacks the prominent rugation of the Australian example, although in part this may reflect the preservation of *Parailsanella* sp. as an internal mould. *Vallatotheca* Foerste, 1914, originally described from the Late Ordovician of Manitoulin Island, Canada, has a globose shell more than ten times larger than *Parailsanella* sp., and was considered by Knight (1941) to be closely

related to the tergomyan *Tryblidium* Lindström, 1880.

A fragment from the Top Springs Limestone (Ordian Stage; Cambrian Stage 4–Wuliuan Stage) in the Georgina Basin of Northern Territory, Australia, illustrated by Kruse (1991, fig. 10K, L) as ?scenellid indet., has a similar shell form to *Parailsanella* sp. from North Greenland, but with coarser comarginal rugae. Both taxa have a prominent comarginal channel delimiting the earliest growth stage. *Bemella wiri* Kruse, 1998 from the Montejinni and Gum Ridge formations of similar age, also in Northern Territory, Australia, is based on larger, more strongly coiled specimens (length 1 cm) in which the apex is curved down close to the plane of the aperture (Kruse 1998). The sub-apical surface of *Bemella wiri* is therefore strongly concave in lateral profile when compared to the almost straight sub-apical surface below the elevated apex of *Parailsanella* sp. (Fig. 10C).

Parailsanella sp. is distinguished from *Scenella*? *siku* by its more tightly coiled shell with a lower rate of whorl expansion, in lateral view, protruding apex and strong rugae.

Genus *Helcionella* Grabau & Shimer 1909

Type species. *Metoptoma*? *rugosa* Hall, 1847 from the Browns Pond Formation, New York State, Cambrian Series 2, Stage 4.

***Helcionella*? sp.**
Fig. 11A, B

Figured material. PMU 39209 from GGU sample 218831, Lauge Koch Land.

Discussion. As preserved, width and length are about equal in this low internal mould, although the sub-apical surface is incomplete (Fig. 11B). The dorsal and lateral areas carry prominent, flared rugae and finer interspersed comarginal cords, the latter most prominent near the apex. Both are crossed by fine radial ribs (Fig. 11B, arrow). A similar low shell, but with more frequent rugae, was illustrated from the Currant Bush Limestone (Gowers Formation) by Runnegar & Jell (1976, fig. 9B.1–B.3) as *Vallatotheca*? sp.

Helcionellids spp. indet.
Figs 10A, E, F, H, 13A–C, E–H

Figured material. PMU 39202 and PMU 39216 from GGU sample 271492, Lauge Koch Land. PMU 39201, PMU 39203, PMU 39213 – 39215, PMU 39217 from GGU sample 271718, Løndal.

Discussion. Smooth internal moulds are common in GGU sample 271718 from Løndal but are difficult to assign due to their variation and lack of distinguishing characters. The apex forms the highest part of the shell in a single internal mould from GGU sample 271718 in which a shallow comarginal constriction is preserved near the broken apertural margin (Fig. 10A). Rare internal moulds with an oval cross-section from GGU sample 271492 have the blunt apex located close to the sub-apical margin, above a vertical sub-apical wall (Figs 10F, 13G). The supra-apical wall is uniformly convex but more strongly curved than in *Scenella*? *siku*. The internal mould is smooth close to the apex, but otherwise covered with fine pits (Fig. 10E). Internal moulds with a similar profile were described by Kruse (1998) from the Ordian Stage (Cambrian Stage 4–Wuliuan Stage) of Northern Territory, Australia. The internal mould of *Parailsanella* sp. has a similar lateral profile, but the apex is overhanging and the surface is traversed by prominent comarginal rugae (Fig. 10C).

The lateral profile of a single internal mould from GGU sample 271718 (Fig. 10H) is similar to that of an upright internal mould illustrated by Runnegar & Jell (1976, fig. 10B.4, B.5) from the Coonigan Formation, although comarginal rugae in the latter specimen are more strongly expressed. The aperture is oval, but its margins are not preserved. The apical area is smooth, but the surface of the rest of the specimen is covered by fine pits.

The apex strongly overhangs the sub-apical margin in several laterally compressed internal moulds from GGU sample 271718 (Fig. 13A,B,C,F), as in *Erugoconus acuminatus* gen. et sp. nov. (Fig. 16F,H), but the rate of expansion in lateral view is greater. Rare internal moulds with a strongly overhanging apex show a conical early growth stage (Fig. 13E). A more tightly coiled internal mould (Fig. 13H) is similar to *Erugoconus acuminatus* (Fig. 16F,H) but the apex overhangs the elongate aperture by a proportionately shorter distance (Fig. 13H).

Genus *Sermeqiconus* gen. nov.

Type species. *Figurina*? *polaris* Peel, 2021d, Aftenstjernesø Formation, Navarana Fjord, northern Lauge Koch Land, North Greenland; Cambrian Series 2, Stage 4 (Peel 2021d).

Derivation of name. From the Greenlandic 'sermeq' meaning an active glacier, referring to the position of the collection locality immediately west of Henson Gletscher (Fig. 1A).

Diagnosis. Isostrophic, low, with oval plan, and swollen apex lying close to the sub-apical margin. Ornamentation of a few widely spaced ribs and finer striations,

the former most prominent on the supra-apical surface, crossed by slightly lamellose comarginal growth lines.

Discussion. Internal moulds from the Parara Formation (Cambrian Series 2) in South Australia, assigned to *Figurina* Parkhaev, 2001a by Parkhaev (2001a), are more laterally compressed, with a narrower, more strongly overhanging apex, and lack the prominent widely spaced radial ribs characteristic of *Sermeqiconus*. *Calyptroconus* Parkhaev, 2001a, also from the Parara Formation (Cambrian Series 2) in South Australia, has broad radial folds distributed all around the low, oval shell and a sub-central apex in contrast to the overhanging apex of *Sermeqiconus*. In North Greenland, *Sermeqiconus* ranges from Cambrian Series 2, Stage 4 (Aftenstjernesø Formation; Peel 2021d) to the Miaolingian Series, Wuliuan Stage (Henson Gletscher Formation).

***Sermeqiconus polaris* (Peel, 2021d)**
Figure 11C, D

2021d *Figurina*? *polaris* Peel, p. 29, fig. 4.7, 4.8.

Figured material. PMU 39210 from GGU sample 218831, Lauge Koch Land.

Diagnosis. As for genus.

Description. The internal mould is isostrophic, low, oval, with width about two-thirds of length; the swollen apex lies above, but just within the sub-apical margin. Supra-apical surface shallowly convex in lateral view, flattening as the supra-apical margin is approached; sub-apical surface concave and steeply inclined (Fig. 11C). Initial growth stage forming one third of the preserved length; smooth, with a shallowly impressed pegma on the sub-apical surface at the junction with the ornamented later shell growth stage. Ornamentation consists of widely spaced, prominent radial ribs with rounded upper surfaces and intervening fine striations, which are crossed by slightly lamellose comarginal growth lines. Fine pits are prominent on the sub-apical surface and lateral margins.

Discussion. *Sermeqiconus polaris* (Peel, 2021d) from the basal Aftenstjernesø Formation, northern Navarana Fjord, northern Lauge Koch Land, North Greenland (Fig. 1A; Cambrian Series 2, Stage 4) was referred tentatively to *Figurina* by Peel (2021d). The distinctive widely spaced radial ribs located mainly on the dorsal area of the holotype of *Sermeqiconus polaris* (Peel, 2021d, fig. 4.7, 4.8) are clearly preserved in the specimen from the Henson Gletscher Formation (Fig. 11C,D). *Sermeqiconus polaris* has a wider shell than the laterally compressed *Figurina figurina* Parkhaev, 2001a, and its broader apex less strongly overhangs the sub-apical surface.

Figurina? *groenlandica* Skovsted, 2004 from the Bastion Formation (Cambrian Series 2, Stage 4) of North-East Greenland has a narrower shell than *Sermeqiconus polaris* in which the supra-apical surface of the internal mould is more strongly curved in lateral view (Skovsted 2004). In lateral view, prominent grooves and ridges present on the half of the internal mould closest to the sub-apical margin slope obliquely, sub-parallel to the supra-apical surface. Similar ridges on the sub-apical surface of *Sermeqiconus polaris* are confined to the sub-apico-lateral areas and run parallel to the sub-apical surface (Fig. 11C). Partial phosphate coating of the outer surface of the shell near the supra-apical margin in some specimens from the Bastion Formation shows weak traces of radial ribs reminiscent of *Sermeqiconus* (Skovsted 2004, fig. 6G).

Genus *Vendrascospira* gen. nov.

Type species. *Vendrascospira troelseni* gen. et sp. nov.

Derivation of name. For Michael J. Vendrasco in recognition of his studies of Cambrian molluscs.

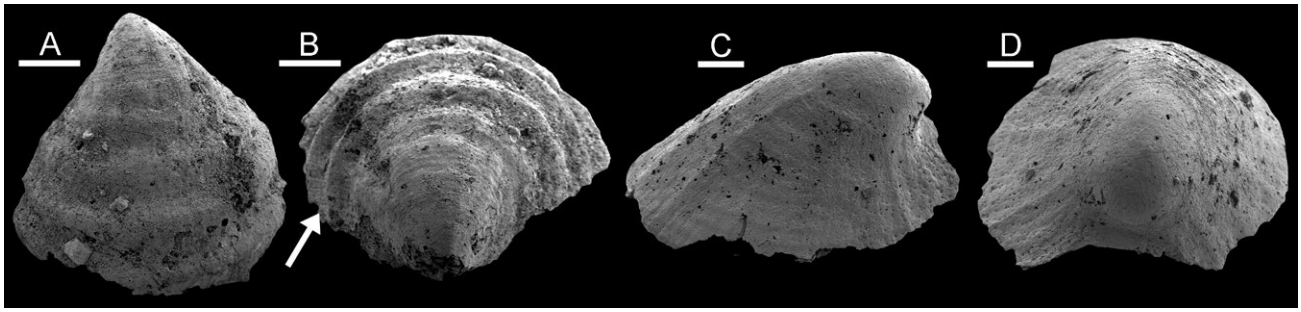

Fig. 11. Helcionelloids from GGU sample 218831, Henson Gletscher Formation, southern Lauge Koch Land, Miaolingian Series, Wuliuan Stage. **A, B:** *Helcionella*? sp., PMU 39209, dorsal (A) and apico-dorsal (B) views. **C, D:** *Sermeqiconus polaris* (Peel, 2021d), PMU 39210, internal mould in oblique lateral (C) and apico-dorsal (D) views. Scale bars: 300 μm (A, B), 100 μm (C, D).

Diagnosis. Isostrophic, laterally compressed to oval, erect, coiled through about one quarter of a whorl, with the blunt apex lying close to the sub-apical margin, slightly overhanging the concave (in lateral view) sub-apical wall of the internal mould. Apertural margin shallowly convex in lateral view, forming a shallow median fold and emargination below the apex. Internal mould surface may develop weakly expressed comarginal rugae and constrictions.

Discussion. Vendrasco *et al.* (2010) assigned this form to *Figurina*, originally described from the Parara Formation of the Stansbury Basin of South Australia (Cambrian Series 2, Stage 4), on the basis of material from the Gowers Formation (Drumian) of the Georgina Basin. *Figurina* differs in its lower shell in which the pointed apex of the internal mould is hooked, overhanging the sub-apical margin. In *Vendrascospira* the crest of the bluntly rounded apex lies at about one quarter of the distance from the sub-apical margin to the supra-apical margin, lying within the shell periphery in dorsal view (Fig. 11A,K).

In terms of its erect and compressed shell form, *Vendrascospira* resembles some species of *Davidonia* Parkhaev, 2017, proposed as a replacement name for the pre-occupied *Mackinnonia* Runnegar *in* Bengtson *et al*., 1990 (see discussion in Peel 2021d, p. 26). While the outer surface of *Davidonia* is smooth, the internal surface is marked by prominent comarginal ridges that produce corresponding channels on the internal mould (Bengtson *et al.* 1990, fig. 159; Skovsted 2004, fig. 3). Such channels are not present in *Vendrascospira*, although the holotype of the type species, *Vendrascospira troelseni* gen. and sp. nov., preserves a low comarginal ruga near the apex (Fig. 11C). *Capitoconus* Skovsted, 2004, originally described from the Bastion Formation (Cambrian Series 2, Stage 4) of North-East Greenland, differs in possessing a swollen early growth stage delimited from the rest of the internal mould by a broad, shallow, constriction. Additionally, while the outer surface of *Capitoconus* varies from ribbed to smooth, the internal mould is ornamented by comarginal rugae.

***Vendrascospira troelseni* gen. et sp. nov.**
Fig. 12A–C, E, F

Holotype. PMU 39211 from GGU sample 271492, internal mould, Lauge Koch Land, Henson Gletscher Formation, Cambrian, Miaolingian Series, Wuliuan Stage.

Other figured material. PMU 39212 from GGU sample 271492, paratype.

Derivation of name. For Johannes C. Troelsen, who first collected Cambrian fossils from southern Peary Land during the 1940s (Peel *et al.* 1974).

Diagnosis. As for genus, but laterally compressed, with aperture almost twice width (Fig. 12E).

Description. The isostrophically coiled shell is laterally compressed, erect, and coiled through about one quarter of a whorl. The apex of the internal mould is bluntly rounded and lies closer to the sub-apical margin, slightly overhanging the concave (in lateral view) sub-apical wall (Fig. 12A). In lateral view, the apertural margin is shallowly convex forming a shallow median fold and emargination below the apex (Fig. 12D,G). Weakly expressed comarginal rugae and constrictions may be present near the apex of the internal mould (Fig. 12C), the surface of which is covered, except for the apical area, with fine pits (Fig. 12D,F). Characters of the external surface are not known.

Discussion. *Vendrascospira troelseni* occurs only rarely in GGU sample 271492. MacKinnon (1985) grouped several similarly coiled shells from the Tasman Formation (Guzhangian Stage) of New Zealand into *Helcionella* sp. Three smooth specimens (MacKinnon 1985, fig. E–L) are similar to *Vendrascospira* in terms of height and the bluntly rounded apex, but MacKinnon (1985) stated that larger specimens developed transverse rugae. Such rugae are have not been seen in the North Greenland material. MacKinnon (1985) commented that the surface of his material was finely tuberculate but the North Greenland material (excluding the smooth initial growth stage) of the holotype and all the marginal areas of the paratype (Fig 11D, G–I) is finely pitted.

The apex in internal moulds of *Davidonia taconica* (Landing & Bartowski, 1996), as illustrated by Peel (2021d) from the Aftenstjernesø Formation (Cambrian Series 2, Stage 4) of northern Lauge Koch Land, barely protrudes beyond the line of the straight sub-apical wall, in contrast to *Vendrascospira troelseni*. Additionally, comarginal channels are well-developed distally, although typically absent in *Vendrascospira troelseni*. Specimens of *Davidonia taconica* illustrated by Skovsted (2004) from the Bastion Formation of North-East Greenland, and by Landing & Bartowski (1996) from the Browns Pond Formation of New York State, have a more steeply inclined supra-apical surface and more strongly developed channeling of the surface of the internal mould than the specimens from northern Lauge Koch Land (Peel 2021c).

Vendrascospira troelseni resembles *Parailsanella sayutinae* Parkhaev, 2004 from the Bystraya Formation (Botoman Stage; Cambrian Series 2, Stage 4) of the Transbaikal region (Parkhaev 2004), but has a more

rounded apex and lacks comarginal rugae. Specimens referred to *Mellopegma uslonica* Parkaev, 2004 from the Botoman part of the Emyaksin Formation have a pointed apex and greater lateral compression (Kouchinsky *et al.* 2015). The latter specimens, and specimens illustrated by Vendrasco *et al.* (2011) are taller and with a more overhanging apex than the elongate specimens described by Parkhaev (2004) from the Bystraya Formation.

***Vendrascospira frykmani* gen. et sp. nov.**
Fig. 10I–L

Holotype. PMU 39208 from GGU sample 271492, internal mould, Lauge Koch Land, Henson Gletscher Formation, Cambrian, Miaolingian Series, Wuliuan Stage.

Derivation of name. For Peter Frykman, with thanks for his companionship in the field and help in the collection of material.

Diagnosis. Species of *Vendrascospira* with width of oval aperture about four fifths of length.

Description. The isostrophical shell is oval in plan view, with width about four fifths of length, and coiled through about a quarter of a whorl. The apex of the internal mould is bluntly rounded and lies close to the sub-apical margin (Fig. 10J). The surface of internal mould lacks comarginal rugae and is finely pitted (Fig. 10L). The apex displays an irregular pattern of closely spaced, low tubercles. Characters of the shell exterior are not known.

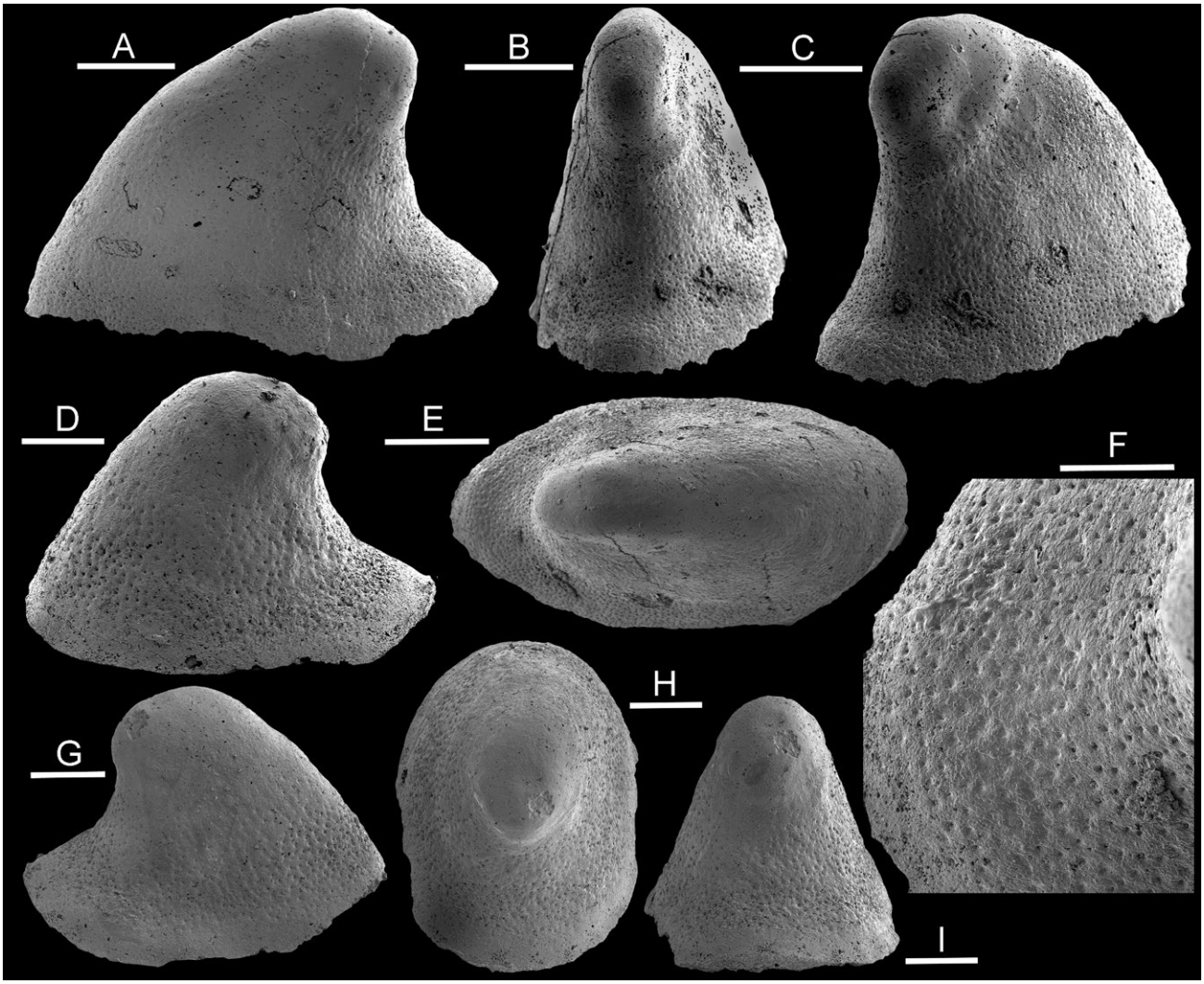

Fig. 12. *Vendrascospira troelseni* gen. et sp. nov., from GGU sample 271492, internal moulds, upper Henson Gletscher Formation, southern Lauge Koch Land, Miaolingian Series, Wuliuan Stage. **A–C, E, F:** PMU 39211, holotype in lateral (A), sub-apical (B), oblique lateral (C) and dorsal (E) views, with detail of sub-apical margin (F). **D, G–I:** PMU 39212, paratype in lateral (D, G) and sub-apical (H, I) views. Scale bars: 200μm (A–C, E), 100 μm (D, G–I), 50 μm (F).

Discussion. The apertural margin is not preserved in the single specimen of *Vendrascospira frykmani* from GGU sample 271492. It is distinguished from *Vendrascospira troelseni* by its less laterally compressed form and oval aperture in plan view (compare Fig. 10J with Fig. 12E). The conspicuous pattern of low tubercles on the apical area of *Vendrascospira frykmani* (Fig. 10I,J) is very weakly developed in the paratype of *Vendrascospira troelseni* (Fig. 12D).

Family Stenothecidae Runnegar & Jell, 1976

Genus *Mellopegma* Runnegar & Jell, 1976

Type species. *Mellopegma georginense* (= *georginensis*) Runnegar & Jell, 1976, Currant Bush Limestone (reassigned in part to the Gowers Formation (Miaolingian Series, Drumian Stage) of Queensland; see discussion in Vendrasco *et al.* 2010).

Discussion. *Mellopegma* was first noted from North Greenland by Peel (1986) from the Ekspedition Bræ Formation (Drumian Stage; Fig. 1C) and subsequently described from the Henson Gletscher Formation (Cambrian Series 2, Stage 4) by Peel *et al.* (2016). A detailed review of the systematics, shell structure and ecology of *Mellopgema* species was given by Vendrasco *et al.* (2011).

***Mellopegma schizocheras* Vendrasco, Kouchinsky, Porter & Fernandez, 2011**
Fig. 14A–F, H–J, M–O

2010 *Mellopegma schizocheras* Vendrasco, Kouchinsky, Porter & Fernandez, 2011, p. 9, figs 7.1–7.2, 8–9.

Figured material. PMU 39219 – PMU 39225 from GGU sample 271492, southern Lauge Koch Land.

Other material. More than 100 specimens from GGU sample 271492; uncommon in GGU sample 271718.

Description. Isostrophic, elongate, laterally compressed, with faint, variable, comarginal rugae on the internal mould that are obscure near the sub-apical and supra-apical margins and across the dorsum. Apex of internal mould bluntly rounded in lateral view (Fig. 14M), slightly bulbous in dorsal view (Fig. 14A,D), although it may seem sharp due to an apical tubercle (Fig. 14E,I). Supra-apical surface uniformly convex in lateral view with the concave sub-apical surface extended distally, becoming almost parallel with the dorsum (Fig. 14C,H). The convex apertural margin, in lateral view, may account for half of the total height (Fig. 14H,J,M). In apertural view, the aperture narrows medially (Fig. 14N) such that lateral areas of the shell may be slightly concave (Fig. 14J).

Tubercles are variably distributed over much of the surface of internal moulds, sometimes in comarginal bands (Fig. 14H), but typically they are most common along the sub-apical and supra-apical margins, including the apex (Fig. 14D), and along the rugae. Between tubercles, the internal mould surface is usually smooth, but it may be locally pitted (Fig. 14J) or with very fine papillae or ridges (Fig. 14C).

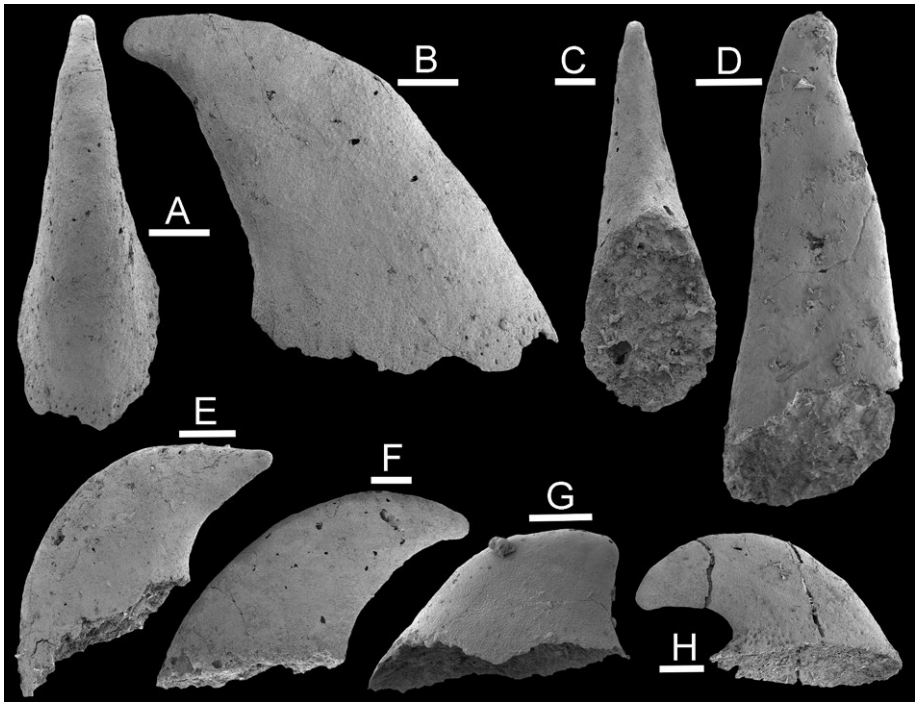

Fig. 13. Helcionellids, internal moulds from the Henson Gletscher Formation, Miaolingian Series, Wuliuan Stage. GGU sample 271718 (Løndal) unless stated. **A–C, E–H:** helcionellids spp. indet. **A, B:** PMU 39213, dorsal (A) and lateral (B) views. **C, F:** PMU 39214, sub-apical (C) and lateral views. **E:** PMU 39215, lateral view. **G:** PMU 39216 from GGU sample 271492, southern Lauge Koch Land, lateral view. **H:** PMU 39217, lateral view. **D:** '*Obtusoconus*' sp., PMU 39218, lateral view showing sigmoidal form. Scale bars: 200 μm except G (300 μm).

Discussion. Vendrasco *et al.* (2011) noted that *Mellopegma schizocheras* and the type species *Mellopegma georginense* Runnegar & Jell, 1976 occurred together in the Gowers Formation but ruled out that they were ontogenetic variants of the same species or sexual dimorphs. Evidence of lamellar shell structures rep-

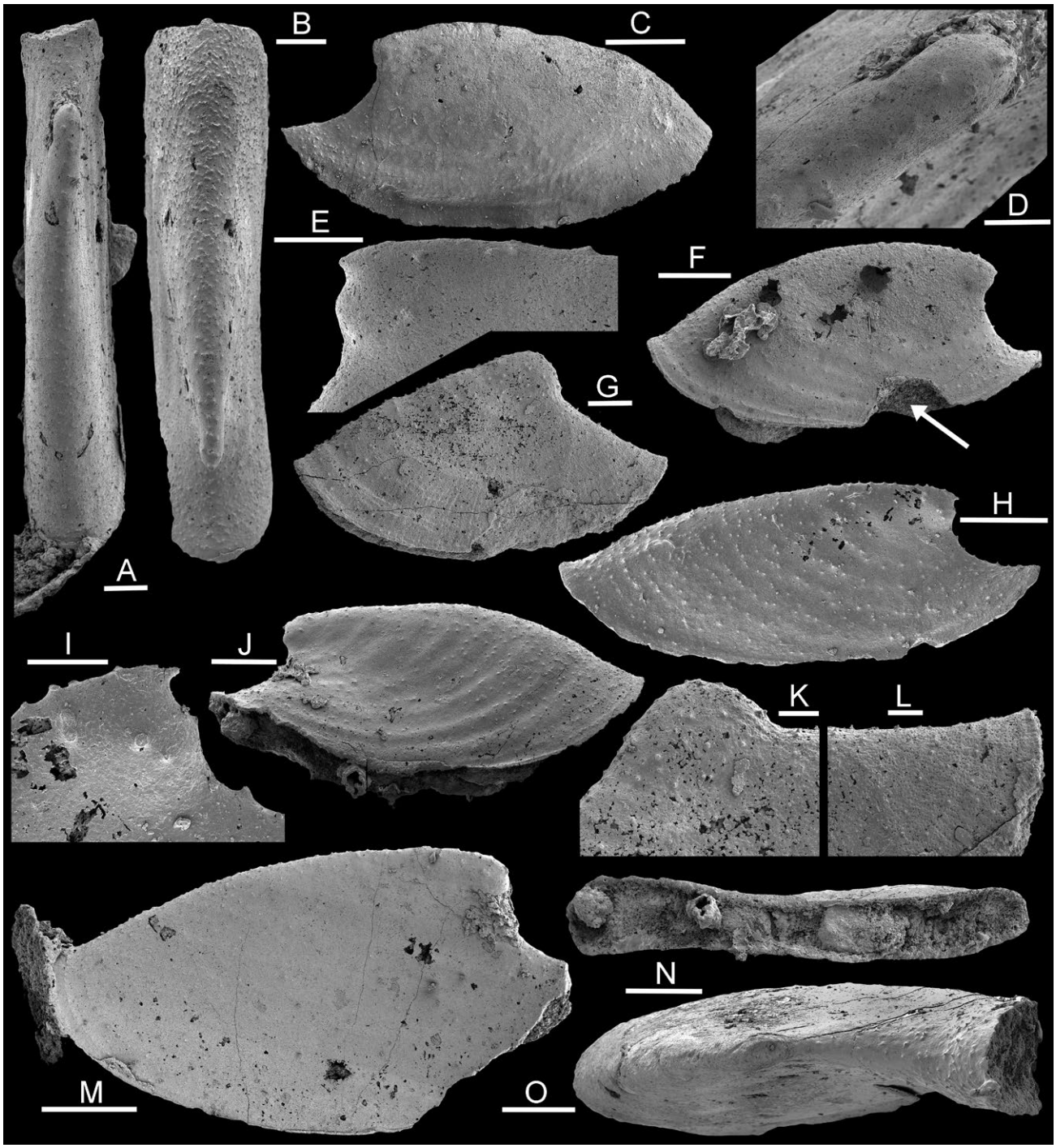

Fig. 14. *Mellopegma*, internal moulds from GGU sample 271492, southern Lauge Koch Land, upper Henson Gletscher Formation, Miaolingian Series, Wuliuan Stage. **A–F, H–J, M–O:** *Mellopegma schizocheras* Vendrasco, Kouchinsky, Porter & Fernandez, 2011. **A, D, M:** PMU 39219, dorsal (A) and lateral (M) views, with detail of apex (D). **B:** PMU 39220, dorsal view. **C, O:** PMU 39221, lateral (C) and oblique dorsal (O) views. **E:** PMU 39222, apex in lateral view. **F:** PMU 39223, lateral view with pre-fossilization fracture in apertural margin (arrow). **H, I:** PMU 39224, lateral view (H) with detail of apex (I). **J, N:** PMU 39225, lateral (J) and apertural view (N). **G, K, L:** *Mellopegma* sp., PMU 39226, lateral view (G) with details of apex (K) and sub-apical margin (L). Scale bars: 200 μm (C, F, H, J, M, N), 100 μm (A, B, G, O), 50 μm (D, E, I, K, L).

licated in the surface of internal moulds is generally absent, although a rudimentary pattern may occur locally (Fig. 14I). Vendrasco *et al*. (2011) described a polygonal network reflecting the imprint of prismatic shell structure in the sub-apical and distal supra-apical areas of internal moulds of *Mellopegma schizocheras*. Such structures are rarely visible in available material, where the surface is often very finely papillate.

Vendrasco *et al*. (2011) summarized observations by Kouchinsky (2000a), Parkhaev (2006) and Feng & Sun (2006) concerning tubercles rising perpendicular from the surface of the internal moulds in helcionelloids that were interpreted as pores entering into, or passing through, the shell. Comparable tubercles are widely and variably distributed in specimens of *Mellopegma schizocheras* from GGU sample 271492. They are often prominent on the apical area (Fig. 14B,E,I) and the sub-apical and supra-apical margins (Fig. 14J,O), but some specimens show tubercles in comarginal rows (Fig. 14H). Individual tubercles are usually conical in shape, with rounded apices, but some are truncated suggesting termination at a shell surface (Fig. 14I).

***Mellopegma* cf. *georginense* Runnegar & Jell, 1976**
Figs 15A

Figured specimens. PMU 39227 from GGU sample 271718, Løndal.

Discussion. *Mellopegma georginense* was originally described by Runnegar & Jell (1976) from the Currant Bush Limestone of Queensland (reassigned in part to the Gowers Formation, Drumian Stage, by Vendrasco *et al*. 2010). It is distinguished from *Mellopegma schizocheras*, with which it occurs in the Gowers Formation (Vendrasco *et al*. 2010), by its more prominent comarginal rugae that are continuous around the shell margins and across the dorsum (Fig. 15A), as is the case in an apical fragment illustrated by Peel *et al*. (2016, fig. 13N) from older strata of the Henson Gletscher Formation in Løndal (Cambrian Series 2, Stage 4, *Ovatoryctocara granulata* beds). The single large specimen from GGU sample 271718 placed here preserves fine radial ridges on the supra-apical surface close to the apex (Fig. 15A, arrow) and a coarse, tuberculate, prismatic pattern in more distal areas.

Specimens from late Cambrian Stage 4 strata at Ville Guay, Québec, assigned to *Mellopegma georginense* by Landing *et al*. (2002, fig. 8.1, 8.2), are closely similar to the earliest growth stage of the Henson Gletscher Formation specimen (Fig. 15A). The much greater length and curved ventral profile of the latter specimen reflects its later ontogenetic stage. Caron *et al*. (2014, supplementary fig. 6r) illustrated a single specimen from the Burgess Shale Formation of Canada that is also comparable in shape to the early growth stages of the specimen from the Henson Gletscher Formation (Fig. 15A), although the comarginal rugae are less strongly expressed in the latter internal mould.

***Mellopegma chelata* (Skovsted, 2006b)**
Fig. 15B–D

2006b *Anabarella chelata* Skovsted, p. 489, fig. 2A–E.

Figured material. PMU 39228 from GGU sample 271718, Løndal.

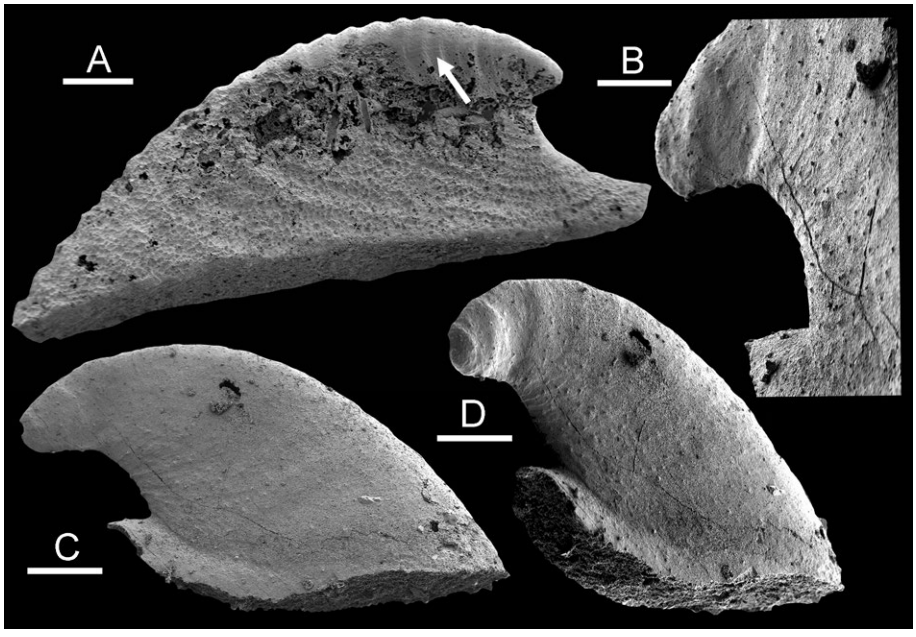

Fig. 15. *Mellopegma*, internal moulds from GGU sample 271718, Løndal, upper Henson Gletscher Formation, Miaolingian Series, Wuliuan Stage. **A:** *Mellopegma* cf. *georginense* Runnegar & Jell, 1976, PMU 39227, lateral view. **B–D:** *Mellopegma chelata* (Skovsted, 2006b), PMU 39228 from GGU sample 271718, in lateral (C) and apico-lateral (D) views, with detail of sub-apical surface (B). Scale bars: 300 μm (A), 100 μm (C, D), 50 μm (B).

Discussion. *Mellopegma chelata* from the basal Emigrant Formation of Nevada (Cambrian Series 2, Stage 4; upper Dyeran) resembles *Mellopegma simesi* (MacKinnon, 1985), originally described from the Tasman Formation (Guzhangian Stage) of New Zealand (MacKinnon 1985), but has a much lower shell in lateral aspect (Fig. 15C). Specimens of *Mellopegma simesi* illustrated from New Zealand by MacKinnon (1985), from Queensland by Vendrasco *et al.* (2011) and by Peel *et al.* (2016), the latter from the Henson Gletscher Formation (Cambrian Series, Stage 4) in Løndal, show greater convexity of the supra-apical surface in lateral view and have a hooked apex.

The single internal mould from GGU sample 271718 displays an incipient pegma at the angular junction between the sub-apical surface and the protruding sinuate marginal field (Fig. 15C, D). A shallow comarginal channel, representing a thickening of the shell interior, extends from the deepest point of this pegma towards the distal supra-apical margin. Constrictions and rugae on the apical area suggest periodic flaring of the aperture in the juvenile shell. Fine tubercles and traces of comarginal growth lines are present on the subapical surface.

***Mellopegma* sp.**
Fig. 14G, K, L

Figured material. PMU 39226 from GGU sample 271492, Lauge Koch Land.

Discussion. The rounded apex of several specimens from GGU sample 271492 forms the highest point on the dorsal surface (Fig. 14G), unlike the dominant, co-occurring specimens of *Mellopegma schizocheras* (Fig. 14C,H,J), and may suggest comparison to *Stenotheca* Salter *in* Hicks, 1872, although the type species of that genus is poorly known (Vendrasco *et al.* 2011). However, the tubercles and fine pits on the internal mould favour assignment to *Mellopegma*. The supra-apical and sub-apical slopes are flattened, and almost equal in inclination when viewed in lateral aspect (Fig. 14G). In addition to tubercles and the finely pitted intervening surface (Fig. 14G,K,L), these specimens show radial ridges and traces of acute, but wrinkled, comarginal growth lines that may reflect the periostracum. Similar radial ridges and growth lines were illustrated by Vendrasco *et al.* (2011, fig. 5.15, 5.18).

Family uncertain

Genus *Erugoconus* gen. nov.

Type species. *Erugoconus acuminatus* gen. et sp. nov., from the Henson Gletscher Formation of North Greenland. Cambrian, Miaolingian Series, Wuliuan Stage.

Derivation of name. From the Latin 'erugo' meaning without wrinkles, relating to the smooth shell.

Diagnosis. Isostrophic, slowly expanding cone coiled through slightly more than one quarter of a whorl. Laterally compressed, with width of the oval aperture about two thirds of its length. Protoconch small on internal mould, bulbous. Early growth stages slender and only slightly coiled, considerably overhanging the sub-apical margin. External surface seemingly smooth. Internal surface smooth, without comarginal rugae. Internal mould with a pair of deep channels on the sub-apical surface in late growth stages.

Discussion. The low rate of whorl expansion and rapid divergence of the logarithmic spiral of the shell in *Erugoconus* produce a widely open-coiled shell in which the apex strongly overhangs the subapical margin. Early growth stages have a tall, almost conical form but curvature increases with passage into the latest growth stage. In this respect, *Erugoconus* is clearly distinct from the tightly coiled hyolith *Protowenella* with which it occurs (Peel 2021a; Fig. 5A–D).

In lateral view, *Erugoconus* is similar in curvature to specimens from the Tommotian regional stage (Cambrian Stage 2) of the Siberian Platform assigned to *Ceratoconus* Chen & Zhang, 1980 by Missarzhevsky (1989), Rozanov *et al.* (2010) and Kouchinsky *et al.* (2017), but these are more strongly curved than the tall Chinese specimens illustrated by Chen & Zhang (1980, pl. 1, figs 29–32). However, the shell of *Ceratoconus* is more slowly expanding and less laterally compressed than *Erugoconus*. *Ceratoconus* Chen & Zhang, 1980 is a junior homonym of *Ceratoconus* Borgmeier, 1928, a parasitic dipteran from South America (Borgmeier 1928; Brown *et al.* 2017). *Masculuconus* Feng, Sun & Qian, 2000 from the Meishucunian (Cambrian Stage 2) of Yunnan, China, has similar curvature to Chinese specimens of *Ceratoconus* but differs by its greater rate of shell expansion and transversely elliptical aperture; it is much less strongly coiled than *Erugoconus*.

Mellopegma simesi (MacKinnon, 1985), as illustrated by Peel *et al.* (2016, fig. 14D–G) from the Henson Gletscher Formation (Cambrian Stage 4) in Løndal, has an extended and slender early growth stage overhanging the sub-apical margin, as in *Erugoconus acuminatus*, but differs in the proportionally longer and narrower aperture and incipient pegma.

Genus incertum et species incerta B of Geyer (1986, pl. 3, fig. 45) from Morocco displays similar curvature to *Erugoconus*, with a strongly overhanging apex, but the exterior is ornamented with rugae that are also present in a subdued form on the internal mould.

***Erugoconus acuminatus* gen. et sp. nov.**
Fig. 16E–N

Derivation of name. From the Latin 'acuminatus' referring to the pointed apex.

Holotype. PMU 39232 from GGU sample 271718, Henson Gletscher Formation, Løndal, western Peary Land, North Greenland. Cambrian, Miaolingian Series, Wuliuan Stage.

Other figured material. PMU 39230, PMU 39231, PMU 39233 – PMU 39235, paratypes, from GGU sample 271718.

Diagnosis. As for genus.

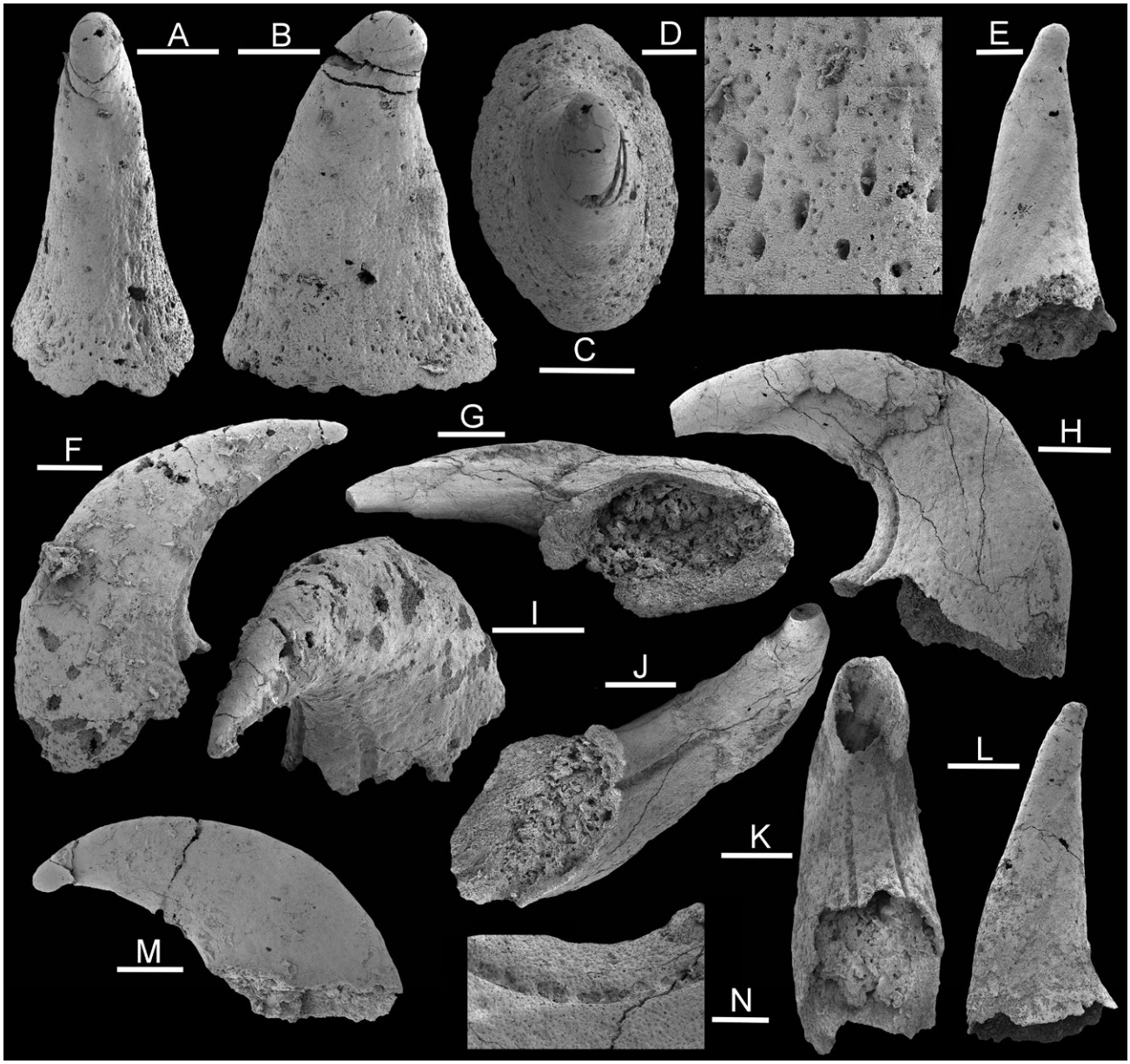

Fig. 16. Helcionellids, internal moulds from the Henson Gletscher Formation, Miaolingian Series, Wuliuan Stage. GGU sample 271718, Løndal. **A–D:** *Tavseniconus erectus* gen. et sp. nov., PMU 39229, holotype, in sub-apical (A), lateral (B) and apical (C) views, with detail of pitted surface (D). **E–N:** *Erugoconus acuminatus* gen. et sp. nov. **E:** PMU 39230, lateral view of early growth stage. **F, I:** PMU 39231, lateral (F) and oblique lateral view with sub-apical grooves (I). **G, H, J, N:** PMU 39232, holotype, in apertural (G), lateral (H) and oblique sub-apical (J) views, with detail of sub-apical groove (N). **K:** PMU 39233, sub-apical view showing grooves. **L:** PMU 39234, lateral view of early growth stage. **M:** PMU 39235, lateral view. Scale bars: 400 μm (F–M), 200 μm (A–C, E), 100 μm (N), 20 μm (D).

Description. Isostrophic, with the slowly expanding cone coiled through slightly more than one quarter of a whorl. Laterally compressed, with width of the oval aperture about two thirds of its length. The protoconch as preserved on internal mould is small and slightly inflated, with a shallow constriction separating it from the following growth stage (Fig. 16E). Early growth stage is slender and with only slight curvature, but the early part of the shell considerably overhangs the sub-apical margin by a distance exceeding the length of the aperture in available material (Fig. 16F,H,M). The external surface is seemingly smooth, as is the internal mould, without comarginal rugae. A pair of deep channels is present on the sub-apical surface of the internal mould in late growth stages. Surface of internal mould with abundant closely spaced fine pits in later growth stages. Larger pits close to the apertural margin on the internal mould, are directed obliquely in and towards the aperture (Fig. 16H).

Discussion. *Erugoconus acuminatus* is very common in GGU sample 271718. The slender early growth stage may develop a slight angulation on the sub-apical surface as it passes into the later shell (Fig. 16L). In its form it is reminiscent of tall specimens described as *Obtusoconus foliaceus* MacKinnon, 1985 from the Tasman Formation (Guzhangian Stage) of New Zealand, which Parkhaev (2001b) referred to *Anuliconus* Parkhaev, 2001b, although these show substantial variation in the rate of expansion and curvature of the shell cone when compared to the early stages of the holotype of *Erugoconus acuminatus*. Most of MacKinnon's (1985) specimens have a lamellose external ornamentation or pronounced comarginal rugae (MacKinnon 1985, fig. 2) not known in available material from Greenland.

Genus novum et species nova? G of Geyer (1986, pl. 2, fig. 27) from the Wuliuan part of the Jbel Wawrmast Formation of the Lemdad Syncline of Morocco, has a longer shell in lateral aspect than the early growth stage of *Erugoconus acuminatus*. It is here assigned to *Tavseniconus* gen. nov. *Tavseniconus erectus* gen. et sp. nov., from GGU sample 271718 differs from the early stages of *Erugoconus acuminatus* in its greater length in lateral view and more rounded apical termination (Fig. 16A–D).

Genus *Tavseniconus* gen. nov.

Type species. *Tavseniconus erectus* gen. et sp. nov., from the Henson Gletscher Formation of North Greenland. Cambrian, Miaolingian Series, Wuliuan Stage.

Derivation of name. From Hans Tavsen Iskappe, the prominent ice field lying north-west of the type locality in Løndal (Fig. 1A).

Diagnosis. Isostrophic, tall, laterally compressed helcionelloid with a sub-conical shell; the rounded apex slightly overhanging the sub-apical surface.

Discussion. Genus novum et species nova? G of Geyer (1986, pl. 2, fig. 27), a mainly exfoliated internal mould about 3 mm tall from the lower part (of Wuliuan age) of the Lemdad Syncline) of the High Atlas, Morocco, has a closely similar shell form and can be assigned to *Tavseniconus*.

***Tavseniconus erectus* gen. et sp. nov.**
Fig. 16A–D

Holotype. PMU 39229 from GGU sample 271718, internal mould, Løndal, Henson Gletscher Formation, western Peary Land, North Greenland. Cambrian, Miaolingian Series, Wuliuan Stage.

Derivation of name. With reference to the upright form.

Diagnosis. As for genus.

Description. The upright, tall, slowly expanding isostrophic shell is slightly curved, such that the rounded apex of the internal mould slightly overhangs the sub-apical surface, but not the sub-apical margin. Length is about two thirds of height in lateral view (Fig. 16B). In plan view, apertural width is about two thirds of length (Fig. 16C). The surface of the internal mould is covered by fine pits except around the smooth apex. Larger, deeper pits close to the apertural margin slope obliquely inwards and down towards the aperture. External ornamentation not known.

Discussion. As with many other internal moulds from GGU sample 271718, the holotype internal mould of *Tavseniconus erectus* has a smooth apical area while the flanks are covered by closely spaced fine pits (Fig. 16A–D). Scattered, larger pits located close to the preserved apertural margin slope obliquely in and down towards the apertural plane (Fig. 16D), a pattern also seen in *Erugoconus acuminatus* gen. et sp. nov. (Fig. 16H).

The specimen illustrated by Geyer (1986, pl. 2, fig. 27) as Genus novum et species nova? G, from the Lemdad Syncline of Morocco, is here referred to *Tavseniconus*. In lateral perspective, it has a longer shell (height:length ratio of 1.2) than the holotype of *Tavseniconus erectus* (1.4).

Genus *Obtusoconus* Yu, 1979

Type species. *Obtusoconus paucicistatus* Yu, 1979 from the early Cambrian of Hubei, China.

'*Obtusoconus*' sp.
Fig. 13D

Figured material. PMU 39218 from GGU sample 271718, Løndal.

Discussion. In addition to the type species and other species illustrated by Yu (1979), several early Cambrian species were referred to *Obtusoconus* by Esakova & Zhegallo (1996) and Vasileva (1990). The single slender internal mould with an oval cross-section from GGU sample 271718 retains the slightly sigmoidal form characteristic of *Obtusoconus*, but no trace of the prominent comarginal ornamentation is seen in most described species. The swollen protoconch overlies a shallowly convex sub-apical surface, while the supra-apical surface is initially convex before becoming shallowly concave (Fig. 13D). However, assignment of the Greenland specimen to '*Obtusoconus*' is just a matter of convenience. It is not inconceivable that it represents the early growth stage of a species of *Erugoconus* gen. nov., although the sigmoidal form is not seen in *Erugoconus acuminatus*.

Tavseniconus erectus has a similar overall shape to '*Obtusoconus*' sp. but its shell has a greater rate of whorl expansion in lateral perspective (Fig. 16B). The pits in the surface of the internal mould of *Tavseniconus erectus* (Fig. 16D) have not been observed in '*Obtusoconus*' sp. (Fig. 13D).

Obtusoconus foliaceus MacKinnon, 1985 from the Tasman Formation (Guzhangian Stage) of New Zealand, shows substantial variation in the rate of expansion and curvature of the shell. Parkhaev (2001b) referred *Obtusoconus foliaceus* to *Anuliconus* but this assignment is rejected. Most of MacKinnon's (1986, fig. 2) illustrated specimens resemble *Tavseniconus*, but one shows a slightly sigmoidal, but more rapidly expanding shell than '*Obtusoconus*' sp. (MacKinnon 1985, fig. 2B).

Acknowledgements

Fieldwork was undertaken as part of the North Greenland Project (1978–80) organised by the Geological Survey of Greenland (GGU). Stratigraphic section logs (Fig. 2) were measured and kindly made available by Jon R. Ineson. Gerd Geyer supplied information concerning the stratigraphic distribution of Moroccan helcionelloids. Yue Liang kindly provided Chinese literature. Gerd Geyer and an anonymous reviewer are thanked for comments on the manuscript.

References

Ahlberg, P., Axheimer, N. & Robison, R.A. 2007: Taxonomy of *Ptychagnostus atavus*: A key trilobite in defining a global Cambrian stage boundary. Geobios 40, 709–714. https://doi.org/10.1016/j.geobios.2007.01.004

Aksarina, N.A. 1968: Probivalvia–novyy klass drevneyshikh mollyuskov. In: Selyatitskiy, G.A. (ed.), Novye dannye po geologii i poleznym iskopaemym Zapadnoy Sibiri, 77–86. Tomsk University Press, Tomsk.

Aksarina, N.A. & Pelman, Yu.L. 1978: Kembriyskie brakhiopodi i dvustvorchati mollyuski Sibiri. Akademiya Nauk SSSR, Sibirskoe otdelenie, Trudy Instituta Geologii i Geofiziki 362, 180 pp.

Atkins, C.J. & Peel, J.S. 2004: New species of *Yochelcionella* (Mollusca; Helcionelloida) from the Lower Cambrian of North Greenland. Bulletin, Geological Society of Denmark 51, 1–9. https://doi.org/10.37570/bgsd-2004-51-01

Atkins, C.J. & Peel, J.S. 2008: *Yochelcionella* (Mollusca, Helcionelloida) from the lower Cambrian of North America. Bulletin of Geosciences 83, 23–38. https://doi.org/10.3140/bull.geosci.2008.01.023

Bengtson, S., Conway Morris, S., Cooper, B.J., Jell, P.A. & Runnegar, B.N. 1990: Early Cambrian fossils from South Australia. Association of Australasian Palaeontologists Memoir 9, 364 pp.

Berg-Madsen, V. & Peel, J.S. 1978: Middle Cambrian monoplacophorans from Bornholm and Australia, and the systematic position of the bellerophontiform molluscs. Lethaia 11, 113–125. https://doi.org/10.1111/j.1502-3931.1978.tb01295.x

Billings, E. 1872: On some new species of Palaeozoic fossils. The Canadian Naturalist 6, 213–222.

Blaker, M.R. & Peel, J.S. 1997: Lower Cambrian trilobites from North Greenland. Meddelelser om Grønland, Geoscience 35, 145 pp. https://doi.org/10.1017/s0016756898258432

Borgmeier, T. 1928: Investigações sobre Phorideos Myrecophilus (Diptera, Phoridae) Arquivos do Instituto Biológico, Sao Paulo, 1928, 1, 159–192.

Brock, G.A. 1998: Middle Cambrian molluscs from the southern New England Fold Belt, New South Wales, Australia. Geobios 31, 571–586. https://doi.org/10.1016/s0016-6995(98)80045-4

Brown, B.V., Hash, J.M., Hartop, E.A., Porras, W. & Amorim, D. de S. 2017: Baby killers: documentation and evolution of scuttle fly (*Diptera*: *Phoridae*) parasitism of ant (*Hymenoptera*: *Formicidae*) brood. Biodiversity Data Journal 2017, 5, e11277, https://doi.org/10.3897/bdj.5.e11277

Caron, J.B., Gaines, R.R., Aria, C., Mángano, M.G. & Streng, M. 2014: A new phyllopod bed-like assemblage from the Burgess Shale of the Canadian Rockies. Nature communications. https://doi.org/10.1038/ncomms4210

Chen, P. & Zhang, F. 1980: Small shell fossil assemblage from the Meishucunian Stage of Yunnan. Wuhan College of Geological Studies 26, 190–197.

Clausen, S. & Peel, J.S. 2012: Middle Cambrian echinoderm remains from the Henson Gletscher Formation of North

Greenland. GFF 134, 173–200. https://doi.org/10.1080/11035897.2012.721003

Cobbold, E.S. 1921: The Cambrian horizons of Comley (Shropshire) and their Brachiopoda, Pteropoda, Gasteropoda, etc. The Quarterly Journal of the Geological Society of London 76, 325–386. https://doi.org/10.1144/gsl.jgs.1920.076.01-04.10

Conway Morris, S. & Peel, J.S. 2013: A new helcionelloid mollusk from the middle Cambrian Burgess Shale, Canada. Journal of Paleontology 87, 1067–1070. https://doi.org/10.1666/13-050

Cushman, J.A. 1910: A monograph of the Foraminifera of the North Pacific Ocean. Part 1. Astrorhizidae and Lituolidae. Smithsonian Institution, United States National Museum, Bulletin 71, 134 pp. https://doi.org/10.5479/si.03629236.71.i

Cuvier, G. 1797: Tableau élémentaire de l'histoire naturelle des animaux. Baudouin, Paris, 710 pp. https://doi:10.5962/bhl.title.11203

Esakova N.V. & Zhegallo E.A. 1996: Stratigrafiya i fauna nizhnego kembriya Mongolii. Trudy Sovmestnaya Rossiysko-Mongol'skaya paleontologicheskaya ekspeditsiya 46, 213 pp.

Feng, W. & Sun, W. 2006: Monoplacophoran *Igorella* type pore-channel structures from the Lower Cambrian in China. Materials Science and Engineering 26, 699–702. https://doi.org/10.1016/j.msec.2005.09.102

Feng, W., Sun, W. & Qian, Y. 2000: Earliest Cambrian Monoplacophora in northeastern Yunnan with some new genera and species. Acta Micropalaeontologica Sinica 17, 378–397.

Foerste, A.F. 1914: Notes on the Agelacrinidae and Lepadocystinae, with descriptions of *Thresheradiscus* and *Brockocystites*. Bulletin of the Scientific Laboratories of Denison University 17, 399–487.

Frýda, J. 1999: Higher classification of the Paleozoic gastropods inferred from their early shell ontogeny. Journal of the Czech Geological Society 44, 137–153.

Frýda, J., Nützel, A. & Wagner, P.J. 2008: Paleozoic Gastropoda. In: Ponder, W.F. & Lindberg, D.L. (eds), Phylogeny and evolution of the Mollusca, 239–270. University of California Press, Berkeley. https://doi.org/10.1525/california/9780520250925.003.0010

Geyer, G. 1986: Mittelkambrische Mollusken aus Marokko und Spanien. Senckenbergiana lethaea 67, 55–118.

Geyer, G. 1994: Middle Cambrian molluscs from Idaho and early conchiferan evolution. New York State Museum Bulletin 481, 69–86.

Geyer, G. & Peel, J.S. 2011: The Henson Gletscher Formation, North Greenland, and its bearing on the global Cambrian Series 2–Series 3 boundary. Bulletin of Geosciences 86, 465–534. https://doi.org/10.3140/bull.geosci.1252

Geyer, G., Valent, M. & Meier, S. 2019: Helcionelloids, stenothecoids and hyoliths from the Tannenknock Formation (traditional lower middle Stage 4/Wuliuan boundary interval) of the Franconian Forest, Germany. PalZ 93, 207–253. https://doi.org/10.1007/s12542-018-0433-5

Golikov, A.N. & Starobogatov, Y.I. 1975: Systematics of prosobranch gastropods. Malacologia 15, 185–232.

Gittenberger, E. 1994: Adaptations of the aperture in terrestrial gastropod-pulmonate shells. Netherlands Journal of Zoology 46, 191–205. https://doi.org/10.1163/156854295x00159

Grabau, A.W. & Shimer, H.W. 1909: North American index fossils, invertebrates, Volume 1. A.G. Seiler & Company, New York, 853 pp. https://doi.org/10.5962/bhl.title.52120

Grube, A.E. 1850: Die Familien der Anneliden. Archiv für Naturgeschichte 16, 249–364.

Gubanov, A.P. & Peel, J.S. 1998: Redescription of the type species of *Latouchella* Cobbold, 1921 (Mollusca) from the Lower Cambrian of Comley, England. GFF 120, 17–20. https://doi.org/10.1080/11035899801201017

Gubanov, A.P., Kouchinsky, A. & Peel, J.S. 1999: The first evolutionary-adaptive lineage within fossil molluscs. Lethaia 32, 155–157. https://doi.org/10.1111/j.1502-3931.1999.tb00534.x

Gubanov, A., Kouchinsky, A., Peel, J.S. & Bengtson, S. 2004: Middle Cambrian molluscs of 'Australian' aspect from northern Siberia. Alcheringa 28, 1–20. https://doi.org/10.1080/03115510408619272

Hall, J. 1847: Palæontology of New-York; Volume 1; Containing descriptions of the organic remains of the lower division of the New York system (equivalent of the Lower Silurian rocks of Europe). C. Van Benthuysen, New York, 338 pp. https://doi.org/10.5962/bhl.title.32878

Harper, J.A. & Rollins, H.B. 2000: The bellerophont controversy revisited. American Malacological Bulletin 15, 147–156.

Higgins, A.K., Ineson, J.R., Peel, J.S., Surlyk, F. & Sønderholm, M. 1991: Lower Palaeozoic Franklinian Basin of North Greenland. Bulletin Grønlands Geologiske Undersøgelse 160, 71–139. https://doi.org/10.34194/bullggu.v160.6714

Horný, R.J. 1964: The Middle Cambrian Pelagiellacea of Bohemia (Mollusca). Sborník Národniho Muzea v Praze 20B, 133–140.

Hu, Y., Holmer, L.E., Liang, Y., Duan, X. & Zhang, Z. 2021: First report of small shelly fossils from the Cambrian Miaolingian Limestones (Zhangxia and Hsuzhuang Formations) in Yiyang County, Henan Province of North China. Minerals 2021, 11, 1104. https://doi.org/10.3390/min11101104

Ineson, J.R. & Peel, J.S. 1997: Cambrian shelf stratigraphy of North Greenland. Geology of Greenland Survey Bulletin 173, 1–120. https://doi.org/10.34194/ggub.v173.5024

Jacquet, S.M. & Brock, G.A. 2016: Lower Cambrian helcionelloid macromolluscs from South Australia. Gondwana Research 36, 333–358. https://doi.org/10.1016/j.gr.2015.06.012

Johnston, P.A. 2019: Morphology and relationships of Cambrian Stenothecoida. Geological Society of Hubei Province, Academic Exchanges, Academic Reports. http://www.hbsdzxh.com.cn/html/dzxh/news/2019/06/10/1906101439 5911700001.html

Johnston, P.A. & Streng, M. 2021: Morphology and relationships of the enigmatic stenothecoid pan-brachiopod *Stenothecoides*—New data from the middle Cambrian Burgess Shale Formation. Acta Palaeontologica Polonica 66, 723–751.

Knight, J.B. 1941: Paleozoic gastropod genotypes. Geological Society of America, Special Papers 32, 510 pp. https://doi.org/10.1130/spe32-p1

Knight, J.B. 1952: Primitive fossil gastropods and their bearing on gastropod classification. Smithsonian Miscellaneous Collections 117(13), 56 pp.

Knight, J.B., Cox, L.R., Keen, A.M., Batten, R.L., Yochelson, E.L. & Robertson, R. 1960: Systematic descriptions [Archaeogastropoda]. In: Moore, R.C. (ed.), Treatise on Invertebrate Paleontology. Part I, Mollusca 1. *I*169–*I*310. Geological Society of America and University of Kansas Press, Boulder, Colorado and Lawrence, Kansas. https://doi.org/10.17161/dt.v0i0.5585

Koken, E. & Perner, J. 1925: Die Gastropoden des baltischen Untersilurs. Mémoires de l'Académie des Sciences de Russie, 8eme Série, Classe physico-mathématique 37, 326 pp. https://doi.org/10.1017/s0016756800103127

Kouchinsky, A.V. 1999: Shell microstructures of the Early Cambrian *Anabarella* and *Watsonella* as new evidence on the origin of the Rostroconchia. Lethaia 32, 173–180. https://doi.org/10.1111/j.1502-3931.1999.tb00537.x

Kouchinsky, A.V. 2000a: Shell microstructures in Early Cambrian molluscs. Acta Palaeontologica Polonica 45, 119–150.

Kouchinsky, A.V. 2000b: Skeletal microstructures of hyoliths from the Early Cambrian of Siberia. Alcheringa 24, 65–81. https://doi.org/10.1080/03115510008619525

Kouchinsky, A., Bengtson, S., Clausen, S., Gubanov, A., Malinky, J.M. & Peel, J.S. 2011: A Middle Cambrian fauna of skeletal fossils from the Kuonamka Formation, northern Siberia. Alcheringa 35, 123–189. https://doi.org/10.1080/03115518.2010.496529

Kouchinsky, A., Bengtson, S., Clausen, S. &Vendrasco, M. 2015: An early Cambrian fauna of skeletal fossils from the Emyaksin Formation, northern Siberia. Acta Palaeontographica Polonica 60, 421–512. https://doi.org/10.4202/app.2012.0004

Kouchinsky, A., Bengtson, S., Landing, E., Steiner, M., Vendrasco, M. & Ziegler, K. 2017: Terreneuvian stratigraphy and faunas from the Anabar Uplift, Siberia. Acta Palaeontologica Polonica, 62, 331–340. https://doi.org/10.4202/app.00289.2016

Kruse, P.D. 1991: Cambrian fauna of the Top Springs Limestone, Georgina Basin. The Beagle, Records of the Northern Territory Museum of Arts and Sciences 8, 169–188. https://doi.org/10.5962/p.262819

Kruse, P.D. 1998: Cambrian palaeontology of the eastern Wiso and western Georgina Basins. Northern Territory Geological Survey Report 9, 68 pp.

Landing, E. & Bartowski, K.E. 1996: Oldest shelly fossils from the Taconic allochthon and late early Cambrian sea-levels in eastern Laurentia. Journal of Paleontology 70, 741–761. https://doi.org/10.1017/s0022336000023799

Landing, E., Geyer, G. & Bartowski, K.E. 2002: Latest Early Cambrian small shelly fossils, trilobites, and Hatch Hill dysaerobic interval on the Québec continental slope. Journal of Paleontology 76, 287–305. https://doi.org/10.1666/0022-3360(2002)076<0287:lecssf>2.0.co;2

Landing, E., Geyer, G., Jirkov, I.A. & Schiaparelli, S. 2021: Lophotrochozoa in the Cambrian evolutionary radiation and the *Pelagiella* problem. Papers in Palaeontology 7, 2227–2244. https://doi.org/10.1002/spp2.1396

Li, L., Zhang, X., Yun, H. & Li , G. 2017: Complex hierarchical microstructures of Cambrian mollusk *Pelagiella*: insight into early biomineralization and evolution. Scientific Reports 7, 1935. https://doi.org/10.1038/s41598-017-02235-9

Li, L., Zhang, X., Skovsted, C.B., Yun, H., Pan, B. & Li, G. 2021: Revisiting the molluscan fauna from the Cambrian (series 2, stages 3–4) Xinji Formation of North China. Papers in Palaeontology 7, 521–564. https://doi.org/10.1002/spp2.1289

Lindström, G. 1880: Fragmenta Silurica e dono Caroli Henrici Wegelin. Samson & Wallin, Stockholm, 60 pp. https://doi.org/10.5962/bhl.title.63278

Linnaeus, C. 1758: Systema naturae per regna tria naturae, 10th Edition. Laurentii Salvii, Stockholm, 824 pp. https://doi.org/10.5962/bhl.title.542. https://doi.org/10.5962/bhl.title.542

Linnarsson, J.G.O. 1869: Om Västergötlands Cambriska och Siluriska aflagringar. Kungliga svensk Vetenskaps-Akademiens Handlingar 8, 89 pp.

Lu, Y.H. 1957: Trilobita. In: Ku, Z.W., Yang, T.Y., Hsu, S.C., Yin, T.H., Yu, C.C., Chao, K.K., Lu, Y.H., & Hou, Y.T. (eds), Index fossils of China, Invertebrates, Part 3, 249–294. Geological Publishing House, Beijing.

MacKinnon, D.I. 1985: New Zealand late Middle Cambrian molluscs and the origin of Rostroconchia and Bivalvia. Alcheringa 9, 65–81. https://doi.org/10.1080/03115518508618959

Malinky, J.M. 2002: A revision of early to mid-Ordovician hyoliths from Sweden. Palaeontology 45, 511–555. https://doi.org/10.1111/1475-4983.00248

Marek, L. 1963: New knowledge on the morphology of *Hyolithes*. Sborník geologických věd, řăda Paleontologie 1, 53–72.

Marek, L. 1966: New hyolithid genera from the Ordovician of Bohemia. Časopis Národního Muzea 135, 89–92. https://doi.org/10.1017/s0022336000040129

Marek, L., Malinky, J.M. & Geyer, G. 1997: Middle Cambrian fossils from Tizi N'Tichka, the High Atlas, Morocco, Part 2. Hyolitha. Journal of Paleontology 71, 638–656.

Matthew, G.F. 1893: Illustrations of the fauna of the St. John Group, No. VIII. Transactions of the Royal Society of Canada 11 (4), 85–129.

Matthew, G.F. 1902: Notes on Cambrian faunas. Transactions of the Royal Society of Canada, 84, 93–112.

Missarzhevsky, V.V. 1980: Early Cambrian Mongolian Hyolitha and Gastropoda. Paleontological Journal 15, 18–25.

Missarzhevsky, V.V. 1989: Drevneyshie skeletnye okamenelosti i stratigrafiya pogranichnykh tolshch dokembriya i kembriya. Trudy Geologicheskogo Instituta, Akademiya Nauk SSSR 443, 237 pp.

Oh, Y., Lee, D.-C., Lee, D.-J., & Lee, J.-G. 2021: Cambrian helcionelloids (univalved molluscs) from the Korean Peninsula: systematic revision and biostratigraphy. Alcheringa 45, 127–139. https://doi.org/10.1080/03115518.2021.1929479

Parkhaev, P.Yu. 2000: The functional Morphology of the Cambrian univalved mollusks – Helcionellids, 1. Paleontological Journal 34, 392–399.

Parkhaev, P.Yu. 2001a: Molluscs and siphonoconchs. In: Alexan-

der, E.M., Jago, J.B., Rozanov, A.Yu. & Zhuravlev, A.Yu. (eds), The Cambrian biostratigraphy of the Stansbury Basin, South Australia, 133–210. Transactions of the Palaeontological Institute, Russian Academy of Sciences 282, 343 pp.

Parkhaev, P.Yu. 2001b: The Functional Morphology of the Cambrian Univalved Mollusks Helcionellids, 2. Paleontological Journal 35, 470–475.

Parkhaev, P.Yu. 2002: Phylogenesis and the system of the Cambrian univalved mollusks. Paleontological Journal 36, 25–36.

Parkhaev, P.Yu. 2004: Malacofauna of the Lower Cambrian Bystraya Formation of Eastern Transbaikalia. Paleontological Journal 38, 590–608.

Parkhaev, P.Yu. 2006: On the genus *Auricullina* Vassiljeva, 1998 and shell pores of the Cambrian helcionelloid mollusks. Paleontological Journal 40, 20–33. https://doi.org/10.1134/s0031030106010035

Parkhaev, P.Yu. 2008: The early Cambrian radiation of Mollusca. In: Ponder, W.F. & Lindberg, D.R. (eds), Phylogeny and evolution of the Mollusca 33–69. University of California Press, Berkeley. https://doi.org/10.1525/california/9780520250925.003.0003

Parkhaev, P.Yu. 2017: On the position of Cambrian Archaeobranchians in the system of the class Gastropoda. Paleontological Journal 51, 453–463. https://doi.org/10.1134/s0031030117050070

Parkhaev, P.Yu. 2019: Cambrian molluscs of Australia: overview of taxonomy, biostratigraphy and paleobiogeography. Stratigrafiya, Geologicheskaya Korrelatsiya 27, 52–79. https://doi.org/10.31857/s0869-592x27252-79

Parkhaev, P.Yu. & Demidenko Yu.E. 2010: Zooproblematica and Mollusca from the Lower Cambrian Meishucun Section (Yunnan, China), and taxonomy and systematics of the Cambrian small shelly fossils of China. Paleontological Journal 44, 883–1161. https://doi.org/10.1134/s0031030110080010

Peel, J.S. 1986: *Mellopegma* (Mollusca) from the Middle Cambrian of North Greenland. Rapport Grønlands Geologiske Undersøgelse 132, 14 (only). https://doi.org/10.34194/rapggu.v132.7958

Peel, J.S. 1988: Molluscs of the Holm Dal Formation (late Middle Cambrian), central North Greenland. Meddelelser om Grønland, Geoscience 20, 145–168.

Peel, J.S. 1989: A Lower Cambrian *Eotebenna* (Mollusca) from Arctic North America. Canadian Journal of Earth Science 26, 1501–1503. https://doi.org/10.1139/e89-127

Peel, J.S., 1991: The Classes Tergomya and Helcionelloida, and early molluscan evolution. Bulletin Grønlands Geologiske Undersøgelse 161, 11–65.

Peel, J.S., 1993: Muscle scars and mode of life of *Carinaropsis* (Bellerophontoidea, Gastropoda) from the Ordovician of Tennessee. Journal of Paleontology 67, 528–534. https://doi.org/10.1017/s0022336000024872

Peel, J.S., 2004: Asymmetry and musculature in some Carboniferous bellerophontiform gastropods (Mollusca). GFF 126, 213–220. https://doi.org/10.1080/11035890401262213

Peel, J.S. 2006: Scaphopodization in Palaeozoic molluscs. Palaeontology 49, 1357–1364. https://doi.org/10.1111/j.1475-4983.2006.00599.x

Peel, J.S. 2017. A problematic cnidarian (*Cambroctoconus*; Octocorallia?) from the Cambrian (Series 2–3) of Laurentia. Journal of Paleontology 91, 871–882. https://doi.org/10.1017/jpa.2017.49

Peel, J.S. 2019: Sponge spicule assemblages from the Cambrian (Series 2–3) of North Greenland (Laurentia): systematics and biogeography. GFF 141, 133–161. https://doi.org/10.1080/11035897.2019.1578261

Peel, J.S. 2021a: In-place operculum demonstrates that the middle Cambrian *Protowenella* is a hyolith and not a mollusc. Alcheringa 45, 385–394. https://doi.org/10.1080/03115518.2021.2004225

Peel, J.S. 2021b: *Pseudomyona* from the Cambrian of North Greenland (Laurentia) and the early evolution of bivalved molluscs. Bulletin of Geosciences 96, 195–215. https://doi.org/10.3140/bull.geosci.1827

Peel, J.S. 2021c: Ontogeny, morphology and pedicle attachment of stenothecoids from the middle Cambrian of North Greenland (Laurentia). Bulletin of Geosciences 96, 381–399. https://doi.org/10.3140/bull.geosci.1839

Peel, J.S. 2021d: An outer shelf shelly fauna from Cambrian Series 2 (Stage 4) of North Greenland (Laurentia). Journal of Paleontology 95, Memoir 83, 1–41. https://doi.org/10.1017/jpa.2020.112

Peel, J.S., Dawes, P.R. & Troelsen, J.C. 1974: Note on some Lower Palaeozoic to Tertiary faunas from eastern North Greenland. Rapport Grønlands Geologiske Undersøgelse 65, 18–23. https://doi.org/10.34194/rapggu.v65.7379

Peel, J.S., Streng, M., Geyer, G., Kouchinsky, A. & Skovsted, C.B. 2016: *Ovatoryctocara granulata* assemblage (Cambrian Series 2–Series 3 boundary) of Løndal, North Greenland. Australasian Palaeontological Memoirs 49, 241–282.

Percival, I.G., Quinn, C.D. & Glen, R.A. 2011: A review of Cambrian and Ordovician stratigraphy in New South Wales. Quarterly Notes, Geological Survey of New South Wales 137, 1–39.

Ponder, W.F., Lindberg, D.R. & Ponder, J.M. 2020: Biology and evolution of the Mollusca, Volume 2, 870 pp. CRC Press, Boca Raton, Florida. https://doi.org/10.1086/711791

Price, R.M. 2004: Columellar muscle of neogastropods: muscle attachment and the function of columellar folds. Biological Bulletin 205, 351–366. https://doi.org/10.2307/1543298

Rasetti, F. 1954: Internal shell structures in the Middle Cambrian gastropod *Scenella* and the problematic genus *Stenothecoides*. Journal of Paleontology 28, 59–66.

Rasetti, F. 1957: Additional fossils from the Middle Cambrian Mt. Whyte Formation of the Canadian Rocky Mountains. Journal of Paleontology 31, 955–972.

Resser, C.E. 1938: Cambrian System (restricted) of the southern Appalachians. Geological Society of America Special Paper 15, 140 pp. https://doi.org/10.1130/spe15

Resser, C.E. 1939: The *Ptarmigania* strata of the northern Wasatch Mountains. Smithsonian Miscellaneous Collections 98, 72 pp.

Resser, C.E. & Howell, B.J. 1938: Lower Cambrian *Olenellus* Zone of the Appalachians. Bulletin of the Geological Society of America 49, 195–248. https://doi.org/10.1130/gsab-49-195

Robison, R.A. 1964. Late Middle Cambrian fauna from western Utah. Journal of Paleontology 38, 510–566.

Robison, R.A. 1984: Cambrian Agnostida of North America and Greenland; part 1, Ptychagnostidae. Paleontological Contributions of the University of Kansas, Paper 109, 59 pp.

Robison, R.A., 1994, Agnostoid trilobites from the Henson Gletscher and Kap Stanton formations (Middle Cambrian), North Greenland. Bulletin Grønlands Geologiske Undersøgelse 169, 25–77. https://doi.org/10.34194/bullggu.v169.6726

Rozanov, A.Yu. & Missarzhevsky, V.V. 1966: Biostratigrafiya i fauna nizhnikh gorizontov kembriya. Akademiya Nauk SSSR, Trudy Geologicheskaya Instituta 148, 125 pp.

Rozanov A.Yu., Missarzhevsky, V.V., Vol'kova, N.A., Voronova, L.G., Krylov, I.N., Keller, B.M., Korolyuk, I.K., Lendzion, K., Michniak, R., Rykova, N.G. & Sidorov, A.D. 1969: Tommotskiy yarus i problema nizhney granitsy kembriya. Akademiya Nauk SSSR, Trudy Geologicheskaya Instituta 206: 379 pp.

Rozanov, A.Yu. *et al*. 2010: Fossils from the Lower Cambrian Stratotypes. Paleontologicheskiy Institut Rossiyksaya Akademiya Nauk, Moscow, 228 pp. [in Russian and English].

Rozov, S.N. 1984: Morfologiya, terminologiya, i sistematicheskoe polozhenie stenotekoid. Akademiya Nauk SSSR, Sibirskoe otdelenie, Trudy Institut geologii i geofiziki 597, 117–133.

Runnegar, B., 1985: Early Cambrian endolithic algae. Alcheringa 9, 179–182. https://doi.org/10.1080/03115518508618966

Runnegar, B. & Jell, P.A. 1976: Australian Middle Cambrian molluscs and their bearing on early molluscan evolution. Alcheringa 1, 109–138. https://doi.org/10.1080/03115517608619064

Runnegar, B. & Jell, P.A. 1980: Australian middle Cambrian molluscs: corrections and additions: Alcheringa 4, 111–113. https://doi.org/10.1080/03115518008619642

Runnegar, B. & Pojeta, J., 1974: Molluscan phylogeny: the palaeontological viewpoint. Science 186, 311–317. https://doi.org/10.1126/science.186.4161.311

Saito, K. 1936: Older Cambrian Brachiopoda, Gastropoda, etc., from northwestern Korea. Journal of the Faculty of Science, the Imperial University of Tokyo, Section 2, 4, 345–367.

Shaw, A.B. 1962: Paleontology of northwestern Vermont IX. Fauna of the Monkton Quartzite. Journal of Paleontology 36, 322–345.

Signor, P.W. & Kat, P.W. 1984: Functional significance of columellar folds in turritelliform gastropods. Journal of Paleontology 58, 210–216.

Skovsted, C.B. 2004: Mollusc fauna of the Early Cambrian Bastion Formation of North–East Greenland. Bulletin of the Geological Society of Denmark 51, 11–37. https://doi.org/10.37570/bgsd-2004-51-02

Skovsted, C.B. 2006a: Small shelly fauna from the upper Lower Cambrian Bastion and Ella Island Formations, North-East Greenland. Journal of Paleontology 80, 1087–1112. https://doi.org/10.1666/0022-3360(2006)80[1087:ssfftu]2.0.co;2

Skovsted, C.B. 2006b: Small shelly fossils from the basal Emigrant Formation (Cambrian, uppermost Dyeran Stage) of Split Mountain, Nevada. Canadian Journal of Earth Science 43, 487–496. https://doi.org/10.1139/e05-119

Smith, P.M., Brock, G.A. & Paterson, J.R. 2015: Fauna and biostratigraphy of the Cambrian (Series 2, Stage 4; Ordian) Tempe Formation (Pertaoorta Group), Amadeus Basin, Northern Territory. Alcheringa 39, 40–70. https://doi.org/10.1080/03115518.2014.951917

Stockfors, M. & Peel, J.S. 2005: Endolithic Cyanobacteria from the Middle Cambrian of North Greenland. GFF 127, 179–185. https://doi.org/10.1080/11035890501273179

Sulikowska-Drozd, A., Walczak, M. & Binkowski, M. 2014: Evolution of shell apertural barriers in viviparous land snails (Gastropoda: Pulmonata: Clausiliidae). Canadian Journal of Zoology 92, 205–213. https://doi.org/10.1139/cjz-2013-0222

Taylor, J.D., Kennedy, W.J. & Hall, A. 1969: The shell structure and mineralogy of the Bivalvia: introduction, Nuculacea–Trigonacea. Bulletin of the British Museum (Natural History) Zoology, Supplement 3, 125 pp. https://doi.org/10.5962/p.312694

Thomas, R.D.K., Runnegar, B. & Matt, K. 2020: *Pelagiella exigua*, an early Cambrian stem gastropod with chaetae: lophotrochozoan heritage and conchiferan novelty. Palaeontology 63, 601–627. https://doi.org/10.1111/pala.12476

Tullberg, S.A. 1880: Om *Agnostus*-arterna i de kambriska aflagringarne vid Andrarum. Sveriges Geologiska Undersökning C42, 1–37. https://doi.org/10.1080/11035898009446304

Ushatinskaya, G.T. & Parkhaev, P.Yu. 2005: Preservation of imprints and casts of cells of the outer mantle epithelium in the shells of Cambrian brachiopods, mollusks, and problematics. Paleontological Journal 39, 251–263.

Vasileva N.I. 1990: Novye rannekembriyskie bryuchonogie mollyuski Sibirskoy platformyi voprosyichsistematiki. In: Nikolaev, A.I. (ed.), Mikrofauna SSSR: sistematika i voprosy biostratigrafii, 4-21, VNIGRI, Leningrad.

Vendrasco, M.J., Porter, S.M., Kouchinsky, A., Li, G. & Fernandez, C.Z. 2010: New data on molluscs and their shell microstructures from the Middle Cambrian Gowers Formation, Australia. Palaeontology 53, 97–135. https://doi.org/10.1111/j.1475-4983.2009.00922.x

Vendrasco, M.J., Kouchinsky, A.V., Porter, S.M. & Fernandez, C.Z. 2011: Phylogeny and escalation in *Mellopegma* and other Cambrian molluscs. Palaeontologia Electronica 14, 2, 11A, palaeo-electronica.org/2011_2/221/index.html

Vermeij, G.J. 2017: Shell features associated with the sand-burying habit in gastropods. Journal of Molluscan Studies 83, 153–160. https://doi.org/10.1093/mollus/eyx001

Voronova, L.G., Drosdova, N.A., Esakova, N.V., Zhegallo, E.A., Zhuravlev, A.Yu., Rozanov, A.Yu., Sayutina, T.A. & Ushatinskaya, G.T. 1987: Iskopaemye nizhnego kembriya gor Makkenzi (Kanada). Akademiya Nauk SSSR, Trudy Paleontologicheskogo Instituta 224, 88 pp.

Vostokova,V.A. 1962: Kembriyskie gastropody Sibirskoyj

platformy i Taymyra. Trudy Nauchno Issledovatel'skogo Instituta Geologii Arktiki 28, 51–74.

Walcott, C.D. 1884: Paleontology of the Eureka district. United States Geological Survey Monograph 8, 298 pp.

Wenz, W. 1938: Gastropoda. Allgemeiner Teil und Prosobranchia. In: O.H. Schindewolf (ed.), Handbuch der Paläozoologie, Band 6, 720 pp. Borntraeger, Berlin. https://doi.org/10.1017/s0016756800072459

Whitehouse, F.W. 1939: The Cambrian faunas of north-eastern Australia, Part 3. Queensland Museum Memoir, new series 1, 179–282.

Wotte, T. 2006: New Middle Cambrian molluscs from the Láncara Formation of the Cantabrian Mountains (northwestern Spain). Revista Española de Paleontología 21, 145–158. https://doi.org/10.7203/sjp.21.2.20487

Yang, Y., Zhao, Y., Peng, J. & Yang, X. 2012: *Oelandiella* from the Cambrian "Tsinghsutung Formation" of Jianhe County, Guizhou. Acta Palaeontologica Sinica 51, 308–319. [in Chinese with English abstract].

Yochelson. E.L. 1968: Stenothecoida, a proposed new class of Cambrian Mollusca. Abstracts, International Palaeontological Union, Prague, Czechoslovakia, August 20–27, 1968, p. 34.

Yochelson, E.L. 1969: Stenothecoida, a proposed new class of Cambrian Mollusca. Lethaia 2, 49-62. https://doi.org/10.1111/j.1502-3931.1969.tb01250.x

Yu, W 1979: Earliest Cambrian monoplacophorans and gastropods from western Hubei with their biostratigraphical significance. Acta Palaeontologica Sinica 18, 233–270 [in Chinese with English abstract].

Zhou, B. & Xiao, L. 1984: Early Cambrian monoplacophorans and gastropods from Hainan and Huoqiu Counties, Anhui Province. Professional Papers of Stratigraphy and Palaeontology 13, 125–140 [in Chinese with English abstract].

Holocene development of Brabrand Fjord, eastern Jylland, Denmark

OLE BENNIKE, PETER MOE ASTRUP, BENT V. ODGAARD, CHRISTOF PEARCE & PETER WIBERG-LARSEN

Geological Society of Denmark
https://2dgf.dk

Received 29 January 2022
Accepted in revised form
5 April 2022
Published online
11 May 2022

Bennike, O., Astrup, P.M., Odgaard, B.V., Pearce, C. & Wiberg-Larsen, P. 2022: Holocene development of Brabrand Fjord, eastern Jylland, Denmark. Bulletin of the Geological Society of Denmark, Vol. 70, pp. 105–115. ISSN 2245-7070. https://doi.org/10.37570/bgsd-2022-70-07

The Brabrand Sø area west of Aarhus in eastern Jylland, Denmark, was deglaciated about 18 000 to 17 000 years ago. Coring in the present-day lake area revealed Early Holocene stream deposits overlain by marine deposits. The area was transgressed by the sea at *c.* 8500 cal. years BP and a 12 km long, narrow fjord was formed. In the beginning, the fjord housed a species-poor marine or brackish-water fauna with molluscs *Hydrobia* sp. (mudsnail), *Littorina littorea* (winkle), *Mytilus edulis* (blue mussel) and *Cerastoderma* sp. (cockle). This phase was followed by a phase during which the fjord housed a species-rich fauna that included *Ostrea edulis* (European flat oyster) and *Ruditapes decussatus* (palourde clam). During this phase the salinity and summer water temperatures were higher than in present day Aarhus Bugt and we also see evidence for strong bottom currents. This phase was probably characterised by a fairly large tidal amplitude. Two radiocarbon ages of *O. edulis* shells of *c.* 6250 and 6700 cal. years BP indicate that such conditions peaked during the period of the Ertebølle culture. The high-salinity phase was followed by a phase with a more species-poor fauna, this phase was also characterised by a high sedimentation rate – a feature seen in other fjords in the region. We suggest that the shift could be due to a decrease in tidal amplitude. Brabrand Fjord was eventually transformed into a lake due to land uplift and closure of the connection to Aarhus Bugt due to longshore sediment transport but the timing of the transition from fjord to lake is still unknown.

Keywords: Quaternary, Brabrand Sø, Littorina Sea, relative sea-level changes, tidal amplitude, *Ostrea*.

Ole Bennike [obe@geus.dk], Geological Survey of Denmark and Greenland (GEUS), Universitetsbyen 81, DK-8000 Aarhus C, Denmark. Denmark. Peter Moe Astrup [pma@moesgaardmuseum.dk], Moesgaard Museum, Moesgård Allé 15, DK-8270 Højbjerg. Bent V. Odgaard [bvo@geo.au.dk] and Christof Pearce [christof.pearce@geo.au.dk], Department of Geoscience, Aarhus University, Høegh-Guldbergs Gade 2, DK-8000 Aarhus C, Denmark. Peter Wiberg-Larsen [pwl@ecos.au.dk], Institute for Ecoscience, Aarhus University, Vejlsøvej 25, DK-8600 Silkeborg, Denmark.

During the Last Glacial Maximum, huge amounts of water was stored in continental ice sheets and global sea level was lowered by *c.* 130 m compared with the present (Lambeck *et al.* 2014). About 20 000 years ago, the sea level began to rise, and vast shallow-water areas were flooded. In Denmark, Storebælt, Lillebælt, Øresund and the North Sea were inundated. Large areas that were dry land or occupied by lakes were transgressed by the sea (e.g. Jensen *et al.* 2002; Bennike *et al.* 2021a). Stone Age settlements, forests and mires were flooded by the sea. However, in the northern part of Denmark, the glacio-isostatic uplift surpassed the eustatic sea-level rise and raised marine deposits are widespread. In the Aarhus Bugt area, the marine limit is *c.* 2.5 m above present sea level (Mertz 1924). According to the deglaciation chronology of Denmark, the last active glacier ice disappeared from the Brabrand Sø region about 18 000 to 17 000 years ago (Houmark-Nielsen *et al.* 2012).

The Holocene history of Denmark has been studied for almost two centuries, but many details are still unknown. Development of radiocarbon dating by means of accelerator mass spectrometry means that it is now possible to date a single shell of a mol-

lusc, small remains of plants or even a single test of a foraminifer. Therefore, the timing of events in the Holocene history of Denmark can be better constrained than earlier. Detailed, high-resolution studies of continuous records are crucial for understanding the late Quaternary palaeogeographical evolution of southern Scandinavia. Here we report on studies of two sediment cores from the former Brabrand Fjord in eastern Jylland, Denmark (Figs 1, 2). We studied macroscopical remains of plants and animals and determined the age of selected samples to provide information on local environmental changes, which must have had a crucial impact on pre-historic people.

In 1900 Stone Age artefacts were found during digging of a ditch near Rugholm at the south-eastern end of Brabrand Sø and in 1903–1904 excavations were conducted by the Danish National Museum and the Geological Survey of Denmark (Thomsen & Jessen 1906). The artefacts were referred to the Ertebølle culture; they came from shallow-water, marine deposits. The deposits located in 1900 were dated by means of pollen analysis by Troels-Smith (1937). Troels-Smith dated the deposits to the late part of pollen zone VII and the early part of pollen zone VIII in the zonation scheme of Jessen (1935) and Troels-Smith (1937, 1942) concluded that the Ertebølle culture was partly contemporaneous with the Early Neolithic.

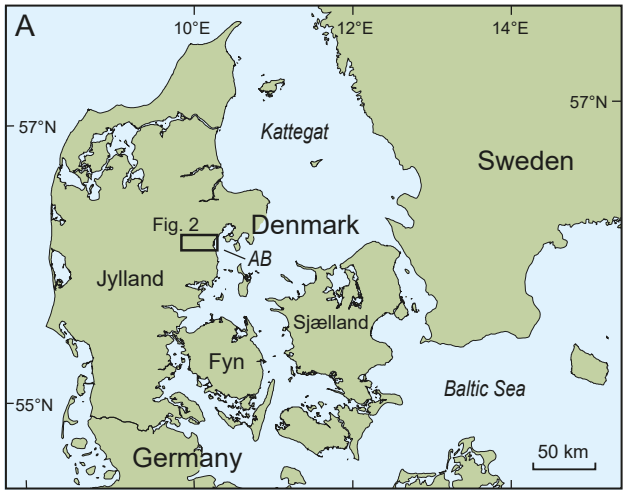

Fig. 1. Map of Denmark showing the location of the study area. AB: Aarhus Bugt. The position of Fig. 2 is indicated.

More recent radiocarbon dating indicates that the artefacts belong to the Ertebølle culture, which is now referred to the Late Mesolithic (Table 1; Fig. 3). The bone assemblage was dominated by *Cervus elaphus* (red deer) but included *Sus scrofa* (wild boar), *Bos primigenius* (aurochs), *Capreolus capreolus* (roe deer), *Martes martes* (pine marten), *Halichoerus grypus* (grey seal), *Alces alces* (elk), *Lagenorhynchus albirostris* (white-beaked dolphin), *Vulpes vulpes* (red fox), *Felis silvestris* (wild cat), *Ursus arctos* (brown bear), *Cygnus cygnus* (whooper swan), *Cygnus columbianus* (tundra swan), *Tetrao urogallus* (capercaillie), *Phalacrocorax carbo* (great cormorant), *Uria aalge* (common guillemot), *Morus bassanus* (gannet) and *Pelicanus crispus* (dalmatian pelican). The bones were identified by Herluf Winge and the results published by Thomsen & Jessen (1906).

An updated list of vertebrate remains from Ertebølle sites in Brabrand Fjord was published by Laursen (2012), based on information from Kim Aaris-Sørensen from the Natural History Museum of Denmark. The list published by Laursen includes *Pagophilus groenlandica* (harp seal), *Aquila chrysaetos* (golden eagle) and *Pinguinus impennis* (great auk). *P. groenlandica* is an arctic species that was common in Danish waters

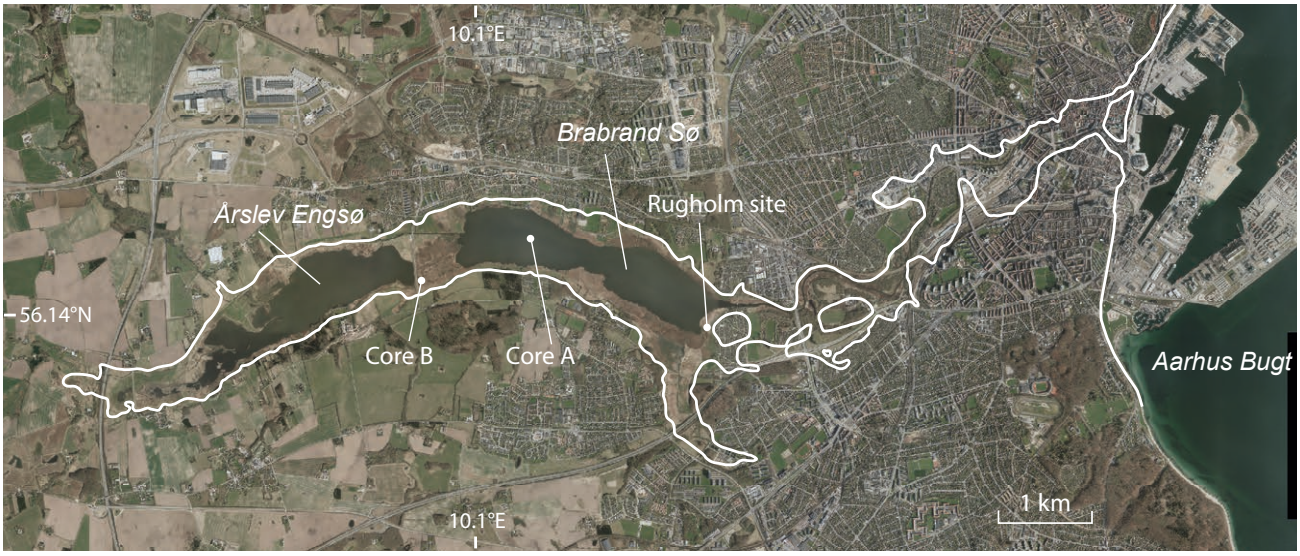

Fig. 2. Orthophoto with the former extension of Brabrand Fjord indicated, based on Rasmussen (2017).

Table 1. Selected radiocarbon ages from Brabrand Fjord and Aarhus, Denmark

Core/ site	N. lat. °	E. long. °	Laboratory number	Material	Depth (m)	Age (^{14}C years BP)[1]	Cal. age (years BP)[2]	Cal. age (y BP)[3]	Ref.
A	56.146	10.109	AAR-30714	*S. lacustris*	2.22	148 ± 25	2–282	142	a
A	56.146	10.109	AAR-30713	*S. lacustris*	2.74	134 ± 23	9–272	112	a
A	56.146	10.109	AAR-30712	Leaf fragments	3.54	4554 ± 29	5052–5431	5169	a
A	56.146	10.109	AAR-30711	Leaf fragments	4.62	4729 ± 32	5326–5579	5470	a
A	56.146	10.109	AAR-30710	Leaf fragments	5.58	4755 ± 33	5330–5584	5519	a
A	56.146	10.109	AAR-30709	Leaf fragments	6.54	4922 ± 27	5592–5716	5638	a
A	56.146	10.109	AAR-30708	*Ostrea edulis*	7.10	6260 ±31	6495–6836	6669	a
A	56.146	10.109	AAR-30707	*Ostrea edulis*	8.65	5862 ± 34	6079–6395	6240	a
A	56.146	10.109	AAR-30706	*Mytilus edulis*	8.77	8512 ± 40	8967–9310	9130	a
A	56.146	10.109	AAR-30705	Twig	8.90	9249 ± 40	10262–10560	10418	a
A	56.146	10.109	AAR-30704	*Populus tremula*	8.98	9377 ± 37	10500–10702	10603	a
B	56.143	10.090	AAR-30093	*S. lacustris*	0.58	2831 ± 32	2853–3058	2934	a
B	56.143	10.090	AAR-30092	*Cerastoderma* sp.	0.62	5428 ± 33	5602–5909	5769	a
B	56.143	10.090	AAR-30091	*Littorina littorea*	2.16	7274 ± 36	7564–7848	7702	a
B	56.143	10.090	AAR-30090	Root, woody plant	2.24	6895 ± 39	7624–7834	7725	a
Rugholm	56.138	10.139	K-2651	*Equus ferus*		5500 ± 75	6016–6450	6299	b
Rugholm	56.138	10.139	Ua-32311	*Bos primigenius*		5425 ± 75	5999–6391	6216	c
Åby rens.	56.152	10.178	Aar-12828	*Cerastoderma* sp.	1.0	5179 ± 39	5325–5648	5503	d
Pustervig	56.158	10.208	Ua-4161	*Littorina* sp.	0.36	4885 ± 50	4943–5366	5167	e

[1] Radiocarbon ages are reported in conventional radiocarbon years BP (before present = 1950; Stuiver & Polach (1977)).

[2] Calibration to calendar years BP (2 sigma) is according to the IntCal20 and Marine20 data (Reimer *et al.* 2020; Heaton *et al.* 2020).

[3] Median probability ages.

References. a: this study, b: Sommer *et al.* 2011, c: Gravlund *et al.* 2012, d: Kveiborg 2014, e: Heinemeier 1999.

during the Middle Holocene (Bennike *et al*. 2008). *P. impennis* is extinct but its bones are well known from Ertebølle sites in Denmark. *P. crispus* is a southern species that no longer lives in Denmark (Hatting 1963).

The bone material excavated by Thomsen & Jessen included two bones of horse, but Winge did not include this species in his list, presumably because he considered the age of them doubtful. Degerbøl (1933) discussed these horse bones and suggested that they represent *Equus ferus* (wild horse). This viewpoint has been confirmed by direct radiocarbon dating of one of the bones, which gave an age of *c.* 6300 cal. years BP, and which fits into a general central European repopulation of wild horse tracing the Neolithic expansion (Table 1; Sommer *et al.* 2011). Degerbøl & Fredskild (1970) discussed if some of the ox bones from Rugholm represent domestic cows but concluded that the bones likely come from *B. primigenius*. One of these bones has been dated to *c.* 6220 cal. years BP (Table 1; Gravlund *et al.* 2012), which predates the arrival of domestic cattle to Denmark (Sørensen 2015).

Data on the fossil marine mollusc fauna from a gyttja layer from the Rugholm excavation were provided by Thomsen & Jessen (1906). They reported the following 13 species of molluscs: *Ostrea edulis* (European flat oyster), *Mytilus edulis* (blue mussel), *Cerastoderma edule* (common cockle), *Parvicardium exiguum*, *Venerupis corrugate* (= *Tapes pullastra*), *Ruditapes decussatus* (palourde clam), *Scrobicularia plana*, *Macoma balthica*, *Littorina littorea* (winkle), *Hydrobia ulvae*, *Bittium reticulatum*, *Tritia reticulata* (= *Nassa reticulata*) and *Retusa truncatula*. The fauna shows that a fjord with a rich and diverse marine mollusc fauna existed in the area during the Stone Age.

In 1944–1945 new excavations were carried out at the Rugholm site. The aim was to collect material for exhibitions in Aarhus (Haugsted *et al.* 1947), however, new pollen analyses were also carried out (Andersen 1947). The analysed samples were referred to the late part of pollen zone VII, corresponding to the late part of the Atlantic chronozone (Mangerud *et al.* 1974) or to *c.* 6000–7000 cal. years BP.

In recent years, archaeological excavations have been conducted in connection with urban development east of Brabrand Sø (Rasmussen 2009a, b, 2012, 2017; Kveiborg 2014) and it is clear that the Brabrand Fjord area has been an important area for pre-historic people. A shell of a marine bivalve (*Cerastoderma*) from the fjord gave an age of *c.* 5500 cal. years BP, and a shell of a marine gastropod (*Littorina*) from Aarhus, at the entrance to the fjord gave an age of *c.* 5170 cal. ka BP (Table 1). However, so far little information is available

on the duration of the fjord stage and no attempt to obtain continuous records of environmental changes has been carried out so far.

Study area

Brabrand Sø is located in a 2–3 km wide buried valley with a Quaternary succession that is over 100 m thick (Lykke-Andersen 1973). This incised valley is interpreted as a tunnel valley, where meltwater has eroded Quaternary and pre-Quaternary strata. The lake is fed by Aarhus Å draining a catchment of 310 km^2. In pre-historic times the Brabrand Sø area (Fig. 2) was a fjord, which was connected to Aarhus Bugt in the east. Brabrand Fjord was *c.* 12 km long, *c.* 700 m wide in the west and more in the east. At present, part of the former fjord is occupied by two lakes, Brabrand Sø and Årslev Engsø. Brabrand Sø is east–west-oriented, 2.8 km long and 300–600 m wide with an area of 154 ha. The maximum water depth was 1.8 m in 1979 (Høy 1979). According to historical maps, 200 years ago the lake was approximately 1 km longer than at present. Lake level lowering and deposition of sediment have reduced the size of the lake. During the period from 1988 to 1995 about 500 000 m^3 of sediment was dredged from the lake, in order to improve the water quality of the eutrophic lake and to prevent overgrowth of the lake. Årslev Engsø is an artificial, shallow lake that was created in 2003. The level of Brabrand Sø is 0.7 m above sea level (Høy 1979). The tidal range in Aarhus is about 40 cm during spring tide (DMI 2021), but sea level variations during stormy weather may exceed 150 cm (Kystdirektoratet 2019).

During the Late Holocene, the former Brabrand Fjord turned into the present lake because the relative sea level gradually fell *c.* 2.5 m (Mertz 1924). Raised marine deposits have been mapped at some sites along the shores of Brabrand Sø (Jupiter 2019).

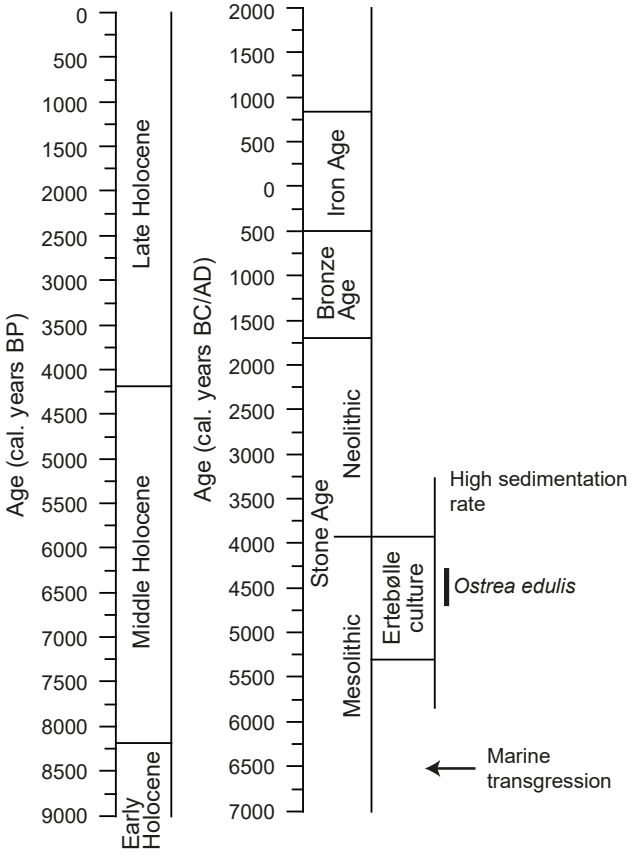

Fig. 3. Chronology and overview of Holocene changes at Brabrand Fjord. The division of the Holocene is from Walker *et al.* 2019 and the archaeological time periods are from Skousen (2008).

Methods

Coring was carried out from a platform on the lake (May 2019) and at a site on land (March 2019), using a Russian peat corer (Jowsey 1966). The chamber was 1 m long and had a diameter of 5 cm. The corer was pushed or hammered into the sediment. The water depth at the lake site was 1.6 m (site A, Fig. 2). The site on land is located south-west of Brabrand Sø, at an elevation of *c.* 1 m above sea level (site B in Fig. 2). Whole cores were brought to the laboratory where they were cleaned and subsampled. Contiguous 4 cm thick samples were taken for macrofossil analyses. Sediment samples were wet sieved on 0.4, 0.2 mm sieves, and the residue left on the sieves was transferred to a petri dish. Macroscopic remains of plants and animals were identified and counted using a dissecting microscope. The numbers in the macrofossil diagrams refer to the number of shells per sample, however, many of the shells represent small juvenile specimens. Many of the shells, especially of *M. edulis*, were fragmented – in this case, hinge fragments were counted. In general, preservation was good to excellent, but at some levels carbonate shells were somewhat dissolved. This means that thin-shelled organisms may be under-represented at these levels. A total of 320 samples were analysed for macrofossils.

Selected remains were dried and submitted for radiocarbon dating using accelerator mass spectrometry. Dating was carried out at the Aarhus AMS Centre, Aarhus University. Radiocarbon ages were calibrated to calendar years before present (BP) using CALIB v. 8.2 with the IntCal20 or Marine20 calibration curves (Reimer *et al.* 2020; Heaton *et al.* 2020). For

marine samples, we used a ΔR value of –150 years, which corresponds to a reservoir age of 400 years. However, the local reservoir age may have varied in the past (Olsen *et al*. 2009), and ages of marine shells are therefore more uncertain than ages of remains of terrestrial plant.

Results and discussion

Sediments

Simplified logs are shown in Figs 4, 5. The sediments at core site A consisted, from the bottom upwards, of (1) 40 cm light-grey homogenous clay and silt, (2) 55 cm brown sand, layered fine- and medium-grained sand in the lower part and homogenous coarse-grained sand in the upper part, (4) 39 cm grey, homogenous shell-rich sand, (5) 8 cm grey silt and fine-grained sand. This layer was almost completely lost during coring. It was followed by (6) 100 cm grey, homogenous shell-rich sand, (7) 428 cm dark olive-grey homogenous gyttja with abundant well-preserved leaves of deciduous woody plants and with scattered marine shells, (8) 80 cm dark-grey homogenous detritus gyttja.

At core site B we found (1) 30 cm grey poorly sorted sand and fine gravel with *in situ* roots in the upper part, (2) 155 cm marine sediments consisting of brown shell-rich sand in the bottom, dark-brown homogenous sandy gyttja with shells and homogeneous gyttja with marine shells and remains of *Phragmites*, (3) 85 cm alternating layers of fine-grained sand and coarse detritus gyttja, and (4) 75 cm brown peat, decomposed in the upper part.

Radiocarbon ages and sedimentation rates

A total of 15 samples were dated (Table 1; Figs 4, 5). At site A a *Populus tremula* (aspen) bud scale and a twig provide ages of the terrestrial vegetation that covered the deeper parts of the fjord before it was inundated by the sea; these samples gave ages of *c.* 10 400 and 10 600 cal. years BP. The oldest dated marine shell yielded an age of *c.* 9100 cal. years BP, however, this age appears to be somewhat too old, according to the relative sea-level curve for the area (Bennike *et al.* 2021b). It is possible that the local reservoir age was

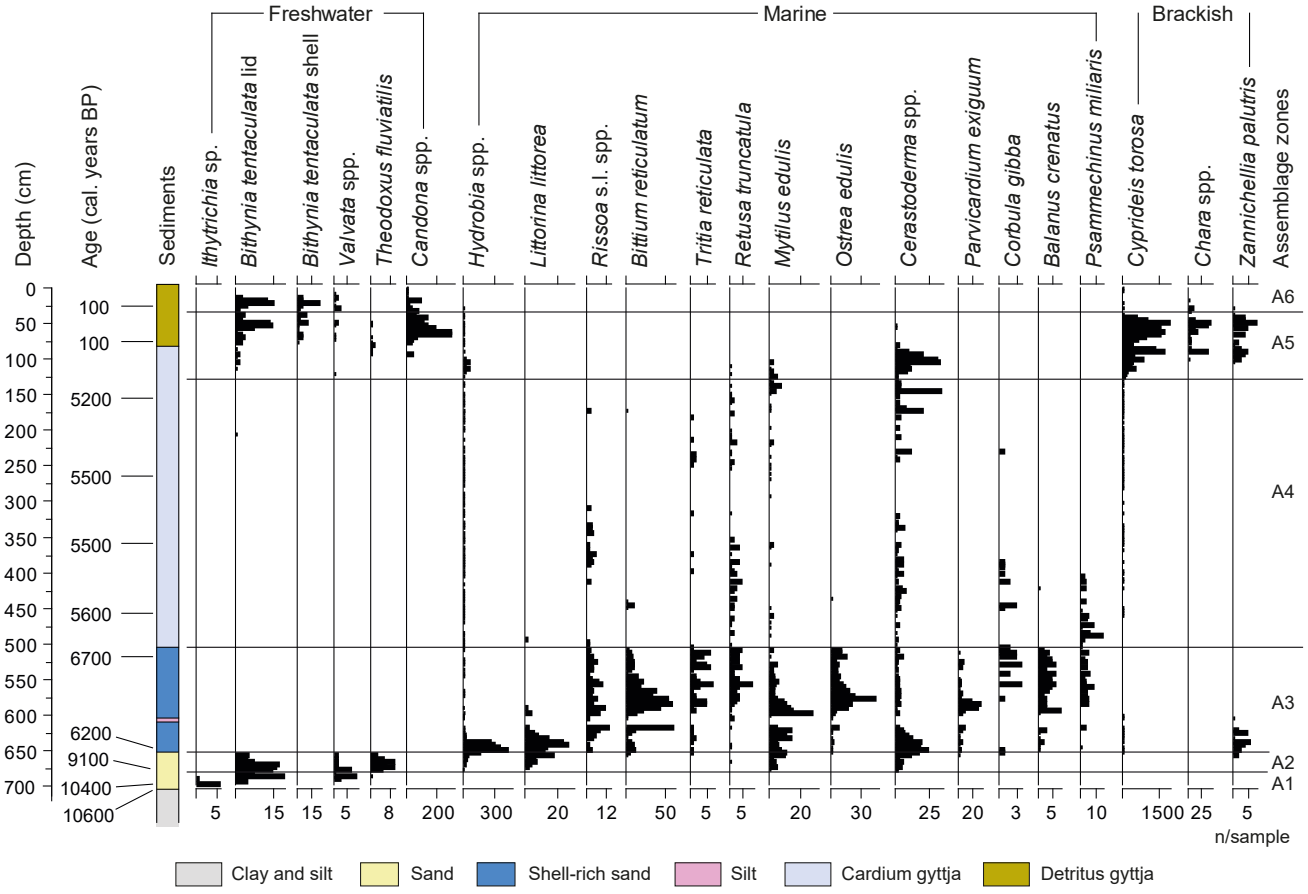

Fig. 4. Simplified macrofossil concentration diagram for core site A from Brabrand Fjord. Note different scales for different taxa.

larger than 400 years during the initial marine transgression and we suggest that the fjord was inundated *c.* 8500 cal. years BP. Dating of two shells of *O. edulis* gave ages of *c.* 6300 and 6700 cal. years BP, however, the ages are reversed, indicating that the shell-rich sandy sediment was deposited during a time period with strong currents that led to reworking of shells. Four samples of leaves from the next layer gave ages between *c.* 5600 and 5100 cal. years BP, indicating a very high sedimentation rate. The high sedimentation rate may be the reason that the leaves were well-preserved. Thus usually, only the veins of the leaves are found in Holocene sediments. Finally, two samples from the upper part of the succession gave young ages. The ages show that the succession is characterised by major hiati and it was not possible to reconstruct an age-depth curve from the dated samples.

At site B a small *in situ* root and a shell of *L. littorea* both gave ages of *c.* 7700 cal. years BP, indicating that the site was inundated by the sea at that time. The youngest shell from the site was dated to *c.* 5800 cal. years BP and a sample of achenes of the reed plant *Schoenoplectus lacustris* (bulrush) gave an age of *c.* 2900 cal. years BP. This shows that a major hiatus is also found at site B.

Macrofossils

Core site A. The macrofossil diagram from core site A was divided into six local assemblage zones (A1–A6; Fig. 4).

Zone A1 is characterised by sand with a mixture of terrestrial, wet-ground and limnic plants such as *P. tremula*, *Betula* sect. *Albae* sp. (tree birch), *Schoenoplectus* spp., *Carex* sp. (sedge), *Urtica dioica* (common nettle), *Filipendula ulmaria* (meadowsweet), *Eupatorium cannabinum* (hemp-agrimony), *Menyanthes trifoliate* (bogbean) and *Nymphaea alba* (white water lily). A single tooth of a small rodent was also found. The lowest fossiliferous samples contained remains of larvae of the caddisflies *Ithytrichia* sp. (probably *Ithytrichia lamellaris*), *Hydropsyche pellucidula* and *Lepidostoma hirtum* and head capsules of larvae of Simuliidae (blackflies; Table 2). Larvae of the recorded caddisflies and blackflies are typical inhabitants of rivers and streams with fairly fast-flowing water (Wiberg-Larsen *et al*. 2001; Bennike & Wiberg-Larsen 2002), and the sandy sediment is interpreted as a stream deposit. Larvae of non-biting midge *Stenochironomus* sp. are miners of macrophytes (Brooks *et al*. 2007). A bit higher up follows shells of the gastropods *Valvata cristata*, *Valvata piscinalis*, opercula of the freshwater gastropod *Bithynia tentaculata*, shells of the small bivalve *Pisidium* sp. and statoblasts of the bryozoan *Cristatella mucedo*. The gastropods are primarily inhabitants of lakes, but the presence of sandy sediment may indicate a at least partly lotic environment.

Zone A2 contains shells of the freshwater gastropods *V. cristata*, *V. piscinalis*, rare shells and common opercula of *B. tentaculata* and shells of *Pisidium* sp. Shells of the gastropod *Theodoxus fluviatilis* (river nerite) are common; this species is usually classified as a freshwater species and it is nowadays widely distributed in Aarhus Å (Wiberg-Larsen, unpubl.), but it also lives in brackish water. Zone A2 also contains shells of marine or brackish-water mollusc species, such as *Hydrobia* sp., *L. littorea*, *M. edulis* and *Cerastoderma* sp. The mixture of freshwater species and marine species may indicate that the salinity alternated between marine and freshwater conditions during the earliest stage of the marine inundation. It is also possible that the remains of freshwater species were transported into the fjord from a nearby stream (no doubt being a former Aarhus Å and its major tributary Lyngbygaards Å), but we consider this option less likely because the shells of the freshwater species are thin and hardly survives transport. The zone forms a transition from freshwater conditions to marine conditions.

Zone A3 contains numerous shells of marine molluscs, whereas shells of fresh-water species are absent. Remains of land plants and limnic plants are also absent. The fauna is dominated by the gastropods *Hydrobia* sp., *L. littorea*, *Rissoa* spp. (*R. parva* and *R. membranacea*) and *B. reticulatum* and the bivalves *M. edulis*, *O. edulis* and *Cerastoderma* sp. The fauna also comprises for example *Musculus discors*, *Mysella bidentata*, *Spisula subtruncata*, *Abra alba*, *R. decussatus*, *P.*

Table 2. Arthropod remains from assemblage zone A1, core site A from Brabrand Fjord, Denmark

Order/family	Genus/species	694 cm	698 cm
Oribatida	*Hydrozetes*?		2 exoskeletons
Trichoptera, Hydropsychidae	*Hydropsyche pellucidula*		1 frontoclypeal apotome
Trichoptera, Hydroptilidae	*Ithytrichia* sp.	1 case	7 cases
Trichoptera, Lepidostomatidae	*Lepidostoma hirtum*	2 genae, 1 pronotum	
Diptera, Simuliidae		6 head capsules	13 head capsules
Diptera, Chironomidae	*Stenochironomus* sp.	1 head capsule	1 head capsule
Diptera, Chironomidae	*Micropsectra* sp.		2 head capsules

exiguum, *Corbula gibba*, *T. reticulata*, *Triphora adversa*, *R. truncatula*, *Onoba semicostata*, *Lacuna divaricata*, the barnacle *Balanus crenatus*, the crab *Carcinus maenas*, the sea urchin *Psammechinus milliaris* and the polychaete worm *Pomatoceros triqueter*. Remains of crabs are rarely reported from Quaternary sediments, but the samples from Brabrand Fjord contained a few dactyls (moveable fingers from the claw) of crabs.

The lower part of the zone is characterised by abundant shells of *Hydrobia* spp., many shells of *L. littorea and Cerastoderma* sp., whereas shells of *O. edulis* are rare; the species becomes common in the upper part of the zone. The fauna is rich and diverse with a total of 24 taxa of molluscs. The fossil assemblage indicates shallow water influenced by currents and increasing salinity and water depth. The presence of *O. edulis* and *R. decussatus* is noteworthy as these species no longer live in the inner Danish waters; they indicate salinities and summer temperatures higher than pre-industrial values. Water plants are represented by fruits of *Zannichellia palustris* in the lower part of the zone and by rare fruits of *Ruppia* sp., both being common in shallow marine or brackish waters.

Zone A4 is characterised by gyttja with *Cerastoderma* sp., *M. edulis* and *Hydrobia* spp., whereas *Rissoa* spp., *B. reticulatum*, *T. reticulata*, *R. truncatula* and *C. gibba* are rare or fairly rare. The fauna also comprises for example *S. subtruncata*, *M. bidentata*, *M. balthica*, jaws of the polychaete worm *Nereis* sp. A total of 15 taxa of molluscs were found in this zone. The fine-grained sediment indicates a low energy environment and the fauna indicate somewhat lowered salinity, although *B. reticulatum* indicates a salinity above 25 ‰.

Zone A5 is characterised by huge numbers of the ostracod *Cyprideis torosa*, fairly high numbers of *Cerestoderma* (in the lower part of the zone), *Chara* sp., *Z. palustris*, *B. tentaculata* and *Candona* sp. *Cyprideis torosa* is typical of brackish-water environments with fluctuating salinities (Pint *et al.* 2012), and we suggest that the sediments accumulated during the transition from fjord to lake. The plants *Chara* and *Zannichellia* are also typical of brackish water, although they may also grow in freshwater. *B. tentaculata* is a freshwater species, whereas some *Candona* species can live in brackish water. This zone marks a transition from fjord to lake.

Zone A6 contains shells of molluscs such as *B. tentaculata*, *V. cristata*, *V. piscinalis*, *Anisus contortus*, *Acroloxus lacustris*, *Pisidium* sp., shells of ostracods (*Candona* sp., *Darwinula stevensoni*, *Cyclocypris laevis*), the caddisfly *Orthotrichia* sp., the bryozoans *Cristatella mucedo* and *Fredericella* sp., the water plants *Ranunculus* sect. *Batrachium* sp., *Potamogeton perfoliatus* and *Callitriche* sp. This assemblage represents a limnic or

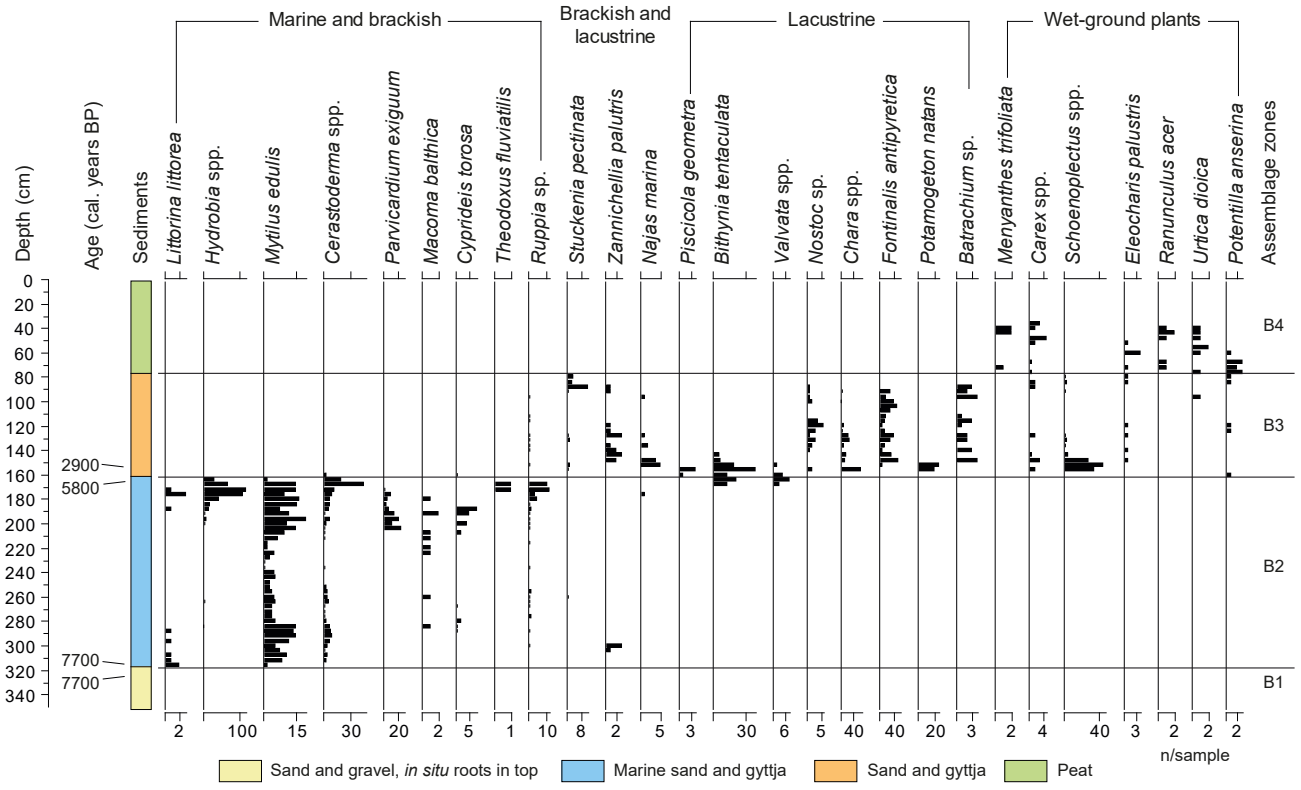

Fig. 5. Simplified macrofossil concentration diagram for core site B from Brabrand Fjord. Note different scales for different taxa.

lentic environment with macrolimnophytes and a rich fauna of invertebrates. The zone contains low numbers of *C. torosa* shells, which we interpret as reworked from zone A5.

Core site B. The macrofossil diagram from core site B was divided into four local assemblage zones (B1–B4; Fig. 5).

Zone B1 contains roots of woody and non-woody plants.

Zone B2 is characterised by shells of marine bivalves and gastropods, in particular *M. edulis* and *Cerastoderma* spp. Rare shells of *L. littorea* occur in the bottom and top of the zone, and shells of *Hydrobia* spp. are abundant in the top. Other marine molluscs comprised the bivalves *P. exiguum* and *M. balthica* and the gastropods *B. reticulatum* and *Aclis walleri*. There is a small peak of the ostracod *C. torosa* below the top of the zone, and two shells of the gastropod *T. fluviatilis* were found near the top of the zone. Remains of water plants are rare but fruits of the vascular plants *Ruppia* sp. and *Zannichellia palustris* were recorded. Shells of freshwater gastropods are found in the uppermost part of the zone. A total of 9 taxa of marine molluscs are recorded in zone B2.

Zone B3 is dominated by remains of water plants such as the vascular plants *Ruppia* sp. (rare), *Stuckenia pectinata*, *Z. palustris*, *Najas marina*¸ *Batrachium* sp., *Ceratophyllum demersum*, *N. lutea*, *Myriophyllum spicatum*, *Potamogeton perfoliatus*, the algae *Nostoc* sp. and *Chara* spp. and the bryophyte *Fontinalis antipyretica*. In the lower part of the zone shells and opercula of freshwater molluscs are found, the most common species are *B. tentaculata*, *V. cristata* and *V. piscinalis*. The zone also contains fruits of wet-ground plants such as the *Scirpus* s.l. spp., *Carex* spp. and *Eleocharis palustris*.

Zone B4 is dominated by vegetative remains of *Phragmites australis*. In the lower part rare fruits and seeds of wet-ground plants such as *Eleocharis palustris*, *Carex* spp., *M. trifoliata*, *Alisma plantago-aquatica*, *Ranunculus flammula*, *Ranunculus acer*, *U. dioeca*, *Caltha palustris* and *Cicuta virosa* occurred. Achenes of *Potentilla anserina* were also fairly common at the base of zone B4, perhaps due to trampling by domestic animals near the core site. The upper part of the peat did not contain fruits or seeds because the peat was decomposed.

Palaeoenvironmental reconstruction of Brabrand Fjord

The light-grey clay and silt at core site A is interpreted as a glaciolacustrine deposit and the poorly sorted sand and fine-grained gravel at core site B as a glaciofluvial deposit. Both sediment types are likely from the last deglaciation of the region.

During the earliest Holocene, the region was covered by open woodland with *Betula*, *Pinus* and *Populus* (Odgaard 1994). A stream, probably the predecessor of present-day Aarhus Å that drained the area west of Aarhus Bugt was found at the bottom of the valley. The stream housed a fauna that included larvae of the caddisflies *Ithytrichia* sp. and *Hydropsyche pellucidula*, confined to rivers and major streams, and *Lepidostoma hirtum*, mainly recorded from major streams. There is no clear indication that a lake existed in Brabrand Fjord prior to the marine transgression, which may indicate that there is no threshold between Brabrand Fjord and Aarhus Bugt. When marine waters began to inundate the area at *c.* 8500 cal. years BP, a brackish-water phase followed, with *Hydrobia* sp., *L. littorea*, *M. edulis* and *Cerastoderma* sp. These taxa are common in shallow-water coastal areas with brackish water in the region at present (Muus 1967).

Somewhat later fully marine conditions with a rich fauna that included *O. edulis* and *R. decussatus*. Thomsen & Jessen (1906) noted that the *O. edulis* shells from the Rugholm site were up to 100–110 mm long. This can be compared with lengths up to 160 mm recorded from the Limfjord (Madsen *et al.* 1900; Nordmann 1903) and a maximum length of 53 mm for shells from southern Lolland (Bennike, unpublished data). The fairly species-rich marine fauna in the former Brabrand Fjord and the large size of *O. edulis* shells indicate favorable conditions with high salinities over 25 ‰, nutrient-rich warm waters and a tidal amplitude larger than at present. However, the conditions were not as favorable for *O. edulis* as in the Limfjord during the Middle Holocene.

Thomsen & Jessen (1906) reported on 13 species of molluscs, and we found a total of 24 taxa of molluscs. Two ages of 6300 and 6700 cal. years BP correspond to the Ertebølle culture (Fig. 3), during which shell middens dominated by *Ostrea edulis* shells accumulated in the region (Andersen 2007). The shell-rich sandy sediments indicate a high-energy environment with strong bottom currents, which was probably caused by a fairly large tidal amplitude.

In the Early Neolithic, fine-grained marine gyttja accumulated in Brabrand Fjord at a high rate, indicating a marked shift to a low-energy environment. A shift to higher sedimentation rates is seen in several other fjords in the region (Lewis *et al.* 2016) and in the former Arrefjord in north-east Sjælland a shift in sedimentation from sand to gyttja occurred (Bennike *et al.* 2017). The shift in Arrefjord was dated to between 6700 and 6200 cal. years BP, apparently earlier than the shift registered in Brabrand Fjord. Lewis *et al.* (2016) discussed if the change in sedimentation rate dated to *c.* 5900 cal. years BP could be due to forest clearance by early farmers. However, only minor changes

in soil erosion rates are seen in lake records from the region during the relevant time interval (Bennike *et al*. 2021c). Increased sedimentation rates could also be caused by a relative sea level fall, which could lead to increasing erosion in the streams entering the fjords but it appears that increasing sedimentation rates occurred prior to sea level fall. Lewis *et al*. (2016) suggested that gradually falling temperatures following the Holocene thermal maximum as reconstructed by for example Brown *et al.* (2011) led to increasing sedimentation rates, but we find it difficult to see how falling temperatures could have a strong influence on sedimentation rates. We suggest that a decline in the tidal amplitude could be the factor that allowed fine-grained sediment to accumulate at a high rate in Brabrand Fjord in the Early Neolithic and caused a major shift in sedimentation rate in other fjords in the region.

We have not been able to provide a precise age for the transition from the fjord stage to the current lake stage, but bracketing ages from the core sites indicate that the shift occurred between 5200 and 2900 cal. years BP. The transition was caused by relative sea-level fall and longshore sediment transport along the shores of Aarhus Bugt, closing off the mouth of the fjord. There is a large hiatus in the upper part of the succession from core site A in Brabrand Fjord. This hiatus could be caused by the dredging of sediments from the lake.

The terrestrial fauna during the time of the Ertebølle culture included the mammals *B. primigenius* (aurochs), *E. ferus* (wild horse) and the bird *T. urogallus* (capercaillie). The presence of the latter two species may indicate that the forests in the area were fairly open. By the time of the Ertebølle culture, aurochs had died out on the Sjælland and Fyn, perhaps the forests on these islands had become too closed for this species. The marine fauna included *P. groenlandica* (harp seal) and *P. impennis* (great auk), bones of which have been recorded from many Middle Holocene sites in Denmark. Overall, the marine invertebrate and vertebrate faunas during the Middle Holocene were rich, reflecting higher than present-day temperatures, more salty water – and probably a larger tidal amplitude.

Conclusions

This macrofossil study of the palaeoenvironmental history of Brabrand Fjord shows that the area has a complex Holocene history. A stream drained the region that was transgressed by the sea at about 8500 years BP. The early marine fauna was species-poor, but during the Ertebølle culture a rich marine fauna with *Ostrea edulis* (oyster) was found in the fjord. The fauna and the presence of sandy sediments in the fjord indicate strong bottom currents, which were likely due to a high tidal amplitude. In the Early Neolithic, fine-grained gyttja accumulated rapidly in Brabrand Fjord and other fjords in the region. We suggest that a marked decrease in the tidal amplitude could be the reason. We could not date the transition from fjord to lake, probably because of dredging of sediments in the lake.

Acknowledgements

We thank Hans Skov and Uffe Rasmussen from Moesgaard Museum for information on archaeological excavations in the Brabrand Fjord area. Renée Enevold from Moesgaard Museum kindly organised a coring platform for us. The study was funded by Geocenter Denmark. We thank journal referees Morten Fischer Mortensen from the National Museum of Denmark and Renée Enevold from Moesgaard Museum for valuable comments on the manuscript.

References

Andersen, A. 1947: Resultatet af pollenanalysen 1945. *In* Haugsted, E. (ed.) 1947: Bopladsen på Rugholm. Aarhus Museums Undersøgelser ved Østenden af Brabrand Sø 1944-45, 32–36. Aarhus: Aarhus Byraad. https://doi.org/10.3109/08039484709139199

Andersen, S.H. 2007: Shell middens ("Køkkenmøddinger") in Danish prehistory as a reflection of the marine environment. In: Milner, N., Craig, O.E. & Bailey, G.N. (eds): Shell middens in Atlantic Europe, 31–45. Barnsley: Oxbow Books.

Bennike, O. & Wiberg-Larsen, P. 2002: Seed-like hydroptilid larval cases (Insecta: Trichoptera) from Holocene freshwater deposits. Journal of Paleolimnology 27, 275–278. https://doi.org/10.1023/a:1014270827121

Bennike, O., Rasmussen, P. & Aaris-Sørensen, K. 2008: The harp seal (*Phoca groenlandica* Erxleben) in Denmark, southern Scandinavia, during the Holocene. Boreas 37, 263–272. https://doi.org/10.1111/j.1502-3885.2007.00015.x

Bennike, O., Pantmann, P. & Aarsleff, E. 2017: Holocene development of the Arresø area, north-east Sjælland, Denmark. Bulletin of the Geological Society of Denmark 65, 25–35. https://doi.org/10.37570/bgsd-2017-65-02

Bennike, O., Jensen, J.B., Nørgaard-Pedersen, N., Andresen, K.J., Seidenkrantz, M.-S., Moros, M. & Wagner, B. 2021a: When were the straits between the Baltic Sea and the Kattegat inundated by the sea during the Holocene? Boreas 50, 1079–1094. https://doi.org/10.1111/bor.12525

Bennike, O., Andresen, K.J., Astrup, P.M., Olsen, J. & Seiden-

krantz, M.-S. 2021b: Late glacial and Holocene shore-level changes in the Aarhus Bugt area, Denmark. GEUS Bulletin 47, 6530. https://doi.org/10.34194/geusb.v47.6530

Bennike, O. *et al*. 2021c: Early historical forest clearance caused major degradation of water quality at Vængsø, Denmark. Anthropocene 35, 100302. https://doi.org/10.1016/j.ancene.2021.100302

Brooks, S.J., Langdon, P.G. & Heiri, O. 2007: The identification and use of Palaearctic Chironomidae larvae in palaeoecology. QRA Technical Guide 10, 276 pp. London: Quaternary Research Association. https://doi.org/10.1007/s10933-007-9191-1

Brown, K.J., Seppä, H., Schoups, G., Fausto, R.S., Rasmussen, P. & Birks, H.J.B. 2011: A spatio-temporal reconstruction of Holocene temperature change in southern Scandinavia. Holocene 22, 165–177. https://doi.org/10.1177/0959683611414926

Degerbøl, M. 1933: Danmarks Pattedyr i Fortiden i Sammenligning med recente Former. Videnskabelige Meddelelser fra Dansk Naturhistorisk Forening 96, 357–641.

Degerbøl, M. & Fredskild, B. 1970: The urus (*Bos primigenius* Bojanus) and the Neolithic domesticated cattle (*Bos taurus domesticus* Linnè) in Denmark. Det Kongelige danske Videnskabernes Selskab, Biologiske Skrifter 17(1), 234 pp. https://doi.org/10.1525/aa.1972.74.4.02a00900

Gravlund, P., Aaris-Sørensen, K., Hofreiter, M., Meyer, M., Bolback, J. & Noe-Nygaard, N. 2012: Ancient DNA extracted from Danish aurochs (*Bos primigenius*): Genetic diversity and preservation. Annals of Anatomy 194, 103–111. https://doi.org/10.1016/j.aanat.2011.10.011

Hatting, T. 1963: On subfossil finds of Dalmatian pelican (*Pelecanus crispus* Bruch.) from Denmark. Videnskabelige Meddelelser fra Dansk naturhistorisk Forening 125, 327–351. https://doi.org/10.5040/9781472926982.0087

Haugsted, E. (ed.) 1947: Bopladsen på Rugholm. Aarhus Museums Undersøgelser ved Østenden af Brabrand Sø 1944-45, 36 pp. Aarhus: Aarhus Byraad.

Heaton, T. J. *et al*. 2020: Marine20 – the marine radiocarbon age calibration curve (0-55,000 cal BP). Radiocarbon 62, 779–820. https://doi.org/10.1017/rdc.2020.68

Heinemeier, J. & Rud, N. 1999: Danske arkæologiske AMS ^{14}C-dateringer, Aarhus 1998. Arkæologiske udgravninger i Danmark 1998, 327–345.

Houmark-Nielsen, M., Linge, H., Fabel, D., Schnabel, C., Xue, S., Wilcken, K.M. & Binnie, S. 2012: Cosmogenic surface exposure dating the last deglaciation in Denmark: discrepancies with independent age constraints suggest delayed periglacial landform stabilisation. Quaternary Geochronology 13, 1–17. https://doi.org/10.1016/j.quageo.2012.08.006

Høy, T. 1979: Brabrand Sø, Århus Kommune, Århus Amt. Map sheet, 1:5000. Aarhus: Århus Amtsråd.

Jensen, J.B., Kuijpers, A., Bennike, O. & Lemke, W. 2002: Balkat – the Baltic Sea without frontiers. Geologi, nyt fra GEUS 2002(4), 19 pp.

Jessen, K. 1935: Archaeological dating in the history of North Jutland's vegetation. Acta Archaeologica 5(3), 185–214.

Jowsey, P.C. 1966: An improved peat sampler. New Phytologist 65, 245–248. https://doi.org/10.1111/j.1469-8137.1966.tb06356.x

Jupiter 2019: http://data.geus.dk/geusmap/?mapname=jupiter#baslay=baseMapGeologyDa25k&optlay=&extent=494988.34981802024,6169843.986865233,653013.041176045,6247457.155589513. Accessed January 2022.

Kveiborg, J. 2014: FHM 4880 Åby Renseanlæg-Regnvandsbassin Åby sogn, Hasle herred, Århus amt. Stednr. 15.03.10 KUAS-journalnummer: 2008-7.24.02/FHM-006. Rapport, Moesgaard Museum, 156 pp.

Kystdirektoratet 2019: Højvandsstatistikker, 86 pp. Lemvig: Kystdirektoratet.
hoejvandsstatistikker2017revideret11022019.pdf (kyst.dk)

Lambeck, K., Rouby, H., Purcell, Y.S. & Sambridge, M. 2014: Sea level and global ice volumes from the Last Glacial Maximum to the Holocene. Proceedings of the National Academy of the United States (PNAS) 111, 15296–15303. https://doi.org/10.1073/pnas.1411762111

Laursen, J.T. 2012: Aarhus Ådal til Brabrand Sø – kultur, natur, dyrelivet før og nu, 111 pp. Aarhus: Klim.

Lewis, J.P., Ryves, D.B., Rasmussen, P., Olsen, J., Knudsen, K.-L., Andersen, S.H., Weckström, K., Clarke, A.L., Andrén, E. & Juggins, S. 2016: The shellfish enigma across the Mesolithic-Neolithic transition in southern Scandinavia. Quaternary Science Reviews 151, 315–320. https://doi.org/10.1016/j.quascirev.2016.09.004

Lykke-Andersen, H. 1973: En begravet dal i Præ-kvartæret ved Århus. Dansk Geologisk Forening, Årsskrift for 1972, 111–118.

Madsen, A P., Müller, S., Neergaard, C., Petersen, C.G.J., Rostrup, E., Steenstrup, K.J.V. & Winge, H. 1900: Affaldsdynger fra Stenalderen i Danmark, 196 pp. Copenhagen: Reitzel.

Mangerud, J., Andersen, S.T., Berglund, B. & Donner, J. 1974: Quaternary Stratigraphy of Norden, a proposal for terminology and classification. Boreas 3, 109–126. https://doi.org/10.1111/j.1502-3885.1974.tb00669.x

Mertz, E.L. 1924: Oversigt over de sen- og postglaciale Niveauforandringer i Danmark. Danmarks Geologiske Undersøgelse II. Række, Vol. 41, 49 pp. https://doi.org/10.34194/raekke2.v41.6827

Muus, B.J. 1967: The fauna of Danish estuaries and lagoons. Meddelelser fra Danmarks Fiskeri- og Havundersøgelser Ny Serie 5, vol. 1, 316 pp.

Nordmann, V. 1903: Østersens (*Ostrea edulis* L.) Udbredelse i Nutiden og Fortiden i Havet omkring Danmark. Meddelelser fra Dansk Geologisk Forening 2 (9), 45–60.

Odgaard, B.V. 1994: Holocene vegetation history of northern West Jutland, Denmark. Opera Botanica 123, 171 pp.

Olsen, J., Rasmussen, P. & Heinemeier, J. 2009: Holocene temporal and spatial variation in the radiocarbon reservoir age of three Danish fjords. Boreas 38, 458–470. https://doi.org/10.1111/j.1502-3885.2009.00088.x

Pint, A., Frenzel, P., Fuhrmann, R., Scharf, B. & Wennrich, V. 2012: Distribution of *Cyprideis torosa* (Ostracoda) in Quaternary

atalassic sediments in Germany and its application for pelaeoecological reconstructions. International Review of Hydrobiology 97, 330–355. https://doi.org/10.1002/iroh.201111495

Rasmussen, U. 2009a: FHM 4879 Carl Blochs Gade. Århus Domsogn, Hasle herred, Århus amt. Stednr. 150311. Rapport, Moesgaard Museum, 10 pp. https://doi.org/10.7146/aul.242.173

Rasmussen, U. 2009b: FHM 5121 Viby Renseanlæg, Viby sogn, Ning herred, Århus amt. Stednr. 150413, Rapport, Moesgaard Museum, 10 pp.

Rasmussen, U. 2012: FHM 5326 Eskelund, Viby Sogn, Ning Herred, Aarhus Amt. Sted nr. 13.07.12, 13 pp. Rapport, Moesgaard Museum, Aarhus. https://doi.org/10.7146/aul.323.219

Rasmussen, U. 2017: FHM 5260 Ceresgrunden, Aarhus sogn, Hasle herred, tidl. Aarhus amt, sted-nr. 15.03.11, SB-nr. 205, KUAS-nr. 2011-7.24.02/FHM-0006, (LP 892). Rapport, Moesgaard Museum, 19 pp. https://doi.org/10.7146/aul.323.219

Reimer, P. *et al*. 2020: The IntCal20 Northern Hemisphere radiocarbon age calibration curve (0-55 cal kB). Radiocarbon 62, 725–757.

Skousen, H. 2008: Arkæologi i lange baner, 248 pp. Aarhus: Forlaget Moesgård.

Sommer, R.S., Benecke, N., Lõugas, L., Nelle, O. & Schmölcke, U. 2011: Holocene survival of the wild horse in Europe: a matter of open landscape? Journal of Quaternary Science 26, 805–812. https://doi.org/10.1002/jqs.1509

Sørensen, L. 2015: From hunter to farmer in northern Europe. Migration and adaptation during the Neolithic and Bronze Age. Acta Archaeologica 85, 276 pp.

Stuiver, M. & Polach, H.A. 1977: Discussion of reporting ^{14}C data. Radiocarbon 19, 355–363. https://doi.org/10.1017/s0033822200003672

Thomsen, T. & Jessen, A. 1906: Brabrand-Fundet fra den ældre Stenalder, arkæologisk og geologisk behandlet. Aarbøger for nordisk Oldkyndighed og Historie II. Række, Vol 21, 74 pp.

Troels-Smith, J. 1937: Pollenanalytisk Datering af Brabrand-Fundet. Danmarks Geologiske Undersøgelse IV. Række, Vol. 2, No. 16, 24 pp. https://doi.org/10.34194/raekke4.v2.6983

Troels-Smith, J. 1942: Geologisk Datering af Dyrholm-Fundet. Det Kongelige danske Videnskabernes Selskab. Arkæologiske Skrifter 1942–1948, Vol. 1(1), 137–212.

Walker, M. J. C. *et al*. 2019: Subdividing the Holocene Series/Epoch: formalization of stages/ages and subseries/subepochs, and designation of GSSPs and auxiliary stratotypes. Journal of Quaternary Science 34, 1–14. https://doi.org/10.1002/jqs.3097

Wiberg-Larsen, P., Bennike, O., Jensen, J.B. & Lemke, W. 2001: Trichoptera remains from early Holocene river deposits in the Great Belt, Denmark. Boreas 30, 299–306. https://doi.org/10.1111/j.1502-3885.2001.tb01049.x

First occurrence of a frog-like batrachian (Amphibia) in the Late Triassic Fleming Fjord Group, central East Greenland

VALERIAN J.P. JÉSUS, OCTÁVIO MATEUS, JESPER MILÀN & LARS B. CLEMMENSEN

Geological Society of Denmark
https://2dgf.dk

Received 21 February 2022
Accepted in revised form
2 July 2022
Published online
24 August 2022

Jésus, V.J.P., Mateus, O., Milàn, J. & Clemmensen, L.B. 2022. First occurrence of a frog-like batrachian (Amphibia) in the Late Triassic Fleming Fjord Group, central East Greenland. Bulletin of the Geological Society of Denmark, Vol. 70, pp. 117–130. ISSN 2245-7070. https://doi.org/10.37570/bgsd-2022-70-08

During the Triassic, Batrachia diverged into ancestors of frogs (Salientia) and salamanders (Caudata). Fossils of Triassic batrachians are rare and found only in a few outcrops, such as the Middle Sakamena Formation of Madagascar (Induan). Only three Triassic taxa have been described, the two early frogs *Triadobatrachus* and *Czatkiobatrachus* and the early salamander *Triassurus*. Here we describe a right ilium, collected in 1991, attributed to the first batrachian from the Late Triassic Carlsberg Fjord Member (Ørsted Dal Formation, Fleming Fjord Group) in the Jameson Land Basin, located in central East Greenland. The fossil specimen only displays the proximal part of a right ilium, missing its shaft. After a thorough comparison with several clades (lizards, temnospondyls, salamanders and frogs), we consider the specimen as a lissamphibian sharing feature with salientians and anurans: squarish acetabular region, deeply concave acetabular surface, laterally projecting acetabular rim, flat mesial surface. It is the youngest Triassic specimen of Batrachia to date and one of the northernmost of the Late Triassic.

Supplementary file: Features potentially used for differentiating ilia of anurans and urodeles with updated nomenclature and specimen NHMD-154502, *Triadobatrachus, Czatkobatrachus, Triassurus* and *Kokartus*.
https://doi.org/10.37570/bgsd-2022-70-08s1

Keywords: Lissamphibia, frogs, salamanders, ilium, Late Triassic, Fleming Fjord Group.

Valerian J. P. Jésus [valerian.jesus@mail.com], Museu da Lourinhã 2530-158 Lourinhã, Portugal. Octávio Mateus [omateus@fct.unl.pt], GEOBIOTEC, Departamento de Ciências da Terra, FCT-UNL Faculdade de Ciências e Tecnologia, Universidade Nova de Lisboa, Portugal & Museu da Lourinhã, Portugal. Jesper Milàn [jesperm@oesm.dk], Geomuseum Faxe, Østsjællands Museum, Rådhusvej 2, DK-4640 Faxe, Denmark. Lars B. Clemmensen [larsc@ign.ku.dk], Department of Geosciences and Natural Resource Management, University of Copenhagen, Øster Voldgade 10, DK-1350 Copenhagen K, Denmark.

Late Triassic lake and fluvial deposits from the Jameson Land Basin of central East Greenland have provided many vertebrates (e.g. Jenkins *et al.* 1994; Clemmensen *et al.* 2016; Agnolin *et al.* 2018; Marzola *et al.* 2018; Sulej *et al.* 2020; Beccari *et al.* 2021). In addition, trackways of archosaurs, including dinosaurs, are known from the same deposits (Jenkins *et al.* 1994; Klein *et al.* 2016; Lallensack *et al.* 2017), as well as coprolites (Hansen *et al.* 2016; Milàn *et al.* 2021) and abundant invertebrate trace fossils (Bromley & Asgaard 1979).

There have been several expeditions to study the Late Triassic deposits of the Jameson Land Basin in East Greenland since the 19th century (Marzola *et al.* 2018). Many expeditions focused on Mesozoic strata in Jameson Land during the late 1960s and early 1970s, leading to the discovery of rare vertebrate fossils from Triassic deposits, most of them being temnospondyl remains (Clemmensen 1980b). From 1988 to 2001, the Late Triassic of the Jameson Land Basin was the subject of successive vertebrate palaeontological expeditions to sample fossil tetrapods by Harvard University

(HU), Massachusetts, USA, in collaboration with the University of Copenhagen (UC), Denmark and the Natural History Museum of Denmark (NHMD). The team from the 1991 expedition recovered a large number of vertebrate fossils. Among them, we identify and describe an amphibian ilium in this paper.

The Triassic period witnessed the development and appearance of most tetrapod groups that constitute modern vertebrate fauna, such as mammaliaforms, squamates, crocodylomorphs and lissamphibians (Jenkins *et al.* 1997; Irmis *et al.* 2013; Ascarrunz *et al.* 2016; Simões *et al.* 2018; Sulej *et al.* 2020).

However, Batrachia Latreille, 1800 is rarely preserved in the fossil record from the first half of the Mesozoic. The cladogenesis of Anura Duméril, 1805 (frogs) and Urodela Duméril, 1806 (salamanders) is obscure, and their divergence is still debated but often estimated as Early Permian (Pyron 2011; Marjanović & Laurin 2014, 2019). The earliest batrachians have been recovered in the Olenekian of Madagascar, with the sub-complete specimen *Triadobatrachus massinoti* (Piveteau, 1936) and Poland, with disarticulated remains of *Czatkobatrachus polonicus* Evans & Borsuk-Białynicka, 1998. Both are members of the clade Salientia Laurenti, 1768, also known as proto-frogs (Piveteau 1936; Evans & Borsuk-Białynicka 1998, 2009a; Rage & Roček 1989; Ascarrunz *et al.* 2016). In Kyrgyzstan, the earliest Caudata Scopoli, 1777 (proto-salamanders) is *Triassurus sixtelae* Ivakhnenko, 1978, known from Middle to Upper Triassic (Ladinian/Carnian), with two reasonably complete specimens (Ivakhnenko 1978; Schoch *et al.* 2020). Recently, some new specimens of Salientia have been reported from the lower part of the Tiki Formation of India (possible Carnian in age), an incomplete jaw of an indeterminate *Eodiscoglossus* sp. (Kumar & Sharma 2019) and from the Chinle Formation of the United States, in Arizona, consisting of several ilia and a partial maxilla from the Late Triassic (Carnian/Norian; Stocker *et al.* 2021). The indeterminate *Eodiscoglossus* sp. identification remains dubious based on the resemblance of the material to one of Grigorescu *et al.* (1999), which had been later reassigned to *Paralatonia transylvanica* Venczel & Csiki, 2003 (see Venczel *et al.* 2016).

Here, we describe the first batrachian remains from the Carlsberg Fjord Member (Ørsted Dal Formation) in the Late Triassic Fleming Fjord Group in the Jameson Land Basin in central East Greenland (Clemmensen *et al.* 2020). This find adds new knowledge to the palaeogeographical distribution of the clade and adds to the diversity of the Late Triassic Greenland vertebrate fauna.

Taxonomic definition

Batrachia includes Salientia (frogs and proto-frogs) and Caudata (salamanders and proto-salamanders).

Salientia includes Anura (extant frogs) and every taxon closer to Anura than Urodela (Milner 1988).

Caudata includes Urodela (extant salamanders) and every taxon closer to Urodela than Anura (Milner 1988).

Geological setting

The Jameson Land Basin is situated in Jameson Land and Scoresby Land in central East Greenland, around 71° N (Clemmensen *et al.* 2020; Fig. 1). Its boundaries are the Stauning Alper in the west, the Liverpool Land area in the east, the fracture zones in the Kong Oscar Fjord region in the north and the Scoresby Sund in the south (Guarnieri *et al.* 2017; Clemmensen *et al.* 2020). During the Late Triassic period, East Greenland was located at 41° N on the northern rim of the supercontinent Pangaea, bordered by the Boreal Sea to the North (Clemmensen 1980a, b; Clemmensen *et al.* 1998; Kent & Tauxe 2005; Nøttvedt *et al.* 2008; Kent *et al.* 2014; Andrews & Decou 2018). The Jameson Land Basin was situated at the southern end of the East Greenland rift system, which formed part of a larger rift complex separating Greenland from Norway before the Atlantic opened (Ziegler 1988; Nøttvedt *et al.* 2008; Guarnieri *et al.* 2017). Since the Late Triassic, the basin has rotated 45° clockwise and translated 30° northward relative to present-day meridians (Kent & Tauxe 2005).

The Jameson Land Basin contains a relatively thick succession (~1.0 to 1.7 km) of Lower Triassic to Lower Jurassic continental sediments, including alluvial fan, braided river, aeolian dune, flood plain, saline playa lake and freshwater lake deposits (Clemmensen 1980a; Dam & Surlyk 1993; Clemmensen *et al.* 1998; Nøttvedt *et al.* 2008; Clemmensen *et al.* 2020). In the uppermost part of the Triassic succession (the Fleming Fjord Group), freshwater lake deposits are particularly well exposed on steep cliff sides facing the Carlsberg Fjord (Clemmensen *et al.* 2016, 2020). The Fleming Fjord Group, which has a thickness of about 350 m, consists of the basal Edderfugledal Formation, the middle Malmros Klint Formation and the uppermost Ørsted Dal Formation, including the Carlsberg Fjord Member (Clemmensen *et al.* 2020). Vertebrate fossils have primarily been found in lake and mudflat deposits from the two uppermost formations (Jenkins *et al.* 1994; Marzola *et al.* 2017; Clemmensen *et al.* 2020).

Material and Methods

Institutional Abbreviations: BSM: Bavarian State Collection for Palaeontology and Geology (Bayerische Staatssammlung für Paläontologie und historische Geologie), Munich, Germany; DMNH: Dallas Museum of Natural History (Perot Museum of Nature and Science), Dallas, Texas, United States; FMNH: Field Museum of Natural History, Chicago, Illinois, United States; GIN: Geological Institute of the Russian Academy of Sciences (Geologicheskiy Institut Ran), Moscow, Russia; JAM: Jósef Attila City Library and Museum Collection (Jósef Attila Városi Könyvtár és Muzeális Gyűjtemény), Komló, Hungary; HU: Harvard University, Cambridge, Massachusetts, United States; MMP: Municipal Museum of Natural Sciences 'Lorenzo Scaglia' (Museo Municipal de Ciencias Naturales 'Lorenzo Scaglia'), Mar del Plata, Argentina; MNHN: National Museum of Natural History (Muséum National d'Histoire Naturelle), Paris, France; NOVA: NOVA University Lisbon (Universidade NOVA de Lisboa), Lisbon, Portugal; NHMD: National History Museum of Denmark (Statens Naturhistoriske Museum), Copenhagen, Denmark; PEFO: Petrified Forest National Park; PIN: Palaeontological Institute of the Russian Academy of Sciences, Moscow, Russia; TMP: Royal Tyrell Museum of Palaeontology, Drumheller, Alberta, Canada; UC: University of Copenhagen (Københavns Universitet), Copenhagen, Denmark; UMNH: Utah Museum of Natural History, Salt Lake City, Utah, United States; ZPAL: Institute of Palaeobiology, Polish Academy of Sciences (Instytut Palaeobiologii, Polskiej Akademii Nauk), Warsaw, Poland; ZIN PH: Palaeoherpetollogical Collection, Zoological Institute, Russian Academy of Sciences, St Petersburg, Russia.

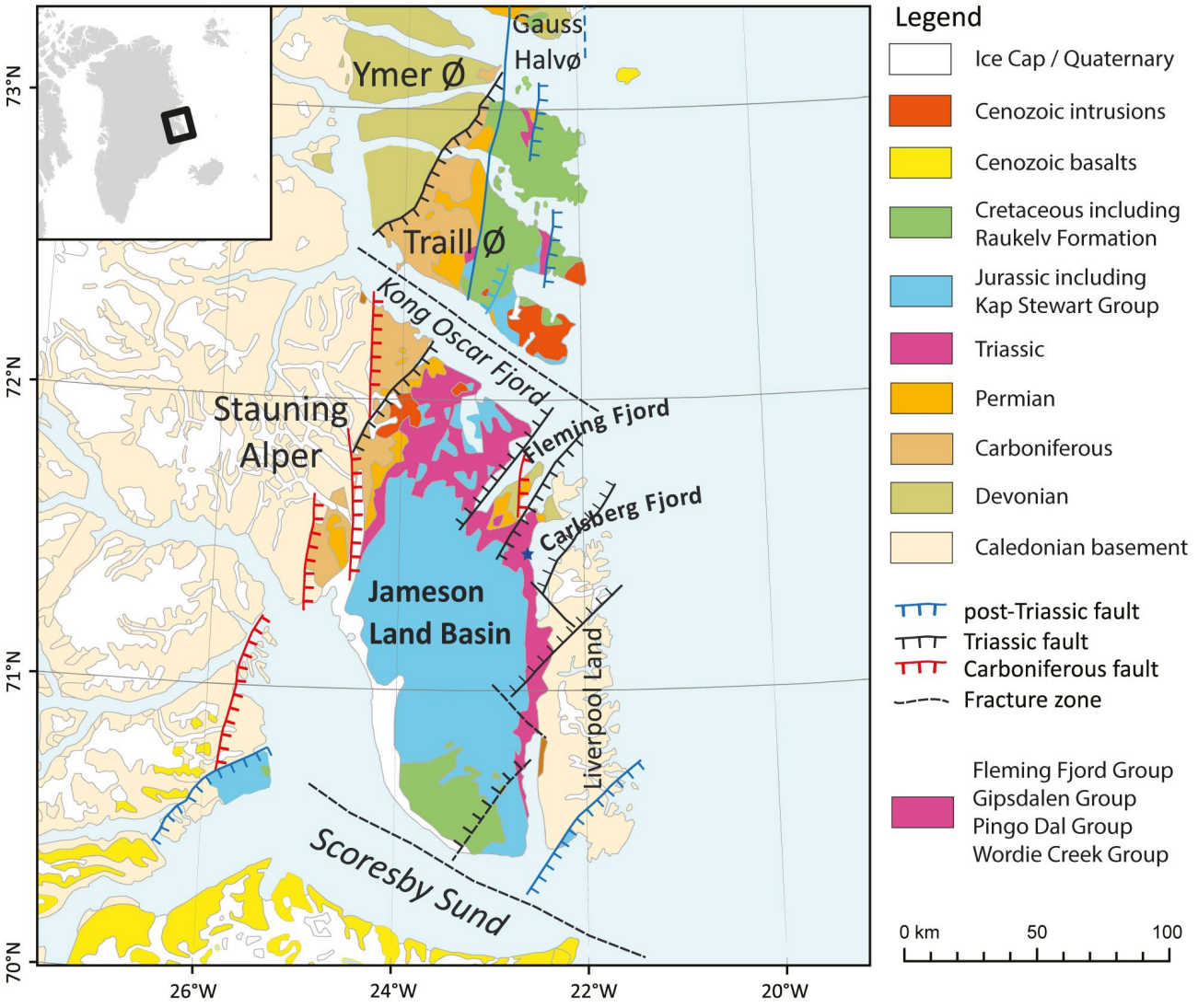

Fig. 1. Geological map of central East Greenland with the Jameson Land Basin. The blue star indicates the location of Tait Bjerg (from Clemmensen *et al.* 2020, modified).

The material presented here (NHMD-154502) was collected in 1991 during an expedition involving collaborations between the NHMD, the UC and HU (Jenkins *et al.* 1994). The specimen described here was sampled at Tait Bjerg from a thin bone bed 50 m above the base of the Carlsberg Fjord Member (Jenkins *et al.* 1994; site 62/91/G). The thin bone bed is situated within chron E15 (Kent & Clemmensen 2021), dating the specimen to approximately 212.5 Ma. The Carlsberg Fjord Member has recently been dated by magnetochronology and covers a period between 214 and 211 Ma within the Norian (Kent & Clemmensen 2021; Mau *et al.* 2022).

The material was photographed with a digital microscope (Dinolite pro AM4111T (R4)) and with an autonomous camera (FLEXACAM C1) fixed to a stereomicroscope (Leica M165 C) by stacking multiple pictures (~50) with the software Leica Application Suite X (LAS X) at the NOVA.

Terminology: We follow herein the terminology of Gómez & Turazzini (2016), slightly modified to adapt the comparison with non-salientian taxa. We decided to use 'acetabular surface' instead of 'acetabular fossa' since it can be flat and add three new terms: 'lateral oblique groove', 'posterior margin' and 'anterior margin'. The specimen has been compared with multiple materials representing various taxa.

Systematic palaeontology

Amphibia Linnaeus, 1758

Lissamphibia Haeckel, 1866

Batrachia Latreille, 1800

?Salientia Laurenti, 1768 (*sensu* Milner 1988) (aff.)

Specimen referred. Proximal part of a right ilium, NHMD-154502.

Locality. The specimen was collected during the 1991 American-Danish expedition to the eastern margin of the Jameson Land Basin, along the west slope of Tait Bjerg (71°28´34´´ North 22°40´43´´ West).

Horizon. A thin bone bed over- and underlain by purple, massive lake mudstone (Jenkins *et al.* 1994). Carlsberg Fjord Member of the Ørsted Dal Formation in the Fleming Fjord Group, Late Norian 212.5 Ma.

Description. The specimen (NHMD-154502) is a right ilium with a broken shaft. The acetabular surface

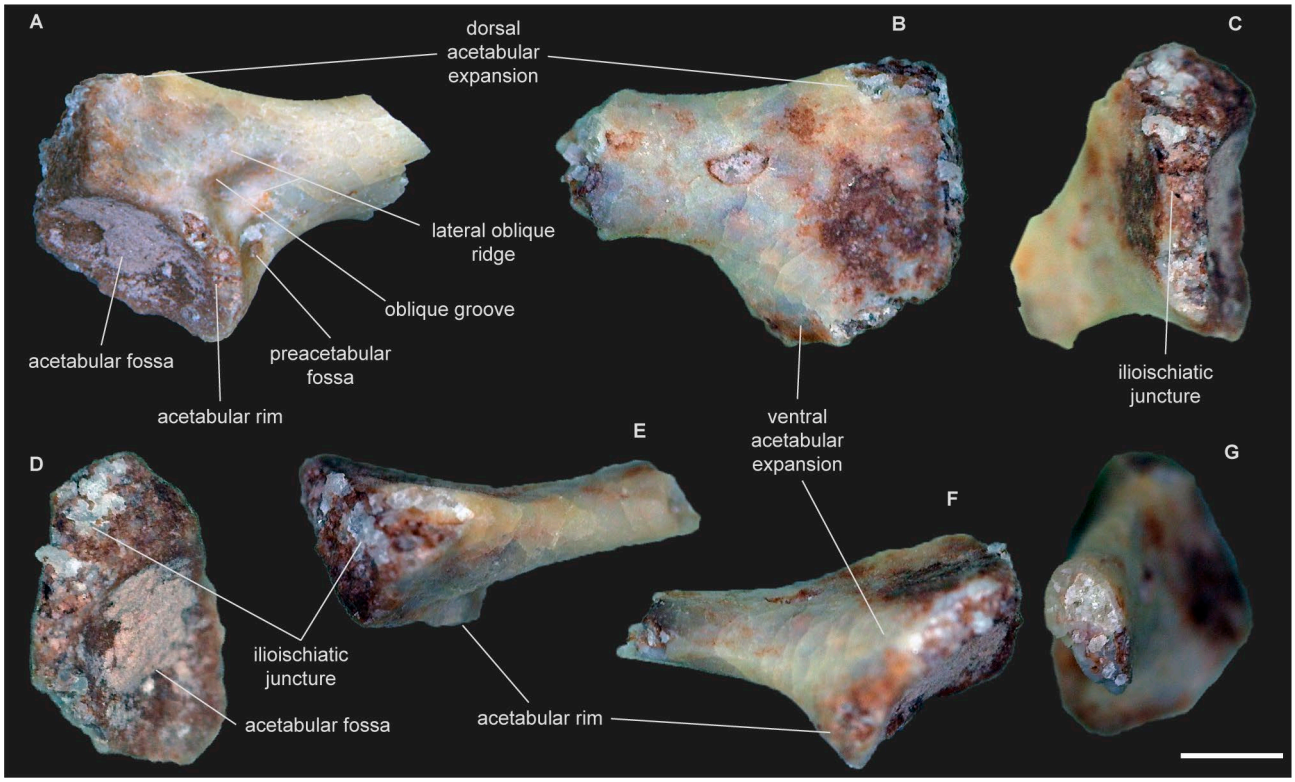

Fig. 2. Right ilium of the Greenland ?Salientia NHMD-154502. **A:** lateral view. **B:** medial view. **C:** proximal view. **D:** proximo-lateral view. **E:** ventral view. **F:** dorsal view. **G:** distal view.

forms a 1 mm wide (from the posteroventral edge to the acetabular rim) and 2 mm long (from posterior to ventral extremity) semi-circular deep concavity in the lateral view, sunk into the bone. It is bordered dorsally, anteriorly and ventrally by a convex acetabular rim strongly projected laterally, easily discernible anteriorly and ventrally (Figs 2A, E–F). Unfortunately, the posterior part of the dorsal acetabular expansion is not preserved, preventing us from fully understanding the actual shape of the ilial body. The dorsal acetabular expansion is well developed and triangular, while the ventral acetabular expansion is absent. The preacetabular zone is visible anterior to the acetabular surface. It is a circular fossa 0.5 mm broad and 0.1 mm deep (Fig. 2A). The medial surface is flat and slightly concave, with no interiliac tubercle (Figs 2B–C, E–F). In a proximal view, the ilioischiatic juncture is asymmetrical, its thickness varying mediolaterally, with the most dorsal part being 1 mm wide and the most ventral part 0.5 mm wide (Figs 2C–D). This difference in wideness is due to the dorsal acetabular expansion and acetabular rim participation and the absence of a ventral acetabular expansion in the shape of the ilioischiatic juncture. Its lateral half part is triangular with a roughened surface with its lateral tip joined by the acetabular rim. The rest of the ilioischiatic juncture surface has been damaged, not allowing us to understand how the ilium was attached to the ischium. The dorsal margin of the body between the shaft and the dorsal acetabular expansion is straight, lacking any dorsal prominence or dorsal tubercle (Figs 2A, F). The lateral surface exhibits two anterodorsally to posteroventrally inclined ridges, oblique to the shaft direction, anterior to the acetabular rim and dorsal to the preacetabular surface on the lateral surface (Fig. 2A). The most ventral ridge borders the preacetabular zone dorsally. It may be difficult to distinguish the dorsal lateral ridge from surface bone as it lacks any discernible process. The most notable features are its height and its flattened shape. The two short ridges are separated by a rectangular groove of 1 mm in length, 0.5 mm in width and as deep as the preacetabular zone (0.1 mm deep). The shaft cross-section is oval, with a height of 1.3 mm and a width of 0.7 mm; its ventral margin is mediolaterally compressed (Fig. 2G).

Discussion

The attribution to Lissamphibia was based on comparisons with several vertebrates known from the Late Triassic of the Jameson Land Basin and nearby localities (see Marzola *et al*. 2018). Despite differences in dimensions, it shares an overall similarity (ilial body and shaft) with several groups of Temnospondyli von Zittel, 1887 and Lepidosauromorpha Benton, 1983.

Comparison to Lepidosauromorpha

The shaft represents less than 50% of the body width in lateral view (Fig. 2A), being thinner than in lepidosauromorphs (Borsuk-Białynicka 2007, fig. 3; Evans & Borsuk-Białynicka 2009b, figs 11A, 11C1; Paparella *et al*. 2019, figs 1A–1C, 1G). Squamates display three distinct processes: the posterior process (or posterior iliac-blade), the preacetabular process and the anterior supracetabular process, lacking in some lepidosauromorphs, like *Sophineta cracoviensis* Evans & Borsuk-Białynicka 2009a, from the Early Triassic of Poland (Paparella *et al*. 2019). None of these features appears in the Greenland specimen, which has a deeper acetabular surface.

Comparison to Temnospondyls

Comparison to large Triassic Temnospondyls

Many temnospondyl specimens have been found in the Jameson Land Basin, lacking an ilium for comparison (see Marzola *et al*. 2018). The material was compared to specimens from other crops in the Early Mesozoic, mostly from Capitosauria Yates & Warren, 2000 and Trematosauria Yates & Warren, 2000, the two main groups that lived during the Late Triassic (Warden & Snell 1991; Yates & Warren 2000; Maisch *et al*. 2004). Since within temnospondyls, the shape of the ilium is highly variable between each clade (Schoch 1999), the specimen was compared to both groups individually (Figs 3A–C).

For Capitosauria, three species have been selected: *Paracyclotosaurus davidi* Watson, 1958, *Stanocephalosaurus pronus* (Howie, 1970) and *Mastodontosaurus giganteus* Jaeger, 1828. Their ilium is a short and stout piece of the pelvic girdle, comprising two parts expanded anteroposteriorly, as in most capitosaurs (Watson 1958, fig. 12; Howie 1970, fig. 18; Schoch 1999, fig. 46). Watson (1958) did not describe the ilium of *Paracyclotosaurus*; it is very similar to *Stanocephalosaurus*, which is described as a dorsoventrally short bone with an elongated, flattened shaft that expands distally (Howie 1970). The shaft is longer in *Mastodontosaurus* (Schoch 1999; Fig. 3B). The cross-section of the shaft is oval to nearly round ventrally and flattens dorsally. The proximal region, bearing most of the acetabulum, is also well expanded anteroposteriorly, especially on the posterior side, with the acetabular surface almost entirely on the ilium and consisting

of a little round concavity (Watson 1958; Howie 1970; Schoch 1999).

Comparison with Trematosauria is based on ilia from two trematosauroids: an indeterminate trematosaurid from the Middle Jurassic (Maisch *et al*. 2004) and *Trematolestes hagdorni* Schoch, 2006, from the Middle Triassic. In addition, we compared NHMD-154502 with two brachyopoids from the Late Triassic, *Compsocerops cosgriffi* Sengupta, 1935 and *Pelorocephalus mendozensis* Cabrera, 1944. Finally, two metoposauroids from the Late Triassic, *Metoposaurus diagnosticus krasiejowensis* Sulej, 2002 and *Apachesaurus gregorii* Hunt, 1993 were also used for comparison. The ilium is very similar to what is seen in Lissamphibia, especially for metaposaurids, with a long shaft, barely expanded to unexpanded anteroposteriorly, corresponding to more than 60% of the total length of the ilium, whereas the ilial body is extended on either side of the acetabular surface (Sengupta 1935, fig. 14; Marsicano 1993, fig. 10; Maisch *et al*. 2004, fig. 2; Schoch 2006, fig. 6; Sulej 2007, figs 58, 59; Spielmann & Lucas 2012, figs 26, 27). *Metoposaurus* differs by having a sinusoidal shaft oval to round in cross-section (Sulej 2007; Fig. 3C). The trematosauroids possess a well-defined acetabulum, though smaller than in the Greenland specimen (Maisch *et al*. 2004, figs 1, 2A; Schoch 2006, fig. 6). *Pelorocephalus* does possess two ridges on its lateral surface running along the shaft and joining each other at mid-length, and only one is close to the acetabular surface, which is limited by a sizeable nail-shaped rim (Marsicano 1993, fig. 10). *Compsocerops* has an acetabular surface that is more similar to our specimen. Its centre is under the edge of the base of the ilium; however, it is confined on both sides of its dorsal edge by two deep grooves (Sengupta 1935, fig. 14). The base of the ilium of metaposaurids has a right-angle shape, the lateral edge being the hypotenuse (Sulej 2007, fig. 59), a considerably different base compared to the Greenland specimen (Figs 2C, D).

Comparison to Amphibamiformes

To help in the allocation of NHMD-154502 to a clade, we also compared it with three representative specimens of Amphibamiformes Schoch, 2019: *Doleserpeton*

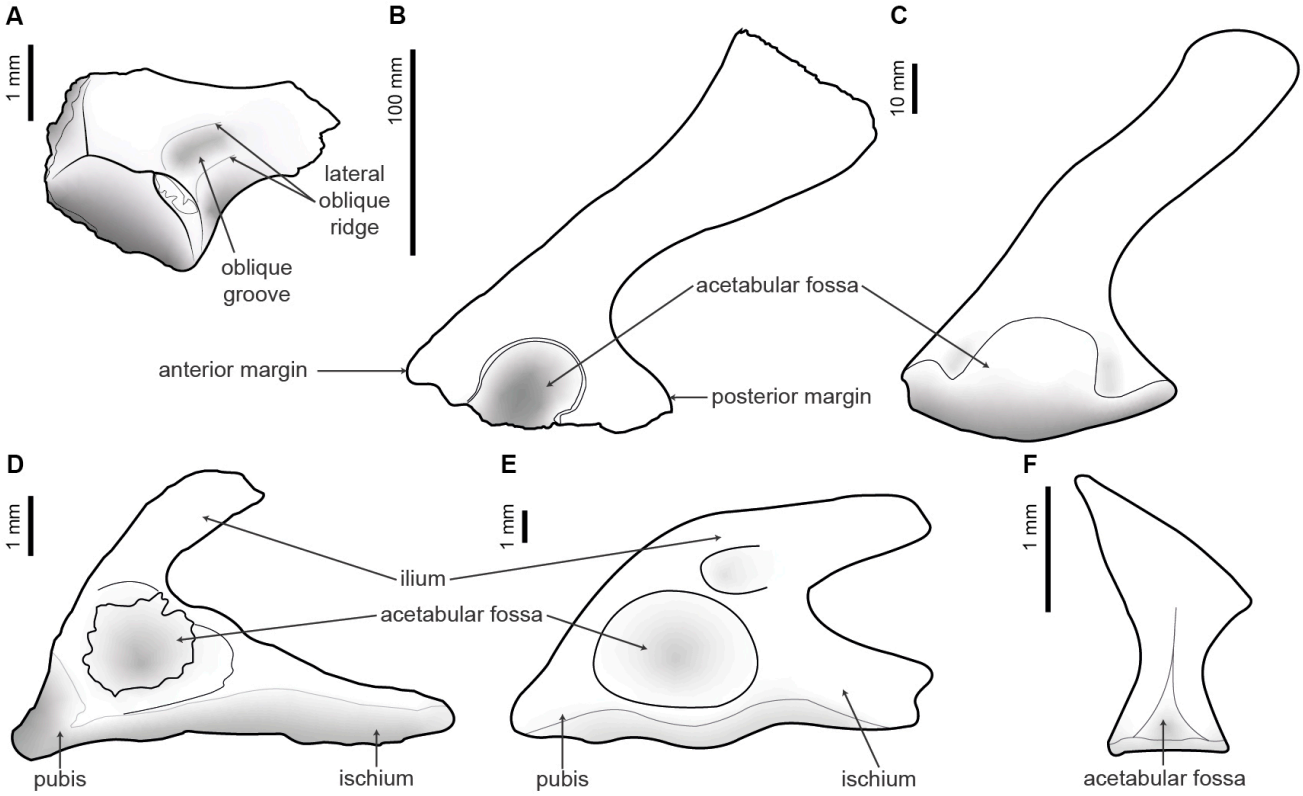

Fig. 3. Compilation of ilia, NHMD-154502 and temnospondyls. **A:** Right ilium of Ørsted Dal Formation specimen (NHMD-154502), Norian. **B:** Left ilium (inversed) of *Mastodonsaurus giganteus*, Ladinian, after Schoch (1999). **C:** Right ilium of *Metoposaurus diagnosticus krasiejowensis*, (ZPAL AbIII/632), Norian, after Sulej (2007). **D:** Right pelvis (ilium, pubis and ischium) of *Doleserpeton annectens*, (FMNH UR1379), Lower Permian, after Sigurdsen & Bolt (2010). **E:** Right pelvis (ilium, pubis and ischium) of *Micropholis stowi*, (BSM 1934 VIII 43C), Induan, after Schoch & Rubidge (2005). **F:** *Tungussogyrinus bergi*, (PIN 4262/4a), Late Permian to Early Triassic, after Wernerburg (2009).

annectens Bolt, 1969 (a Lower Permian amphibamid), *Micropholis stowi* Huxley, 1859 (a Lower Triassic micropholid) and *Tungussogyrinus bergi* Efremov, 1939 (a Late Permian – Early Triassic branchiosaurid); this clade, although mainly known in the Permian, is phylogenetically close to lissamphibians according to several analyses. We could not compare our specimen to *Gerobatrachus* due to a lack of details on the ilium of the specimen in the original publication.

The 4 mm long ilium of *Doleserpeton* is fused with pubis and ischium and has a dorsal blade oriented posterolaterally as large as two-thirds of the acetabular surface (Sigurdsen & Bolt 2010; Fig. 3D). The authors have lightly described the ilium of *Doleserpeton* in itself; the drawing suggests that the concave acetabular surface occupies a large part of the body of the ilium, and the anterior margin is fine and straight, although the posterior margin is concave and skinny. It reminds NHMD-154502 if we consider the dorsal acetabular expansion as the posterior margin, the main difference being that *Doleserpeton* has a wider ilial shaft, corresponding to two-thirds of the width of the acetabular surface, and a thinner anterior margin. The shaft of NHMD-154502 only represents half of its acetabular surface, and its dorsal acetabular expansion is extremely large (Fig. 3A). According to the drawing and the authors, no lateral structure has been spotted.

Similarly, *Micropholis* has an ilium fused with the other pelvic belt bones (Schoch & Rubidge 2005; Fig. 3E). The body is vast, the acetabulum occupying about 55% with a skinny and angular posterior margin forming a slope with the dorsal margin of the blade and an extensive anterior margin. The dorsal blade, shorter, is more inclined horizontally and narrows ventrodorsally at the tip. The bone has an oval fossa positioned anterodorsally to the acetabulum on the lateral surface, but Schoch & Rubidge (2005) did not mention it.

Tungussogyrinus has an ilium shaped like an hourglass (Fig. 3F). It is shaped like an isosceles triangle and framed by anterior and posterior margins of the same width. The dorsal shaft extends in the anteroposterior axis, especially in the anterior direction (Werneburg 2009). The acetabulum occupies only a tiny proportion of the body.

NHMD-154502 differs from the typical ilia of Triassic temnospondyls. First, there is an essential variation in size between the multiple temnospondyl taxa and NHMD-154502. For example, the ilia of *Mastodontosaurus* are around 25 cm long (Fig. 3B), while the ilia of *Metoposaurus* vary from 6 cm to 10 cm long (Sulej 2007). NHMD-154502 is closer to amphibamiforms in size (*e.g. Doleserpeton*: 4 mm long). As seen before, temnospondyl ilia have an anteroposteriorly expanded dorsal blade and a massive anteroposteriorly expanded ventral part bearing the dorsal part of the acetabular surface (Warden & Snell 1991). The acetabular surface is mainly centred in large temnospondyls (Schoch 1999, fig. 46; Maisch *et al.* 2004, fig. 1; Sulej 2007, figs 58, 59). On the other hand, this surface is offset in amphibamiforms and the Greenland specimen (Figs 3A, D–F), as in many salientians (Shubin & Jenkins 1995; Evans & Borsuk-Białynicka 1998; Ascarrunz *et al.* 2016; Stocker *et al.* 2019). Moreover, most temnospondyls lack any structure on the lateral surface of the ilium, as seen in the specimen presented here (Fig. 3A), refuting the possibility of attribution of the Greenland ilium to this group.

Comparison to Caudata/Urodela

The ilium of salamander and frog are very alike. Thanks to a few papers, it is now easier to differentiate the two groups when only scattered fragments are present, such as, for example, the ilium. For salamanders, this element shares some similarities with ilia of non-lissamphibian temnospondyls (Fig. 4).

Comparison to Caudata

Unfortunately, among the few ilia of stem-Caudata preserved, they are generally flattened due to the preservation, making it difficult to appreciate their actual shapes. Among the caudate species known in the bibliography, only ilia of *Triassurus sixtelae* and *Kokartus honorarius* Nesov, 1988 could have been observed, the other taxa missing this element (see Skutschas *et al.* 2018 for *Kulgeriherpeton*; Evans *et al.* 1988 for *Marmorerpeton*; Skutschas & Krasnolutskii 2011 for *Urupia*). The ilium of *Triassurus* is very similar to those of temnospondyl, looking like an hourglass in lateral view, with a triangular acetabular region (Schoch *et al.* 2020: figs 1C, 2B).

Seven ilium fragments have been identified for *Kokartus*, preserving only the acetabulum region and the base of the shaft (Averianov *et al.* 2008; Fig. 4B). According to the authors, the acetabular surface has the shape of a kidney and is bordered anteriorly and posteriorly by slit-like depressions. The ilioischiatic juncture is asymmetrical and convex, thickened anteriorly in a similar way to NHMD-154502, although it is thickened dorsally for the latter (see Averianov *et al.* 2008: fig. 7O). The authors did not mention the form of the acetabular surface, but it seems shallowly concave. The presence of a protuberance projecting laterally at the dorsal margin of the acetabular surface distinguishes it from our specimen.

Comparison to Urodela

The ilium of Urodela does not differ significantly from stem-Caudata: a triangular acetabular region in lateral

view, with posterior and anterior margins almost subequally developed, with a smooth medial surface, either flat or convex and a thin asymmetrically concave ilioischiatic juncture with lateral edge excavated and grading into the acetabular surface (Gardner *et al.* 2010). The acetabular surface of Urodela varies highly in shape: generally, distally elongate, longer than larger (kidney-shape), subtriangular or semi-circular (Gardner *et al.* 2010; Figs 4C–E). The acetabular surface varies from shallowly concave or flat to flat saddle-shaped or sinuous (Gardner *et al.* 2010; Roček *et al.* 2012). *Kokartus* shows that the acetabular surface can be delimited by a low rim that does not extend laterally (Averianov *et al.* 2008). In some cases, the portion closest to the base of the shaft can project laterally in a ramp-like structure (Roček *et al.* 2012), as seen in *Andrias scheuchzeri* (Holl, 1831) and the indeterminate Urodela (Roček *et al.* 2012, fig. 2S; Szentesi *et al.* 2020; Figs 4D–E).

Comparison to Salientia/Anura

Contrary to salamanders, the pelvic girdle of frogs and their relatives had changed significantly from its ancestral state to allow the jumping locomotion specific to the group. Instead of projecting globally dorsally in salamanders, their elongated ilia display a shaft oriented anteriorly to anterodorsally (Milner 1988; Ford & Cannatella 1993) temnospondyls. This condition is present among the earliest salientians, *Triadobatrachus* and *Czatkobatrachus*, in the Chinle specimens and anurans (Gardner *et al.* 2010), although the shaft is shorter in the former. Due to this rotation, the acetabular surface turns posterolaterally to laterally in extant frogs (Gardner *et al.* 2010; Roček *et al.* 2012). We note a similar condition in *Triadobatrachus*, where the acetabulum faces more laterally (Ascarrunz *et al.* 2016). Since the Greenland specimen is only an isolated ilium without its shaft, we can only suggest the putative direction of the acetabular surface being oriented posterolaterally and ventrally if considering the shaft is oriented laterally as in Salientia (Ford & Cannatella 1993).

Comparison to Salientia

In contrast to Caudata, isolated ilia of Salientia have been found multiple times and described. The outline of their ilial body in lateral view, excluding the acetabulum fossa, is triangular as in *Triadobatrachus* and the Chinle specimens, or squarish as seen in *Czatkobatrachus*, with a dorsal acetabular expansion well developed and barely developed (or absent) ventral acetabular expansion for all three (Figs 5B–E). The acetabular surface on their ilia is semi-circular and concave (Rage & Roček 1989; Stocker *et al.* 2019), whereas in *Czatkobatrachus*, the whole surface is subtriangular and shallow (Evans & Borsuk-Białynicka 2009). The acetabular rim does not stand out in *Czatkobatrachus* while it is easily discernible anteriorly and ventrally for *Triadobatrachus* and the Chinle specimens (Stocker *et al.* 2019; Figs 5B, D–E).

The medial surface is smooth, flat (or slightly concave) and does not bear any trace of an interiliac tubercle in *Triadobatrachus* and *Czatkobatrachus*, while it is not visible in the Chinle specimens (Rage & Roček

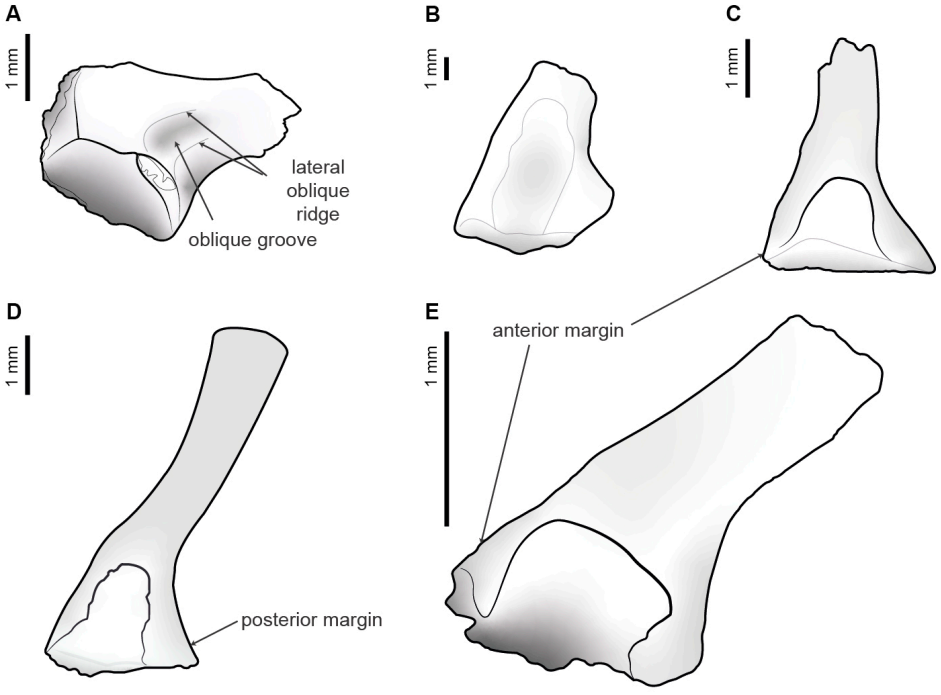

Fig. 4. Compilation of ilia, NHMD-154502 and salamanders. **A:** Right ilium of Ørsted Dal Formation specimen (NHMD-154502), Norian. **B:** Left ilium of *Kokartus honorarius*, (ZIN PH 48/47), Bathonian, after Averianov *et al.* (2008). **C:** Left ilium of Urodela indet., (TMP 96.78.199), Campanian, after Roček *et al.* (2012). **D:** Left ilium of *Ambystoma mexicanum*, (TMP 2010.30.06), Recent, after Gardner *et al.* (2010). **E:** Left ilium of *Andrias scheuchzeri*, (JAM 2006.185.47), Miocene, after Szentesi *et al.* (2020).

1989; Evans & Borsuk-Białynicka 2009; Stocker *et al*. 2019: see supplementary file).

The ilioischiatic juncture has not been described or shown for *Triadobatrachus*, *Czatkobatrachus* or the Chinle specimens. For the first, ilia and ischia junctions are obscured because of overlapping in the fossil (Ascarrunz *et al*. 2016) In the case of *Czaktobatrachus*, the ilia are fused with the ischia, preventing any accurate description of the juncture (Evans & Borsuk-Białynicka 2009). Furthermore, for the Chinle specimens, this area is too damaged for accuracy (Stocker *et al*. 2019).

Both earliest salientians, *Triadobatrachus* and *Czaktobatrachus*, share a dorsal prominence positioned between the dorsal acetabular expansion and the ilial shaft (Rage & Roček 1989; Evans & Borsuk-Białynicka 2009), which differs them from NHMD-154502.

Comparison to Anura

Frogs possess an ilium remarkably similar to stem-Salientia: a triangular to squarish ilial body in lateral view, with strongly divergent dorsal and ventral acetabular expansions; a small to a large semi-circular or subtriangular acetabular surface whose deepness varies from deeply concave to bowl-shaped and partially sunk into the bone; the medial surface is smooth and flat to shallowly concave and may bear an interiliac tubercle; an ilioischiatic juncture flat or shallowly convex with a sharp posterolateral edge to distinct itself from the acetabular surface (Gardner *et al.* 2010).

Concerning the interiliac tubercle, anurans may bear a triangular one on the medial surface of the ilial body (Gardner *et al.* 2010; Roček *et al*. 2012), confirmed by Gómez & Turazzini (2016), who stated its absence in neobatrachians (except two genera), and that it is significantly developed only in aquatic taxa (e.g. pipids and palaeobatrachids). In extant frogs, the ilioischiatic juncture is thickened mediolaterally in most pipimorph and narrow in most other anurans (Gómez & Turazzini 2016), meaning that its thickness does not help in the differentiation between Anura and Urodela, as stated by Gardner *et al*. (2010) and Roček *et al*. (2012), even more, if we consider that both papers contradict them on that point.

As the description shows, NHMD-154502 displays various features on its lateral surface, like two ridges and a groove. A single lateral oblique ridge has been spotted in several pipimorphs (see Báez *et al*. 2012, figs 3B, 4A; Gómez & Turazzini 2016, fig. 3D; Fig. 5H). More

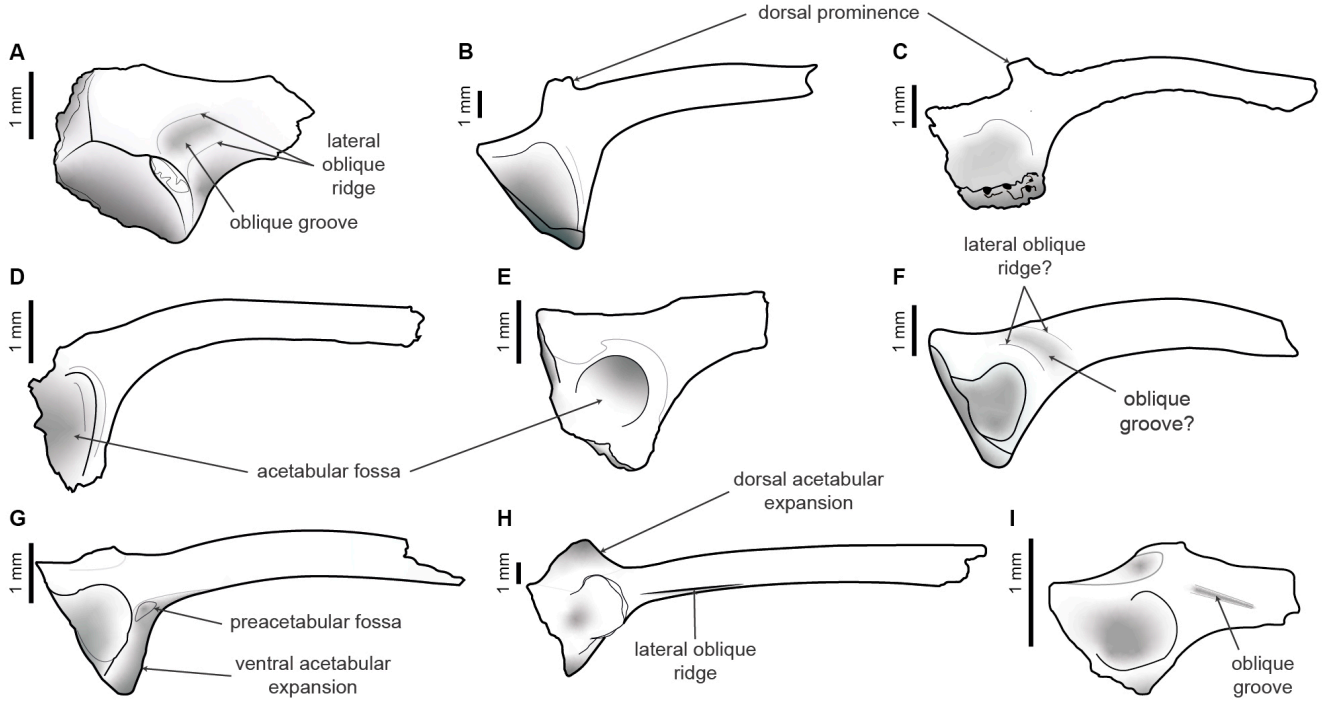

Fig. 5. Compilation of ilia, NHMD-154502 and frogs. **A:** Right ilium of Ørsted Dal Formation specimen (NHMD-154502), Norian. **B:** Right ilium of *Triadobatrachus massinoti*, (MNHN.F.MAE126), Induan, after Ascarrunz *et al.* (2016). **C:** Right ilium of *Czatkobatrachus polonicus*, (ZPAL AbIV/114), Induan, after Evans & Borsuk-Białynicka (2009a). **D–E:** Right ilia of Chinle Formation specimens (**D**, DMNH 2018-05-0002; **E**, PEFO 41743), Norian, after Stocker *et al.* (2019). **F:** Right ilium of *Prosalirus bitis*, (MCZ 9324A), Pliensbachian, after Jenkins & Shubin (1998). **G:** Left ilium (inversed) of *Bufo viridis*, (GIN-11142/120), early Middle Pleistocene, after Tesakov *et al.* (2019). **H:** Right ilium of a pipid from Daireaux (MMP M-5121), Upper Pleistocene, after Báez *et al.* (2012). **I:** Left ilium (reversed) of Dakota Formation specimen (UMNH 13158), late Cenomanian, after Roček *et al.* (2010).

interestingly, *Prosalirus bitis* Shubin & Jenkins, 1995, an early Jurassic anuran, possesses two lateral oblique ridges, although they are located more dorsally and are inclined in the opposite directions, perpendicular to the ilial shaft (Shubin & Jenkins 1995; Gardner *et al.* 2010; Fig. 5F). The groove separating the two lateral ridges is reminiscent of a similar wider and shorter structure described in anurans from the Late Cretaceous of Utah (Roček *et al.* 2010, figs 5J–K; Fig. 5I). NHMD-154502 shows both types of structures, ridges and a groove; thus, both structures could be present on other specimens, but their presence means nothing concerning the inclusion of NHMD-154502 in Anura since they have not been considered in numerous phylogenetic analyses, except Báez *et al.* (2012), and are typically absent in the majority of anuran (Gómez & Turazzini 2016).

Summary of the comparison

The supplementary file (adapted from Gardner *et al.* 2010, Appendix 1) helps to differentiate the ilia of anurans, urodeles, NHMD-154502, two salientians (*Triadobatrachus* and *Czatkobatrachus*) and two caudates (*Triassurus* and *Kokartus*). The specimen shares more features with salientians and anurans than any other clade: squarish acetabular region, deeply concave acetabular surface, laterally projecting acetabular rim and flat mesial surface. Triassic caudates are incomplete or not detailed enough, and the features concerning the shaft cannot be treated for NHMD-154502. Based on these statements, NHMD-154502 is considered as a batrachian closer to Salientia than to Caudata.

Triassic lissamphibians are poorly documented, with only three well-known genera: *Triadobatrachus*, *Czatkobatrachus* and *Triassurus* (Piveteau 1936; Ivakhnenko 1978; Evans & Borsuk-Białynicka 1998). The Greenland specimen is the first lissamphibian reported from the Jameson Land Basin in East Greenland. Therefore, it is one of the northernmost Triassic occurrences of Lissamphibia and most likely the youngest, dated to 212.5 Ma (Fig. 6). The earliest frogs (including at least a complete ilium) described from the Late Triassic are the Chinle specimens from Arizona, dated from 217 Ma to 213 Ma (Stocker *et al.* 2019).

Conclusion

This study describes the first lissamphibian discovered from the Triassic of the Jameson Land Basin, Greenland, based on an incomplete right ilium from the Norian of the Carlsberg Fjord Member (Ørsted Dal Formation) in the Fleming Fjord Group.

The ilium has been compared to various taxa such as lepidosauromorphs, temnospondyls, salamanders and frogs. It is identified as a batrachian displaying

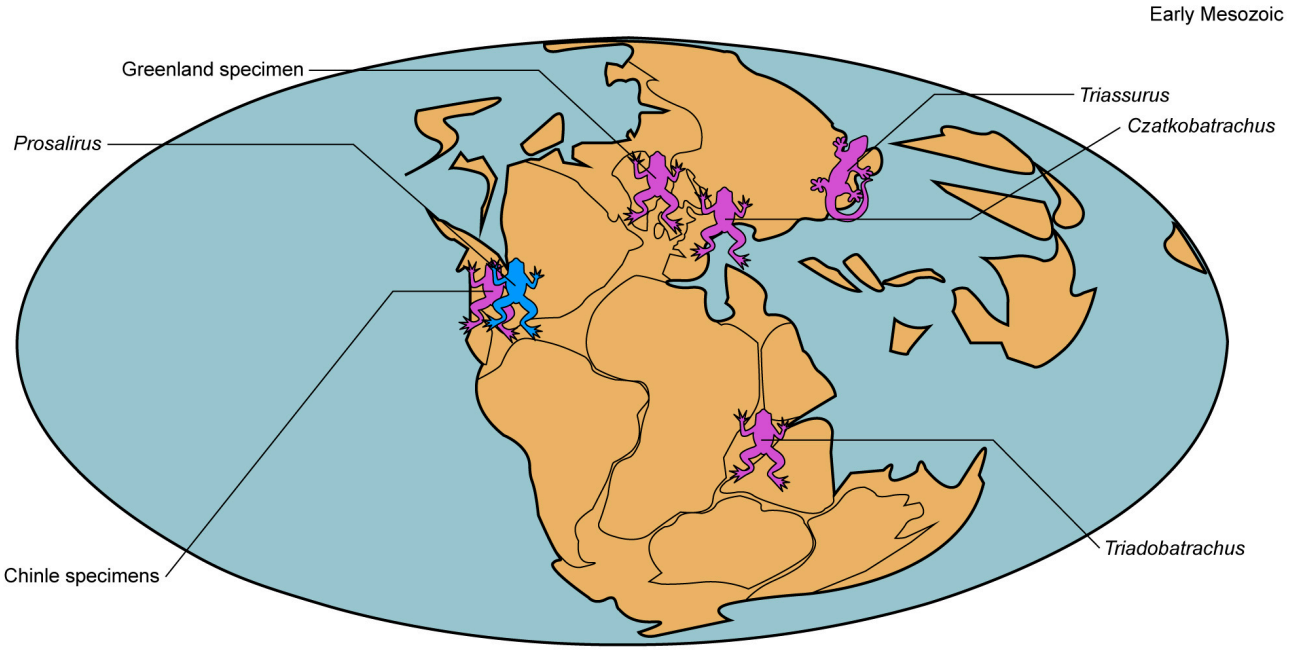

Fig. 6. Triassic palaeogeography, with localities of Triassic batrachian and the Greenland specimen. Frog and salamander icons mark the location of each specimen; purple for a Triassic locality and blue for an Early Jurassic locality (Paleobiology Database; Authorizers: M. Carrano, R. Butler, T. Cleary and J. Alroy).

several features suggesting an affinity with salientians: a squarish acetabular region, deeply concave acetabular fossa, laterally projecting acetabular rim, and flat mesial surface. This study reinforces the view that, during the Late Triassic, batrachians were more widespread than previously known and reached as far north as 41° palaeolatitude. It is also one of the northernmost occurrences of Batrachia from the Late Triassic.

Acknowledgements

This research benefited from the GeoBioTec-GeoBioSciences, GeoTechnologies and GeoEngineering NOVA [GeoBioCiências, GeoTecnologias e GeoEngenharias], grant UIDB/04035/2020 by the Fundação para a Ciência e Tecnologia. This study could not have been possible without the team that uncovered this specimen, Farish A Jenkins Jr., William W. Amaral, William R. Downs III, Stephen M. Gatesy, Neil H. Shubin Niels Bonde and Lars B. Clemmensen. We thank Harvard University and Bent Lindow from the Natural History Museum of Denmark. Thanks to Alexandre Guillaume and Vincent Cheng for reviewing and bringing improvements to the original manuscript and Carla Tomás for laboratory support. Alfred Lemierre and an anonymous reviewer are thanked for their comments on the manuscript.

References

Agnolin, F.L., Mateus, O., Milàn, J., Marzola, M., Wings, O., Adolfssen, J.S. & Clemmensen, L.B. 2018: *Ceratodus tunuensis* sp. nov., a new lungfish (Sarcopterygii, Dipnoi) from the Late Triassic of central East Greenland. Journal of Vertebrate Paleontology 38, e1439834, 1–6. https://doi.org/10.1080/02724634.2018.1439834

Andrews, S. & Decou, A. 2018: The Triassic of Traill Ø and Geographical Society Ø, East Greenland: Implications for North Atlantic palaeogeography. Geological Journal 54, 2124–2144. https://doi.org/10.1002/gj.3287

Ascarrunz, E., Rage, J.-C., Legreneur, P. & Laurin, M. 2016: *Triadobatrachus massinoti*, the earliest known lissamphibian (Vertebrata: Tetrapoda) re-examined by μCT scan, and the evolution of trunk length in batrachians. Contributions to Zoology 85, 201–234. https://doi.org/10.1163/18759866-08502004

Averianov, O.A., Martin, T., Skutschas, P.P., Rezvyi, A.S. & Bakirov, A.A. 2008: Amhibians from the Middle Jurassic Balabansai Svita in the Fergana Depression, Kyrgystan (Central Asia). Palaeontology 51(2), 471–485. https://doi.org/10.1111/j.1475-4983.2007.00748.x

Báez, A.M., Gómez, R.O. & Taglioretti, M.L. 2012: The archaic ilial morphology of an enigmatic pipid frog from the Upper Pleistocene of the South American Pampas. Journal of Vertebrate Paleontology 32, 304–314. https://doi.org/10.1080/02724634.2012.637591

Beccari, V., Mateus, O., Wings, O., Milàn, J. & Clemmensen, L.B. 2021: *Issi saaneq* gen. et sp. nov. – A new sauropodomorph dinosaur from the Late Triassic (Norian) of Jameson Land, Central East Greenland. Diversity 13, 561. https://doi.org/10.3390/d13110561

Benton, M.J. 1983: The Triassic reptile *Hyperodapedon* from Elgin: functional morphology and relationships. Philosophical Transactions of the Royal Society, Series B 302, 605–717. https://doi.org/10.1098/rstb.1983.0079

Bolt, J.R. 1969: Lissamphibian Origins: Possible Protolissamphibian from the Lower Permian of Oklahoma. Science 166, 888–891. https://doi.org/10.1126/science.166.3907.888

Borsuk-Białynicka, M. 2007: Evolution of the iliosacral joint in diapsid phylogeny. Neues Jahrbuch für Geologie und Paläontologie – Abhandlungen 249, 297–311. https://doi.org/10.1127/0077-7749/2008/0249-0297

Bromley, R.G., & Asgaard, U. 1979: Triassic freshwater ichnocoenosis from Carlsberg Fjord, East Greenland. Palaeogeography, Palaeoclimatology, Palaeoecology 28, 39–80. https://doi.org/10.1016/0031-0182(79)90112-3

Cabrera, A. 1944 : Sobre un estegocéfalo de la provincia de Mendoza. Notas Museo Universidad Nacional de La Plata IX, Paleontología 69, 421–429.

Clemmensen, L.B. 1980a: Triassic lithostratigraphy of East Greenland between Scoresby Sund and Kejser Franz Josephs Fjord. Grønlands Geologiske Undersøgelse Bulletin 139, 56 pp. https://doi.org/10.34194/bullggu.v139.6681

Clemmensen, L.B. 1980b: Triassic rift sedimentation and palaeogeography of central East Greenland. Grønlands Geologiske Undersøgelse Bulletin 136, 72 pp. https://doi.org/10.34194/bullggu.v136.6678

Clemmensen, L.B., Kent, D.V. & Jenkins, F.A. Jr. 1998: A Late Triassic lake system in East Greenland: facies, depositional cycles and palaeoclimate. Palaeogeography, Palaeoclimatology, Palaeoecology 140, 135–159. https://doi.org/10.1016/S0031-0182(98)00043-1

Clemmensen, L.B., Milàn, J., Adolfssen, J.S., Estrup, E.J., Frobøse, N., Klein, N., Mateus, O. & Wings, O. 2016: The vertebrate-bearing Late Triassic Fleming Fjord Formation of central East Greenland revisited: stratigraphy, palaeoclimate and new palaeontological data. In: Kear, B.P. *et al.* (eds): Mesozoic Biotas of Scandinavia and its Arctic Territories. Geological Society, London, Special Publications 434, 31–47. https://doi.org/10.1144/SP434.3

Clemmensen, L.B., Kent, D.V., Mau, M., Mateus, O. & Milàn, J. 2020: Triassic lithostratigraphy of the Jameson Land Basin (central East Greenland), with emphasis on the new Fleming Fjord Group. Bulletin of the Geological Society of Denmark 68, 95–132. https://doi.org/10.37570/bgsd-2020-68-05

Dam, G. & Surlyk, F. 1993: Cyclic sedimentation in a large wave

and storm-dominated anoxic lake; Kap Stewart Formation (Rhaetian–Sinemurian), Jameson Land, East Greenland. Special publication of the International Association of Sedimentologists 18, 419–448.

Duméril, A.M.C. 1805: Zoologie analytique, ou méthode naturelle de classification des animaux, rendue plus facile à l'aide de tableaux synoptiques, 344 pp. https://doi.org/10.5962/bhl.title.44835

Efremov, J.A. 1939: First representative of Siberian early Tetrapoda. Comptes-Rendus des Seances de l'Academie des Sciences de l'URSS 23(1), 106–110.

Evans, S. & Borsuk-Białynicka, M. 1998: A stem-group frog from the early Triassic of Poland. Acta Palaeontologica Polonica 43, 573–580.

Evans, S. & Borsuk-Białynicka, M. 2009a: The Early Triassic stem-frog *Czatkobatrachus* from Poland. Palaeontologica Polonica 65, 79–105.

Evans S.E. & Borsuk-Białynicka, M. 2009b: A small lepidosauromorph reptile from the Early Triassic of Poland. Paleontologica Polonica 65, 179–202.

Evans, S.E., Milner, A.R. & Mussett, F. 1988: The earliest known Salamanders (Amphibia, Caudata): A record from the Middle Jurassic of England. Geobios 21, 539–552. https://doi.org/10.1016/s0016-6995(88)80069-x

Ford, L.S., & Cannatella, D.C. 1993: The major clades of frogs. Herpetological Monographs 7, 94–117. https://doi.org/10.2307/1466954

Gardner, J.D., Roček, Z., Přikryl, T., Eaton, J.G., Blob, R.W. & Stankey, J.T. 2010: Comparative morphology of the ilium of anurans and urodeles (Lissamphibia) and a re-assessment of the anuran affinities of *Nezpercius dodsoni* Blob *et al*. 2001. Journal of Vertebrate Paleontology 30, 1684–1696. https://doi.org/10.1080/02724634.2010.521605

Gómez, R.O. & Turazzini, G.F. 2016: An overview of the ilium of anurans (Lissamphibia, Salientia), with a critical appraisal of the terminology and primary homology of main ilial features. Journal of Vertebrate Paleontology 36, e1030023. https://doi.org/10.1080/02724634.2015.1030023

Guarnieri, P., Brethes, A. & Rasmussen, T.M. 2017: Geometry and kinematics of the Triassic rift basin in Jameson Land (East Greenland). Tectonics 36, 602–614. https://doi.org/10.1002/2016TC004419

Grigorescu, D., Venczel, M., Csiki-Sava, Z. & Limberea, R. 1999: New latest Cretaceous microvretebrate fossil assemblage from the Haţeg Basin (Romania). Geologie en Mijnbouw 78, 301–314. https://doi.org/10.1023/A:1003890913328

Hansen, B.B., Milàn, J., Clemmensen, L.B., Adolfssen, J.S., Estrup, E.J., Klein, N., Mateus, O. & Wings, O. 2016: Coprolites from the Late Triassic Kap Stewart Formation, Jameson Land, East Greenland: Morphology, classification and prey inclusions. Geological Society, London, Special Publications 434, 46–49. https://doi.org/10.1144/SP434.12

Hunt, A.P. 1993: Revision of the Metoposauridae (Amphibia: Temnospondyli) and description of a new genus from western North America. Museum of Northern Arizona Bulletin 59, 67–97.

Huxley, T.H. 1859: On some amphibian and reptilian remains from South Africa and Australia. Quarterly Journal of the Geological Society 15, 642–649.

Holl, F. 1831: Handbuch der Petrefaktenkunde. Dresden

Howie, A.A. 1970: A new capitosaurid labyrinthodont from East Africa. Palaeontology 13, 210–253.

Irmis, R.B., Nesbitt, S.J. & Sues, H.-D. 2013: Early Crocodylomorpha. In: S.J. Nesbitt, J.B. Desojo & R.B. Irmis (eds): Anatomy, Phylogeny and Paleobiology of Early Archosaurs and their Kin. Geological Society, London, Special Publications 379, 275–302. https://doi.org/10.1144/SP379.24

Ivakhnenko, M.F. 1978: Tailed amphibians from the Triassic and Jurassic of Middle Asia. Paleontological Journal 3, 84–89.

Jaeger, G.F. 1828: Über die fossile Reptilien, welche in Würtemberg aufgefunden worden sind, 48 pp. Verlag der Metzler'schen Buchhandlung, Stuttgart.

Jenkins, F.A., Jr., Shubin, N.H., Amaral, W.W., Gatesy, S.M., Schaff, C.R., Clemmensen, L.B., Downs, W.R., Davidson, A.R., Bonde, N. & Osbaeck, F. 1994: Late Triassic continental vertebrates and depositional environments of the Fleming Fjord Formation, Jameson Land, East Greenland. Meddelelser om Grønland, Geoscience 32, 25 pp.

Jenkins, F.A., Jr., Gatesy, S.M., Shubin, N.H. & Amaral, W.W. 1997: Haramiyids and Triassic mammalian evolution. Nature 385, 715–718. https://doi.org/10.1038/385715a0

Kent, D.V. & Clemmensen, L.B. 2021: Northward dispersal of dinosaurs from Gondwana to Greenland at the mid-Norian (215–212 Ma, Late Triassic) dip in atmospheric pCO2. Proceedings of the National Academy of Sciences 118, e2020778118. https://doi.org/10.1073/pnas.2020778118

Kent, D.V. & Tauxe, L. 2005: Corrected Late Triassic latitudes for continents adjacent to the North Atlantic. Science 307, 240–244. https://doi.org/10.1126/science.1105826

Kent, D.V., Malnis, P.S., Colombi, P.S., Alcober, O.A. & Martínez, R.N. 2014: Age constraints on the dispersal of dinosaurs in the Late Triassic from magnetochronology of the Los Colorados Formation (Argentina). Proceedings of the National Academy of Sciences 111, 7958–7963. https://dx.doi.org/10.1073%2Fpnas.1402369111

Klein, H., Milàn, J., Clemmensen, L.B., Frobøse, N., Mateus, O., Klein, N., Adolfssen, J.S., Estrup, E. & Wings, O. 2016: Archosaur footprints (cf. *Brachychirotherium*) with unusual morphology from the Upper Triassic Fleming Fjord Formation (Norian–Rhaetian) of East Greenland. In: Kear, B.B. *et al*. (eds): Mesozoic Biotas of Scandinavia and its Arctic Territories. Geological Society, London, Special Publications 434, 71–85. https://doi.org/10.1144/SP434.1

Kumar, J. & Sharma, M. 2019: Micro and mega-vertebrate fossils from the Late Triassic Tiki Formation, South Rewa Gondwana Basin, India: paleoenvironmental and palaeobiogeographic implications. Journal of the Paleontological Society of India 64, 151–168.

Lallensack, J.N., Klein, H., Milan, J., Wings, O., Mateus, O. & Clemmensen, L.B. 2017: Sauropodomorph dinosaur trackways

from the Fleming Fjord Formation of East Greenland: Evidence for Late Triassic sauropods. Acta Palaeontologica Polonica 64(4), 833–843. https://doi.org/10.4202/app.00374.2017

Laurenti, J.N. 1768: Specimen medicum, exhibens synopsin reptilium emendatam cum experimentis circa venena et antidota reptilium austriacorum [Medical ideas, showing an emended synopsis of the reptiles together with experiences in poisoning by and antidotes of Austrian reptiles]. Published and printed by Johann Thomas von Trattner, Vienna. https://doi.org/10.5962/bhl.title.5108

Linnaeus C. 1758: Systema Naturae per Regna Tria Naturae, Secundum Classes, Ordines, Genera, Species, cum Characteribus, Differentiis, Synonymis, Locis. Editio Decima 1, 824 pp. https://doi.org/10.5962/bhl.title.156765

Maisch, M.W. & Matzke, A.T. 2004: A relict trematosauroid (Amphibia: Temnospondyli) from the Middle Jurassic of the Junggar Basin (NW China). Naturwissenschaften 91, 589–593. https://doi.org/10.1007/s00114-004-0569-x

Marjanović, D. & Laurin, M. 2014: An updated paleontological timetree of lissamphibians, with comments on the anatomy of Jurassic crown-group salamanders (Urodela). Historical Biology 26, 535–550. https://doi.org/10.1080/08912963.2013.797972

Marjanović, D. & Laurin, M. 2019: Phylogeny of Paleozoic limbed vertebrates reassessed through revision and expansion of the largest published relevant data matrix. PeerJ 6, e5565. https://doi.org/10.7717/peerj.5565

Marsicano, C.A. 1993: Postcranial skeleton of a brachyopoid (Amphibia, Temnospondyli) from the triassic of Mendoza (Argentina). Alcheringa: An Australasian Journal of Palaeontology 17, 185–197. https://doi.org/10.1080/03115519308619603

Marzola, M., Mateus, O., Milàn, J. & Clemmensen L.B. 2018: A review of Palaeozoic and Mesozoic tetrapods from Greenland. Bulletin of the Geological Society of Denmark 66, 21–46. https://doi.org/10.37570/bgsd-2018-66-02

Mau, M., Kent, D.V. & Clemmensen, L.B. 2022: Planetary chaos and inverted climate phasing in the Late Triassic of Greenland. Proceedings of the National Academy of Sciences 119, e2118696119. https://doi.org/10.1073/pnas.2118696119

Milàn, J., Mateus, O., Mau, M., Rudra, A., Sanei, H. & Clemmensen, L.B. 2021: A possible phytosaurian (Archosauria, Pseudosuchia) coprolite from the Late Triassic Fleming Fjord Group of Jameson Land, central East Greenland. Bulletin of the Geological Society of Denmark 69, 71–80. https://doi.org/10.37570/bgsd-2021-69-05

Milner, A.R. 1988: The relationships and origin of living amphibians. In: Benton, M.J. (ed.): The Phylogeny and Classification of the Tetrapods, Volume 1: Amphibians, Reptiles, Birds. Systematics Association Special Volume 35A, 59–102. Clarendon Press, Oxford. https://doi.org/10.1017/s0016756800006476

Nesov, L.A. 1988: Late Mesozoic amphibians and lizards of Soviet Middle Asia. Acta Zoologica Cracoviensa 31, 475–486.

Nøttvedt, A., Johannessen, E.P. & Surlyk, F. 2008: The Mesozoic of western Scandinavia and East Greenland. Episodes 31, 1–7.

Paparella, I., LeBlanc, A.R.H., Doschak, M.R. & Caldwell, M.W. 2019: The iliosacral joint in lizards: an osteological and histological analysis. Journal of Anatomy 236, 668–687. https://doi.org/10.1111/joa.13132

Piveteau, J. 1936: Origine et évolution morphologique des amphibiens anoures. Comptes Rendus Hebdomadaires des Séances de l'Académie des Sciences 103, 1084–1086. https://doi.org/10.5962/bhl.part.5840

Pyron, R.A. 2011: Divergence time estimation using fossils as terminal taxa and the origins of Lissamphibia. Systematic Biology 60, 466–481. https://doi.org/10.1093/sysbio/syr047

Rage, J.-C. & Roček, Z. 1989: Redescription of *Triadobatrachus massinoti* (Piveteau, 1936) an anuran amphibian from the Early Triassic. Palaeontographica Abteilung A206, 1–16.

Roček, Z., Eaton, J.G., Gardner, J. & Prikryl, T. 2010: Evolution of anuran assemblages in the Late Cretaceous of Utah, USA. Palaeobiodiversity and Palaeoenvironments 90, 341–393. https://doi.org/10.1007/s12549-010-0040-2

Roček, Z., Gardner, J.D., Eaton, J.G. & Přikryl, T. 2012: Similarities and differences in the ilia of Late Cretaceous anurans and urodeles. Bulletin de la Société Géologique de France 183, 529–535. https://doi.org/10.2113/gssgfbull.183.6.529

Schoch, R.R. 1999: Comparative osteology of *Mastodonsaurus giganteus* (Jaeger, 1828) from the Middle Triassic (Lettenkeuper: Longobardian) Germany (Baden-Württemberg, Bayern, Thüringen). Stuttgarter Beiträge zur Naturkunde B278, 175 pp.

Schoch, R.R. 2006: A complete trematosaurid amphibian from the Middle Triassic of Germany. Journal of Vertebrate Paleontology 26, 29–43. https://doi.org/10.1671/0272-4634(2006)26[29:actaft]2.0.co;2

Schoch, R.R. 2019: The putative lissamphibian stem-group: Phylogeny and evolution of the dissorophoid temnospondyls. Journal of Paleontology 93, 137–156. https://doi.org/10.1017/jpa.2018.67

Schoch, R.R. & Rubidge, B.S. 2005: The amphibamid *Micropholis* from the Lystrosaurus assemblage zone of South Africa. Journal of Vertebrate Paleontology 25, 502–522. https://doi.org/10.1671/0272-4634(2005)025[0502:tamftl]2.0.co;2

Schoch, R.R., Wernebug, R. & Voigt, S. 2020: A Triassic stem-salamander from Kyrgyzstan and the origin of salamanders. Proceedings of the National Academy of Sciences 117, 11584–11588. https://doi.org/10.1073/pnas.2001424117

Scopoli, G.A. 1777: Introductio ad Historiam Naturalem, Sistens Genera Lapidium, Planatarum, et Animalium Hactenus Detecta, Caracteribus Essentialibus Donata, in Tribus Divisa, Subinde ad Leges Naturae. Gerle, Prague. https://doi.org/10.5962/bhl.title.10827

Sengupta, D.P. 1935: Chigutisaurid temnospondyls from the Late Triassic of India and a review of the family Chigutisauridae. Palaeontology 38, 313–339.

Shubin, N.H. & Jenkins, F.A., Jr. 1995: An Early Jurassic jumping frog. Nature 377, 49–51. https://doi.org/10.1038/377049a0

Sigurdsen, T. & Bolt, J.R. 2010: The Lower Permian amphibamid *Doleserpeton* (Temnospondyli: Dissorophoidea), the interrelationships of amphibamids, and the origin of modern amphibians. Journal of Vertebrate Paleontology 30, 1360–1377. https://doi.org/10.1080/02724634.2010.501445

Simões, T.R., Caldwell, M.W., Talanda, M., Bernardi, M., Palci, A., Vernygora, O., Bernardini, F., Mancini, L. & Nydam, R.L. 2018: The origin of squamates revealed by a Middle Triassic lizard from the Italian Alps. Nature 557, 706–709. https://doi.org/10.1038/s41586-018-0093-3

Skutschas, P.P, Kolchanov, V.V., Averianov, A.O., Martin, T., Schellhorn, R., Kolosov, P.N. & Vitenko, D.D. 2018: A new relict stem salamander from the Early Cretaceous of Yakutia, Siberian Russia. Acta Palaeontologica Polonica 63, 519–525. https://doi.org/10.4202/app.00498.2018

Skutschas, P.P. & Krasnolutskii, S.A. 2011: A new genus and species of basal salamanders from the Middle Jurassic of western Siberia, Russia. Proceedings of the Zoological Institute of the Russian Academy of Sciences 315,167–175.

Spielmann, J.A. & Lucas, S.G. 2012: Tetrapod fauna of the Upper Triassic Redonda Formation, East-central New Mexico: the characteristic assemblage of the Apachean Land-vertebrate Faunachron. New Mexico Museum of Natural History and Science Bulletin 55, 119 pp.

Stocker, M.R., Nesbitt, S.J., Kligman, B.T., Paluh, D.J., Marsh, A.D., Blackburn, D.C. & Parker, W.G. 2019: The earliest equatorial record of frogs from the Late Triassic of Arizona. Biology Letters 15, 1–5. https://doi.org/10.1098/rsbl.2018.0922

Sulej, T. 2002: Species discrimination of the Late Triassic temnospondyl amphibian *Metoposaurus diagnosticus*. Acta Palaeontologica Polonica 47, 535–546.

Sulej, T. 2007: Osteology, variability, and evolution of *Metoposaurus*, a temnospondyl from the Late Triassic of Poland. Paleontologica Polonica 64, 29–139.

Sulej, T., Krzesiński, G., Tałanda, M., Wolniewicz, A.S., Błażejowski, B., Bonde, N., Gutowski, P., Sienkiewicz, M. & Niedźwiedski, G. 2020: The earliest-known mammaliaform fossil from Greenland sheds light on origin of mammals. Proceedings of the National Academy of Sciences 117, 26861–26867. https://doi.org/10.1073/pnas.2012437117

Szentesi, Z., Sebe, K. & Szabó, M. 2020: Giant salamander from the Miocene of the Mecsek mountains (Pécs-Danitzupuszta, southwestern Hungary). Paläontologische Zeitschrift, 94, 353–366. https://doi.org/10.1007/s12542-019-00499-2

Tesakov, A.S., Simakova, A.N., Frolov, P.D., Sytchevskaya, E.K., Syromyatnikova, E.V., Foronova, I.V., Shalaeva, E.A. & Trifonov, V.G. 2019: Early-Middle Pleistocene environmental and biotic transition in north-western Armenia, southern Caucasus. Palaeontologia Electronica 22, 1–39. https://doi.org/10.26879/916

Venczel, M., Gardner, J.D., Codrea, V.A., Csiki-Sava, Z., Vasile, S. & Solomon, A.A. 2016: New insights into Europe's most diverse Late Cretaceous anuran assemblage from the Maastrichtian of western Romania. Palaeobiodiversity and Palaeoenvironments 96, 61–65. https://doi.org/10.1007/s12549-015-0228-6

Venczel, M. & Csiki, Z. 2003: New frogs from the latest Cretaceous of Haţeg Basin, Romania. Acta Palaeontologica Polonica 48, 609–616.

Warden A.A & Snell, N. 1991: The postcranial skeleton of Mesozoic temnospondyl amphibians: a review. Alcheringa: An Australasian Journal of Paleontology 15, 43–64. https://doi.org/10.1080/03115519108619009

Watson, D.M.S. 1958: A new labyrinthodont (*Paracyclotosaurus*) from the Upper Trias of New South Wales. Bulletin of the British Museum of Natural History of Geology 3, 233–263.

Werneburg, R. 2009: The Permotriassic branchiosaurid *Tungussogyrinus* Efremov, 1939 (Temnospondyli, Dissorophoidea) from Siberia restudied. Fossil Record 12, 105–120. https://doi.org/10.1002/mmng.200900001

Yates A.M. & Warren A.A. 2000: The phylogeny of the 'higher' temnospondyls (Vertebrata: Choanata) and its implications for the monophyly and origins of the Stereospondyli. Zoological Journal of the Linnean Society 128, 77–121. https://doi.org/10.1111/j.1096-3642.2000.tb00650.x

Ziegler, P.A. 1988: Evolution of the Arctic-North Atlantic and the Western Tethys. American Association of Petroleum Geologists, Memoirs 43, 164–196. https://doi.org/10.1306/M43478

von Zittel, K.A. 1887: Handbuch der Palæontologie. I. Abtheilung – Palæozoologie. III. Band – Vertebrata (Pisces, Amphibia, Reptilia, Aves), 900 p. R. Oldenburg, München.

Cutting through sponge and time – a new record of *Koptichnus rasmussenae* (trace fossil) from the Kerteminde Marl (middle Paleocene), Denmark

LOTHAR H. VALLON & ANDREW K. RINDSBERG

Geological Society of Denmark
https://2dgf.dk

Received 6 February 2022
Accepted in revised form
21 July 2022
Published online
24 August 2022

Vallon, L.H. & Rindsberg, A.K. 2022: Cutting through sponge and time – a new record of *Koptichnus rasmussenae* (trace fossil) from the Kerteminde Marl (middle Paleocene), Denmark. Bulletin of the Geological Society of Denmark, Vol. 70, pp. 131–137. ISSN 2245-7070. https://doi.org/10.37570/bgsd-2022-70-09

A new trace fossil, *Koptichnus rasmussenae*, was recently reported from the Cretaceous of Denmark. This burrow is thickly lined with cuboids that the tracemaker cut from siliceous sponges. A newly discovered specimen from the lower Selandian Kerteminde Marl, found in a loose boulder in the Gundstrup gravel pit (Fyn, Denmark), extends the stratigraphical range of this ichnotaxon from the previously known Coniacian to the middle Paleocene and demonstrates that this distinct behaviour of harvesting and shaping building material survived the K-Pg extinction event.

Keywords: domichnia, armoured burrow, sponge, Selandian, K-Pg extinction event.

Lothar H. Vallon [kv@oesm.dk], Geomuseum Faxe, Østsjællands Museum, Rådhusvej 2, 4640 Faxe, Denmark. Andrew K. Rindsberg [arindsberg@uwa.edu], Dept. of Biological & Environmental Sciences, University of West Alabama, Livingston, AL 35470, USA.

The trace fossil *Koptichnus rasmussenae* was recently described by Vallon *et al*. (2020). It is an armoured burrow system (Buatois *et al*. 2017) similar to *Ophiomorpha* Lundgren, 1891, but using cuboids (cubelike polyhedra) of siliceous sponges instead of sediment nodules as lining material. These building blocks are characterised by having a fairly uniform size and shape and they are interpreted as being cut from sponges by an arthropod tracemaker (Vallon *et al*. 2020).

Previous records of this peculiar trace fossil from Denmark include the Coniacian (Arnager Limestone; Bornholm) and Maastrichtian chalk localities at Stevns Klint (Sjælland) and northern Jylland (Fig. 1; Vallon *et al*. 2020). Although the newly recovered specimen derives from ice-rafted loose material in a gravel pit, the specimen can be assigned with certainty to the Kerteminde Marl by lithological comparison. Micropalaeontological analyses of lithologically similar blocks from the same locality have proved that they represent the Kerteminde Marl (Schnetler & Nielsen 2018).

Geological setting

The Gundstrup gravel pit is located about 20 km north of Odense on Fyn (Fig. 1). There, glacially transported boulders represent the Kerteminde Marl, which crops out in the northern and eastern parts of Fyn (Gry 1935, Schnetler & Nielsen 2018). The boulders, therefore, are expected to have been transported less than 50 km (Schnetler & Nielsen 2018; see also Fig. 1). The Kerteminde Marl was deposited during the lowermost Selandian, immediately above the Danian–Selandian transition, and has a similar if not identical age as the Lellinge Greensand Formation of Sjælland (Schnetler & Nielsen 2018).

The Kerteminde Marl is predominantly a monotonous, light grey silty marl, in places with slightly silicified layers. It may contain pyrite (Gry 1935) and has been homogenised by intensive bioturbation (Heilmann-Clausen 1995), probably by meiofauna. Body fossils are diverse and common at the Gundstrup locality (Foraminifera, Porifera, Annelida,

Decapoda, Cirripedia, Bryozoa, Brachiopoda, Echinodermata, and Vertebrata including 'ganoid fishes', Elasmobranchii, Cheloniidae, and Aves). Only a few groups (e.g. molluscs: Schnetler & Nielsen 2018 and some vertebrates, e.g. Myrvold *et al*. 2018) have been treated systematically. Trace fossils have so far only been briefly mentioned in other studies (e.g. *Teredolites* by Schnetler & Nielsen 2018; *Lepidenteron* by Schwarzhans *et al*. 2021).

In the palaeoenvironmental interpretation of Clemmensen & Thomsen (2005), the Kerteminde Marl was deposited under fully marine conditions at a water depth between 100 and 150 m (see also King 1994, 2016, who inferred an outer to middle neritic setting). Compared to those of other localities, the silicified boulders from Gundstrup are of coarser sediment than the typical Kerteminde Marl and have a higher content of benthic fossils (Heilmann-Clausen & Surlyk 2017, p. 195). A relatively high sedimentation rate is indicated by reworking of Cretaceous chalk sediments from the uplifted Tornquist–Sorgenfrei Zone (Fig. 1; Heilmann-Clausen & Surlyk 2017). Slight silicification of the sediment (Gry 1935; Heilmann-Clausen 1995) might have its origin in the occurrence and dissolution of abundant siliceous sponges (Fig. 3; see also Gry 1935). According to Clemmensen & Thomsen (2005), the bottom water was well ventilated at least in more arenaceous and glauconitic strata of the Kerteminde Marl (Gry 1935, p. 77), but planktonic production was low, resulting in a reduction of benthic food supply to the depositional environment of the Kerteminde Marl. The seafloor was probably influenced by weak water currents, as deduced from small, patchy accumulations of molluscs, together with driftwood containing *Teredolites* isp. (Schnetler & Nielsen 2018). The other trace fossils, however, are deeper-tier structures that imply oxygen-depleted sediments – as is usual below the redox potential discontinuity within a soft substrate. Oxygen depletion below this discontinuity is also suggested by micropyrite (cf. Gry 1935; Wilkins & Barnes 1997).

Fig. 1. Map of Denmark and adjacent countries with major tectonic units. The locality of the Gundstrup gravel pit (star) is shown within the outcrop of Selandian sediments. Previously documented localities from the Cretaceous are indicated with arrows. Modified from Schnetler & Nielsen (2018) and Schwarzhans *et al*. (2021) with additional data from Brandes *et al*. (2018) and Vallon *et al*. (2020).

Description of the specimen

The specimen (Fig. 2) was collected and donated by Mette Hofstedt and Peter Mortensen in 2019. It is preserved in full relief, split longitudinally into two slabs. As in the specimens from the Cretaceous Arnager Limestone (Vallon *et al*. 2020), the sponge spicules have completely dissolved and only their moulds are preserved. These moulds have a light orange stain from metal oxides.

The two halves of the rock sample (Fig. 2A) have approximately the shape of a triangular prism. The slightly larger piece has edge lengths of about 10 cm each and contains the burrow itself. The burrow is flattened and individual cuboids of the lining material are somewhat weathered. The preserved burrow stretch is fairly rectilinear and unbranched. It is about 73 mm long and about 12 mm wide. Individual cuboids are about 3–4 mm in edge length.

The slightly smaller other half of the rock sample (Fig. 2B) contains the outermost area of the lining and shows well-preserved moulds of bundles of monaxone sponge needles (Fig. 2C). According to Dorte Janussen (written communication, 2021), the spicules appear to be rather similar and potentially derive from the same sponge genus. The monaxones appear to be root tuft spicules, probably belonging to the order Lyssacinosida, perhaps to the modern family Rossellidae.

The surrounding sediment is slightly silicified and contains an abundance of small bioclasts, most of them indeterminable. Amongst the identifiable bioclasts are mollusc and echinoderm fragments and an abundance of isolated sponge spicule moulds (Fig. 3).

Both halves of the specimen are housed in the collection of the National Museum of Natural History of Denmark, Copenhagen: MGUH 34070.

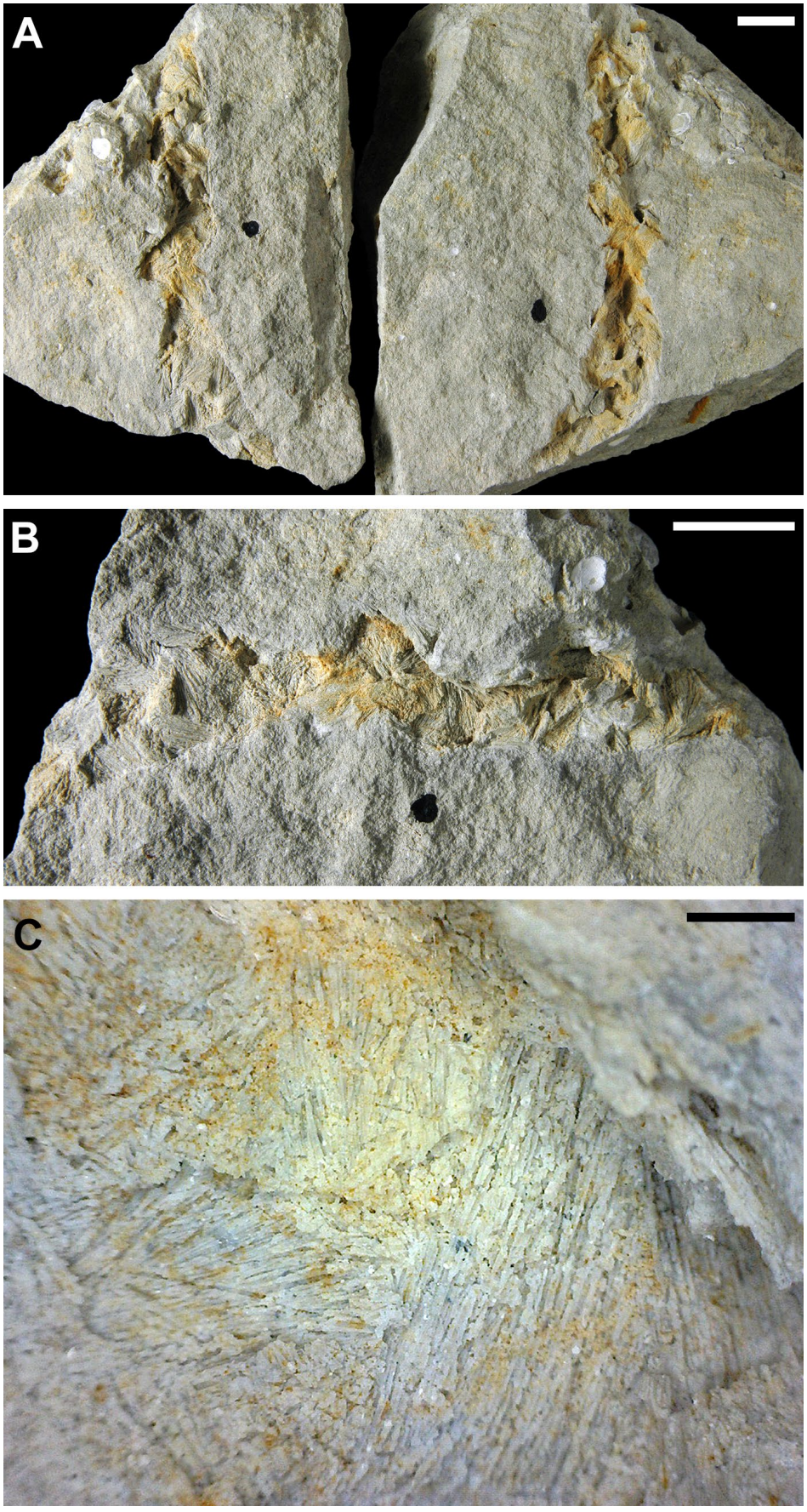

Fig. 2. *Koptichnus rasmussenae* (MGUH 34070) from the Gundstrup gravel pit. Scale bar: 10 mm. **A:** Overview of the two halves of the specimen. **B:** Smaller half. **C:** Detail of B. Imprints of monaxone spicular bundles cut into cuboids as building material for the burrow's lining.

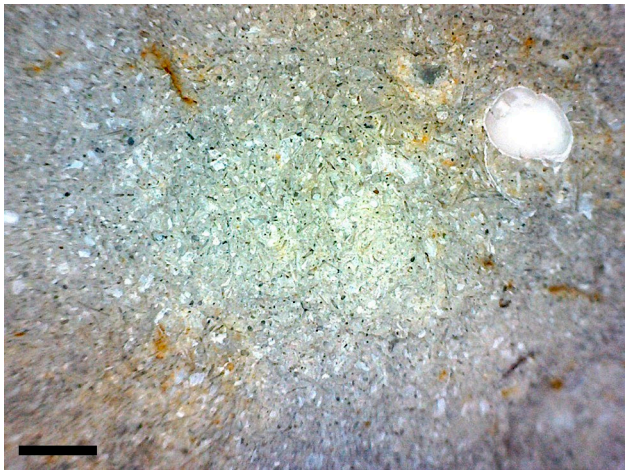

Fig. 3. Detail of the surrounding sediment with numerous cross-cuts of unoriented sponge spicules and other bioclasts. Scale bar: 1 mm.

Interpretation

Vallon *et al.* (2020) inferred that *Koptichnus* is a shallow-tier trace fossil and that its thick lining was constructed to prevent collapse within soft chalk sediments. It particularly occurs close to small sponge accumulations or patch reefs. These not only provided the tracemakers with building material for the trace's lining, but also aided preservation of the burrows. At the previously described Cretaceous locations where *Koptichnus* occurs (Vallon *et al.* 2020), most other burrows lack such thick linings, suggesting that they were constructed in subsequently firmer substrates in the lower tier (Bromley & Ekdale 1984a; Ekdale & Bromley 1991). The preserved fauna, however, shows adaptations to softgrounds (e.g. cf. Heinberg 2012; Hansen & Surlyk 2014).

This apparent contradiction has its origin in continuous sedimentation. Most burrows from these locations were constructed in deep tiers below the seafloor, where the sediment was much firmer than in shallower tiers. With continuous sedimentation, the tracemakers and their burrows gradually moved upward. Under normal circumstances, bioturbation by these deep-tier burrowers erases the record of previous shallow-tier tracemakers (e.g. Howard 1978; Bromley 1996). However, the tiny sponge reefs were evidently impenetrable to these deep-tier burrowers and therefore acted, first, as shields against colonisation by deep-tier burrowers, and later as protection for shallow-tier traces that were made immediately below the sponge thickets.

The trace and body fossils occurring in the Kerteminde Marl indicate a very similar condition on the Paleocene seafloor with softgrounds at the sediment-water interface grading into firmgrounds at some distance below the seafloor characterised by deep-tier trace fossils. The abundance of sponge spicules in the host sediment surrounding the new *Koptichnus* specimen points to a close proximity of sponges. These needles seem not to have been fused and therefore probably belong to the order Lyssacinosida. Most sponges associated with the previously described *Koptichnus rasmussenae* at Arnager (Vallon *et al.* 2020) also belong to the Lyssacinosida (e.g. Brückner 2006).

No systematic treatment of the Kerteminde Marl trace fossils is yet available, but in our own brief observations, the assemblage includes common *Chondrites* ispp., *Zoophycos* ispp. and very abundant *Lepidenteron mortenseni* (see also Schwarzhans *et al.* 2021). These deep-tier ichnotaxa generally are present below the redox potential discontinuity (e.g. Bromley & Ekdale 1984b; Ekdale & Mason 1988; Savrda 2007 and references therein). Typical trace-fossil taxa from upper tiers (except *Koptichnus*) have either been erased, eroded by glacial transport or have never been established. Together with *Koptichnus,* however, this association places the Kerteminde Marl in a transitional zone between the Seilacherian *Cruziana* and *Zoophycos* ichnofacies.

Seilacher (1964, 1967) recognised that certain trace fossils occur more frequently in specific environments because they express an assertive response (ethology) of their tracemakers to these particular environmental conditions (e.g. Buatois & Mángano 2011; MacEachern *et al.* 2012). The *Cruziana* ichnofacies is dominated by horizontal trace fossils, and inclined and vertical burrows occur subordinately. Its typical ethological trace-fossil groups belong to repichnia, fodinichnia, cubichnia, domichnia and pascichnia with a dominance of deposit- and detritus-feeding strategies. Most traces are produced by mobile organisms, but sedentary burrow-dwellers are present as well. The *Cruziana* ichnofacies is characterised by high ichnodiversity and abundance of trace fossils (Buatois & Mángano 2011). Only deep-tier trace fossils have been recovered so far in the Kerteminde Marl boulders from Gundstrup. Common ichnotaxa therefore belong to the fodinichnia and domichnia: e.g. *Rhizocorallium commune* and *Thalassinoides paradoxicus*? together with fanlike feeding burrows. The *Cruziana* ichnofacies is typically associated with medium-energy, sandy to silty substrates which can be found in shelf settings (Bromley 1996).

Originally, the *Zoophycos* ichnofacies was defined as dominated by deep-tier fodinichnia, ranging from relatively simple forms to rather complex structures having a spreite. Many of these deep-tier structures have been reinterpreted and are now regarded as

belonging to the recently introduced ethological category sequestrichnia (Uchman & Wetzel 2016, 2017; Uchman & Rattazzi 2017; Jurkowska *et al.* 2018; Rodríguez-Tovar *et al.* 2019; Uchman *et al.* 2019, 2020). This category comprises storage behaviour that is predominantly applied by tracemakers in deep-sea settings, where food availability fluctuates seasonally or episodically. In times of food abundance, the tracemakers store it within the deeper tiers, an activity that can be referred to as *stowing*, after Schäfer (1972); the tracemakers are then *stowers*. Here, the organic matter is preserved in poorly oxygenated sediments out of the reach of shallow-dwelling deposit feeders (Uchman & Wetzel 2016, 2017; for shallower environments see also Bromley 1996, pp. 100–101, fig. 4.25; Seilacher 2007, p. 54, pl. 18). Subordinately to sequestrichnia, pascichnia may also be present. The *Zoophycos* ichnofacies typically is dominated by deposit feeders and characterised by a low ichnodiversity with a high trace-fossil abundance (Buatois & Mángano 2011). In light of recent discoveries, stowing traces (sequestrichnia) should be added to the list (cf. Uchman & Wetzel 2016). Typical ichnotaxa of the *Zoophycos* ichnofacies that occur in the Kerteminde Marl are *Zoophycos* and *Chondrites*. This ichnofacies is characteristic of low-energy environments with muddy substrates in slope to abyssal settings (e.g. Bromley 1996).

Because elements of both Seilacherian ichnofacies are present, the Kerteminde Marl was likely deposited in the transitional zone between the *Cruziana* and *Zoophycos* ichnofacies. The trace-fossil content further supports previous palaeoenvironmental interpretations for the Kerteminde Marl as being deposited under fully marine conditions at water depths between 100 and 150 m (Clemmensen & Thomsen 2005; King 1994, 2016). Clemmensen & Thomsen (2005) inferred well ventilated bottom waters. Although the ichnocoenosis at hand was adapted to oxygen-depleted conditions, there is no contradiction. Most observed ichnotaxa derive from deeper tiers where oxygen availability was reduced (e.g. Bromley 1996).

Many shallow-tier tracemakers need to strengthen their burrows within the relatively soft sediment in order to prevent collapsing (e.g. Bromley 1996; Vallon *et al.* 2020). The use of bioclasts in such linings is rather uncommon compared to mucus-bound sediment because the tracemakers need to expend much time to collect, shape and assemble suitable material (Vallon *et al.* 2020). In *Koptichnus*, the collection and shaping of cuboids cut from hexactinellid sponges is unique (Vallon *et al.* 2020). Therefore, the range extension of *Koptichnus* across the K-Pg boundary suggests the persistence not only of an unusual behavior, but also of its makers, through the end-Cretaceous mass extinction. This is consistent with the hypothesis that animals living in deep burrows were relatively well protected during this event (Robertson *et al.* 2004; Labandeira *et al.* 2016; Martin 2017).

Acknowledgements

We thank the amateur collectors Mette Hofstedt and Peter Mortensen for collecting and donating the above-described specimen. Arne Thorshøj Nielsen (University of Copenhagen), Jesper Milán and Sten Lennart Jakobsen (both Østsjællands Museum, Faxe) directed us to important literature about the Kerteminde Marl. Dorte Janussen (Senckenberg Museum, Frankfurt) determined the sponge spicules. The manuscript benefited from the reviews of Arne Thorshøj Nielsen (University of Copenhagen) and Alfred Uchman (Jagiellonian University, Kraków).

References

Brandes, C., Steffen, H., Sandersen, P.B.E, Wu, P. & Winsemann, J. 2018: Glacially induced faulting along the NW segment of the Sorgenfrei-Tornquist Zone, northern Denmark: Implications for neotectonics and Lateglacial fault-bound basin formation. Quaternary Science Reviews 189, 149–168. https://doi.org/10.1016/j.quascirev.2018.03.036

Bromley, R.G. 1996: Trace fossils: biology, taphonomy and applications. 2nd ed., 384 pp. London: Chapman & Hall.

Bromley, R.G. & Ekdale, A.A. 1984a: Trace fossil preservation in flint in the European Chalk. Journal of Paleontology 58, 298–311. https://www.jstor.org/stable/1304785

Bromley, R.G. & Ekdale, A.A. 1984b: *Chondrites:* a trace fossil indicator of anoxia in sediments. Science 224, 872–874. https://doi.org/10.1126/science.224.4651.872

Brückner, A. 2006: Taxonomy and paleoecology of lyssacinosan Hexactinellida from the Upper Cretaceous (Coniacian) of Bornholm, Denmark, in comparison with other Postpaleozoic representatives. Abhandlungen der Senckenbergischen Naturforschenden Gesellschaft 564, 103 pp.

Buatois, L.A. & Mángano, M.G. 2011: Ichnology – organism-substrate interactions in space and time, 358 pp. New York: Cambridge.

Buatois, L., Wisshak, M., Wilson, M. & Mángano, M.G. 2017: Categories of architectural designs in trace fossils: a measure of ichnodisparity. Earth-Science Reviews 164, 102–181. https://doi.org/10.1016/j.earscirev.2016.08.009

Clemmensen, A. & Thomsen, E. 2005: Palaeoenvironmental changes across the Danian–Selandian boundary in the North Sea Basin. Palaeogeography Palaeoclimatology Palaeoecology 219, 351–394. https://doi.org/10.1016/j.palaeo.2005.01.005

Ekdale, A.A. & Bromley, R.G. 1991: Analysis of composite ichnofabrics: an example in uppermost Cretaceous Chalk of Denmark. Palaios 6: 232–249. https://doi.org/10.2307/3514904

Ekdale, A.A. & Mason, T.R. 1988: Characteristic trace-fossil associations in oxygen-poor sedimentary environments. Geology 16, 720–723. https://doi.org/10.1130/0091-7613(1988)016%3C0720:CTFAIO%3E2.3.CO;2

Gry, H. 1935: Petrology of the Paleocene sedimentary rocks of Denmark. Danmarks Geologiske Undersøgelse Række II, vol. 61, 172 pp. https://doi.org/10.34194/raekke2.v61.6849

Hansen, T. & Surlyk, F. 2014: Marine macrofossil communities in the upper Maastrichtian Chalk of Stevns Klint, Denmark. Palaeogeography, Palaeoclimatology, Palaeoecology 399, 323–344. https://doi.org/10.1016/j.palaeo.2014.01.025

Heilmann-Clausen, C. 1995: Palæogene aflejringer over danskekalken. In: Nielsen, O.B. (ed.): Danmarks geologi fra Kridt til i dag, 69–114. Århus: Geologisk Institut, Aarhus Universitet.

Heilmann-Clausen, C. & Surlyk, F. 2017: Koralrev og lerhav: Palæogen. In: Larsen, G. (ed.): Naturen i Danmark: Geologien, 3rd ed., 181–226. Copenhagen: Gyldendal.

Heinberg, C. 2012: Livet i Kridthavet, 62 pp. Store Heddinge: Stevns Museum (Østsjællands Museum).

Howard, J.D. 1978: Sedimentology and trace fossils. In: Basan, P.B. (ed.): Trace fossil concepts. SEPM Short Course Notes 5, 13–45. Tulsa, Oklahoma: Society of Economic Paleontologists and Mineralogists. https://doi.org/10.2110/scn.77.01.0013

Jurkowska, A., Uchman, A. & Świerczewska-Gładysz, E. 2018: A record of sequestration of plant material by marine burrowing animals as a new feeding strategy under oligotrophic conditions evidenced by pyrite microtextures. Palaios 33, 312–322. https://doi.org/10.2110/palo.2018.002

King, C. 1994: Late Paleocene microfaunas of the Harre borehole (North Jylland, Denmark). In: Nielsen, O.B. (ed.): Lithostratigraphy and biostratigraphy of the Tertiary sequence from Harra Borehole, Denmark. Aarhus Geoscience 1, 65–72.

King, C. 2016: A revised correlation of Tertiary rocks in the British Isles and adjacent areas of NW Europe (edited by Gale, A.S. & Barry, T.L.). Geological Society of London Special Report 27, 718 pp. https://doi.org/10.1144/SR27

Labandeira, C.C., Rodríguez-Tovar, F.J. & Uchman, A. 2016: The end-Cretaceous extinction and ecosystem change. In: Mángano, M.G. & Buatois, L.A. (eds): The trace-fossil record of major evolutionary events. Topics in Geobiology 40, 265–300. https://doi.org/10.1007/978-94-017-9597-5_5

Lundgren, B. 1891: Studier öfver fossilförande lösa block. Geologiska Föreningens i Stockholm Förhandlingar 13, 111–121. https://doi.org/10.1080/11035899109446863

MacEachern, J.A., Bann, K.L., Gingras, M.K., Zonneveld, J.-P., Dashtgard, S.E. & Pemberton, S.G. 2012: The ichnofacies paradigm. In: Knaust, D. & Bromley, R.G. (eds): Trace fossils as indicators of sedimentary environments. Developments in Sedimentology 64, 103–138. https://doi.org/10.1016/B978-0-444-53813-0.00004-6

Martin, A.J. 2017: The evolutionary advantage of burrowing underground. American Scientist 105, 306. https://doi.org/10.1511/2017.105.5.306

Myrvold, K.S., Milàn, J. & Rasmussen, J.A. 2018: Two new finds of turtle remains from the Danian and Selandian (Paleocene) deposits of Denmark with evidence of predation by crocodilians and sharks. Bulletin of the Geological Society of Denmark 66, 211–218. https://doi.org/10.37570/bgsd-2018-66-11

Robertson, D.S., McKenna, M.C., Toon, O.B., Hope, S. & Lillegraven, J.A. 2004: Survival in the first hours of the Cenozoic. GSA Bulletin 116, 760–768. https://doi.org/10.1130/B25402.1

Rodríguez-Tovar, F.J., Miguez-Salas, O., Dorador, J. & Duarte, L.V. 2019: Opportunistic behaviour after the Toarcian Oceanic Anoxic Event: the trace fossil *Halimedides*. Palaeogeography, Palaeoclimatology, Palaeoecology 520, 240–250. https://doi.org/10.1016/j.palaeo.2019.01.036

Savrda, C.E. 2007: Trace fossils and marine benthic oxygenation. In: Miller, W. III. (ed.): Trace fossils: concepts, problems, prospects, 149–158. Amsterdam: Elsevier. https://doi.org/10.1016/B978-044452949-7/50135-2

Schäfer, W. 1972: Ecology and palaeoecology of marine environments (transl. Oertel, I.; ed. Craig, G.Y.), 568 pp. Edinburgh: Oliver & Boyd.

Schnetler, K.I. & Nielsen, M.S. 2018: A Palaeocene (Selandian) molluscan fauna from boulders of Kerteminde Marl in the gravel-pit at Gundstrup, Fyn, Denmark. Cainozoic Research 18, 3–81.

Schwarzhans, W., Milàn, J. & Carnevale, G. 2021: A tale from the middle Paleocene of Denmark: a tube-dwelling predator documented by the ichnofossil *Lepidenteron mortenseni* n. isp. and its predominant prey, *Bobbitichthys* n. gen. *rosenkrantzi* (Macroridae, Teleostei). Bulletin of the Geological Society of Denmark 69, 35–52. https://doi.org/10.37570/bgsd-2021-69-02

Seilacher, A. 1964: Biogenic sedimentary structures. In: Imbrie, J. & Newell, N. (eds): Approaches to paleoecology, 296–316. New York: Wiley.

Seilacher, A. 1967: Bathymetry of trace fossils. Marine Geology 5, 413–428. https://doi.org/10.1016/0025-3227(67)90051-5

Seilacher, A. 2007: Trace fossil analysis, 226 pp. Berlin: Springer. https://doi.org/10.1007/978-3-540-47226-1

Uchman, A. & Rattazzi, B. 2017: The trace fossil *Polykampton cabellae* isp. nov. from the Pagliaro Formation (Paleocene), northern Apennines, Italy: a record of nutritional sediment sequestration by a deep sea invertebrate. Ichnos 25, 1–10. https://doi.org/10.1080/10420940.2017.1308362

Uchman, A. & Wetzel, A. 2016: Sequestrichnia – a new ethological category of trace fossils in oligotrophic deep-sea environments. In: Baucon, A., de Carvalho, C.N. & Rodrigues, J. (eds): Ichnia 2016: Abstract Book, p. 190; UNESCO Geopark Naturtejo/International Ichnological Association, Castelo Branco.

Uchman, A. & Wetzel, A. 2017: Hidden subsurface garden on own faeces – the trace fossil *Tubulichnium rectum* (Fischer-

Ooster, 1858) from the Cretaceous-Palaeogene deep-sea sediments. Palaeontologica Electronica 20.2.40A. https://doi.org/10.26879/777

Uchman, A., Wetzel, A. & Rattazzi, B. 2019: Alternating stripmining and sequestration in deep-sea sediments: the trace fossil *Polykampton* – an ecologic and ichnotaxonomic evaluation. Palaeontologica Electronica 22.2.21A. https://doi.org/10.26879/930

Uchman, A., Lebanidze, Z., Beridze, T., Kobakhidze, N., Lobzhanidze, K., Khutsishvili, S., Chagelishvili, R., Makadze, D., Koiava, K., & Khundadze, N. 2020: Abundant trace fossil *Polykampton* in Palaeogene deep-sea flysch deposits of the Lesser Caucasus in Georgia: palaeoecological and palaeoenvironmental implications. Palaeogeography, Palaeoclimatology, Palaeoecology 558, 109958. https://doi.org/10.1016/j.palaeo.2020.109958

Vallon, L.H., Milàn, J., Rindsberg, A.K., Madsen, H. & Rasmussen, J.A. 2020: Cutting-edge technology: burrows lined with sponge bioclasts from the Upper Cretaceous of Denmark. Ichnos 27, 317–325. https://doi.org/10.1080/10420940.2020.1744581

Wilkin, R.T. & Barnes, H.L. 1997: Formation processes of framboidal pyrite. Geochimica et Cosmochimica Acta 61, 323–339. https://doi.org/10.1016/S0016-7037(96)00320-1

Further holocephalian remains from the Hasle Formation (Early Jurassic) of Denmark

CHRISTOPHER J. DUFFIN & JESPER MILÀN

Geological Society of Denmark
https://2dgf.dk

Received 26 August 2022
Accepted in revised form
12 November 2022
Published online
30 November 2022

Duffin, C.J. & Milàn, J. 2022: Further holocephalian remains from the Hasle Formation (Early Jurassic) of Denmark. Bulletin of the Geological Society of Denmark, Vol. 70, pp. 139–149. ISSN 2245-7070. https://doi.org/10.37570/bgsd-2022-70-10

Oblidens bornholmensis, known from isolated upper posterior (palatine) and lower posterior (mandibular) tooth plates, was the first myriacanthid holocephalian to be described from the Hasle Formation (Pliensbachian, Early Jurassic) of Bornholm (Denmark). Further collecting in the Hasle Formation has yielded seven more specimens of myriacanthid tooth plates. Two mandibular tooth plates are assigned to *Myriacanthus paradoxus*, thereby extending both the geographical and stratigraphic range of the genus. In addition to new material of *Oblidens bornholmensis*, some distinctive myriacanthid palatine and mandibular tooth plates are described and left in open nomenclature. The Early Pliensbachian deposits of Bornholm preserve the most diverse myriacanthid fauna known to date.

Keywords: Bornholm, tooth plate, Holocephali, Myriacanthidae, Pliensbachian, Early Jurassic.

Christopher J. Duffin [cduffin@blueyonder.co.uk], Earth Sciences Department, The Natural History Museum, Cromwell Road, London SW7 5BD, UK and 146, Church Hill Road, Cheam, Sutton, Surrey SM3 8NF, UK. Jesper Milàn [jesperm@oesm.dk], Geomuseum Faxe/Østsjællands Museum, Østervej 2, DK-4640 Faxe, Denmark.

Remains of holocephalians are much rarer in the fossil record than those of elasmobranchs, their chondrichthyan sister-group. Unlike elasmobranchs, in which the teeth are shed from the crest of the jaw continuously throughout life in a conveyor belt-like fashion, holocephalian teeth grow from their lingual surface throughout the life of the individual and are not shed. This means that a tooth plate specimen represents the death of an individual in holocephalians, whereas an isolated shark's tooth might represent loss during a single feeding episode.

Mesozoic holocephalians all belong to the Order Chimaeriformes, and can be classified into three suborders: the squalorajoids are represented only by the type genus (*Squaloraja*; Hettangian to Sinemurian of Europe); myriacanthoids range from the Rhaetian (Late Triassic) to the Tithonian (Late Jurassic) of Europe; true chimaeroids, whose oldest known representatives are *Eomanodon simmsi* and *Brachymylus latus* from the Pliensbachian of England and Germany respectively (Ward & Duffin 1989; Duffin 1996). The discovery of tooth plates of *Oblidens bornholmensis*, a myriacanthid, on Bornholm (Duffin & Milàn 2017) marked the first record of the group in Pliensbachian deposits and the earliest point in the overlap of the ranges of the myriacanthoids and chimaeroids. Myriacanthoid remains seem to dominate the holocephalian fossil record in the Early Jurassic, but chimaeroid remains are more abundant and diverse by the Late Jurassic and Early Cretaceous.

Further specimens of myriacanthid holocephalian tooth plates have come to light since the initial work of Duffin & Milàn (2017). The purpose of the present paper is to describe and discuss this additional material and highlight holocephalian diversity in the Pliensbachian Hasle Formation.

Geological Setting

Bornholm (Fig. 1), a Danish island located south of Sweden in the Baltic Sea, is an upstanding, fault-bounded block. It is situated adjacent to the NW–SE-

trending Sorgenfrei-Tornquist Zone, separating the Danish Basin from the Baltic Shield, and whose movements had direct consequences for Mesozoic sediment supply and pulses of sedimentation. The type section for the Hasle Formation is exposed just south of Hasle town (Fig. 1B), approximately 1 km west of a fault line which controlled the shoreline geography during the deposition of the formation (Surlyk & Noe-Nygaard 1986; Milàn & Surlyk 2015). The formation is dominated by arenaceous deposits; reddish-brown, hummocky cross-stratified sandstones and swaley cross-stratified siltstones are interbedded with very fine sandstones (Duffin & Milàn 2017, fig. 1C). Most of the vertebrate remains come from a fossiliferous conglomerate where they are mixed with basement rock clasts draping the bases of individual swales (Surlyk & Noe-Nygaard 1986; Larsen & Friis 2001).

The Hasle Formation is dated to the Early Pliensbachian based on its ammonite fauna, which places the formation within the lower Pliensbachian *Uptonia jamesoni* zone together with the *Acanthopleuroceras valdani* subzone of the overlying *Tragophylloceras ibex* zone (Donovan & Surlyk 2003). Other invertebrates include several species of bivalves, scaphopods and belemnites (Malling & Grönwall 1909; Malling 1911, 1914, 1920; Höhne 1933; Donovan & Surlyk 2003). The Hasle Formation further yields a diverse vertebrate fauna comprising hybodont and neoselachian sharks (Rees 1998), isolated scales of as yet undetermined actinopterygians, and at least three plesiosaurian taxa (Milàn & Bonde 2001; Smith 2008). Recently remains of terrestrial animals have been described in the form of dinosaurian bone fragments and a mammalian tooth (Molin 2021), an osteoderm from a thallatosuchian crocodile (Milàn & Mueller-Töwe 2021), and a single, small theropod footprint (Milàn & Surlyk 2015).

Material and Methods

Six virtually complete holocephalian tooth plates were collected in 2019 and 2020 by Marianne Nattestad, and one specimen by Anton Wulff Jensen from the out-

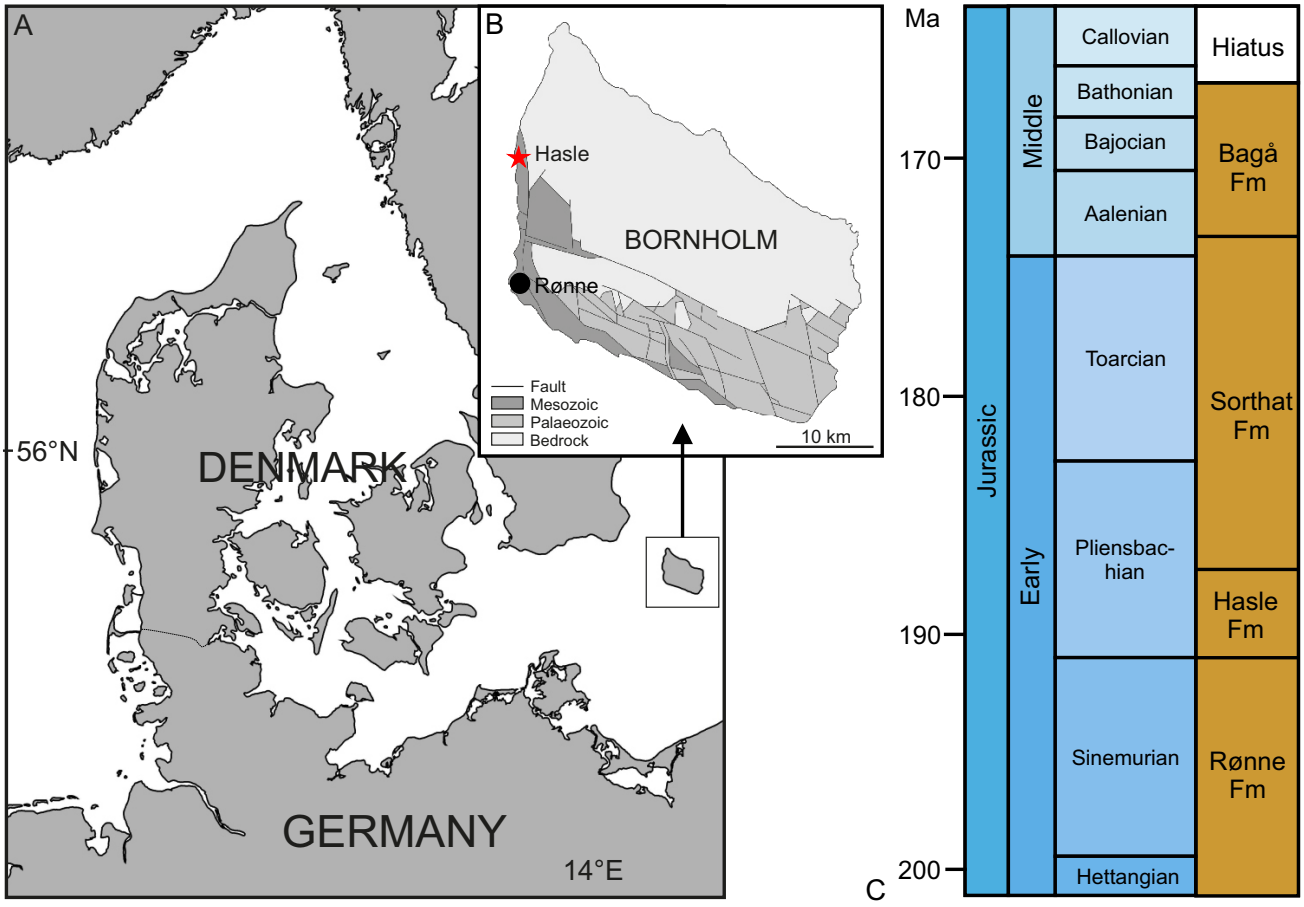

Fig. 1. Bornholm and the Hasle Formation. **A**: Location map showing the position of Bornholm in the Baltic Sea. **B:** Outline geological map of Bornholm, showing the location of Hasle. **C:** Late to Middle Jurassic stratigraphy of Bornholm, modified after Sandersen *et al.* (2014).

crop of Hasle sandstone just south of Hasle harbour, Bornholm. The specimens are declared Danekrae NHMD 633649–633653, NHMD 633654 and NHMD 873668. Danekræ are fossils, minerals or meteorites of exceptional scientific merit or value as items for exhibition purposes; the discoverer is rewarded for the material by the Danish state. All the specimens are now part of the collections of the Natural History Museum of Denmark (NHMD), Øster Voldgade 5-7, DK-1350 Copenhagen. The tooth plates were removed from the surrounding matrix by mechanical preparation using an air scribe.

Other institutional abbreviations used in this paper are as follows: NHMUK PV – Fossil Fish section, Earth Science Faculty, The Natural History Museum, Cromwell Road, South Kensington, London SW7 5BD, UK; SMNS – Staatliches Museum für Naturkunde in Stuttgart, Rosenstein 1-3, 70191 Stuttgart, Germany.

Myriacanthid holocephalians

Ranging in age from the Late Triassic (Rhaetian) to the Early Jurassic (Toarcian; Patterson 1965; Stahl 1999), members of the chimaeriform Family Myriacanthidae are characterised by the presence of a specialised hypermineralised tissue covering the greater part of the occlusal surfaces of the single pair of upper (palatine) tooth plates and the single pair of lower (mandibular) tooth plates. Anterior to the palatine tooth plates, the paired vomerine tooth plates usually have the hypermineralised tissue arranged in distinct units or tritors. There is also a single medial tooth plate, the symphyseal tooth plate, anterior to the mandibular tooth plate pair. The hypermineralised dentine pillars sit upon a base of lamellar tissue. The occlusal surface of the tooth plate is often transected by a series of ridges with intervening depressions. These give rise to sufficient variation in occlusal surface topography to permit development of a sectorial component to the largely crushing function of the tooth plates. Recent work on the histology of the tooth plates of extant chimaeroids (Smith *et al.* 2019; Lijima & Ishiyama 2020; Johanson *et al.* 2021) has demonstrated that the phosphate mineral phase forming the dentinal pillars in the dental hypermineralised tissue of holocephalians is whitlockite (a magnesium and iron-rich calcium phosphate) rather than apatite. This has prompted the use of the term 'whitlockin' for the hypermineralised tissue formerly known as pleromin. Whilst the mineralogy of myriacanthid tooth plates has not yet been checked directly it is most likely to be identical to that of the chimaeroids. However, in the absence of definitive clarification of the chemical composition of the phosphate minerals forming the

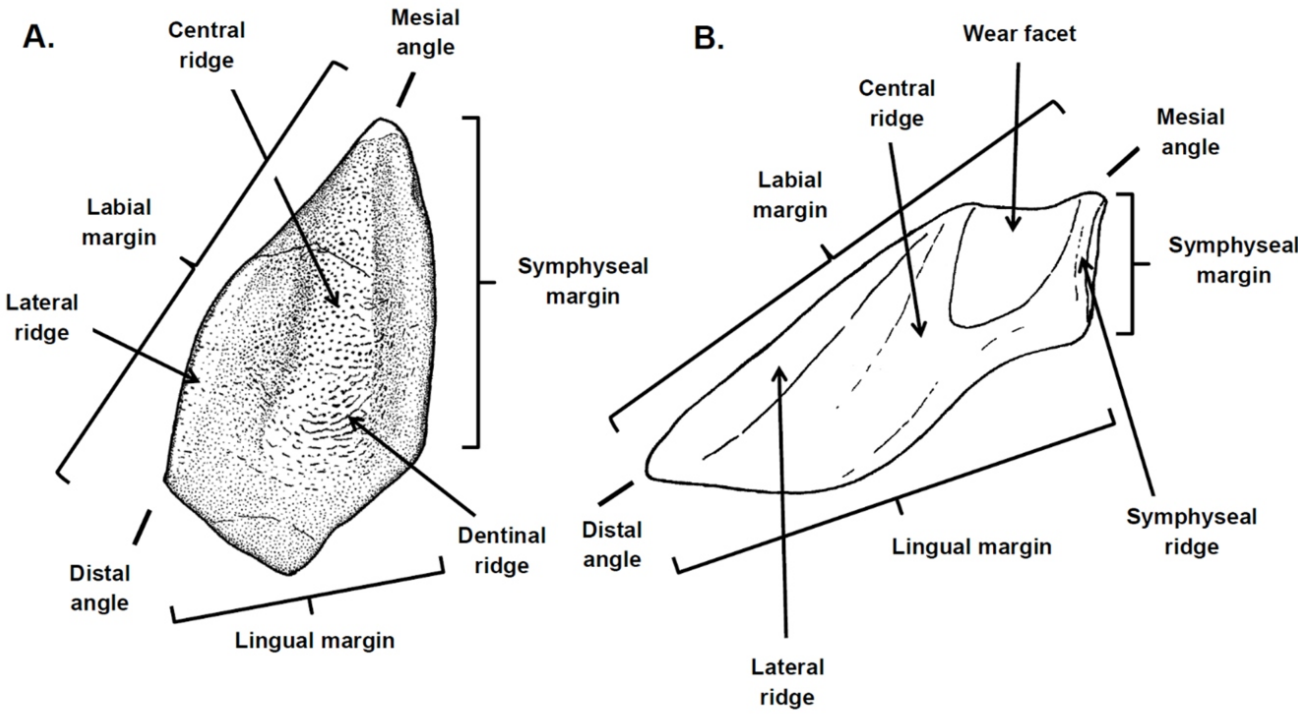

Fig. 2. Diagram showing the technical descriptive terms used in the text: **A:** NHMD 11740, a right upper posterior (palatine) tooth plate of *Oblidens bornholmensis* in occlusal view. **B:** NHMD 633652, a left lower posterior (mandibular) tooth plate of *Myriacanthus paradoxus* in occlusal view.

hypermineralised tissue of the tooth plates described here, the term 'pleromin' is the name retained here.

The most common myriacanthid fossils are isolated tooth plates whose robust structure favours preservation. Unlike the teeth of sharks, holocephalians do not shed their teeth during life, so the discovery of a tooth plate represents the death of an individual fish. Like their elasmobranch sister group within the chondrichthyans, holocephalians possess cartilaginous skeletons with a high organic content, and consequently low preservation potential. A few specimens preserving parts of the endoskeleton in varying degrees of articulation are known from certain conservation lagerstätten (*Myriacanthus* and *Metopacanthus* from the Hettangian to Sinemurian 'Lower Lias' of Lyme Regis in the UK, and *Acanthorhina* from the Toarcian Posidonienschiefer of SW Germany; Patterson 1965; Duffin 1983a). Dorsal fin spines are also commonly preserved as isolated elements. The Myriacanthidae currently contains 10 species distributed amongst eight genera, plus some material which remains in open nomenclature (Stahl 1999; Duffin & Milàn 2017).

A guide to the descriptive terminology used in this paper, originally developed by Duffin (1984), subsequently modified by Patterson (1992), and now in general use (Stahl, 1999) is given in Fig. 2.

Systematic Palaeontology

Class Chondrichthyes Huxley, 1880

Superorder Holocephali Bonaparte, 1832–1841

Order Chimaeriformes Obruchev, 1953

Suborder Myriacanthoidei Patterson, 1965

Family Myriacanthidae Woodward, 1889

Genus *Myriacanthus* Agassiz, 1836

Type species by monotypy. *Myriacanthus paradoxus* Agassiz, 1836, 'Lower Lias', Sinemurian (Early Jurassic) of Lyme Regis, Dorset, UK.

Myriacanthus paradoxus Agassiz, 1836

Fig. 3A, B

1822 "External defensive organ" De la Beche, vol. 1, p. 44, pl. 5 figs 1, 2.
1836 *Myriacanthus paradoxus* Agassiz, vol. 3, pl. 6.
1837 *Myriacanthus paradoxus* Agassiz, vol. 3, p. 38.
1837 *Myriacanthus retrorsus* Agassiz, vol. 3, 39.
1838 *Myriacanthus retrorsus* Agassiz, vol. 3, pl. 8a figs 14, 15.
1855 *Chimaera (Ischyodon) johnsoni* Terquem, p. 241, pl. 14 fig. 1.
1872 *Prognathodus guentheri* Egerton, p. 233, pl. 8.
1891 *Myriacanthus paradoxus* Woodward, p. 44, pl. 2 figs 1–3.
1906 *Myriacanthus paradoxus* Woodward, p. 2, pl. 1 figs 1–5.
1906 *Myriacanthus paradoxus* Dean, p. 143, text-figs 119, 119A, 142.
1965 *Myriacanthus paradoxus* Patterson, p. 128, text-figs 13-19, pl. 22 fig. 46, pl. 25 fig. 59, pl. 26 fig. 60, pl. 28 fig. 67.
1992 *Myriacanthus paradoxus* Patterson, p. 45, figs 7A–C.
1993 *Myriacanthus paradoxus* Duffin & Delsate, text-fig. 5f.
1994 *Myriacanthus paradoxus* Duffin, p. 12, figs 8a-b.
1995 *Myriacanthus paradoxus* Duffin & Delsate, p. 4, text-figs 3a, 4, pl. 1. figs a–b.
1999 *Myriacanthus paradoxus* Stahl, p. 120, figs 117C, 120-122, 123F.
1999 *Myriacanthus paradoxus* Duffin, p. 211, text-figs 23A–B.
2016 *Myriacanthus paradoxus* Duffin, p. 12, figs 8a.
2017 *Myriacanthus paradoxus* Duffin & Milàn, figs 4D, 5B.

Holotype. NHMUK PV P 6095, a dorsal fin spine (Agassiz, 1836 pl. 6 figs 1–2) from the Lower Lias (?Sinemurian, Early Jurassic) of Lyme Regis, Dorset, England.

Bornholm material. NHMD 633652, an isolated left lower posterior (mandibular) tooth plate freed from the matrix (Fig. 3A); NHMD 873668, an isolated right lower posterior (mandibular) tooth plate (Fig. 3B).

Horizon. Hasle Formation.

Age. 'Carixian', Early Pliensbachian, Early Jurassic (probably *Uptonia jamesoni* subzone to *Acanthopleuroceras valdani* subzone based on the Hasle Formation ammonite fauna collected from inland quarries; Donovan & Surlyk, 2003). No ammonites have been described from the coastal exposures.

Locality. Cliff section 100 m south of Hasle, Bornholm, Denmark; 55°10'44.18"N, 14°42'8.58"E.

Description of the Bornholm material. NHMD 633652 is an isolated left mandibular (lower) tooth plate measuring 27.5 mm across the diagonal from the mesial angle to the distal angle (Fig. 3A). The symphyseal margin is short (7.5 mm long) and straight, 4 mm deep and D-shaped in symphyseal view. It is marked

Fig. 3. The tooth plates of *Myriacanthus paradoxus* from the Hasle Formation (Early Pliensbachian) of Bornholm, Denmark. **A:** NHMD 633652 in occlusal and basal views. **B:** NHMD 873668 in occlusal and basal views. **C:** Left lower posterior (mandibular) tooth plate of *Myriacanthus paradoxus* (NHMUK PV P.477) from the Lower Lias (Sinemurian) of Lyme Regis, Dorset, UK, in occlusal view. The specimens are reproduced to the same scale.

by a slight symphyseal ridge. The occlusal surface of the tooth plate is completely covered with a carpet of hypermineralised hard tissue with the exception of a triangular wear facet with broad (6.5 mm long) edge lying along the labial border adjacent to the mesial angle. The straight distal margin of the triangular wear facet is parallel to the symphyseal margin of the tooth plate while the gently curved lingual margin sweeps toward the mesial angle from the wear facet apex. A long, well-developed longitudinal ridge defines the labial border of the tooth plate, widens distally, and has its origin adjacent to the distal limit of the wear facet on the labial border. A second ridge, the central ridge, arises from this same point of origin, flanks the distal margin of the wear facet and crosses the central part of the tooth plate toward the lingual margin. The labial and central ridges diverge at approximately 35° to each other from their common point of origin and are separated by a deep groove. The mesiolabial and mesiolingual borders of the tooth plate are subparallel to each other for a distance of approximately 7 mm.

In basal view it is clear that the mesial angle is sharply defined with fairly deep labial and symphyseal walls. The mesial angle itself is underlain by a deep circular pit. Vascular canals can be seen perforating the basal tissue of the root at low angles of entry.

NHMD 873668 is an isolated right mandibular tooth plate whose overall morphology agrees well with that of the holotype. Rather smaller, it measures 13.4 mm diagonally from the mesial angle to the (incomplete) distal angle (Fig. 3B). Like the holotype, it has a straight symphyseal margin, D-shaped in symphyseal view. The symphyseal margin is 6 mm long. The occlusal surface is covered with pleromin, except for the triangular or V-shaped wear facet occupying the mesiolabial portion of the tooth plate. A lateral ridge follows the labial margin of the plate, strengthening distally and is separated by means of a groove from the broad central ridge which crosses the tooth plate diagonally. The lateral and central ridges have closely adjacent points of origin at a point on the labial margin distal to the mesial angle and diverge from each other at an angle of approximately 30°. Growth lines are visible in the body of the tooth plate lingual to the wear facet.

Although trapezoid in shape, NHMD 873668 is much less gracile and rather broader labio-lingually than NHMD 633652. Also, the lateral ridge along the labial border is not as well developed as in NHMD 633652.

Comparisons. NHMD 633652 and NHMD 873668 clearly belong to the same taxon, based on their closely similar morphologies. The comparatively slender, elongate shape of the holotype is similar to that in *Alethodontus bavariensis* (Duffin 1983b) and *Acanthorhina jaekeli* (Duffin 1983a); the mandibular tooth plates of *Halonodon* and *Agkistracanthus* are much broader labio-lingually (Duffin 1984; Duffin & Furrer 1981).

Several myriacanthid genera show topographic variation in the form of distinct ridges which either cross or border the occlusal surface. The specimens described above are similar to the mandibular tooth plate in *Alethodontus* in that the central and lateral ridges meet at a common point of origin on the labial border and diverge lingually from each other at an angle of 30°-35°. *Alethodontus* does not show any sign of a triangular wear facet, however. The type and only specimen of *Alethodontus bavariensis* (SMNS 51956) probably belongs to a juvenile, based on the sharply defined ridges and lack of any significant antemortem wear (Duffin 1983a).

Acanthorhina possesses a similar wear facet to that shown in the Bornholm material, but in the Toarcian specimen, two diagonal ridges arise from the labial margin just lateral to the mesial angle, converging lingually (Duffin 1983a).

Myriacanthus and *Metopacanthus* both have a fairly simple arrangement with a symphyseal, central and lateral ridge. The latter lacks the distinctive V-shaped wear facet shown in NHMD 633652 and NHMD 873668 (Stahl 1999, fig. 118). In the case of mandibular tooth plates of *Myriacanthus paradoxus*, however, some specimens show the development of a comparable wear facet. NHMUK PV P.477 consists of associated symphyseal, palatine and mandibular tooth plates (Fig. 3C). The mandibular tooth plate in this specimen is an excellent match for the Danish specimens described above, in spite of being much larger (measuring 80 mm across the diagonal from the mesial angle to the distal angle) and less slender in outline. The Bornholm specimens can therefore be attributed to *M. paradoxus*, thereby extending (1) the geographical range of the genus from the UK (Patterson 1965), France (Terquem 1855) and Belgium (Duffin & Delsate 1995) to Denmark, and (2) the stratigraphical range of the genus from the Rhaetian (Duffin 1994) and Sinemurian (Patterson 1965) into the Pliensbachian. The comparatively diminutive size of the Bornholm specimens in comparison to the Lyme Regis material suggests either that (1) the Danish tooth plates are both from juveniles, or (2) that a reduction in body size took place from Sinemurian to Pliensbachian times. Note also the differences in sedimentary facies at the two localities; the 'Lower Lias' consists of an interbedded sequence of marine near- and off-shore calcareous and organic-rich mudstones, whilst the arenite-dominated Bornholm sequence represents a higher energy nearshore environment with greater terrigenous clastic input.

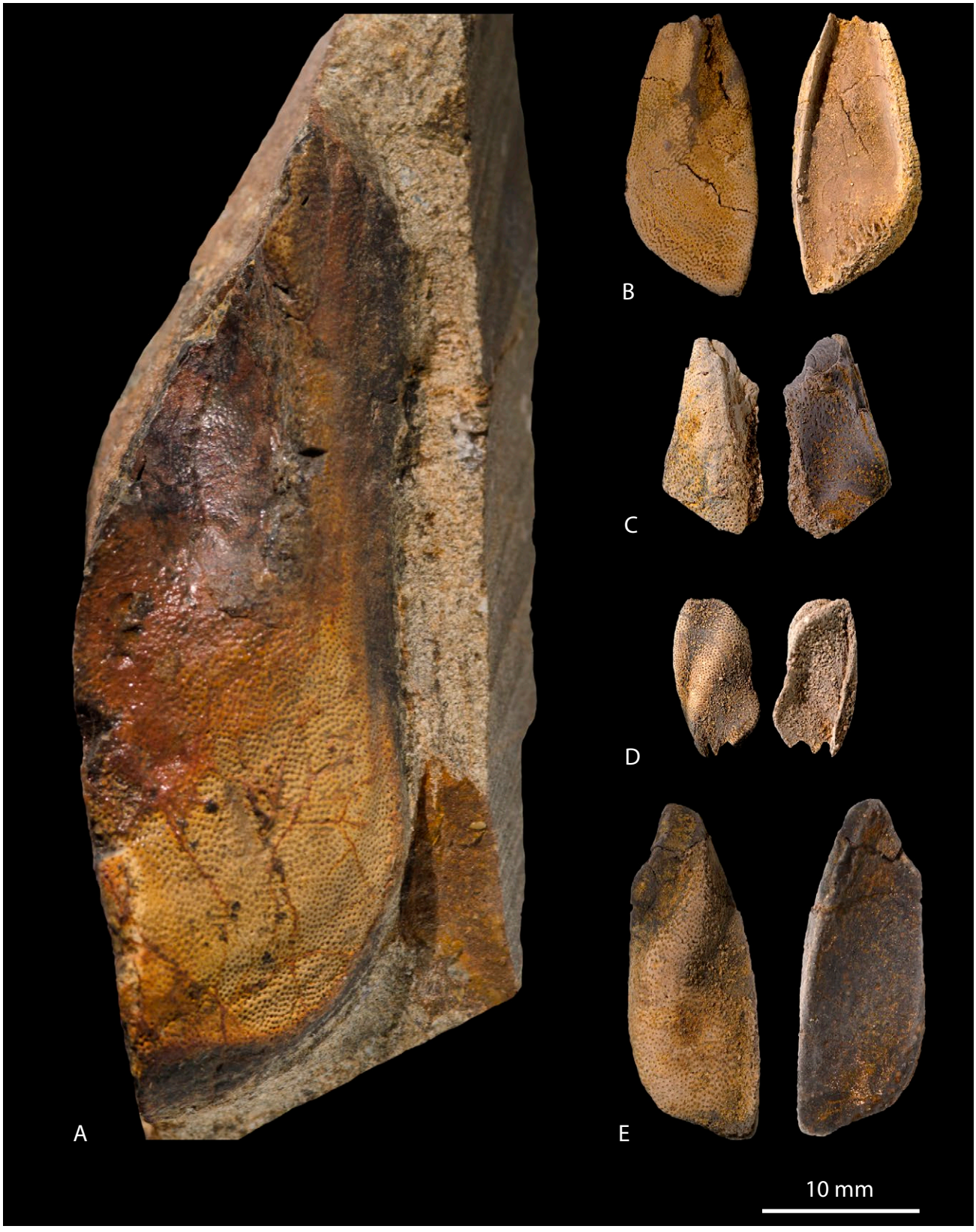

Fig. 4. Myriacanthid holocephalian tooth plates from the Hasle Formation (Early Pliensbachian) of Bornholm, Denmark. **A:** NHMD 633649 (note the left side is eroded) in occlusal view. **B:** NHMD 633651: left upper posterior (palatine) tooth plate of *Oblidens bornholmensis* in occlusal and basal views. **C:** NHMD 633650: probably a left upper posterior (palatine) tooth plate of *Oblidens bornholmensis* in occlusal and basal views. **D:** NHMD 633654: right lower posterior (mandibular) tooth plate of an undetermined myriacanthid holocephalian in occlusal and basal views. **E:** NHMD 633653: left upper posterior (palatine) tooth plate of an undetermined myriacanthid holocephalian in occlusal and basal views. The specimens are reproduced to same scale.

The mandibular tooth plates of *M. paradoxus* can be clearly distinguished from those of the coeval *Oblidens bornholmensis* on the basis of overall shape, and the fact that the latter species has only a single ridge which crosses the tooth plate in a central position (Duffin & Milàn 2017).

Genus *Oblidens* Duffin & Milàn, 2017

Type species. Oblidens bornholmensis Duffin & Milàn, 2017

Revised diagnosis. Myriacanthid genus known from isolated palatine (upper posterior) and mandibular (lower) tooth plates only. The palatine tooth plate is covered with pleromin (no tritoral areas) and possesses a prominent central ridge which expands lingually in juveniles and terminates in the central region of the tooth plate in mature individuals. A weak ridge flanks the labial margin of the palatine tooth plate, and a deep ovoid wear facet is developed on the mesio-labial flanks of the central ridge in mature individuals. The mandibular tooth plate is elongate mesio-distally, the occlusal surface is covered with pleromin (no tritoral areas) and transected by a convex central ridge running from the labial angle to the lingual angle, giving way laterally to flattened labial and lingual fields.

Oblidens bornholmensis

2017 *Oblidens bornholmensis* Duffin & Milàn, 2017; Duffin & Milàn, p. 164, figs 3A-E.

Fig. 4A-C

Material. NHMD 633649, an isolated partial right (?) palatine tooth plate (Fig. 4A); NHMD 633650, an isolated left palatine tooth plate (Fig. 4C); NHMD 633651, an isolated fragment of a left palatine tooth plate (Fig. 4B).

Stratigraphical position. Hasle Formation.

Age: 'Carixian', Early Pliensbachian, Early Jurassic (probably *Uptonia jamesoni* subzone to *Acanthopleuroceras valdani* subzone).

Locality. Cliff section 100m south of Hasle harbour, Bornholm, Denmark; 55°10′44.18″N, 14°42′8.58″E.

Description. NHMD 633651 is the best preserved and most complete of the new specimens which can be assigned to *Oblidens bornholmensis* (Fig. 4B). Missing only the mesial angle, the specimen has been completely freed from the matrix and is a left palatine (upper posterior) tooth plate whose preserved diagonal length is 17 mm. The preserved length of the straight symphyseal margin is 11 mm and that of the arcuate labial margin is 16 mm. These dimensions mean that it is slightly larger than the holotype (NHMD 117400). NHMD 633651 conforms well with the overall form of previously described palatine tooth plates belonging to the genus. The central ridge is clearly developed and extends around halfway toward the lingual margin of the plate from the broken mesial angle. A few dentinal ridges are developed on the symphyseal flanks of the central ridge centrally. The overall shape of the tooth plate is rather more oval than that of the holotype; the labial margin curves rather more gently toward the lingual angle and has a barely developed ridge, in contrast to the holotype. NHMD 633651 probably comes from an older individual than NHMD 11740. A shallow sub-oval wear facet has started to develop on the labial flanks of the central ridge but is still floored with hypermineralised tissue. This wear facet has limited the central expansion of the central ridge toward the center of the occlusal surface of the tooth plate. In basal view, the narrow labial wall and the slightly thicker symphyseal wall of the tooth plate can be clearly discerned. Longitudinal vascular canals enter the lingual underside of the root tissues at a shallow angle.

NHMD 633649 is another palatine tooth plate, this time from the right side (Fig. 4A). In overall morphology it agrees well with NHMD 633651. Still attached to matrix by its basal surface, the tooth plate has a broken labial margin. 66 mm long across the diagonal from the mesial angle to the point on the lingual margin closest to the position of the distal angle (now lost), the occlusal surface is completely covered with hypermineralised tissue. The central ridge is well developed and, as in NHMD 633649, extends to about the mid-point of the tooth plate. Dentinal ridges are missing in this specimen, all the individual pillars of pleromin being normal to the biting surface. The ovoid wear facet flanking the mesio-labial border of the central ridge forms a deeply excavated concavity. The symphyseal border of the tooth plate is not as straight as in the holotype and NHMD 633649, being slightly sinuous along its length. By far the largest of the specimens assigned to *Oblidens bornholmensis*, this example probably comes from a mature individual on the basis of both its size and the development of the wear facet.

NHMD 633650 is probably a fragmentary left palatine tooth plate of *Oblidens bornholmensis* (Fig. 4C). Triangular in shape in occlusal view, the pleromin-covered occlusal surface shows no sign of either a symphyseal or a labial ridge. The maximum preserved diagonal is 14 mm long and there is faint evidence of

a short length of central ridge present near the mesial angle. The symphyseal margin is straight and measures 11.6 mm in length. No dentinal ridges are present.

Undetermined myriacanthid remains

NHMD 633654 is an isolated right mandibular tooth plate which is trapezoid in shape measuring 10 mm across the diagonal from the mesial angle to the distal angle (Fig. 4D). The symphyseal margin of the tooth plate is incomplete but the preserved portion is straight and does not seem to be D-shaped in symphyseal view. The symphyseal ridge is weak to moderate. Pleromin covers the whole of the occlusal surface and no differentiated dentine ridges are present. A lateral ridge is present along the labial margin, getting stronger distally. Broader than in NHMD 633652, it is better developed than in NHMD 633653. A central ridge crosses the occlusal surface of the tooth plate diagonally, expanding distally. The lateral ridge and central ridge are separated from each other by a shallow groove mesially, and the two ridges do not meet or have a common origin anywhere on the labial margin. No wear facets are present on the tooth plate. In basal view, the tooth plate clearly possesses a deep labial wall, but details of the vascularisation are obscure.

This tooth plate is much less gracile and much broader labio-lingually than the mandibular tooth plates of *A. bavariensis*, *Acanthorhina* and *Metopacanthus*. The more robust tooth plate shape in NHMD 633654 is more reminiscent of that in *Myriacanthus*, *Halonodon* and *Akgistracanthus*, although the details of the wear facets and distribution of the pleromin on the occlusal surface is significantly different compared to these three genera. The outline of NHMD 633654 is markedly different to the situation in mandibular tooth plates of *Oblidens bornholmensis*.

NHMD 633653 is an isolated left palatine tooth plate, somewhat tear-dropped in shape, measuring 22 mm across the diagonal (Fig. 4E). The symphyseal margin is slightly concave, measures 5.4 mm in length, is not D-shaped in symphyseal view and is surmounted by a very weak symphyseal ridge. Similarly, a very weak lateral ridge marks the labial margin of the plate, becoming slightly stronger toward the distal angle. An increasingly broad central ridge crosses the tooth plate diagonally but does not meet the lateral ridge on the labial border of the tooth plate. No dentinal ridges are developed and no distinctive wear facets are visible in the pleromin, which covers the occlusal surface of the specimen. Basal view reveals a weak to moderately deep labial wall.

In terms of overall shape, NHMD 633653 is similar to NHMD 633651 (*O. bornholmensis*). In the latter specimen, however, the central ridge is developed differently being limited to the mesial half of the occlusal surface and confined to the mid-line of the tooth plate (rather than crossing it diagonally). NHMD 633653 therefore does not belong to *O. bornholmensis*. Furthermore, the specimen does not pertain to *Myriacanthus paradoxus*, in which the occlusal surface is crossed by two diagonal ridges, or *Halonodon*, which has hypermineralised tissue concentrated in several tritoral areas. In *Acanthorhina jaekeli*, occlusal pleromin is restricted to two triangular areas (Duffin 1983a, p.9), whilst details of the occlusal surface of the palatine tooth plate of *Agkistracanthus mitgelensis* (Rhaetian to Hettangian of Switzerland) are lacking (Duffin & Furrer 1981, p. 818). The material of *A. mitgelensis* described from the British Rhaetian (Duffin 1994) is more oval in shape than the Danish specimen and shows the development of an oval wear facet in larger specimens (Duffin 1994, fig. 5).

NHMD 633654 and NHMD 633653 are left in open nomenclature for the moment, awaiting clarification from further discoveries before their potential relationships can be reassessed.

Conclusions

It used to be that the Pliensbachian marked a stage in the Early Jurassic where our knowledge of myriacanthid holocephalians was negligible. Indeed, the only known holocephalian taxa from the Pleinsbachian were the earliest true chimaeroids, represented by *Eomanodon simmsi* Ward & Duffin (1989) from the *margaritatus* zone of Gloucestershire, UK, and *Brachymylus latus* Duffin (1996) from the *Amaltheus* Shale (*Pleuroceras spinatum* zone, Late Pliensbachian) of Bavaria, Germany. The recent discoveries of myriacanthid tooth plates in the Early Pliensbachian of the cliff sections near Hasle on the Danish island of Bornholm (Duffin & Milàn 2017) have changed this situation dramatically; indeed, although only a relatively small number of tooth plates have been discovered in the succession, they now represent the greatest diversity of Jurassic holocephalians known to date.

The most recent finds of myriacanthid holocephalian tooth plates on Bornholm present a number of problems of interpretation. The mandibular tooth plates can clearly be separated into two groups based upon overall tooth plate shape, wear facet development and ridge development on the occlusal surface. Every myriacanthid taxon is based upon only a small number of specimens which means that there is only limited appreciation of tooth plate variation and ontogeny in the population; this somewhat restricts meaningful comparison and suggests that the dis-

covery of further material may require revision of the conclusions presented here. One of the two groups of mandibular tooth plates is here assigned to *Myriacanthus paradoxus*, previously known from the Rhaetian and Sinemurian of the UK, and the Sinemurian of France and Belgium. The other group of mandibular tooth plates is left in open nomenclature.

The newly discovered palatine tooth plates from Bornholm also fall into two groups – those belonging to *O. bornholmensis* and a further specimen currently left in open nomenclature.

Acknowledgements

We are extremely grateful to the amateur geologists Marianne Nattestad and Anton Wulff Jensen who found the holocephalian teeth in Hasle, brought them to our attention and donated them to the NHMD. Mette Agersnap Grejsen Hofstedt kindly prepared the teeth for us and Sten Lennart Jakobsen provided photographs of the specimens. We are very grateful to the two referees, Dr. David Ward (NHMUK) and Dr. Evgeny Popov (Saratov) for their helpful and constructive comments at the review stage.

References

Agassiz, J.L.R. 1833–1843. Recherches sur les Poissons Fossiles. Petitpierre, Neuchâtel. https://doi.org/10.5962/bhl.title.4275

Beche, H.T. de la. 1822. Remarks on the geology of the south coast of England, from Bridport Harbour, Dorset, to Babbacombe Bay, Devon. Transactions of the Geological Society of London series 2, 1, 40–47. https://doi.org/10.1144/transgslb.1.1.40

Bonaparte, C.L.J.L. 1832–1841: Iconografia della Fauna Italica per le Quattro classi degli animali vertebrati di Carlo L. Bonaparte, principe de Canino. V. iii. Pesci. Rome: Salviucci. https://doi.org/10.5962/bhl.title.70395

Dean, B. 1906. Chimaeroid fishes and their development. Publications of the Carnegie Institution 32, 1–194.

Donovan, D.T. & Surlyk, F. 2003: Lower Jurassic (Pliensbachian) ammonites from Bornholm, Baltic Sea, Denmark. In: Ineson, J.R. & Surlyk, F. (eds): The Jurassic of Denmark and Greenland. Geological Survey of Denmark and Greenland Bulletin 1, 555–583. https://doi.org/10.34194/geusb.v1.4684

Duffin, C.J. 1983a: Holocephalans in the Staatliches Museum fur Naturkunde in Stuttgart. 1. Myriacanthoids and Squalorajoids. Stuttgarter Beitrage zur Naturkunde B97, 1–41.

Duffin, C.J. 1983b: Holocephalans in the Staatliches Museum fur Naturkunde in Stuttgart. 2. A myriacanthid tooth plate from the Hettangian (Lower Jurassic) of Bavaria. Stuttgarter Beitrage zur Naturkunde B98, 1–7.

Duffin, C.J. 1984: A new myriacanthid holocephalan from the Sinemurian (Lower Jurassic) of Belgium. Zoological Journal of the Linnean Society 82 (1), 55–71. https://doi.org/10.1111/j.1096-3642.1984.tb00535.x

Duffin, C.J. 1994: Myriacanthid holocephalans (Chondrichthyes) from the British Late Triassic. Neues Jahrbuch *für* Geologie und Paläontologie Abhandlungen 192 (1), 1–16. https://doi.org/10.1127/njgpm/1993/1993/669

Duffin, C.J. 1996: Holocephalans in the Staatliches Museum für Naturkunde in Stuttgart. 4. The earliest German chimaeroid. Stuttgarter Beitrage zur Naturkunde B 240, 1–10.

Duffin, C.J. 1999. Fish, 191–222, In: Swift, A. & Martill, D.M. (eds): Fossils of the Rhaetian Penarth Group. Cambridge: Palaeontological Society.

Duffin, C.J. & Delsate, D. 1993: A new myriacanthid Holocephalan (Chondrichthyes) from the Early Jurassic of Luxembourg. Neues Jahrbuch für Geologie und Paläontologie Monatshefte 1993 (11), 669–680. https://doi.org/10.1127/njgpm/1993/1993/669

Duffin, C.J. 2016: Cochliodonts and chimaeroids: A.S. Woodward and the Holocephalians. In: Johanson, Z., Barrett, P. M., Richter, M. & Smith, M. (eds): Arthur Smith Woodward: His life and influence on modern vertebrate palaeontology. Geological Society, London, Special Publications 430, 137–154. https://doi.org/10.1144/sp430.9

Duffin, C.J. & Delsate, D. 1995: New record of the Early Jurassic myriacanthid holocephalan *Myriacanthus paradoxus* AGASSIZ, 1836 from Belgium. Belgian Geological Survey. Professional Paper 278, 1–9. https://doi.org/10.1127/njgpm/1993/1993/669

Duffin, C.J. & Furrer, H. 1981: Myriacanthid holocephalan remains from the Rhaetian (Upper Triassic) and Hettangian (Lower Jurassic) of Graubünden (Switzerland). Ecolgae Geologicae Helvetiae 74 (3), 803–829.

Duffin, C.J. & Milàn, J. 2017: A new myriacanthid holocephalian from the Early Jurassic of Denmark. Bulletin of the Geological Society of Denmark 65, 161–170. https://doi.org/10.37570/bgsd-2017-65-10

Egerton, P. de M.G. 1872: On *Prognathodus guentheri* Egerton, a new genus of fossil fish from the Lias of Lyme Regis. Quarterly Journal of the Geological Society of London 28, 233–238. https://doi.org/10.1144/gsl.jgs.1872.028.01-02.35

Höhne, R. 1933: Beiträge zur Stratigraphie, Tektonik und Paläogeographie des südbaltischen Rhät-Lias, insbesondere auf Bornholm. Abhandlungen aus dem Geologisch-Paläontologischen Institut der Universität Greifswald 12, 1–105.

Huxley, T.H. 1880: On the application of the laws of evolution to the arrangement of the vertebrata, and more particularly of the mammalia. Proceedings of the Zoological Society of London 1880, 649–662.

Iijima, M. & Ishiyama, M. 2020: A unique mineralization mode of hypermineralized pleromin in the tooth plate of Chimaera phantasma contributes to its microhardness. Scientific Reports 10, 18591. https:// doi.org/10.1038/s4159 8-020-75545-0.

Johanson, Z., Manzanares, E., Underwood, C., Clark, B., Fer-

nandez, V. & Smith, M. 2021: Ontogenetic development of the holocephalan dentition: Morphological transitions of dentine in the absence of teeth. Journal of Anatomy 239 (3): 704–719. https://doi.org/10.1111/joa.13445

Larsen, O. & Friis, H. 1991: Petrography, diagenesis and pore-water evolution of a shallow marine sandstone (Hasle Formation, Lower Jurassic, Bornholm, Denmark). Sedimentary Geology 72, 269–284. https://doi.org/10.1016/0037-0738(91)90015-6

Malling, C. 1911: Hasle-Sandstenens alder. Meddelelser fra Dansk Geologisk Forening 3, 629–631.

Malling, C. 1914: De Jespersenske Buelag i Lias paa Bornholm. Meddelelser fra Dansk Geologisk Forening 4, 265–270.

Malling, C. 1920: Den marine Lias og Wealden-Aflejringer paa Bornholm. Meddelelser fra Dansk Geologisk Forening 5, 55–57.

Malling, C. & Grönwall, K.A. 1909: En Fauna i Bornholms Lias. Meddelelser fra Dansk Geologisk Forening 3, 271–316.

Milàn, J. & Bonde, N. 2001: Svaneøgler, nye fund fra Bornholm. Varv 2001, 3–8.

Milàn, J. & Mueller-Töwe, I. 2021: En havkrokodille fra Hasles fjerne fortid. Natur På Bornholm 2021, 14–16.

Milàn, J. & Surlyk, F. 2015: An enigmatic, diminutive theropod footprint in the shallow marine Pliensbachian Hasle Formation, Bornholm, Denmark. Lethaia 48, 429–435. https://doi.org/10.1111/let.12115

Molin, E. 2021: Rare terrestrial vertebrate remains from the Pliensbachian (Lower Jurassic) Hasle Formation on the island of Bornholm, Denmark. Dissertations in Geology at Lund University 612, 39 pp

Obruchev, D.M. 1953: Edestid researches in the works of A.P. Karpinskii. Trudy Paleozoologicheskogo Instituta. Akademiya Nauk SSSR 45, 1–85. [In Russian]

Patterson, C. 1965: The phylogeny of the Chimaeroids. Philosophical Transactions of the Royal Society of London B249, 101–219.

Patterson, C. 1992: Interpretation of the tooth plates of chimaeroid fishes. Zoological Journal of the Linnean Society 106, 33–61. https://doi.org/10.1111/j.1096-3642.1992.tb01239.x

Rees, J. 1998: Early Jurassic selachians from the Hasle Formation on Bornholm, Denmark. Acta Palaeontologica Polonica 43, 439–452.

Sandersen, P.B.E., Rasmussen, E.S., Bjerager, M., Jensen, J.B., Schovsbo, N. & Vosgerau, H. 2014: Skitser til opbygningen af en national 3D geologisk model for Danmark, Forslag til legende for den danske del af den nationale 3D geologiske model. Internal GEUS working paper, Rapport 2, 47 pp. https://doi.org/10.34194/raekke2.v78.6867

Smith, A.S. 2008: Plesiosaurs from the Pliensbachien (Lower Jurassic) of Bornholm, Denmark. Journal of Vertebrate Paleontology 28, 1213–1217. https://doi.org/10.1671/0272-4634-28.4.1213

Smith, M.M., Underwood, C., Goral, T., Healy, C. & Johanson, Z. 2019: Growth and mineralogy in dental plates of the holocephalan *Harriotta raleighana* (Chondrichthyes): Novel dentine and conserved patterning combine to create a unique chondrichthyan dentition. Zoology Letters, 5, 11. https://doi.org/10.1186/s40851-019-0125-3

Stahl, B.J. 1999: Chondrichthyes III. Holocephali. In: Schultze, H.-P. (ed.): Handbook of Paleoichthyology, 164 pp. München: Verlag Dr. Friedrich Pfeil.

Surlyk, F. & Noe-Nygaard, N. 1986: Hummocky cross-stratification from the Lower Jurassic Hasle Formation of Bornholm, Denmark. Sedimentary Geology 46, 259–273. https://doi.org/10.1016/0037-0738(86)90062-x

Terquem, O. 1855: Paléontologie de l'étage inférieur de la formation liasique de la province de Luxembourg d 'Hettange. Mémoires de la Société Géologique de France (2) 5, 219–343. https://doi.org/10.5962/bhl.title.11874

Ward, D.J. & Duffin, C.J. 1989: Mesozoic chimaeroids. 1. A new chimaeroid from the Early Jurassic of Gloucestershire, England. Mesozoic Research 2 (2), 45–51.

Woodward, A.S. 1889: On the Myriacanthidae – an extinct family of Chimaeroid Fishes. Annals and Magazine of Natural History, Series 6, 4, 275–280. https://doi.org/10.1080/00222938909460526

Woodward, A.S. 1891: Catalogue of the fossil fishes in the British Museum (Natural History), II. London: British Museum (Natural History). https://doi.org/10.5962/bhl.title.162355

Woodward, A.S. 1906: On a new specimen of the chimaeroid fish, *Myriacanthus paradoxus*, from the Lower Lias near Lyme Regis, Dorset. Quarterly Journal of the Geological Society of London 62, 1–4. https://doi.org/10.1144/gsl.jgs.1906.062.01-04.03

Instructions to authors

See also www.2dgf.dk/publikationer/bulletin/vejledning.html

The Bulletin publishes articles normally not exceeding 30 printed pages, and short contributions not longer than 4 pages. Longer articles and monographs are also published, but in this case it is advisable to consult the chief editor before submitting long manuscripts. Short contributions may be comments on previously published articles, presentation of current scientific activities, short scientific notes, or book reviews.

Manuscripts with complete sets of illustrations, tables, captions, etc., should be submitted electronically to the chief editor (obe@geus.dk). The **main text** with references and figure captions should be in Word format, figures should be in either pdf, jpeg, or tiff format, and tables should be in Excel or Word format. Word tables should be ordinary text files with tab spacing between table columns; Word's 'table function' is discouraged. Compare published articles for table layout.

Manuscripts will be reviewed by two referees; suggestions of referees are welcome. The final decision on whether or not a manuscript will be accepted for publication rests with the chief editor, acting on the advice of the scientific editors. Articles will be published in the order in which they are accepted and produced for publication.

Manuscript

Language – Manuscripts should be in English. Authors who are not proficient in English should ask an English-speaking colleague for assistance before submission of the manuscript.

Title – Titles should be short and concise, with emphasis on words useful for indexing and information retrieval. An abbreviated title to be used as running title may also be submitted.

Abstract – An abstract in English must accompany all papers. It should be short, factual, and stress new information and conclusions rather than describing the contents of the manuscript. Conclude the abstract with a list of key words.

Main text – Use 1.5 or double spacing throughout, and leave wide margins. Italics should be used only in generic and species names and in some Latin abbreviations (e.g. c, *et al.*, ibid., op. cit).

Spelling – Geological units named after localities in Greenland, formal lithostratigraphical units and intrusions named after localities in Greenland remain unchanged even if the eponymous locality names have since been changed in accordance with modern Greenlandic orthography.

References to figures, tables and papers – References to figures and tables in the text should have the form: Fig. 1, Figs 1–3, Table 3 or as (Smith 1969, fig. 3) when the reference is to a figure in a cited paper.

References to papers are given in the form Smith (1969) or (Smith 1969). Combined citations by different authors are separated by a semicolon; two or more papers by same author(s) are separated by commas. Citations are mentioned chronologically and then alphabetically. Use '*et al.*' for three or more authors, e.g. Smith *et al.* (1985).

Reference list

Use the following style:

Smith, A.A. 1989: Geology of the Bulbjerg Formation. Bulletin of the Geological Society of Denmark 38, 119–144. [Note that name of journal is given in full].

Smith, A.A., Jensen, B.B. & MacStuff, C.C. 1987: Sandstones of Denmark, 2nd edition, 533 pp. New York: Springer Verlag. [For more than 10 authors, use first author followed by *et al.*].

Smith, A.A., Jensen, B.B. & MacStuff, C.C. 1992: Characterization of Archean volcanic rocks. In: Hansen, D.D. *et al.* (eds): Geology of Greenland. Geological Survey of Denmark and Greenland Bulletin 40, 1397–1438. [More than three editors – therefore *et al.* form is used].

Sorting – Danish letters æ, ø and å (aa) are treated as ae, o and a (aa), respectively.

References are sorted by:

1) Alphabetically by the first author's surname. 2) Papers by one author: two or more papers are arranged chronologically. 3) Papers by two authors: alphabetically after second author's name. Two or more papers by the same two authors: chronologically. 4) Papers by three or more authors: chronologically. Papers from the same year are arranged alphabetically after second, third, etc. author's name. Authors themselves are responsible for the accuracy and completeness of their references. The reference list must include all, and only, the references cited in the paper (including figures, tables etc).

CrossRef

Please add hyperlinks to Crossref DOI when you create your citation list whenever possible.

Illustrations

May be prepared in either black and white or colour. There is no colour charge. Horizontal illustrations are much to be preferred. Size of smallest letters in illustrations should not be less than 5.5 pt. Remember scale.

All figures (including photographs) should be submitted in electronic form ready for direct reproduction, i.e. having the dimensions of the final figure with a standard resolution of 300 dpi for photographs. Preferred formats are pdf, tiff and jpg.

Size – Width: All widths up to full page width (170 mm) are accepted. Maximum height is 223 mm. Design figure contents to match the preferred figure size.

Captions – Captions to figures and plates must be delivered on separate pages, preferably at the end of the manuscript.

Supplementary data files

Supplementary files are accepted. Such files may provide e.g. analytical data tables, detailed data documentation, illustrations with special effects, or videos.

Proofs

Authors receive page proofs of the article after technical production. The cost of any alterations against the final manuscript will be charged to the author.

Content, vol. 70

Instructions to authors:
See inside the back cover and also www.2dgf.dk/publikationer/bulletin/vejledning.html